Uncovering the functions of novel m^{6}A and Nm writers in *Drosophila melanogaster*

Dissertation

Zur Erlangung des Grades

Doktor der Naturwissenschaften

Am Fachbereich Biologie

Der Johannes Gutenberg-Universität Mainz

Vor- und Zunahme des Doktoranden

Mariangela Spagnuolo

geboren in Eboli (Italien)

Mainz, 2024

Dekan: Prof. Dr. Eckhard Thines

1. Berichterstatter: Prof. Dr. René Ketting

2. Berichterstatter: Dr. Julian Koenig

Tag der mündlichen Prüfung: 24 Juni 2024

JOHANNES GUTENBERG
UNIVERSITÄT MAINZ

Table of Contents

List of Figures

List of Supplementary figures

List Of Tables

List of abbreviations

acp^3U	3-(3-amino-3-carboxypropyl)uridine
ac^4C	N4-acetylcytidine
A	Adenosine
aa	Amino acid(s)
a^6A	N6-allyl Adenosine
a^6m^6A	N6-allyl. N6-methyl Adenosine
ADAR	Adenosine deaminases acting on RNA
ALKBH	AlkB homolog
ALYREF	Aly/REF export factor
ANOVA	Analysis of variance
APA	Alternative polyadenylation
ARID	Autosomal recessive intellectual disability
ATM	Ataxia-telangiectasia mutated
BCSC	Breast cancer stem cells
bp	Base pair(s)
Btz	Barentsz
C	Cytidine
CBC	Cap-binding complex
CBLL1	Casitas B-lineage lymphoma-transforming sequence-like protein 1
cDNA	Complementary DNA
CDK	Cyclin-dependent kinase
CDS	Coding sequence
Chr	Chromosome
CMTR1/2	Cap-specific mRNA 2′-O-methyltransferase 1/2
CNOT complex	CCCR4-NOT complex
CNS	Central nervous system
CPSF	Cleavage and polyadenylation specificity factors
CRC	Colorectal cancer cell line
CRISPR-Cas9	Clustered regularly interspaced short palindromic repeats-CRISPR-associated protein 9
cryo-EM	Cryogenic electron microscopy
CTRL	Control
D	Dihydrouridine
DC	Decoding centre
DART-seq	Deamination adjacent to RNA modification targets sequencing
dm^6A	N6-dithiolsitolmethyladenosine
DNA	Deoxyribonucleic acid
DNMT	DNA methyltransferase
dNTP	Deoxynucleotide triphosphate
ds	Double-stranded
Dxo	Decapping exoribonuclease
ESC	Embryonic stem cells
eIF	Eukaryotic translation initiation factor
eTAM-seq	Evolved TadA-assisted m^6A seq
EB	Embryoid body
EMT	Epithelial to mesechymal transition
FASN2	Fatty acid synthase 2
FBXW7	F-box and WD repeat domain containing 7
FDR	False discovery rate
Fl(2)d	Female-lethal(2)d
Flacc	Fl(2)d-associated complex component
FMR1	Fragile X messenger ribonucleoprotein 1
FTO	Fat mass and obesity-associated protein
FXS	Fragile X syndrome
G	Guanine
GFP	Green fluorescent protein
GLORI-seq	Glyoxial and nitrite-mediated deamination of unmethylated Adenosine
GO	Gene ontology
gRNA	Guide RNA
GSC	Glioblastoma stem cell
GWAS	Genome-wide association study
H	histone
HCC	Hepatocellular carcinoma
HCT116	Human colon tumor cell line 116
HEK293	Human embryoid kidney 293
HIV	Human immunodeficiency virus
HEN1	Hua enhancer 1
hm^5C	5-hydroxymethylcytidine
HNRNP	Heterogeneous nuclear ribonucleoprotein

HPLC	High-performance liquid chromatography
HRP	Horse radish peroxidase
I	Inosine
IFIT1	Interferon-induced proteinwith tetratricopeptiderepeats 1
IGF2BP	Insulin-like growth factor 2 mRNA-binding proteins
INDY	I'm not dead yet
IP	Immunoprecipitation
IRES	Internal ribosome entry site
kb	Kilobase(s)
KD	Knock down
kDa	Kilodalton(s)
KH domain	K-homology domain
KO	Knock out
LARP7	La-related protein 7
LCD	La-motif containing domain
LC-MS/MS	Liquid chromatography with tandem mass spectrometry
lncRNA	Long non-coding RNA
m^1A	N1-methyladenosine
$m^1acp^3\Psi$	N1-methyl-N3-aminocarboxypropylpseudouridine
m^2G	N2-methylguanosine
$m_2{}^2G$	N2,N2-dimethylguanosine
m^3C	3-metyhlcytidine
m^3U	3-methyluridine
m^5C	5-methylcytidine
m^6A	N6-methyladenosine
$m_2{}^6A$	N6-N6-dimethyladenosine
m^6ACE-seq	m^6A crosslinking exonuclease sequencing
m^6A-LAIC-seq	Level and isoform characterization sequencing
m^6A-REF-seq	m^6A-Sensitive-RNA-Endonuclease-Facilitated sequencing
m^6A-SAC-seq	m^6A-selective allyl chemical labeling and sequencing
m^6A-SEAL	FTO-assisted m^6A selective chemical labelling
m^6Am	N6,2′-O-dimethyladenosine
m^7G	N7-methylguanosine
MAC	m^6A–METTL complex
MACOM	m^6A-METTL-associated complex
MALAT1	Metastasis-associated lung adenocarcinoma transcript 1
MAT2A	Methionine adenosyltransferase 2A
MAZTER-seq	MazF RNase assisted cleave of RNA at unmethylated sites within ACA motifs
MeRIP	m^6A-methylated RNA immunoprecipitation
mES cells	Mouse embryonic stem cells
METTL	Methyltransferase Like
Mg2+	Magnesium ion
miCLIP	m^6A-Methylation iCLIP
miRNA	Micro RNA
MLASA	myopathy lactic acidosis sideroblastic anaemia
mRNA	Messenger RNA
MRM	Mitochondriam RNA methyltransferase
msl-2	male-specific lethal-2
mtTFB	Mitochondrial transcription factor B
MTase	Methyltransferase
MTS	Methyltransferase small domain
NAT10A	N-Acetyltransferase 10A
ncRNA	Non-coding RNA
ND5	NADH dehydrogenase 5
Nito	Spenito
NGD	No-go-decay
NLS	Nuclear localisation signal
Nm	2′-O-ribose methylation
NMD	Non-sense mediated mRNA decay
Nm-REP-seq	Nm mapping based onRNA exoribonuclease and periodate oxidative reactivity coupled with sequencing
NSUN	NOP2/Sun RNA Methyltransferase
NXF1	Nuclear RNA export factor 1
nt	Nucleotide(s)
OED	Oxidation-elimination-dephosphorylation
ONT	Oxford nanopore technologies
P bodies	Processing bodies
PA-m^6A-seq	photo-crosslinking assisted m6A-seq
PABP	Poly(A) binding protein
PCBP1	Poly-(c)-Binding Protein 1
PCIF1	PDX1 C-terminal inhibiting factor 1
piRNA	PIWI-interacting RNA
PLD	Peptidylprolyl isomerase (PPI)-like

	domain
poly(A) RNA	Poly-adenylated RNA
PRC2	Polycomb repressive complex 2
PTC	Peptidyl transferase center
Pus	Pseudouridine synthase
RBM15	RNA Binding Motif Protein 15
RBP	RNA binding protein
regRNP	Regulatory ribonucleoprotein
RISC	RNA-induced silencing complex
RNA	Ribonucleic acid
RNAi	RNA interference
RNA Pol	RNA polymerase
RNP	Ribonucleoprotein complex
ROS	Reactive oxygen species
RP-HPLC	Reverse phase-high performance liquid chromatography
rRNA	Ribosomal RNA
RTL-P	Reverse Transcription at Low deoxy-ribonucleoside triphosphate (dNTP) concentrations followed by polymerase chain reaction
RT-qPCR	Quantitative reverse transcription-PCR
SAH	S-adenosylhomocysteine
SAM	S-Adenosyl methionine
scaRNA	Small Cajal-body specific RNA
SCARLET	Site-specific cleavage and radioactive-labelling followed by ligation-assisted extraction and thin-layer chromatography
SELECT	single-base elongation and ligation-based qPCR amplification
SMRT	single-molecule, real-time
siRNA	Small interfering RNA
snoRNA	Small nucleolar RNA
snoRNP	Small nucleolar ribonucleoproteins
snRNA	Small nuclear RNA
SRS	Substrate recognition sequence
SRSF	Serine/arginine-rich splicing factor
ss	Single-stranded
Sxl	Sex lethal
T	Thymine
TARBP1	TAR- binding protein 1
TET	Ten-eleven translocation
TGIRT	Thermostable group II intron reverse transcriptase
TLR7	Toll-like receptor 7
TNT-seq	Transient N6-methyladenosine transcriptome sequencing
TRIBE	ADAR-editing based detection of methylated region
tRF	tRNA fragments
TRMT	tRNA methyltransferase
TRMT112	tRNA methyltransferase activator subunit 11-2
tRNA	Transfer RNA
TSS	Transcription start site
U	Uridine
U2AF	U2 small nuclear ribonucleoprotein auxiliary factor
UPR^{ER}	Endoplasmic reticulum unfolded protein response
USP5	Ubiquitin specific peptidase 5
UTR	Untranslated region
VCR	Vertebrate conserved region
Vir	Virilizer
VIRMA	Vir-like m^6A methyltransferase associated
WDR4	WD repeat domain 4
WT	Wild type
WTAP	Wilms' tumour 1-associating protein
XIST	X-inactive specific transcript
XLID	X-linked intellectual disability
YTH	YT521-B homology
YTHDC	YTH domain-containing protein
YTHDF	YTH domain-containing family protein
yW	wybutosine
ZC3H13	Zinc finger CCCH domain-containing protein 13
ZCCHC4	Zinc finger CCHC-type containing 4
Ψ	Pseudouridine
20-HE	Hydroxyecdysone
8-oxoG	8-Oxo-7,8-dihydroguanosine

Abstract

RNA modifications have emerged as an important regulatory layer of gene expression, decorating all RNA species in the three kingdoms of life. N6-methyladenosine (m^6A), the most prevalent modification in messenger RNA (mRNA), and its methyltransferase, the METTL3-METTL14 complex, is to date the best characterized, known to fulfill important regulatory functions during development through the modulation of mRNA biogenesis. For non-coding RNAs, on the other hand, despite being abundant and heavily modified, the functions and the identity of writers of m^6A and some other modifications are less characterized. One of such modifications, 2'O-methylation of the ribose (Nm), is highly enriched on ribosomal RNA (rRNA) and transfer RNA (tRNA). The improvement of mapping methodologies has unveiled its dynamic nature during development and upon stress, suggesting its importance in these processes, yet the knowledge about its writers is still incomplete. The goal of my PhD is to characterize novel m^6A and Nm methyltransferases in *Drosophila melanogaster* in order to get more insights into these 2 modifications and their impact on non-coding RNAs.

To achieve this goal, the CRISPR/Cas9 system was employed to generate loss-of-functions fly lines for putative m^6A and Nm writers: *CG7544* (ortholog of METTL16), *CG9666* (ortholog of METTL5, identified as novel m^6A writer in this study), and the novel Nm writer *CG33964* (ortholog of human METTL25) The obtained mutant lines were used for molecular studies, proteomic and transcriptomic analysis, as well as behavioural assays.

We identified Mettl5 as a m^6A writer acting in concert with Trmt112, a conserved partner, to methylate the 18S rRNA, and show that m^6A loss upon Mettl5 depletion has a significant impact on brain development and fly behaviour, providing molecular insight to the METTL5-dependent intellectual disability observed in human (Leismann, Spagnuolo et al., 2020). Our data also confirm the binding of Mettl16, another m^6A methyltransferase, to spliceosomal RNA U6 and prove its essential role for fly ovarian development and fertility.

The second part of my PhD, dedicated to the study of novel Nm writers, uncovers $tRNA^{GlyGCC}$ as target of Mettl25 ortholog in flies and shows important translational and metabolic impairments, as well as a significant lifespan reduction, upon depletion of the enzyme. Lastly, the functions of another Nm writer: CG8939, orthologous of human FTSJ3, were addressed by RNAi, nanopore and transcriptomic analysis, uncovering a methylated target in the RNase MRP, essential for ribosome biogenesis.

Altogether, our findings expand the repertoire of m^6A and Nm writers, and demonstrate their specialization and their significance in the context of gene expression and animal health, providing important resource data for future studies.

Zusammenfassung

RNA-Modifikationen haben sich als wichtige Regulationsebene der Genexpression erwiesen und schmücken alle RNA-Arten in den drei Reichen des Lebens. N6-Methyladenosin (m6A), die am weitesten verbreitete Modifikation in Boten-RNA (mRNA), und ihre Methyltransferase, der METTL3-METTL14-Komplex, sind bis heute am besten charakterisiert, und es ist erwiesen, dass sie wichtige regulatorische Funktionen durch die Modulation der mRNA-Biogenese während der Entwicklung erfüllen. Für nicht-kodierende RNAs hingegen sind die Funktionen und die Identität der m6A-Schreiber und einigen anderen Modifikationen weniger gut charakterisiert, obwohl diese RNA-Species reichlich vorhanden und stark modifiziert sind. Eine dieser Modifikationen, die 2'O-Methylierung der Ribose (Nm), ist auf ribosomaler RNA (rRNA) und Transfer-RNA (tRNA) stark angereichert. Die Verbesserung der Kartierungsmethoden hat ihre dynamische Natur während der Entwicklung und bei Stress enthüllt, was auf ihre Bedeutung in diesen Prozessen hindeutet, aber das Wissen über ihre Schreiber ist noch unvollständig. Das Ziel meiner Doktorarbeit ist es, neue m6A-und Nm-Methyltransferasen in Drosophila melanogaster zu charakterisieren, um mehr Einblicke in diese beiden Modifikationen und ihre Auswirkungen auf nicht-kodierende RNAs zu erhalten.

Hierzu wurde das CRISPR/Cas9-System eingesetzt, um Fliegenlinien mit Funktionsverlustmutationen in mutmaßlichen m6A-und Nm-Schreiber zu erzeugen: CG7544 (Ortholog von menschlichem METTL16), CG9666 (Ortholog von METTL5, in dieser Studie als neuartiger m6A-Schreiber identifiziert) und der neuartige Nm-Autor CG33964 (Ortholog von METTL25). Die generierten Mutantenlinien wurden für molekulare Studien, Proteom- und Transkriptomanalysen sowie Verhaltenstests verwendet.

Wir haben Mettl5 als m6A-Schreiber identifiziert, der zusammen mit Trmt112, einem evolutionär konservierten Partner, die 18S rRNA methyliert, und zeigen, dass der m6A-Verlust bei der Deletion von Mettl5 erhebliche Auswirkungen auf die Gehirnentwicklung und das Verhalten der Fliege hat, was einen molekularen Einblick in die von METTL5 abhängige geistige Behinderung beim Menschen ermöglicht (Leismann, Spagnuolo et al., 2020). Unsere Daten bestätigen auch die Bindung von Mettl16, einer weiteren m6A-Methyltransferase, an die spleißosomale RNA U6 und belegen ihre wesentliche Rolle für die Eierstockentwicklung und Fruchtbarkeit der Fliege.

Der zweite Teil meiner Doktorarbeit, der sich mit der Untersuchung neuartiger Nm-Schreiber befasst, deckt tRNAGlyGCC als Zielsequenz des Mettl25-Orthologs in Fliegen auf und zeigt erhebliche Beeinträchtigungen der Translation und des Stoffwechsels sowie eine deutliche Verkürzung der Lebensspanne, wenn das Enzym ausgeschaltet wird. Zuletzt wurden die Funktionen eines weiteren Nm-Schreibers untersucht: CG8939, ein Ortholog des menschlichen FTSJ3, wurde mit Hilfe von RNAi, Nanopore- und Transkriptomanalysen untersucht, wobei eine methylierte Zielsequenz in der RNase MRP entdeckt wurde, das für die Ribosomenbiogenese wesentlich ist.

Insgesamt erweitern unsere Ergebnisse das Repertoire der m6A-und Nm-Schreiber, zeigen ihre Spezialisierung und ihre Bedeutung im Zusammenhang mit der Genexpression und der Tiergesundheit und liefern wichtige Daten für zukünftige Studien.

1. INTRODUCTION

1.1-Gene expression regulation

Gene expression is the process by which the information stored in the DNA is turned into its functional output, like a protein or a non-coding RNA, and it is at the base of every biological process, such as cell division, cell differentiation, cell death. In higher organisms, it provides the instructions for the development and functioning of tissues and organs to regulate more complex processes, like the immune response, or the ability to learn and store memories. Multiple mechanisms come into play to ensure a tight cell-specific regulation of gene expression, ranging from chromatin remodelling and epigenetic modifications, to post-transcriptional events such as microRNA (miRNA)-mediated silencing, alternative splicing, and RNA modifications.

1.1.1-Epigenetics

DNA is organised, in higher organisms, into chromatin, of which the constitutive monomer is the nucleosome. Nucleosomes are composed of proteins called histones, two copies of histones H2, H3 and H4, wrapped by 1.5 turns of DNA. The DNA stretches between adjacent nucleosomes are decorated with a fourth histone, H1.

The first layer of transcriptional regulation occurs at the chromatin level, where insulators and chromatin remodelling factors create long range interactions between enhancer and promoters and shape the chromatin into its two major forms: a compacted and inaccessible heterochromatin, and an open euchromatin, to promote or block transcription of specific genes (Morrison & Thakur, 2021).

High-throughput techniques like assay for transposase-accessible chromatin with high-throughput sequencing (ATAC-seq), chromatin immunoprecipitation and sequencing (ChIP-seq), fluorescence in situ hybridisation (FISH), 3C and its most developed version Hi-C, have allowed scientists to understand chromatin organisation in different contexts (Kempfer & Pombo, 2020; Shaoqian Ma & Zhang, 2020). For example, ChIP-seq experiments have permitted the mapping of epigenetic marks, chemical groups added at the N-terminal tail of histones, associated with active promoters and enhancers, such as acetylation of lysine 27 and methylation of lysine 4 and 36 on histone 3 (H3K27ac; H3K4me3; H3K36me); or marks associated with inactive, heterochromatic, regions, such as H3K9me3 and H3K27me3 (Morrison & Thakur, 2021). The study of the changes that occur at the chromatin level without affecting the DNA sequence are part of the field known as EPIGENETICS(Peixoto et al., 2020).

1.1.2-Post-transcriptional regulation

Once a gene is transcribed into a messenger RNA (mRNA), it undergoes multiple modifications before being translated into a functional protein and/or being degraded. The precursor of mRNA (pre-mRNA) gets **polyadenylated** and **capped,** the former being a stretch of adenosines added at the pre-mRNA 3' terminus, and the latter being an m^7G modification (see chapter 1.2 Epitranscriptomics, m^7G), also known as cap, added at the pre-mRNA 5' terminus, to protect it from the action of exonucleases, and to regulate translation (Manley, 1988; Ramanathan et al., 2016).

In most of the cases, the pre-mRNA also goes through **splicing**, a process by which non-coding sequences, or introns, are removed from a transcript and the coding exons are re-ligated. Splicing is carried out by a complex of RNA and proteins known as spliceosome and contributes to increase the coding complexity of the genome of higher organisms, as a pre-mRNA can undergo "alternative splicing" and generate multiple isoforms, hence more variability, from a single transcript (House & Lynch, 2008).

To ensure that the right amount of a transcript is being translated into a functional protein, gene expression inhibition can also occur at a post-transcriptional level. Major actors of this process, known as RNA interference (RNAi), are small non-coding RNAs (ncRNA) such as microRNAs (miRNA). These are 20-25 nt long oligos and are part of the RNA-Induced Silencing Complex (RISC), which degrades the target mRNA, recognised by mean of sequence complementarity with the miRNA (Agrawal et al., 2003; Shang et al., 2023). miRNAs have been revealed essential in development and immunity for their role in gene expression regulation, and found associated with many cancers, neurological and immune disorders, such that they are nowadays often used for therapeutic applications (Agrawal et al., 2003; Shang et al., 2023), showing the importance of a tight regulation of gene expression.

The last decades have paved the way to a new field of research in molecular biology, called EPITRANSCRIPTOMICS, which share the same prefix, "epi-", as the word epigenetics, meaning in Greek "above, beyond". While epigenetics, from the Greek ἐπί (*epì*) and γεννητικός (*gennitikòs)*, refers to modifications that alter a phenotype without changing the genetic material, the DNA sequence; epitranscriptomics studies the role of modifications on the RNA, that happen "on top of" its sequence, hence affecting the RNA fate without changing its sequence. Over time more and more discoveries have increased interest in the field, shedding light on the importance of RNA modifications in the regulation of RNA metabolism and functions, yet the recent birth of the field still leaves a lot to be unveiled (Fig.1).

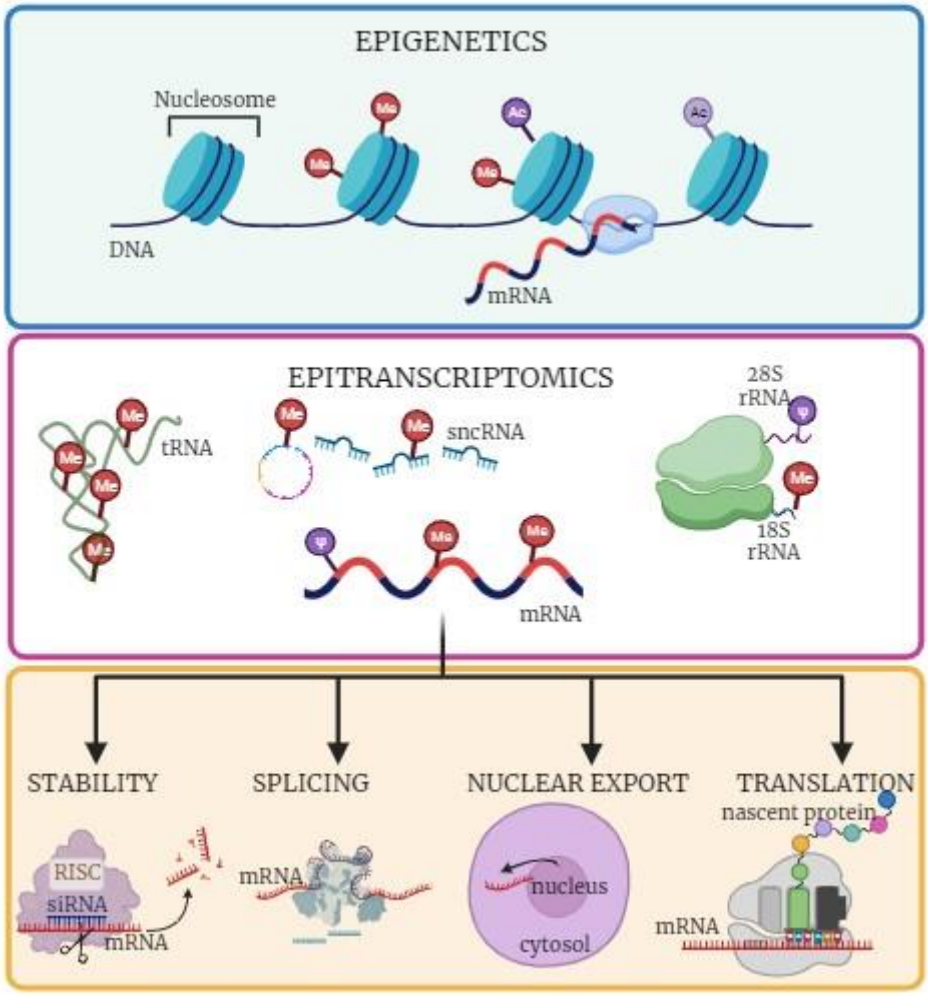

Figure 1: Major mechanisms of gene expression regulation: epigenetis and epitranscriptomics.
Transcriptional regulation is modulated by epigenetics modifications and chromatin remodelling which affects the chromatin status and foster or inhibit the expression of specific genes. Once RNA is transcribed can be subjected to the addition of chemical groups (epitranscriptomics) which affect several aspects of the RNA fate, including its stability, nuclear export, mRNA splicing and translation.

1.2-Epitranscriptomics

The first experiment leading to the identification of RNA modification was anion exchange chromatography carried out by Cohn and Volkin in 1951 (Waldo E. Cohn & Volkin, 1951). The discovered modification was at first mistaken for a fifth nucleotide, to be later identified as a uridine isomer by nuclear magnetic resonance and called pseudouridine (ψ)(W. E. Cohn, 1960). Transfer RNAs (tRNAs) and ribosomal RNAs (rRNAs) had been for long the main subjects of studies directed at the identification of modifications, as they are the most abundant RNA species and the most heavily modified. In 1974 the first internal mRNA modifications, 2'O-methylation of the ribose (2'Ome or Nm) and N-6 methyladenosine (m^6A), were identified in mammals and viruses (Desrosiers et al., 1974; Furuichi, 1974; Mer Wei & Moss, 1974; Perry & Kelley, 1974; Shatkin, 1974). Up to that point, a 7-methylguanosine, attached to the 5'-terminus of a transcript via a 5'-5' phosphodiester bond, was the only known mRNA modification, referred to as "mRNA cap". This has been shown to contribute to transcript stability, splicing, nuclear export and translation initiation(Ramanathan et al., 2016).

Despite their initial discovery in the '70s, the field of mRNA modifications underwent an initial lack of interest due to experimental limitations. But a major progress for their detection occurred in 2012. Dominissini et al. and Meyer et al. were able to map more than 12000 m^6A sites on mammalian mRNA, by developing an antibody-based technique to pull down m^6A-decorated transcripts and coupling it with high-throughput sequencing (Dominissini et al., 2012; K. D. Meyer et al., 2012). Other studies identified the so called "writers", "readers" and "erasers", enzymes responsible respectively for the deposition, binding, and removal, of an RNA modification(Shi et al., 2019). Loss of function studies of these enzymes in multicellular organisms have unveiled many molecular functions of RNA modifications, ranging from regulation of splicing and nuclear export to stability, interaction with proteins, and translation. At the physiological level they have been connected to diseases of neurological and immunological nature as well as cancer onset and progression, becoming important potential therapeutic targets (Boccaletto et al., 2022; Boo & Kim, 2020; L. Han et al., 2015; Jonkhout et al., 2017; Roignant & Soller, 2017; Roundtree, Evans, et al., 2017). Moreover, the identification of erasers proved the versatile nature of some RNA modifications(Jia et al., 2012; K. D. Meyer & Jaffrey, 2017; Shi et al., 2019; Zheng et al., 2013), suggesting their time and/or context-dependent function (Alings et al., 2015; Dedon & Begley, 2014).

Nowadays among the most abundant modifications on mRNA are, **m^6A, Nm** (Desrosiers et al., 1974) and **ψ** (Carlile et al., 2014; Schwartz et al., 2014); and at a lower prevalence N6,2'-O-dimethyladenosine (**m^6Am**) (Mauer et al., 2017), N1-methyladenosine (**m^1A**) (Dominissini et al., 2016; X. Li et al., 2016, 2017; Safra et al., 2017), 7-methylguanosine (**m^7G**) (Malbec et al., 2019; L. S. Zhang et al., 2019), 8-Oxo-7,8-dihydroguanosine

(8-oxoG) (Yan & Zaher, 2019), and cytosine modifications such as 5-methylcytosine (m^5C) (Squires et al., 2012), 5-hydroxymethylcytosine (hm^5C) (Delatte et al., 2016), 3-methylcytosine (m^3C) (Luang Xu et al., 2017) and N4-cytosine acetylation (ac^4C) (Arango et al., 2018, 2022), as well as irreversible modifications caused by deamination of adenine and cytidine, respectively known as adenosine-to-inosine, and cytidine-to-uracile, editing (A-to-I and C-to-U) (Blanc et al., 2014; Hogg et al., 2011).

Non-coding RNAs, on the other hand, include the most abundant and most highly modified species, with eukaryotic tRNA containing on average 13 modifications per molecule (Roundtree, Evans, et al., 2017). Modifications on tRNAs and rRNAs, as well as small nuclear RNAs (snRNAs), in most cases occur in functional sequences and have been associated with RNA biogenesis, stability or translation regulation. tRNAs show the widest chemical diversity of modifications, with the most relevant and widespread being m^1A, m^7G, m^5C, Nm, wybutosine (yW) and ψ (Lorenz et al., 2017), while m^6A has not been detected on tRNA, with the exception of bacterial $tRNA^{Val}$ (Lence et al., 2019). Some of these modifications are generated by the sequential action of different enzymes, like yW (Noma et al., 2006) and N1-methyl-N3-aminocarboxypropylpseudouridine ($m^1acp^3ψ$) (Babaian et al., 2020; Brand et al., 1978).

rRNAs are the most abundant RNA species and are part of the ribosome machinery, which translates the mRNA into functional proteins. Ribosomes are made up of a small subunit (SSU or 40S), comprising the 18S rRNA and 33 proteins, and a large subunit (LSU or 60S), comprising the 5S, 5.8S, 28S rRNAs and 47 proteins in human (Sharma & Lafontaine, 2015). The biogenesis of the ribosomal components begins in the nucleolus, where a polycistronic precursor (pre-rRNA) is transcribed by RNA Pol I and undergoes a series of modifications, cleavages and structural changes to produce the mature rRNAs (Aubert et al., 2018; Sloan et al., 2017). Interestingly, some modifications are deposited co-transcriptionally in the nucleolus, suggesting a role in early steps of pre-rRNA maturation (Sloan et al., 2017). In other cases, binding of a rRNA modification enzyme in the nucleolus is essential for the maturation to occur, yet the modification is deposited only when the rRNA reaches the nucleus or the cytosol (Létoquart et al., 2014; J. White et al., 2008; Zorbas et al., 2015). Despite being the most abundant RNA species, rRNA does not show a great variety of modifications, as it is mainly enriched with Nm and ψ (Sloan et al., 2017). Other modifications decorating this RNA species are ac^4C, m^1A, m^5C, m_2^6A, and N1-methyl-N3-aminocarboxypropylpseudouridine ($m^1acp^3ψ$), which is unique to rRNA(Sloan et al., 2017).

SnRNAs also bear modifications that are important for regulation of their functions. For instance, m^6A decorates several components of the spliceosome machinery and unlike for mRNA, it is not almost exclusively deposited by one complex but distinct RNAs are specifically targeted by different m^6A writers

(Goh et al., 2020; Pendleton et al., 2017; Warda et al., 2017). Less abundant ncRNAs, like micro RNAs (miRNA) or circular RNAs (circRNA) are also modified, for instance **m^{6}A** and **Nm** have been shown to play a role in their maturation and translation (Shuai Ma et al., 2019; Y. Yang et al., 2017).

Nowadays, more than 170 modifications have been found to decorate all RNA species in all kingdoms of life, with m^{6}A on mRNA being the best characterized (Fig. 2) (Boccaletto et al., 2018, 2022; Helm & Motorin, 2017; Machnicka et al., 2013).

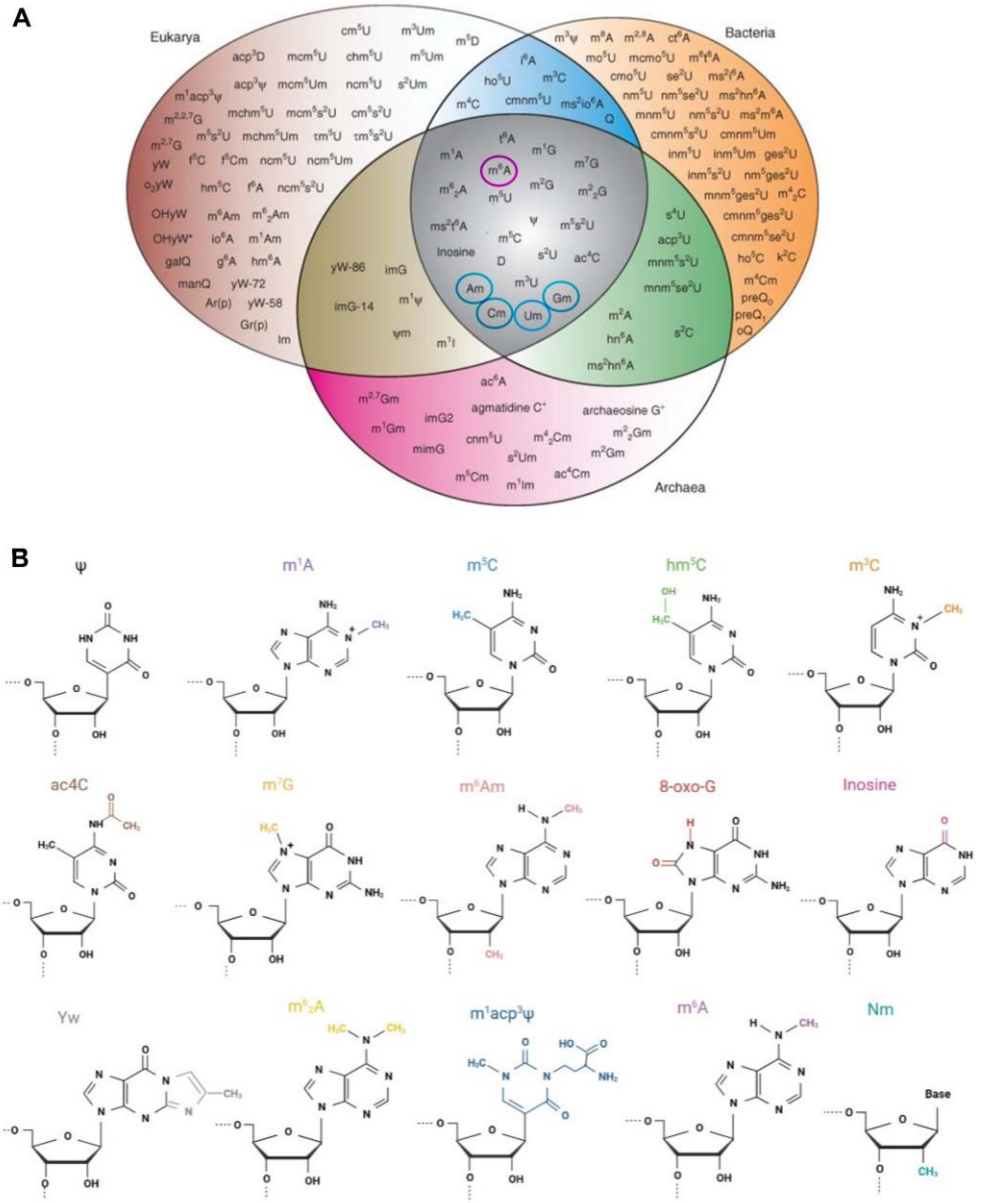

Figure 2. RNA modifications in all kingdom of life.
(A) *Figure adapted from [Motorin (2015), RNA Modifications] showing the modifications detected in the 3 kingdoms of life. N6-methyladenosine (m6A) and 2'O-methylations (Nm) are common of all 3 life domains.*
(B) *Chemical structure of the most relevant RNA modifications of one or more RNA species.*

1.2.1-Main RNA modifications:

Pseudouridine Ψ

Ψ is an isomer of the base uridine, generated by a rotation of uracil and a formation of a new bond between C1 of the ribose and C5 of uracil, instead of the canonical C1-N1 bond(C. T. Yu & Allen, 1959). The C-C bond of Ψ confers more rotational flexibility; moreover, it leaves the N1 of uracil free to establish new hydrogen bonds, increasing RNA stability (Schwartz et al., 2014). Together with 2'O-methylation, Ψ is the most abundant modification on tRNA, rRNA and snRNA, particularly enriched on rRNA, which counts 45 sites in yeast and more than 100 in human (Boccaletto et al., 2018; Piekna-Przybylska et al., 2008; Schwartz et al., 2014). It plays an important role in structural stabilisation and ribosome biogenesis (Garus & Autexier, 2021; Sloan et al., 2017), as well as in translation, as depletion of some Ψ sites from the ribosome peptidyl-transferase centre (PTC) causes translation impairment in yeast with consequences on the growth rate (King et al., 2003).

Most of the modified sites on rRNA depend on a complex whose catalytic subunit, named Dyskerin in human, is guided to its target by H/ACA box snoRNAs, by mean of sequence complementarity (Watkins & Bohnsack, 2012). Dyskerin depletion has been associated with cancer progression (Barbieri & Kouzarides, 2020) and dyskeratosis congenita, a disease characterized by premature aging (Brault et al., 2013).

In tRNA Ψ decorates many sites and it plays a role in tRNA structural stability and translation regulation, as depletion of Pus4, Ψ_{55} writer, leads to a four-fold reduction in $tRNA^{Arg}$ levels in yeast (Copela et al., 2006). tRNA fragments (tRFs), which are implicated in different ways in gene expression regulation, from heterochromatin formation, to post-transcriptional silencing and translation inhibition (Kumar et al., 2016), can be pseudouridylated by Pus7, and thus sequester polyadenylate-binding-protein 1 (PABPC1) to inhibit translation in stem cells (Guzzi et al., 2018). Depletion of Pus7, responsible for this Ψ as well as Ψ_{13} in cytosolic tRNA, has been linked to intellectual disability, microcephaly and aggressive behaviour in human, and these functions are conserved in flies, which upon Pus7 depletion lose Ψ_{13} and exhibit aggressive behaviour (de Brouwer et al., 2018).

Ψ is also involved in tRNA nuclear export, as depletion of the Ψ writer Pus1 causes accumulation of tRNA in the nucleus leading to growth defects in yeast (Hellmuth et al., 2000), and the development of myopathy lactic acidosis sideroblastic anaemia (MLASA) in human (Patton et al., 2005).

Ψ can also regulate splicing. When deposited on the snRNA U2, Ψ is essential for branch point recognition in yeast, and two Ψ sites on U2 are dynamically modulated by snoRNPs and Pus7, to regulate splicing in response to starvation and heat stress, respectively (Y. Lin & Kielkopf, 2008; G. Wu et al., 2011).

Ψ prevalence on mRNA seems to be approximately 0.2-0.7% in mammals (Carlile et al., 2014; Schwartz et al., 2014), although another study identified over 2000 sites on human mRNA (X. Li et al., 2015), ten folds more than previous studies, suggesting a possible underestimation of its abundance. Pus family members, Ψ writers, have their own target and localisation and context specificity, some of them particularly active in the context of stress, like Pus7, whose activation upon heat stress has been linked to increased transcript stability (Carlile et al., 2014; Schwartz et al., 2014).

N1-methyladenosine m^1A

m^1A has the property of carrying a methyl group and a positive charge, which strongly affect RNA structure and RNA-protein interactions (Grosjean et al., 1995). In mRNA, m^1A was initially suggested to decorate the 5' region of the transcript where it would modulate translation (Dominissini et al., 2016; X. Li et al., 2017; Safra et al., 2017), but this was later disproven as it was shown that the identified sites were due to crossreactivity of the m^1A antibody with the Cap structure (Grozhik et al., 2019). The only exception is represented by a mitochondrial mRNA, *ND5*, coding for a component of the respiratory chain and bearing m^1A in its coding sequence, where it affects base pairing with tRNA, leading to ribosome stalling (X. Li et al., 2017).

tRNAs are, on the other hand, highly enriched in m^1A, in particular in position 58, where it is important for stability and translation regulation: absence of m^1A_{58} on the initiator tRNA ($tRNA^{iMet}$) leads to its nuclear degradation in yeast and therefore general translational impairments (Anderson et al., 1998; Kadaba et al., 2004). It has been also associated with weakened response to human immunodeficiency virus type 1 (HIV-1), because tRNAs lacking m^1A can be used by HIV as primer for its replication(Renda et al., 2001).

The enzymes responsible of this modification are highly conserved, Trm61 in yeast (in higher eukaryotes Trmt61A) is the catalytic subunit, and requires its non-catalytic partner Trmt6 for RNA binding (Anderson et al., 1998, 2000; Ozanick et al., 2005). m^1A methyltransferases have been found in Archaea and Eubacteria as well, but in these prokaryotes the non-catalytic subunit is missing, suggesting that it appeared later by duplication of the Trm61 gene (Bujnicki, 2001). Yeast (Anderson et al., 1998) and flies (from this PhD project, data not shown) lacking the catalytic subunit, Trmt61A, die early in development, suggesting that the functions of m^1A_{58} in tRNA stability and translation are conserved. m^1A can be present in other positions

along the tRNA molecule, for example mammalian mitochondrial tRNA bears m^1A_9, which is responsible for the typical cloverleaf folding (Helm et al., 1999; Suzuki et al., 2020; Suzuki & Suzuki, 2014). While this position is methylated by Trmt10C, the same position on cytosolic tRNA is methylated by Trmt10B (Vilardo et al., 2018, 2021).

In addition, this modification is dynamic as its level can fluctuate in response to environmental stimuli (X. Li et al., 2016). It can indeed be removed by the erasers AlkB homolog 1 and 3 (ALKBH1 and ALKBH3) and fat mass and obesity- associated factor (FTO) (Dominissini et al., 2016; X. Li et al., 2016; F. Liu et al., 2016; Wei et al., 2018). Readers have been identified in YTH domain family 1, 2 and 3 (YTHDF1/2/3) and YTH domain containing protein 1 (YTHDC1) (X. Dai et al., 2018).

On rRNA there are two identified sites, in position 645 and 2142 in yeast (Bousquet-Antonelli et al., 2000; Peifer et al., 2013; Sharma et al., 2013) corresponding to human positions 1309 and 3749 (Sharma et al., 2018; Taoka et al., 2018). Loss of m^1A_{645} in yeast is associated with growth defects at low temperatures and impairment in the production of proteins involved in ribosome biogenesis (Bousquet-Antonelli et al., 2000; Sharma et al., 2018), whereas m^1A_{2142} has been found involved in anysomycin and peroxide resistance(Sharma et al., 2013).

5-methylcytosine and 5-hydroxymethylcytosine (m^5C and hm^5C):

m^5C decorates tRNA, rRNAs, lncRNA and mRNAs (Hussain et al., 2013; Khoddami & Cairns, 2013; Squires et al., 2012). On tRNA m^5C is essential to stabilize its structure, achieved through the recruitment of Mg^{2+} (Motorin & Helm, 2010; Tuorto et al., 2012). In human and mice, Nsun2-dependent m^5C is essential to inhibit tRNA cleavage by angiogenin and the subsequent formation of 5' tRNA fragments (tRFs), which lead to the activation of cellular stress pathways, neuronal apoptosis and neurological defects (Blanco et al., 2014), and to increase the sensitivity to 5-fluorouracil in skin cancer cells (Blanco et al., 2016).

In rRNA m^5C has been also implicated in stability and stress response, in particular, Gigova et al. show that lack of m^5C_{2278} and Gm_{2288} in yeast reduces ribosome stability (Gigova et al., 2014), but at the same time, it modulates translation under stress. According to Schosserer et al. loss of this m^5C alters the ribosome structure favouring the recruitment to polysomes of transcripts involved in the oxidative stress response. Loss of the responsible methyltransferase, Nsun5, increases stress tolerance and lifespan in yeast, *C. elegans* and *D. melanogaster* (Schosserer et al., 2015).

The enzymes depositing m^5C are DNMT2 and enzymes of the NSUN family, with only Nsun2 and Nsun6 methylating mRNA (K. E. Bohnsack et al., 2019; Hussain et al., 2013; Selmi et al., 2021). On mRNA, this modification is particularly enriched in the UTR near the translation start site and it has been associated to translation regulation (Selmi et al., 2021; Squires et al., 2012) and nuclear export (Xin Yang et al., 2017). These processes are mediated by the readers Aly/REF (RNA and export factor-binding protein 2), which promotes nuclear export, and YBX1 (Y-box-binding protein 1). YBX1 promotes mRNA stability through the recruitment of ELAV1 to oncogenes in human cancer cells, and Pabpc1a to maternal transcripts in zebrafish embryos, modulating cancer progression and maternal to zigotic transition, respectively (Y. S. Chen et al., 2021). By oxidation of m^5C, hm^5C is generated, and, as for DNA, actors of this reaction are Tet family enzymes (Fu et al., 2014). A relevant study on this modification has shown how in *Drosophila*, which lacks the correspondent modification on DNA, the dTet enzyme generates hm^5C in the coding region of mRNAs to foster their translation in the context of neuronal development (Delatte et al., 2016).

3-methylcytidine and N4-acetylcytidine (m3C and ac4C)

While studies of acetylation on mRNA are quite recent, the identification of acetylated residues on yeast tRNA traces back to the 60s (Zachau et al., 1966). Besides its deposition at the wobble position of $tRNA^{Met}$ in *E. coli* (Ohashi et al., 1972) where it has been suggested to contribute to correct codon reading (Stern & Schulman, 1978), in Eukaryotes it is found only at position 12 of some tRNAs (Kruppa & Zachau, 1972) where it is essential for tRNA stability (Johansson & Byström, 2004).

In rRNA two sites in the small subunit bear an ac^4C in helix 34 and 45, important for translational accuracy in yeast (Chernoff et al., 1996). NAT10 (in yeast Kre33), an ac^4C writer, can acetylate tRNA or rRNA depending on whether it interacts with THUMPD1 (yeast Tan1) or snoRNA U13, respectively (Ito, Akamatsu, et al., 2014; Ito, Horikawa, et al., 2014; Sharma et al., 2015). Loss of rRNA acetylation impaired the late steps of maturation of the 18S rRNA, and therefore ribosome assembly, and has been suggested as one of the reasons behind the onset of laminopathies (Ito, Akamatsu, et al., 2014; Sharma et al., 2015).

m^3C has been found on coding and non-coding RNAs, in particular on tRNA, where it is deposited by METTL2 and METTL6 in mammals (Luang Xu et al., 2017). Mitochondrial tRNAs are instead modified by METTL8, of which depletion impairs translation of components of the respiratory chain, leading to incomplete cortical neurogenesis in mice (Feng Zhang et al., 2023) and poor prognosis in pancreatic cancer patients (Schöller et al., 2021).

About these modifications on mRNA not much is known, although recent studies link cytosine acetylation to mRNA stability and translation efficiency. More specifically, when acetylation occurs within the coding sequence, translation is fostered, whereas when it lays in the 5' region of the transcript, initiation at the canonical Kozak-flanked AUG codon is inhibited and shifted at an upstream sequence (Arango et al., 2018, 2022).

N7-methylguanosine (m^7G)

Known since decades as the mRNA cap, N7-methylguanosine also decorates a plethora of tRNA and rRNA, while its presence on internal position of coding RNAs, is the subject of debate.

m^7G has been found on tRNA from bacteria to eukaryotes, including yeast, plants and animals, but not in Archaea (Alexandrov et al., 2002). Absence of m^7G_{46} in yeast tRNAs leads to growth defects, due to tRNA decay (Alexandrov et al., 2006).

In rRNA, m^7G in position 1575 (m^7G_{1575}) of yeast rRNA and m^7G_{1639} of human rRNA, is deposited only in the nucleus, where it is important for nuclear export of the rRNA, but its writer, the dimer Bud23-Trm112 (WBSCR22-TRMT112 in human), binds to the rRNA from the nucleolus and biogenesis does not proceed if this binding is disrupted or delayed (Létoquart et al., 2014; J. White et al., 2008; Zorbas et al., 2015).

In mRNA, controversial opinions about its prevalence on internal positions have been raised. For example, the development of AlkAniline-Seq led to the identification of very few and possibly false positive internal sites in mRNA (Marchand et al., 2018). On the other hand, other studies, employing chemical or antibody-based methods, were able to map this modification on internal positions, and suggested that is is deposited by METTL1 to modulate translation upon stress (Malbec et al., 2019; L. S. Zhang et al., 2019).

N6-2'O-dimethyladenosine (m^6Am)

m^6Am is the result of the activity of 2 methyltransferases, one depositing a methyl group in position 2 of the ribose, generating a 2'O-me, and a second one, called Phosphorylated CTD-Interacting Factor 1 (PCIF1) (Akichika et al., 2019; Boulias et al., 2019; Sendinc et al., 2019) methylating the base adenosine in position 6. It has been mainly found on the first and sometimes second nucleotides after the cap structure of mRNA and has been proposed to increase mRNA stability (Mauer et al., 2017). However, this finding was not corroborated by other studies, which suggest that m^6Am main function is translation regulation (Akichika et

al., 2019; Sendinc et al., 2019). FTO, previously known as an m^6A eraser, has been found responsible for m^6Am removal as well (Mauer et al., 2017), particularly in response to stress (Akichika et al., 2019).

8-Oxo-7,8-dihydroguanosine (8-oxoG)

8-Oxo-7,8-dihydroguanosine is generated by oxidation of guanosine in presence of reactive oxygen species (ROS) (Yan & Zaher, 2019). This modification is known to interfere with RNA-RNA interactions and translation, causing ribosome stalling (Yan & Zaher, 2019) and the subsequent intervention of no-go-decay (NGD) pathway proteins which degrade the defective mRNA (D'Orazio et al., 2019). Independently of NGD, a specific reader of 8-oxoG, AUF1, binds to and mediates degradation of 8-oxoG bearing transcripts (Ishii et al., 2015), while another reader, Poly-(c)-Binding Protein 1 (PCBP1), binds to two proximal 8-oxoG sites and promotes cellular apoptosis (Ishii et al., 2018), suggesting that higher ROS and therefore higher mRNA oxidation are necessary for its binding.

A-to-I and C-to-U editing

Some modifications do not result from the addition of a chemical group, but from a deamination reaction which converts one base into another. The best known is adenosine to inosine editing, performed by Adenosine Deaminase Acting on RNA (ADAR) enzymes (Bass & Weintraub, 1988; Hogg et al., 2011). This modification is irreversible and can change base pairing, therefore affecting both RNA structure and the decoding ability of the translation machinery (Licht et al., 2019). Decreased ADARs activity has been associated with several cancer types (Hogg et al., 2011). Cytidine to uridine conversion (C-to-U) also affects translation, it has been indeed correlated with altered protein levels of modified transcripts, often due to the introduction of a premature stop codon (Blanc et al., 2014).

Wybutosine (yW)

yW decorates the 3' end of $tRNA^{Phe}$ anticodon in Archaea and Eukarya of a conserved guanosine (G_{37}), to stabilise codon-anticodon pairing during translation, while bacteria have m_1G (Noma et al., 2006; Urbonavičius et al., 2009). This modification is bulky and complex, consisting of a tricyclic guanosine further modified with addition of methyl and amino-carboxy-propyl groups, whose biosynthesis in yeast requires the sequential action of multiple enzymes (Noma et al., 2006). Some organisms, like *Drosophila*, lack this modification, and m_1G, the first step for the production of yW, is effective in codon-anticodon stabilization (Helm & Alfonzo, 2014). In mammals, on the other hand, yW is further modified into other derivatives, like

hydroxy-wybutosine (OHyW) (Urbonavičius et al., 2009), showing a complexity that led to the idea that $tRNA^{Phe}$ yW_{37} and its intermediates shape the "frameshifting potential" to increase codon diversity. Waas et al. proved indeed that frameshifting probability is high when G_{37} is hypomodified, into m^1G_{37} and decreases with intermediates closer to the final product, yW (Helm & Alfonzo, 2014; Waas et al., 2007).

N6-N6-dimethyladenosine ($m^6{}_2A$)

$m^6{}_2A$ is deposited on two adjacent positions of the 18S rRNA, located at the base of the decoding centre (DC), and represent the two most highly conserved rRNA modifications. These correspond in yeast to position 1781 and 1782, and are deposited by Dim1p only in the cytosol, but the presence of the enzyme is required already in the nucleolus for 18S rRNA processing (Lafontaine et al., 1995). The same mechanism has been recently unveiled about the human ortholog of Dim1p, DIMT1L, although in human cells the adenosines A_{1850}/A_{1851} are methylated by DIMT1L in the nucleus and not in the cytosol, still respecting the same sequential order of deposition as in yeast, with DIMT1L-dependent methylations occurring after the WBSCR22-dependent m^7G deposition (Zorbas et al., 2015), suggesting an involvement of these modifications in different rRNA maturation steps. This shows in the two organisms the evolution of unique features, regarding the subcellular localization of the catalytic activity, of an otherwise conserved mechanism, to ensure that only rRNA that will be faithfully modified will reach the mature form.

1-methyl-3-α -amino-α-carboxyl-propyl pseudouridine ($m^1acp^3\psi$)

$m^1acp^3\psi$ is a modification exclusively found on the rRNA of the small ribosomal subunit, at the level of the DC. It is generated by sequential action of distinct enzymes. The first step of this chain is regulated by the H/ACA snoRNP sn35, which converts yeast U_{1191} (corresponding to human U_{1248}) into ψ (Liang et al., 2009), exposing N1 of Uridine for the methylation step that generates $m^1\psi$. This methylation has been suggested to contribute to the 18S rRNA maturation and absence of its writer, Emg1/Nep1, associates with growth defects in yeast and the Bowen-Conradi syndrome, characterised by developmental defects and childhood lethality, in human (Leulliot et al., 2008; B. Meyer et al., 2011; Wurm et al., 2010). While pseudouridylation and N1-methylation occur in the nucleolus, the α-amino-α-carboxypropyl group is added only in the cytosol, independently of the presence of the first two, just before the last 3' cleavage of the 18S rRNA, suggesting that it is important for late ribosome maturation (Brand et al., 1978; B. Meyer et al., 2011). A recent study found in several cancer types, in particular colorectal cancer (CRC), up to 45% reduction of this modification, feature referred to as hypo-$m^1acp^3\psi$. This feature was associated with the production of high levels of ribosomal proteins, maybe as a consequence of increased proliferation rate and ribosome turnover in CRC.

Hypo-$m^1acp^3\Psi$ ribosomes are therefore referred to as “onco-ribosomes”, becoming a potential therapeutic target for colorectal cancer (Babaian et al., 2020).

1.3-m^6A

N6-methyladenosine (m^6A) is the most well characterised mRNA modification. It involves the addition of a methyl group to the nitrogen atom at the 6th position of adenine in the RNA molecule (Fig. 2b). Since its first discovery on mRNA, in 1974 (Desrosiers et al., 1974), thousands of papers have been published. In 2012, Dominissini et al. and Meyer et al. developed an antibody-based approach and parallel sequencing to unveil the human and mouse m^6A landscape, revealing over 12,000 m^6A sites characterized by the consensus sequence RRACH (where R = A/G and H = A/C/U), in more than 10,000 human genes, decorating preferentially long internal exons and the stop codon vicinity (Dominissini et al., 2012; K. D. Meyer et al., 2012). These sites are methylated by a large complex known as Mettl3-Mettl14 complex, or MAC/MACOM (m^6A-METTL complex/m6A-METTL-associated complex). While being well known on mRNA, m^6A also decorates non-coding RNAs, like spliceosomal RNAs, ribosomal RNAs (rRNA), and small and long non-coding RNA, for which the functions and the feature of the responsible methyltransferases have only recently started to be unveiled. The next chapters focus on the description of the well-known Mettl3-Mettl14 complex as well as the other, less known, methyltransferases, with particular focus on Mettl5, a recently identified rRNA methyltransferase, which is one of the main focus of my thesis project.

1.3.1-m^6A on mRNA, lncRNA and sncRNA and its writers

METTL3

The methyltransferase complex responsible for m^6A deposition on mRNA is the METTL3-METTL14 complex comprising seven proteins, with METTL3 and METTL14 being the catalytic core. The complex is conserved from yeast to mammals, with the exception of *S. pombe* and *C. elegans*, suggesting important roles for m^6A on mRNA (Roignant & Soller, 2017).

METTL3 and METTL14 belong to the group of the N6-type MTase enzymes, characterized by a Rossman fold structure, of seven alternating β-strands and α-helices, where the β-strands are linked by hydrogen bonds and flanked by α-helices in an αβα sandwich structure (Iyer et al., 2016; Xiang Wang et al., 2016). The Rossmann-fold bears the [DNSH]PP[YFW] motif which is important for RNA and S-adenosylmethionine (SAM) binding, and therefore for the catalytic transfer of the methyl group from SAM to adenine, although only METTL3 conserved this motif and is therefore the only catalytic component of the complex (Iyer et al., 2016; Xiang Wang et al., 2016). Interestingly, METTL3 can also act independently of its catalytic activity, as it shuffles to the cytosol and directly promotes Cap-independent translation by binding to the 3’UTR and eIF3h,

enhancing translation by ribosome recycling, and thus also promoting oncogenic transformation (Choe et al., 2018).

The other components of the complex are Wilms Tumour Associated Protein (WTAP), VIR-like Methyltransferase Associated (VIRMA/KIAA1429), RNA Binding Motif 15/15B (RBM15/15B), CBLL1/HAKAI and Zinc-finger CCCH-type containing 13 (ZC3H13), each of them influencing different features of the complex. WTAP, the largest protein of the complex, acts as scaffold, bridging the catalytic METTL3-METTL14 core with the rest of the complex, and is essential for its localization to the nuclear speckles, where m^6A influences splicing regulation (Horiuchi et al., 2013; Ping et al., 2014). WTAP binds to VIRMA and RBM15/15B which guide METTL3 methylation to the 3'UTRs and U-rich regions of mRNAs, respectively (J. Liu et al., 2018; Patil et al., 2016). In *Arabidopsis* and in *Drosophila melanogaster*, HAKAI presence in the complex is important for its stabilization and catalytic activity (Bawankar et al., 2021; Růžička et al., 2017), while ZC3H13 binding to WTAP and RBM15/15B participates to m^6A deposition to regulate splicing in mice and flies and sex determination in flies (Knuckles et al., 2018).

m^6A is involved in the regulation of many molecular processes, including splicing, 3'-end processing, nuclear export, translation and stability (Roignant & Soller, 2017; Z. W. Wang et al., 2022). These functions are modulated by factors known as "readers", able to recognise m^6A transcripts and generate a cascade of events regulating to the abovementioned processes. Readers can be divided in direct and indirect according to whether they can specifically recognise and bind m^6A (Z. W. Wang et al., 2022). Direct readers include YTHDC and YTHDF families (Chang et al., 2020; X. Lin et al., 2019; Roignant & Soller, 2017; Roundtree, Luo, et al., 2017; Xiao Wang et al., 2014; W. Xiao et al., 2016).
Indirect readers binding to m^6A transcripts depends on structural changes, caused by m^6A, that expose sequences otherwise hidden (m^6A switch). To this group belong heterogeneous nuclear ribonucleoproteins (hnRNPs) and insulin-like growth factor 2 mRNA-binding proteins (IGF2BPs) (Huilin Huang et al., 2018; N. Liu et al., 2015; Sun et al., 2019). For other readers, like the fragile X mental retardation protein (FMRP) (Edens et al., 2019; Worpenberg et al., 2021; Feiran Zhang et al., 2018) it is not clear whether the binding directly depends on m^6A (S. Wang et al., 2022), although a study from our lab recently showed that fly Fmr1 binds to a consensus sequence independently of m^6A (Worpenberg et al., 2021).

In mammals, members of YTHDF family have been associated to translation regulation and stability in different physiological context, for example YTHDF1 promotes translation in the context of epithelial to mesenchymal transition (EMT) in cancer cells (X. Lin et al., 2019) and YTHDF3 promotes cap-independent translation and has been linked to breast cancer and brain metastasis (Chang et al., 2020). These studies are

divergent to other studies showing that the three mammalian cytosolic readers YTHDF1/2/3 are functionally redundant, in that they all promote mRNA decay to regulate cellular differentiation (Zaccara & Jaffrey, 2020). Future studies might be able to identify new context-specific mechanisms that clarify this discrepancy about their functions.

YTHDF2 was instead unanimously shown to promote mRNA decay (Xiao Wang et al., 2014). The nuclear reader YTHDC1 on the other hand, promotes splicing by interacting with Serine Arginine Rich Factor 3 (SRSF3) and inhibiting SRSF10 (W. Xiao et al., 2016); nuclear export, through the nuclear export receptor NXF1 (Roundtree, Luo, et al., 2017); and alternative polyadenylation (Liutao Chen et al., 2022). Its ortholog in flies, YT521-B, has been associated with splicing regulation in the context of sex determination and X chromosome compensation, as well as neuronal functions (Lence et al., 2016). The reader FMRP has been also linked to neuronal functions, and found impaired in patients with fragile X syndrome, a syndrome with high incidence of autism, caused by defects during neuronal development (Bagni & Zukin, 2019). At a molecular level, it was shown that FMRP binds to m^6A and YTHDF2 to promote mRNA stability (Feiran Zhang et al., 2018), and nuclear export (Edens et al., 2019), or to inhibit translation in flies (Worpenberg et al., 2021).

In mammals m^6A has been shown to be dynamically deposited and removed during development and in response to stimuli, like external stressors (Dominissini et al., 2012; He & He, 2021) and two erasers have been identified: Fat mass and obesity associated protein (FTO) and Alkb homolog 5 (ALKBH5) (Jia et al., 2012; Zheng et al., 2013). FTO can also demethylate m^6Am on mRNA and m^1A on tRNA (Wei et al., 2018) while ALKBH5 exclusively demethylates m^6A. Impaired activity of these enzymes has been linked to metabolic and immune diseases as well as the onset of several cancer types, showing the importance of an efficient plastic regulation of m^6A (He & He, 2021).

METTL3 methylates ncRNAs as well, to modulate their stability, splicing and nuclear export and has been found dysregulated in several cancer types (Shuai Ma et al., 2019). For example, methylated lncRMRP is more stable and leads to the activation of the SMAD2/SMAD3 pathway, promoting non-small cell lung cancer (Yin et al., 2023). Other functions of Mettl3-dependent m^6A deposition on lncRNA involves nuclear accumulation and splicing; for example, m^6A-dependent nuclear accumulation of lncRNA RP11 promotes degradation of ubiquitin ligase mRNAs, and the consequent increase of the protein Zeb1 levels that favours the dissemination of colorectal cancer (CRC) (Y. Wu et al., 2019). The role of m^6A on lncRNA extends to broader functions, like the X-chromosome inactivation, that occurs in female mammals to compensate for the presence of a double X chromosome. For this silencing to occur, an interaction between YTHDC1 and

m^{6}A-decorated lncRNA *Xist* is necessary (Patil et al., 2016). Interestingly, *Xist* is also bound by YTHDF2 in a m^{6}A-dependent manner, to foster its degradation and inhibit metastasis in CRC cells (Xiao Yang et al., 2020). While in the context of gene silencing RBM15/15B proteins are essential for *Xist* methylation, in CRC cells the process depends on Mettl14 (Patil et al., 2016; Xiao Yang et al., 2020), suggesting context-dependent differences in sites selection for *Xist* methylation..

miRNAs also bear m^{6}A which is important for their maturation and in some context with deleterious effects on health. For instance, many miRNAs, of which maturation is promoted by the Mettl3/Mettl14 complex, have been found upregulated in many cancer types in an m^{6}A-dependent manner, like miR-1246 in colorectal cancer (Peng et al., 2019) and *miR-143-3p* in lung cancer (H. Wang et al., 2019).

CircRNAs are generated from back-splicing events and show tissue-specific expression (C. Zhou et al., 2017). Mettl3 deposits m^{6}A on circRNAs to modulate their localization and translation and it is also involved in cancer onset, stress response, and immunity (Y. G. Chen et al., 2019; Y. Yang et al., 2017; C. Zhou et al., 2017). Yang et al. show that m^{6}A on circRNAs can promote cap-independent translation, for which the translation factor eIF4G2 and the m^{6}A reader YTHDF3 are required, particularly upon heat stress (Y. Yang et al., 2017). The reader YTHDF2 modulates their stability in mammalian cells (C. Zhou et al., 2017) and is also involved in the innate immunity, by binding to m^{6}A "self" circRNAs and hence inhibiting RIG-I activity, a receptor that senses foreign nucleic acids (Y. G. Chen et al., 2019). Chen et al. showed that Mettl3 promotes circRNAs expression by methylating repeat elements flanking the circRNAs, and demonstrated that *circ1662*, is involved in CRC invasion and metastasis (C. Chen et al., 2021). Beside regulating circRNAs fate, Mettl3 transcript can actually also generate its own circRNA, named *circMettl3*. circMettl3 overexpression has been associated with inhibition of an oncosuppressor miRNA, *miR-31-5p*, which leads to the overexpression of CDK1 and is positively associated with breast cancer progression (Z. Li et al., 2021).

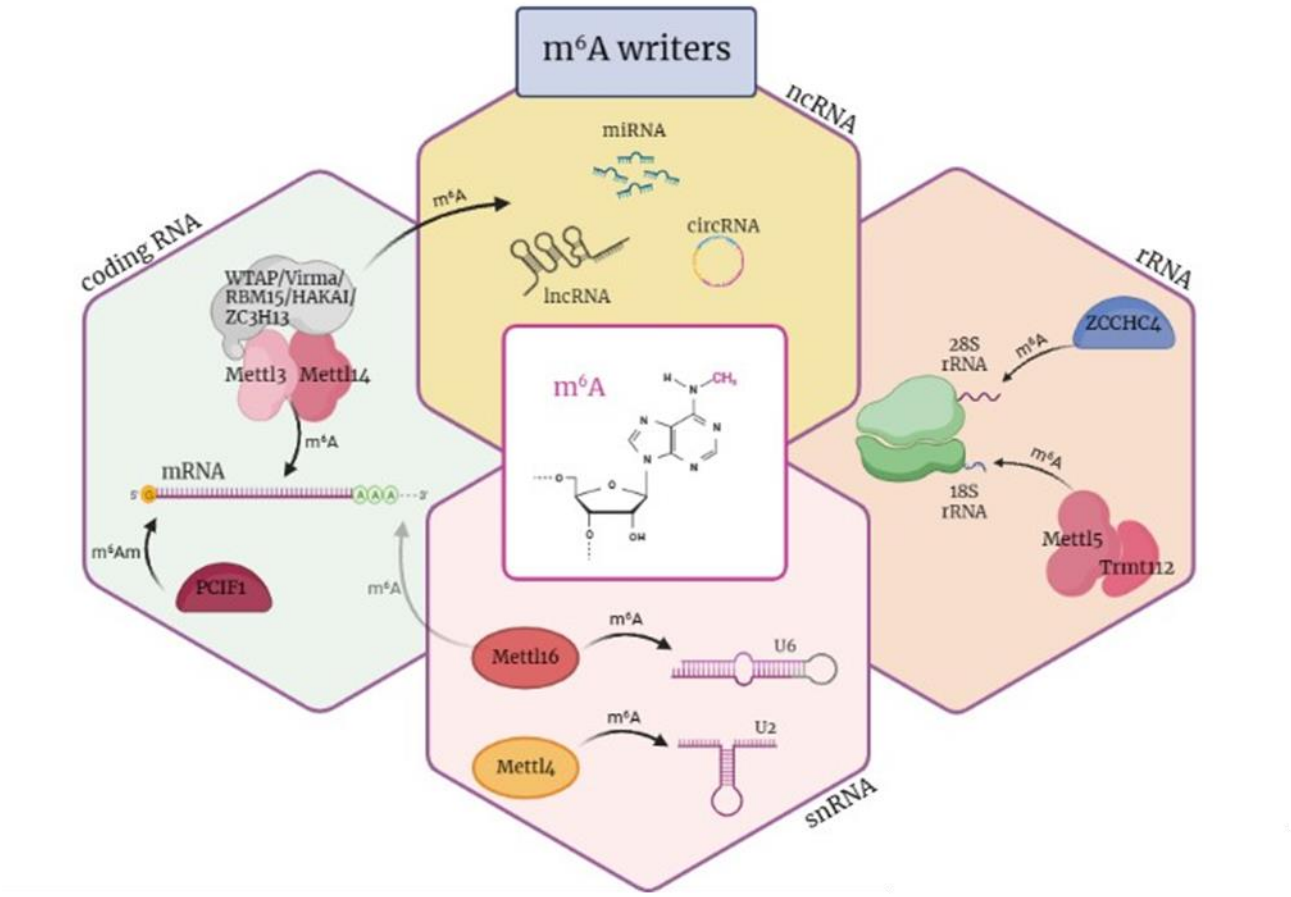

Figure 3. Known m6A writers and their targeted RNA species.

METTL16

METTL16 is another m^{6}A methyltransferase highly conserved from bacteria to eukaryotes (Mendel et al., 2018; Pendleton et al., 2017). Like METTL3, it belongs to class I methyltransferase and is therefore characterized by a catalytic domain containing the conserved [DNSH]PP[YFW] motif (NPPF in this case) shaped in a Rossmann fold structure. Its structure has been published and reviewed by Ruzskwoska et al. as well as other groups (Aoyama et al., 2020; Doxtader et al., 2018; Mendel et al., 2018; Ruszkowska et al., 2018). Differently from METTL3, the catalytic Rossmann fold structure of METTL16 is preceded by a stretch of positively charged amino acids (AA 1 to 78) which accommodates the RNA molecules and guides it into the catalytic core (Aoyama et al., 2020; Doxtader et al., 2018; Mendel et al., 2018; Ruszkowska et al., 2018), and is possibly responsible of the distinct substrate specificity of this enzyme. In addition, METTL16 contains an auto-regulatory K-loop (AA 163–167) which blocks the SAM binding pocket to lower its methylation efficiency (Doxtader et al., 2018).

Beside a self-regulatory function, METTL16 is phosphorylated post-translationally in the context of DNA damage by ATM, in order to reduce its RNA-binding affinity and inhibitory function towards MRE11, key

factor in DNA repair by homologous recombination (HR) (Zeng et al., 2022). These findings suggest the importance of a tight regulation of METTL16 in different contexts and its involvement in essential cellular mechanisms.

The C-terminus of METTL16 is instead important for its homodimerization, although for binding its targets dimerization is dispensable (Ruszkowska et al., 2018). Differently from METTL3, METTL16 binds to the nonamer consensus sequence [UACm^6AGAGAA] when embedded in a complex stem-loop structure (Brown et al., 2016; Warda et al., 2017). The enzyme was shown to bind thousands of coding and non-coding RNAs, yet, until recently its methylation activity was demonstrated solely on two targets: the spliceosomal RNA U6 and the mRNA *Mat2A*, encoding a SAM synthetase (Pendleton et al., 2017; Warda et al., 2017).

The snRNA U6 is methylated by METTL16 in a sequence important for base pairing with the 5' splice site of pre-mRNAs, indicating that it might be regulating the splicing process (Pendleton et al., 2017; Warda et al., 2017). In line with this, a recent study in yeast shows that lack of methylation on the U6 RNA impairs the splicing only of a subset of transcripts (Ishigami et al., 2021), suggesting a context-dependent effect of this methylation on spliceosome functions.

For its second known target, *Mat2A*, METTL16 can directly regulate its splicing in response to the cellular levels of SAM. When SAM levels are high, METTL16 uses SAM as methyl donor to methylate *Mat2A* on a stem-loop structure within its 3'UTR, which leads to intron retention and degradation of *Mat2A*. When SAM levels are low, METTL16 does not methylate the *Mat2A* transcript but lingers on it long enough to recruit the splicing machinery (Mendel et al., 2018; Pendleton et al., 2017). In vertebrates, the C-terminus of METTL16 contains two conserved regions (VCR) (AA 289–562), proven responsible for the recruitment of the splicing machinery on *Mat2A* (Pendleton et al., 2017) and for the binding to U6 snRNA to foster its methylation (Aoyama et al., 2020). Loss of cellular SAM in METTL16 mutant mice has been reported as a cause of massive transcription dysregulation in embryos, which is unfit for development (Mendel et al., 2018), proving the critical role of METTL16 in maintaining cellular SAM homeostasis. Interestingly, invertebrates lack the VCRs to recruit the spliceosome, yet METTL16 ortholog in *C.elegans* (Mendel et al., 2021; Watabe et al., 2021), and *Drosophila melanogaster* (from this study) targets the SAM synthetase transcript and U6, suggesting that different mechanisms might take place in these organisms. Indeed, two recent studies showed that METT-10, the METTL16 ortholog in *C.elegans*, methylates its consensus sequence on the SAM synthetase transcript, which conveniently lies in the 3' AG splicing site of an intron, preventing the binding of the splicing factor U2AF35 to this intron and leading to non-sense mediated decay and overall reduced levels of

SAM synthetase (Mendel et al., 2021; Watabe et al., 2021). These are interesting examples of convergent evolution by which a protein evolved different mechanisms to achieve the same goal.

Another target bound by METTL16 is the long non-coding RNA (lncRNA) metastasis-associated lung adenocarcinoma transcript 1 (MALAT1), which carries the nonamer motif within a complex triple helix structure, and has been implicated in many cancers, especially lung adenocarcinoma (Brown et al., 2016; Goyal et al., 2021; Warda et al., 2017). Interestingly, METTL16 acts as a homodimer to bind MALAT1, but it does not methylate it, suggesting that its functions extend beyond its catalytic activity (Brown et al., 2016; Ruszkowska et al., 2018).

METTL16 has been linked to cancer also through the regulation of an oncosuppressor lncRNA, known as RAB11B-AS1. In hepatocellular carcinoma cells (HCC), METTL16 is overexpressed and methylates RAB11B-AS1, leading to its downregulation and increase in proliferation, migration and invasion of HCC cells, while METTL16 downregulation reinstates RAB11B-AS1 levels and HCC apoptosis and reduces tumour growth *in vivo* (Y. zhang Dai et al., 2022). A recent study by Mikutis et al. could identify many transcripts that are not only bound but methylated by METTL16, in particular near intronic polyadenylation sites (IPA) (Mikutis et al., 2020) which are widely spread in cancers (S. H. Lee et al., 2018), suggesting a role in internal, intronic polyadenylation, and hence splicing (Tian et al., 2007).

While its functions in splicing regulation restricts METTL16 to the nucleus, other non-catalytic functions localise it in the cytosol, where it regulates translation through the interaction with the initiation factor 3a/b (eIF3a/b); interaction that, if impaired, suppresses the proliferating ability of hepatocellular carcinoma (Nance et al., 2020; Su et al., 2022).

In conclusion, despite the plethora of studies showing METTL16 role in SAM homeostasis, development and cancer, there are still many unanswered questions, about the molecular and physiological effects of its activity on the many unmethylated targets, a temporal or cell type-dependent activity during development, as well as the presence of other possible methylated RNAs.

METTL4

Another spliceosomal RNA m^6A writer is **Mettl4**, initially identified in *C. elegans* as adenine N6-methyltransferase on DNA (6mA) (Greer et al., 2015) and later on in mammalian cells, where it positively correlates with the maintenance of a ubiquitin group on histone H2A, a known inhibitory epigenetic mark (Kweon et al., 2019). In recent years, different groups identified Mettl4 as m^6A methyltransferase on Am_{30} of

mammalian U2 spliceosomal RNA, forming m^6Am_{30}, a site located just upstream the branch point recognition site and therefore suggesting a role in the splicing process (H. Chen, Gu, et al., 2020; Goh et al., 2020). As Goh et al found out, depletion of human METTL4 causes exon inclusion of transcripts with weak 3' splice site (Goh et al., 2020). Interestingly, in the same year, the ortholog of human METTL4 in flies, CG14906, was identified as writer for m^6A formation, rather than m^6Am, on U2 snRNA. This m^6A mark has been suggested to play sex-specific functions in splicing modulation as its levels are higher in female flies, and depletion of its writer in *Drosophila* Kc cells, derived from female embryos, led to defects in differentiation and increased proliferation (L. Gu et al., 2020). Interestingly, a hyper-proliferative phenotype was not observed in human cells, perhaps hinting at distinct functions played by m^6A and m^6Am marks. Very recently the *Arabidopsis* ortholog of Mettl4 was identified in the gene At1G19340, as a U2 m^6Am writer, important for the modulation of flowering (Luo et al., 2022). Structural studies show that Mettl4, as the other MT-A70 adenine methyltransferase Mettl3, is characterised by a Rossman fold structured methyltransferase domain and a typical [DSH]PP[YFW] catalytic motif and conserves the same mechanism for SAM binding. Differently from Mettl3, SAM binding is achieved by interaction among its N-, mid, and C-terminal domains, without the need of another partner (Luo et al., 2022).

1.3.2-m^6A on rRNA and its writers

rRNAs are the most abundant RNA species in our cells and are essential part of the ribosome, without which protein synthesis would not be possible. This RNA species is heavily modified, and RNA modifications play an important role for their biogenesis, structural conformations and functions. Despite this, m^6A has been identified only on one residue on the 28S rRNA and on one residue on the 18S rRNA. These modifications are highly conserved, suggesting an important regulatory role, but their functions have not been documented until recently, when the respective methyltransferases have been identified. Their functions mainly involve the regulation of translation, cell proliferation, differentiation and stress response (Ignatova et al., 2020; Liberman et al., 2020; H. Ma et al., 2019; Pinto et al., 2020; Rong et al., 2020; Xing et al., 2020). The first rRNA m^6A writer was identified in *E. coli* in the gene ybiN, responsible for the methylation of adenosine 1618 of the 23S rRNA, which, when impaired, reduced cell growth and fitness (Sergiev et al., 2008). After this, several groups independently identified the methyltransferases responsible for m^6A_{4220} on human 28S rRNA, and for m^6A_{1832} on human 18S rRNA: ZCCHC4 and METTL5, respectively.

ZCCHC4

ZCCHC4 forms m^6A_{4220} on human 28S rRNA. As other known m^6A writers, it is characterized by a Rossmann-fold structure with a DPPF catalytic motif, but flanked in this case in the N-terminus by a GRF and a C2H2 zinc finger domains and in the C-terminus by CCHC zinc finger domains, all contributing to the formation of the

RNA binding surface (H. Ma et al., 2019; Pinto et al., 2020; Ren et al., 2019). Differently from the other known m^6A writers, ZCCHC4 keeps its DPPF motif hidden in the vicinity of a "regulatory loop", which interacts with the so-called "cofactor loop", that hides the SAM binding pocket, suggesting an autoinhibitory conformation for this enzyme (Ren et al., 2019). Moreover, ZCCHC4 target specificity is not determined by the sequence context, but rather by the presence of the stem-loop structure in which A_{4220} resides, as disruption of this structure leads to a 50-fold reduction of m^6A at this position (Ren et al., 2019). Ma et al. suggest that m^6A_{4220} contributes to the stacking between its two adjacent nucleotides, suggesting a role for m^6A in structure stability. To strengthen this, ZCCHC4 KO in HepG2 cells led to a decrease of 60S and of the polysome population and hence impaired translation (H. Ma et al., 2019). ZCCHC4 is located in the nucleolus, suggesting that this modification is deposited early during ribosome biogenesis, yet lack of m^6A_{4220} did not affect rRNA maturation (Pinto et al., 2020). The effect on translation seems to depend on the codon-anticodon interaction strength, with the presence of m^6A_{4220} favouring the enrichment in the ribosome A-site of weak codons (bearing A-T in the first and/or second nucleotide), and a decreased occupancy by strong codons (C-G in the first two nucleotides of the codon) (Pinto et al., 2020).

The lack of ZCCHC4 in HepG2 cells impaired cell proliferation, which is reminiscent of the growth defects found in *E. coli*, and decreased tumour size in a xenograft mouse model. In line with this, ZCCHC4 is overexpressed in hepatocellular carcinoma cells (H. Ma et al., 2019). On the other hand, this effect on proliferation was not observed in the colon cancer cell line HCT116 upon ZCCHC4 KO (Van Tran et al., 2019), suggesting cell type-specific role for this enzyme in translation regulation. Interestingly, in the hepatocarcinoma cell line used by Ma et al., approximately 55% of ribosomes was methylated at position 4220, while in the kidney line HEK293T almost complete methylation was found (H. Ma et al., 2019; Pinto et al., 2020). This is an example of ribosome heterogeneity, which means that ribosomes within a cell differ in their protein and rRNA components to actively steer translation according to the cellular needs (Norris et al., 2021). Another example of m^6A-dependent ribosome heterogeneity has been described in an interesting study, by Liu et al., which reverses the concept of the irreplaceability of $m^6{}_2A$ on the adjacent A_{1850}/A_{1851} sites on human 18S rRNA. Liu et al. show that upon sulfur starvation the highly conserved $m^6{}_2A$ sites on human and yeast rRNA are monomethylated (m^6A) rather than di-methylated, and this change correlates with specific increased translation of sulfur metabolism genes, even with m^6A present at sub-stochiometric levels (K. Liu et al., 2021), showing that ribosomes can actively shape the proteome to adapt to environmental stimuli.

1.4-METTL5

1.4.1-History and structure

The m^6A site on the 18S rRNA was first discovered in 1986 (B. E.H. Maden, 1986), yet the identity of its responsible methyltransferase remained for long elusive. In recent years, independent efforts by different research groups, including ours, have led to the identification of METTL5 as the responsible 18S rRNA methyltransferase in human (Van Tran et al., 2019), *Drosophila* (Leismann et al., 2020), mouse (Ignatova et al., 2020) and *C. elegans* (Liberman et al., 2020). Structural insights of the enzyme has been complicated to achieve since METTL5 is not soluble. However, this problem was solved when by similarity with HVO-1475, the 16S A_{1432} methyltransferase in *Haloferax volcanii*, van Tran et al. decided to co-express METTL5 with the human ortholog of HVO-1475 interactor: TRMT112. TRMT112 is a common cofactor shown to stabilise and modulate the activity of 6 other enzymes (Brūmele et al., 2021). It comprises a central domain composed by 3 α-helices and a terminal domain, which is sometimes referred to as "zinc binding domain" from the zinc binding feature of some eukaryotic Trmt112, lost in the human ortholog. This terminal domain comprises the N- and C- terminal residues of the enzyme, structured to form 4 β-sheets and 1 α-helix. The β-sheets contribute to the interaction with METTL5.

METTL5 is a typical class I SAM-dependent methyltransferase, comprising 7 β-sheet flanked on both sides by α-helices and forming, together with TRMT112, a continuous eleven-stranded β-sheet (Van Tran et al., 2019). The interface between the two enzymes comprises a large surface of hydrophobic residues that are in this way hidden from the hydrophilic cellular environment. These residues are surrounded by polar amino acids from both factors which stabilise the complex by forming hydrogen bonds and salt bridges. This conserved region of the complex comprises many positively charged residues which help bind the RNA, while the SAM binding pocket belongs exclusively to METTL5 (Van Tran et al., 2019).

Comparison with the other known RNA m^6A methyltransferases surprisingly shows not many commonalities, beside the highly conserved [DNSH]PP[YFW] motif (NPPF). Its nucleic acid binding mechanism is instead reminiscent of *Thermus aquaticus* DNA binding Taq I, which binds to a target Adenine extruding from a DNA helix and guides it to the catalytic NPPY motif thanks to Val21 and Phe196. Similarly, METTL5 binds to the extruding A_{1832} and residues Tyr29 and Tyr184 guide it to the NPPF catalytic motif (Van Tran et al., 2019). From crystal structures of several stages of immature 40S subunit, it was pointed out that helix 44, where A_{1832} resides, is rotated outward compared to the mature form of the 40S, probably to expose A_{1832} for METTL5-dependent methylation, which would occur only at later steps of 40S maturation. In line with this, the enzyme has been found both in nucleoli and cytosol in different eukaryotes (Leismann et al., 2020; Van

Tran et al., 2019; Xia et al., 2023) and has been mainly suggested to modulate translation, rather than ribosome biogenesis. Structurally, m^6A_{1832} is located more further apart from Cm_{1703}, compared to *E. coli* and yeasts, which lack Mettl5 and the corresponding m^6A, favouring the positioning of m^6A_{1832} and Cm_{1703} closer to the ribosome P-site to make stronger bonds with the mRNA during translation (H. Chen, Liu, et al., 2020; Rong et al., 2020). This suggests that Mettl5 appeared during evolution to shape the ribosome decoding centre and favour a stronger mRNA bond.

1.4.2-Biological functions of Mettl5

Despite being identified as m^6A writer only four years ago, many studies, including ours, have contributed in shedding light on the functions of this enzyme at a molecular as well as physiological level, and showed its impact in development and disease. Despite the fact that METTL5 is nucleolar in different human cell lines, m^6A_{1832} is dispensable for the regulation of rRNA biogenesis (Ignatova et al., 2020; Leismann et al., 2020; Van Tran et al., 2019). As previously suggested, m^6A_{1832}, at the base of helix h44 and very close to the ribosome decoding centre, plays a role in shaping ribosomal conformations to modulate translation (Rong et al., 2020), globally or restricted to specific transcripts, according to cell type and context (Liberman et al., 2020; Rong et al., 2020; Xing et al., 2020). The effects of m^6A_{1832} on translation affect many cellular processes, from proliferation, differentiation and the stress response, to glucose and lipid metabolism (H. Chen, Liu, et al., 2020; Ignatova et al., 2020; Liberman et al., 2020; Rong et al., 2020; Sepich-Poore et al., 2022; L. Wang et al., 2020; Xia et al., 2023; Xing et al., 2020).

Several studies associated METTL5 loss with decreased proliferation, in particular of pancreatic and hepatocellular cancer cell lines (like HCC-Huh7, HCC-LM3, HepG2) and HEK293T (Hua Huang et al., 2022; Rong et al., 2020; Sepich-Poore et al., 2022; Xia et al., 2023), although other cancer lines grow unaffected by METTL5 absence, like leukaemia, cervical and colon cancer lines (HAP1, HeLa, HCT116 respectively) (Rong et al., 2020; Van Tran et al., 2019), suggesting that some cancers use distinct mechanisms that bypass METTL5 functions for their growth. Mouse embryonic stem cells (mESC) maintain their proliferation and self-renewal potential, but are unable to differentiate, particularly into the neuroectodermal lineage, in absence of Mettl5 (Ignatova et al., 2020; L. Wang et al., 2020; Xing et al., 2020), suggesting an important function for Mettl5 in early development. In particular, it was shown that Mettl5 KO mESCs form smaller embryoid bodies (EB) and fail to complete differentiation, due to reduced global translation, which results in failure in transcription of neuroectodermal and mesodermal markers. These studies further correlate the Mettl5-dependent differentiation defects to compromised development and behaviour in mice. Specifically, Ignatova et al. describe craniofacial abnormality, infertility and hypoactivity of Mettl5 KO mice, suggesting severe developmental impairments (Ignatova et al., 2020; L. Wang et al., 2020). In addition, Wang et al. noticed

smaller size and impaired learning ability of Mettl5 KO mice and suggested that Mettl5 absence affects axon myelination and neurotransmitter transport, which are critical for learning and intelligence (L. Wang et al., 2020). Xing et al., on this same line, observed differentiation defects, although in their case mESCs differentiation potential was compromised, but not completely lost, differently from Ignatova et al.'s study (Xing et al., 2020).

At a molecular level, the absence of Mettl5 in mESCs wires the ribosomes to preferentially translate transcripts rich in G/C, whereas A/T rich codons show reduced ribosome occupancy (Xing et al., 2020). Falling in the latter category, the F-Box and WD Repeat Domain Containing 7 (FBXW7) transcript is downregulated upon Mettl5 KO, and this might explain how Mettl5 fosters embryonic development, as FBXW7 ensures cell differentiation through c-Myc degradation (Xing et al., 2020). Interestingly, two recent studies show a different mechanism, by which Mettl5 correlates with c-Myc stabilization, rather than degradation, to promote proliferation and metastasis of hepatocarcinoma and pancreatic cells and therefore suggest an oncogenic role for METTL5 in these cancer types (Hua Huang et al., 2022; Xia et al., 2023). Xia et al., in particular, show that METTL5 is responsible of the upregulation of the Ubiquitin specific peptidase 5 (USP5), which binds to c-Myc and inhibits its polyubiquitination and degradation by the proteasome (Xia et al., 2023). It is interesting to note that METTL5 functions in shaping the cellular proteome can take opposite outcomes according to the cellular context, promoting differentiation in embryos, but proliferation and growth in some cancer lines. This suggest that METTL5 functions might be further shaped by the presence of other factors or different ribosomal modifications, bringing back the possibility of a ribosomal heterogeneity as a contributor for an oncogenic or developmental role of Mettl5.

Mettl5 has been also associated with the regulation of the stress response, in particular in mouse B16 melanoma cells, where Mettl5 depletion reduces translation of stress response mRNAs, like *Atf4*, transcription factor involved in the Integrated Stress Response (ISR) (H. Chen, Liu, et al., 2020). On the contrary, in *C. elegans* depletion of METL-5, the ortholog of human METTL5, increases lifespan and stress resistance, through the activation of the endoplasmic reticulum unfolded protein response (UPR^{ER}) (Liberman et al., 2020; Rong et al., 2020). Libermann et al. showed that METL-5 methylates A_{1717} on *C.elegans* 18S rRNA and removal of this methylation increases the translation of cytochrome Cyp-29A3, which oxidizes ω3 poly-unsaturated fatty acids eicosapentaenoic acid into eicosanoids, key stress signalling molecules, making *C. elegans* more resistant to Paraquat, heat, cold and UV irradiation (Liberman et al., 2020). Interestingly, eicosanoids are involved in inflammation, immunity and cancer (J. Hu et al., 2018; Kendall & Nicolaou, 2013), suggesting a new link for Mettl5 implications in cancer.

In mouse, a correlation between Mettl5 and lipid metabolism has also been found, with Mettl5 KO mice showing an altered transcriptome leading to impaired lipid metabolism, resulting in smaller mice, not able to produce lipid storage (Sepich-Poore et al., 2022). Though these mice did not show the behavioural defects previously observed by other groups, one main reason for this might be that KO mice were compared to heterozygotes, rather than WT, suggesting that some features might already be altered in heterozygotes (Sepich-Poore et al., 2022). Beside lipid metabolism, METTL5 can promote glucose metabolism through the c-Myc pathway in hepatocarcinoma cells and pancreatic cancer cells, fostering cancer growth and metastatization (Hua Huang et al., 2022; Xia et al., 2023).

1.4.3-Mettl5 and diseases

METTL5 has been defined as an oncogene, since it is found upregulated in several cancer types, particularly hepatocarcinoma and pancreatic cancer, for which METTL5 upregulation is associated to poor prognosis (Hua Huang et al., 2022; Xia et al., 2023). Cancer growth might be promoted by METTL5 through its role in the stabilization of the oncogene c-Myc, or the upregulation of Atf4, which help proliferation and survival under hypoxia and nutrient deficiency, respectively (H. Chen, Liu, et al., 2020; Hua Huang et al., 2022; Xia et al., 2023). Mettl5 has been recently associated with cardiac problems, where its deficiency leads to a transcriptional shift that translates into cardiac remodelling and heart failure in mice. The study shows that Mettl5 modulates cardiomyocytes growth through translational regulation of the chromatin remodeler factor SUZ12, component of the Polycomb repressive complex 2 (PRC2) (Y. Han et al., 2022).

Many studies, including ours, demonstrated an essential role for Mettl5 in nervous system development and functions. Animal studies associated Mettl5 deficiency with a plethora of developmental defects, from craniofacial dysplasia, to hearing and visual problems, to microcephaly and learning impairments in mice, *Zebrafish* and *Drosophila* (Ignatova et al., 2020; Leismann et al., 2020; Richard et al., 2019; L. Wang et al., 2020). This is reminiscent of the phenotype of Mettl5 human patients with autosomal recessive intellectual disability (ARID) (Riazuddin et al., 2017; Richard et al., 2019; Torun et al., 2022), showing a highly conserved and essential function of Mettl5 in ensuring brain functions. Indeed, three variants of METTL5 have been identified in human, that alter its stability or catalytic activity (C344_345delGA, c571_572delAA and c362A>G), and have been associated with intellectual disorders, microcephaly and short stature, poor speech and walking behaviour, aggressivity and craniofacial dysmorphias (Richard et al., 2019; Torun et al., 2022).

All these studies reveal rRNA m^6A as a major player in shaping ribosomes functions. The major developmental defects caused by the absence of this rRNA m^6A can be associated to the category of

"ribosomopathies", developmental ribosome-related diseases, of which known example is diskeratosis congenita, caused by disregulation of the ψ rRNA writer Dyskerin (Orgebin et al., 2020). Major insights into its structure, its role in translation regulation, development, and disease, have emerged in recent years, yet many questions about this enzyme remain unanswered. For example, the only known target of Mettl5 in different species is one single site in rRNA, it remains unclear if Mettl5 catalytic activity extends beyond rRNA, especially considering that from an *in vitro* methylation assay, by Ignatova et al., Mettl5 was able to methylate poly(A)-enriched RNAs (Ignatova et al., 2020). It would be interesting to identify such potential targets and understand whether they conserve structural features that resemble the rRNA helix44 bound by Mettl5. It is also not clear how Mettl5 can cause such different outcomes in translation, cell differentiation, immune response in different cell types or organisms; if there are factors that via direct interaction or indirectly shape Mettl5 functions; and whether Mettl5 activity is regulated by post-translational modifications. It would also be interesting to know whether different functions can be identified between nucleolar and cytosolic Mettl5 and therefore explain why in higher mammals it is exclusively nucleolar. For example, the subcellular localization of Mettl5 might unveil additional functions that do not rely on its catalytic activity. Finally, the findings that both rRNA methyltransferases seem to favour translation of A/T-rich transcripts raises the question of whether rRNA m^6A erasers exist to foster translation of G/C-rich transcripts in particular contexts.

1.5-Mapping methods for m^6A

The main method for m^6A quantification has for long been liquid chromatography-mass spectrometry (LC/MS) based on biophysical features like the retention time of methylated nucleotides in a chromatographic column and their mass/charge ratio. Nevertheless, due to the fact that mass spectrometry requires fragmentation of the oligos into mononucleotides, any sequence information is lost (Thüring et al., 2017). Many efforts to obtain better methods have been put since 2012, when an antibody-based approach was developed by Meyer et al. and Dominissini et al. (Dominissini et al., 2012; K. D. Meyer et al., 2012). Nowadays, beside the antibody-based techniques, there are methods relying on enzymatic or chemical approaches, and direct sequencing. (Table 1)

Table 1. Methods for m^{6}A detection and mapping

	Technique	Advantages	Disadvantages	References
Biophysical	**LC-MS/MS**	absolute quantification can distinguish m6A from m6Am	no sequence context	Thuring et al., 2017
Antibody-based	**MeRIP/m6A-seq**	transcriptome-wide low input material required	ab crossreactivity inability to distinguish m6A from m6Am	Meyer et al., 2012 Dominissini et al., 2012
	miCLIP/PA-m6A-seq	nucleotide resolution transcriptome-wide mapping	high input material complex long protocol	Linder et al., 2015
	m6A-LAIC-seq	characterization of m6A pattern among isoforms	low resolution relative quantification with the use of spike-in	Molinie et al., 2016
	TNT-seq	characterization of m6A pattern in nascent RNA	pretreatment of cells low resolution	Louloupi et al., 2018
	m6ACE-seq	nucleotide resolution, improved by XNR digestion writer/eraser m6A specific sites	high quantity of starting material	Koh et al., 2019
Enzymatic	**MAZTER-seq/m6A-REF-seq**	nucleotide resolution mapping based on MazF inability to digest in presence of m6A	motif dependency, it misses m6A in non ACA motifs	Garcia-Campos et al., 2019;
	DART-seq	nuceotide resolution low input material required	motif dependency, it require a C next to m6A	Zhang et al, 2019b Meyer, 2019
	TRIBE	low input material writer/reader specific methylation landscape	low resolution depending on presence of A for A → I editing near m6A	Worpenberg et al., 2019
	eTAM-seq	low input material nucleotide resolution	inability to distinguish m6A from m6Am inability to deaminate A in structured RNA	Xiao et al., 2023
	m6A-SAC-seq	low input material nucleotide resolution	GA motif preference of Dim enzyme,	Hu et al., 2022
	SCARLET	precision	only site-specific validation long and complicated, use of radioactivity	Liu et al., 2013
	SELECT	simple, fast, radioactivity-free	only site-specific validation	Xiao et al., 2018
Chemical	**GLORI-seq**	nucleotide resolution	limited by successful and specific A deamination	Liu et al., 2022
	m6A-SEAL	high specificity	low resolution no stoichiometric information	Wang et al., 2020b
	m6A-label-seq	nucleotide resolution high specificity	depending on successful incorporation of allylic group, limited by incubation time	Shu et al., 2020
Direct sequencing	**Nanopore**	direct sequencing, no RT-PCR bias nucleotide resolution, low input material	high cost not perfectioned on cellular mRNA	Liu et al., 2020
	SMRT	nucleotide resolution, direct sequencing	high cost, high error rate	Vilfan et al., 2013

Antibody-based methods:

The first studies aiming at mapping m^{6}A transcriptome-wide came from Jaffrey's and Rechavi's laboratories. The two methods, **m6A-seq** (Dominissini et al., 2012) and methylated RNA immunoprecipitation sequencing (**meRIP-seq**) (K. D. Meyer et al., 2012) are both based on immunoprecipitation of fragmented Poly(A) RNAs using an anti-m^{6}A antibody. The fragments generated are 100-200 nt long, which is the resolution of the technique as there is no way to distinguish, within the fragment, methylated from unmethylated adenosines, nor the m^{6}A stoichiometry per fragment. To increase the resolution of the mapping, m^{6}A-individual-nucleotide-resolution crosslinking and immunoprecipitation (**miCLIP**) was developed, adding to the previous protocols an extra step of UV crosslinking at 254 nm which leads to a covalent bond between the antibody and an m^{6}A residue. The following proteinase K digestion degrades all but a small peptide of the antibody

that remains attached to m^{6}A, causing a T-to-C shift during the final PCR of the library preparation, and allowing the identification of the exact methylated site (Linder et al., 2015). On the same line, photo-crosslinking assisted m^{6}A-seq (**PA-m6A-seq**) uses the propensity of 4-thiouridine (4SU) to react to photons to crosslink 4SU close to m^{6}A to anti-m^{6}A antibody at 365 nm (K. Chen et al., 2015). In the same period, m^{6}A-level and isoform characterization sequencing (**m6A-LAIC**) was developed, providing a better understanding of m^{6}A distribution among transcripts isoforms, due to the absence of the fragmentation step (Molinie et al., 2016). Despite losing in resolution, this method allowed to distinguish the methylation on specific isoforms of the same gene, associating methylated isoforms with the usage of proximal alternative adenylation sites (APA) (Molinie et al., 2016). More recently, transient-N6-methyladenosine-transcriptome sequencing (**TNT-seq**) has linked early m^{6}A deposition with splicing kinetics regulation. In particular, m^{6}A deposited co-transcriptionally near splice junctions accelerate splicing, while m^{6}A within introns slows it down or leads to exon inclusion and therefore regulate alternative splicing. This method captures early deposited m^{6}A because it adds a bromouridine (BrU) IP before the m^{6}A IP, to isolate nascent RNA (Louloupi et al., 2018). m^{6}A-Crosslinking-Exonuclease-sequencing (**m6ACE-seq**) still relies on the use of antibodies following a crosslinking step like for miCLIP protocol, but the IP is followed in this case with a digestion by the 5' exonuclease XRN1 which selectively stops when it encounters a m^{6}A site, improving the resolution of the method (Koh et al., 2019).

Enzymatic methods:

To overcome the limitations of the antibody-based methods, being the need of a large input material and the irreproducibility due to cross-reactivity of the antibody with other modifications, techniques relying on enzymatic activity have been developed. For example, **MAZTER-seq** and m^{6}A-Sensitive-RNA-Endonuclease-Facilitated sequencing (**m^{6}A-REF-seq**) rely on the activity of the *E. coli* toxin and endonuclease MazF, which specifically digests ACA motifs but not m^{6}ACA motifs, providing specificity and reducing the need of a large input material. On the other hand this techniques limits the identification of the m^{6}A sites to only 15-25% of them due to the dependency on a single specific motif (Garcia-Campos et al., 2019; Z. Zhang et al., 2019).

Another interesting method, developed by Kate Meyer, is based on the use of the cytidine deaminase APOBEC1 fused to an m^{6}A-binding YTH motif, to induce specific C-to-U mutations in sites next to m^{6}A which will be detected by standard RNA-seq. The method, known as Deamynation-adjacent-to-RNA-modification Target followed by sequencing (**DART-seq**), does not require fragmentation, providing info about m^{6}A distribution along the whole transcript, but loses sensitivity as it will not capture m^{6}A in non DRACH motif, due to the potential absence of citydine in the vicinity (K. D. Meyer, 2019). On the same line, Targets of RNA-bindng proteins Identified by Editing (**TRIBE**) has been used to map m^{6}A by fusing the RNA binding domain of

m^6A readers and writers with the catalytic domain of ADAR, obtaining deaminated adenosines in the vicinity of m^6A reader/writer binding sites (Worpenberg et al., 2019). An improved protocol based on deamination is evolved-TadA-assisted N6-methyladenosine sequencing (**eTAM-seq**), which relies on *E. coli* deaminase TadA, acting with high precision on unmethylated adenosines for a A-to-I conversion, allowing high resolution and a clear distinction between m^6A and A, read by reverse transcriptase as A and G, respectively (Y. L. Xiao et al., 2023). This method provides the precision missing in the DART-seq and TRIBE approaches, and it dramatically reduces the amount of required starting material. As limitations, deamination is not efficient for highly structured RNA, and the presence of $m^6{}_2A$ can mislead in the interpretations of the final results. Another method based on the high mutation rate caused by reverse transcriptase is m^6A-Selective Allyl Chemical-labelling and sequencing (**m6A-SAC-seq**), which makes use of the dimethyl-transferase of the Dim1/KsgA family. This enzyme in presence of an allylic SAM edits m^6A into N6-allyl, N6-methyl Adenosine (a6m6A), and A into N6-allyl Adenosine (a^6A), which get then cyclized in a following step. The method makes then use of HIV1 RT which induces tenfold higher mutation rate at cyclized a^6m^6A residues than at the unmethylated adenosine. One limitation of this method is that the Dim1 enzyme shows activity preferentially towards GA motifs, leaving other m^6A sites uncovered.Yet, as little as 30ng of poly(A) or ribodepleted RNA is sufficient to provide reliable quantitative information on m^6A distribution (L. Hu et al., 2022).

An enzymatic method used to validate the methylation status of a specific target is site-specific cleavage and radioactive-labelling followed by ligation-assisted extraction and TLC (**SCARLET**) (N. Liu et al., 2013). This method measures the m^6A status of a specific target RNA, which is first cleaved at a 5'site flanking the potential methylated adenosine by RNaseH, with the use of a complementary guide RNA. The cleaved site is then radiolabelled with 32P and ligated to a DNA oligo. The following step involves RNase T1/A treatment, which just leaves the nucleotide attached to the DNA oligo intact. This oligo is then gel extracted, digested into mononucleotides with nuclease P1 and the m^6A status analysed via thin-layer chromatography. A simpler method developed to validate individual sites at high resolution, which is faster and avoids the use of radioactivity, is single-base elongation and ligation-based qPCR amplification (**SELECT**). This method uses one oligo complementary to a region upstream and one downstream of the target adenosine, and is based on elongation of these oligos by Bst, followed by their splint ligation, to quantify the m^6A level at that site. Given that m^6A hinders both the elongation and ligation steps, m^6A levels are then measurable by qPCR in comparison with the qPCR results of a control, unmethylated site, in the same target RNA (Y. Xiao et al., 2018).

Chemical methods:

Glyoxial and nitrite-mediated deamination of unmethylated Adenosine (**GLORI-seq**), like eTAM-seq, is based on unmethylated adenosine deamination. In this case the deamination is achieved chemically, using nitrous acid to induce deamination, and glyoxal to protect guanosine during the deamination reaction, as guanosine is the most sensitive base to nitrous acid-dependent deamination (C. Liu et al., 2023). Another chemical method makes use of FTO ability to oxidise m^6A into hydroxy-m^6A (hm^6A) which can be stabilised by the addition of dithiothreitol (DTT) converting hm^6A into a more stable N6-dithiolsitolmethyladenosine (dm^6A). This method, called FTO-assisted m^6A selective chemical labelling method (**m^6A-SEAL**), is followed by biotin labelling and enrichment of m^6A fragments via streptavidin pulldown prior to sequencing (Y. Wang et al., 2020). A simpler labelling method, termed **m^6A-label-seq**, involves feeding cells with a methionine analog, Se-allyl-l-selenohomocysteine, so that the methyltransferase cofactor SAM carries an allylic group rather than a methyl group, leading to the formation of allyl-N6-A (a^6A) in place of m^6A. The subsequent iodine-mediated cyclisation of a^6A leads to a high A-to-T/G/C mutation rate during reverse transcription which allows to map with base precision the exact location of the m^6A site (Shu et al., 2020). Being dependent on the incorporation of the allyic group, the detection of all potential m^6A sites strongly depends on the labelling efficiency and incubation period.

Direct sequencing:

All of the above-mentioned methods have in common the fact that the detection of the modification happens after library preparation which involves reverse transcription and PCR amplification and therefore relies on some signature/modification happening during these steps to be able to detect m^6A at nucleotide resolution. More recent technological advances have made possible the direct sequencing of DNA and RNA molecules thanks to the development of the Nanopore sequencers by Oxford Nanopore technologies (ONT). Nanopore sequencers comprise hundreds of pores which carry out the sequencing in parallel of individual molecules passing through them via electrophoresis, and generating unique changes in the applied current, known as “squiggles”, which allow sequencing and RNA modifications prediction (Liu Xu & Seki, 2020). This involves training an algorithm to recognise the specific squiggle caused by the modification of interest. While theoretically it is the best way to directly detect modifications, false positives are common, and the method still needs improvements. A similar direct sequencing approach to map m^6A is single-molecule, real-time (**SMRT**), which is mainly based on photon detection during the reverse transcription process (Vilfan et al., 2013). The dNTPs are associated to fluorophores and the frequency of fluorescence pulses released during the RT step can be monitored. Since the kinetics of the DNA polymerase is influenced by the m^6A presence and RNA structure, specific changes in the pulses are indicative of these specific features.

1.6-Nm

Ribose 2'O-methylation (Nm or 2'O-me) represents the most abundant RNA modification on ncRNA, especially on rRNA and tRNA, where it was firstly identified in the 60's (Baskin & Dekker, 1967), but it is also found on other ncRNAs, such as small nuclear RNA (snRNA), small nucleolar RNA (snoRNA), microRNA (miRNA), short interfering RNA (siRNA) and Piwi-interacting RNA (piRNA) (Borges & Martienssen, 2015; J. Gu et al., 1996; Ji & Chen, 2012; Krogh et al., 2017; Y. T. Yu et al., 1998). In more recent years, it has been identified on coding RNA as well (Bartoli et al., 2018; Kuge et al., 1998).

This modification consists of a methyl group added on the position 2'-OH of the ribose, and it can be found in all four nucleotides in organisms from all three life domains (Fig. 2) (Sloan et al., 2017). Structurally, Nm has been shown to stabilise RNA into the 3' endo conformation, typical of A-type RNA chain. Chemically, it reduces the nucleophilic nature of the 2'-OH group, increasing RNA resistance to alkaline hydrolysis and enzymatic cleavage (Prusiner et al., 1974), a feature that has been exploited for the development of mapping methodologies (see chapter 1.4.5). Recent years have also witnessed the discovery and characterization of its writers. To date, two distinct classes of Nm methyltransferases are known: stand-alone protein enzymes and a ribonucleoprotein complex containing the catalytic subunit **Fibrillarin** and snoRNAs (**sno(s)RNPs**). The specificity of this complex is provided by base pairing of the snoRNAs with the target RNA. This complex is responsible for almost all Nm sites on rRNA (Erales et al., 2017; Krogh et al., 2016; Sharma et al., 2017; Taoka et al., 2018). The other class of Nm writers comprises different enzymes with distinct specificities, which are incompletely understood.

Human Cap methyltransferases 1 and 2 (**CMTr1** and **CMTr2**) are responsible for methylation of mRNA cap1 and cap2, respectively; TAR binding protein 1 (**TARBP1**, or **Trm3**), tRNA methyltransferases 7, 13 and 44 (**TRMT7**, also known as **FTSJ1**; **TRMT13** and **TRMT44**) are tRNA methyltransferases; FTSJ RNA 2'O-methyltransferase 3 (**FTSJ3**) methylates rRNA; mitochondrial RNA methyltransferases 1, 2 and 3 (**MRM1; MRM2**, also known as **FTSJ2**; and **MRM3**) methylate mitochondrial rRNA (mt-rRNA); and HUA enhancer 1 (**HEN1**) methylates small non-coding RNAs (sncRNAs) (Fig. 4).

The second part of my PhD aimed at understanding the functions of Nm methyltransferases, for several of which *Drosophila* mutant lines have been generated, with particular focus on the characterization of 2 novel, unknown, tRNA writers, called **Mettl25** and **Mettl25b**, which are described in Chapter 4.

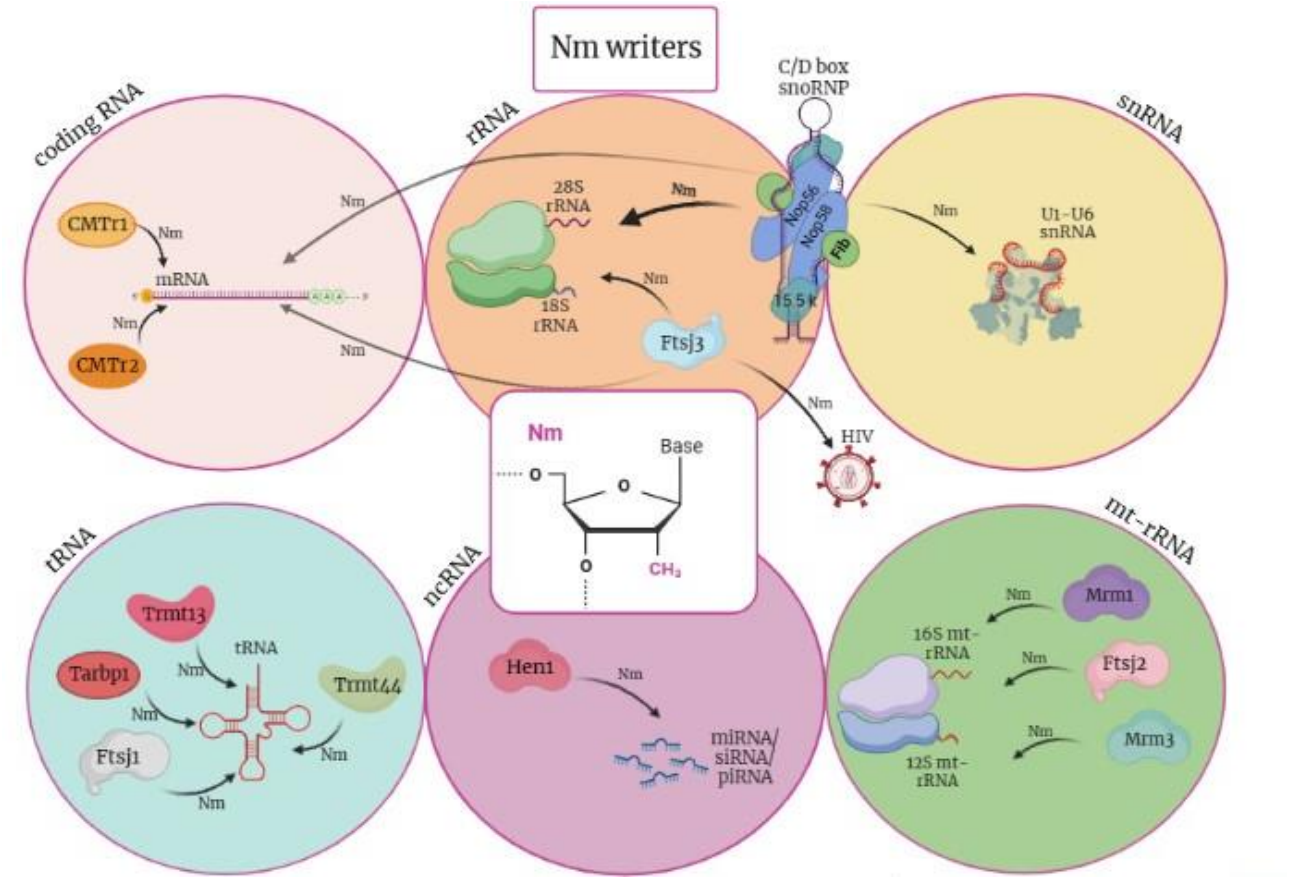

Figure 4. Known Nm writers and their target RNA species.

1.6.1-Nm on rRNA and its writers

rRNA is the most enriched RNA species that contains this modification. Human bears over 100 Nm sites (Sloan et al., 2017). The vast majority of these sites gets methylated co-transcriptionally, especially on the 18S rRNA, suggesting the importance of many Nm sites in early steps of rRNA maturation. Nevertheless, in human several sites are methylated at later stages, made accessible to the writer machinery by the RNA helicase DDX21 (Koš & Tollervey, 2010; Sloan et al., 2015). Beside a role in rRNA biogenesis, Nm also confers resistance to thiostrepton in *Streptomyces azureus*, an antibiotic which binds to the 23S rRNA and inhibits protein synthesis. Am_{1067} on the 23S rRNA recruits protein L11 to the ribosome, preventing thiostrepton binding (Thompson et al., 1982).

Multiple studies have demonstrated an essential role for Nm in protein synthesis. For example, the depletion of Nm on rRNA leads to embryonic lethality in zebrafish and inhibition of translation and ribosome assembly in yeast and bacteria, with consequences on cell growth, while over-methylation has been associated to leukemogenesis in mammals (Arai et al., 2015; Baudin-baillieu et al., 2009; Higa-Nakamine et al., 2012; F. Zhou et al., 2017). Consistently, it is not surprising that Nm sites cluster at the ribosome functional sites, like

the decoding centre (DC), the peptidyl transferase centre (PTC), tRNA binding sites and the interface between the small and large subunits. Depletion of a subset of Nm from the DC was found to affect reading frame maintenance and correct translation termination (Baudin-baillieu et al., 2009; Sloan et al., 2017).

Recent findings show a high diversity of Nm levels on different rRNAs according to the site, tissue, and upon different stimuli, suggesting that Nm is a plastic modification that generates ribosome heterogeneity to accommodate the translational needs of the cell (Buchhaupt et al., 2014; Erales et al., 2017; Krogh et al., 2016). For example, different cancer cell types showed distinct Nm patterns with a core of constitutive Nm sites, and many partially methylated and variable Nm sites (Krogh et al., 2016), the latter probably fulfilling regulatory functions. Erales et al. show how the KD of Fibrillarin, the main rRNA Nm writer, leads in human cells to a global reduction of Nm, impairing ribosome biogenesis, but leaving unaffected the Nm sites in the vicinity of the peptidyl transferase centre (PTC) (Erales et al., 2017), hinting that some sites are more protected than others. Among the less protected, fractionally methylated sites, in human rRNA there is Cm_{174}, of which methylation increases upon upregulation of the oncogene Myc. Higher Cm_{174} levels result in impaired translation of AU-rich transcripts, and increased translation of GC-rich transcripts (Jansson et al., 2021). A context-dependent Nm variability is also observed in *Drosophila melanogaster,* when upon stress, mild but very specific changes in Nm levels were detected. These changes were different, according to the type of stress that flies were subjected to (Sklias et al., 2024), suggesting that a minor change in Nm pattern on rRNA might be enough for the translational specialization of ribosomes to achieve the desired response.

To maintain a tight regulation of Nm levels on rRNA different mechanisms are involved. For example, upon inflammation, in mouse and human, macrophages secrete extracellular vesicles containing C/D box snoRNAs which stimulate distant recipient cells to increase Nm levels at specific sites (Rimer et al., 2018).

In bacteria, on the other hand, only standalone enzymes methylate rRNA, each having its own specific site. An interesting study from Prof. Dr. Suzuki lab, provides structural insight into how depletion of one Nm writer, responsible for the methylation of a single rRNA site, Um_{2552}, seriously affects ribosome assembly in *E. coli,* leading to the accumulation of the 50S precursor, 45S, and impairing cell growth (Arai et al., 2015). According to the study, removal of the Um_{2552} writer, *RlmE*, impeded the Um_{2552}-mediated stabilisation of helices 92 and 71, resulting in impaired incorporation of ribosomal protein L36 in the ribosome (Arai et al., 2015).

Nm deposition is further modulated in Eukaryotes by auxiliary proteins or RNAs which promote or inhibit methylation at specific sites. Fragile-X Mental Retardation protein (FMRP), for example, binds to and affects

several snoRNAs in the nucleus of human embryonic stem cells, shaping the rRNA methylome, only affecting sites that are partially methylated, with no impact on the constitutive, fully methylated sites (D'Souza et al., 2018).

Small Cajal body-specific RNAs (scaRNAs) can also modulate Nm levels. For example, *scaRNA17* gets processed into smaller fragments and becomes part of a complex referred to as regulatory RNP (regRNP) which negatively influences the Nm level of 18S A_{484} as well as C_{62} of U6 snRNA (Burke et al., 2018; Poole et al., 2017), suggesting a regulatory role for scaRNA-derived fragments in both translation and splicing, through modulation of 2'O-methylation levels.

Fibrillarin

The **snoRNP/Fibrillarin** complex is guided to the rRNA by snoRNAs, which carry an antisense element complementary to the rRNA target sequence (Kiss-László et al., 1996). These box C/D short nucleolar RNAs (<100 nt long) are spliced out as part of an intron of a host gene, and, as their name suggests, contain specific motifs known as box C [RUGAUGA] and box D [CUGA], which interact with each other to form a kink-turn conformation that is bound by the proteins of the complex. While box C and D occupy the extremities of the snoRNA, a box C' and a box D' motifs occupy the middle of the molecule, to form a kink-loop conformation. Each snoRNA can in principle recognise two targets, as it contains two 9-10 nt long substrate recognition sequences (SRS) (Lapinaite et al., 2013; Z. Yang et al., 2016), but binds to them with different efficiency (Graziadei et al., 2016).

In Archaea the complex comprises two molecules of Fibrillarin, Nop5 and L7Ae, with Nop5 dimer acting as scaffold for the other two proteins and the C/D box motifs. The Eukaryotic complex, on the other hand, contains Fibrillarin, Snu13 (15.5k in human; ortholog of Archaea L7Ae), and Nop56/Nop58 heterodimer, which are paralogs of Nop5, and show binding specificity for both box C/D (bound by Nop58) and box C´/D´ (bound by Nop56), (Z. Yang et al., 2020). Fibrillarin is the catalytic subunit of the complex. It is a SAM-dependent methyltransferase, and can methylate both rRNA and proteins, as it methylates Histone H2A at rDNA loci to modulate rRNA transcription (Tessarz et al., 2014). The methyltransferase domain occupies the C-terminus and comprises a seven-stranded β-sheet flanked by three α-helices on both sides, typical of most methyltransferases. The C-terminus also includes the RNA-binding domain. In most Eukaryotes, the N-terminus comprises a glycine and arginine-rich domain (GAR) which is essential for its nucleolar localisation (Shubina et al., 2016).

Given the essential role of Nm in ribosome biogenesis and translation regulation, defects in the snoRNP machinery have been linked to reduced ribosomes in human cells and yeast as well as reduced efficiency of IRES-dependent translation (Erales et al., 2017). Dysregulation of Nm levels has been also associated to a plethora of cancer types, as many snoRNAs have been classified as oncosnoRNAs for their role in increasing translation and promoting cell cycle progression, although there are also snoRNAs acting as oncosuppressors (Barros-Silva et al., 2021). Fibrillarin, indeed, has been widely used as therapeutic target in chemotherapies (El Hassouni et al., 2018).

Fibrillarin also methylates small nuclear RNAs (U1 to U6) on several sites to increase base-stacking and hence RNA stability (M. T. Bohnsack & Sloan, 2018), and impairment of these methylations compromises splicing. For example, loss of Nm on U6 snRNA has been implicated in alterations of the splicing pattern typical of the Alazami syndrome, a developmental disorder characterized by dwarfism, mental disabilities and facial dysmorphies (Alazami et al., 2012; Hasler et al., 2020).

Interestingly, METTL3-mediated m^6A has been found on box D or D´, where it modulates snoRNA structure impeding 15.5k binding in human (L. Huang et al., 2017), suggesting that METTL3 might play a role in the regulation of Nm deposition.

FTSJ3

Ftsj/Rrmj is a bacterial SAM-dependent rRNA methyltransferase, essential for ribosome biogenesis and cell growth under normal as well as heat stress conditions. Its N-terminus bears a typical SAM-dependent catalytic domain, comprising a seven-stranded β-sheet layer and five α-helices, which show a high degree of conservation in Eukaryotes (Bügl et al., 2000). Eukaryotes developed three paralogs from this gene, which mainly differ by the length and properties of their C-terminal domain. While FTSJ1 and FTSJ2 differ from their bacterial ancestor in their target specificity and subcellular localization, the third paralog, FTSJ3, maintained the function of the bacterial ortholog. It is indeed a rRNA methyltransferase. While maintaining similarities with the N-terminus of its ortholog in *E. coli*, the C-terminus of the Eukaryotic enzyme acquired a Spb domain, which is responsible of the interaction with the pre-ribosome complex, while the central domain, DUF3381, is uncharacterized (Simabuco et al., 2012).

Interesting studies in yeast show the importance of some Ftsj3-dependent Nm sites in ribosome biogenesis and nuclear export. The yeast ortholog of FTSJ3, Spb1, methylates residue G_{2922} in the ribosome A-loop at a late maturation step, but it also methylates U_{2921} in absence of the snoRNA snR52 (Lapeyre & Purushothaman, 2004). During ribosome biogenesis, Um_{2921} is methylated on the early 35S precursor, while

Spb1 comes into play only when reached the 27S stage, suggesting that Spb1-mediated methylation works as check point to proceed for further maturation; its absence causes growth defects and impaired biogenesis in yeast (Kressler et al., 1999; Lapeyre & Purushothaman, 2004; Pintard et al., 2000). A recent study shows that Gm_{2922} inhibits Nog2 GTPase activity, important for ribosome export. Structural changes, occurring only in an advanced ribosome maturation stage, stop the inhibitory effect of Gm_{2922} on Nog2, allowing ribosome export. In absence of this methyl group, water molecules are coordinated to form hydrogen bonds between G_{2922}, Alf4 and Nog2, stimulating Nog2 GTPase activity and release from the pre-60S subunit, and fostering a premature binding by export factor Nmn3 (Sekulski et al., 2023).

In human cells, FTSJ3 is recruited to the pre-rRNA and is essential for processing and maturation of the 18S rRNA, via interactions with NIP7, which dissociate from pre-rRNA as it completes its maturation. FTSJ3 depletion has been associated with impaired cell proliferation and accumulation of the 34S pre-rRNA (Morello et al., 2011).

FTSJ3 seems to also play a role in breast cancer growth (Manning et al., 2020) and in the immune response. A study from Ringeard et al. shows how FTSJ3 is hijacked by the human immunodeficiency virus (HIV) in mammalian cells to get its genome methylated, preventing interferon (IFN) production by the host dendritic cells (Ringeard et al., 2019). Degradation of HIV RNA is carried out by Interferon-stimulated gene 20kDa protein (ISG20), of which antiviral activity is blocked in presence of Nm on the viral genome, due to a steric hindrance caused by the methyl group (El Kazzi et al., 2023).

Besides its specificity towards rRNA, recent studies suggest a more diverse target repertoire, including ncRNAs and mRNA (Bartoli et al., 2018), hinting that knowledge about its functions is yet at its infancy.

MRM1, FTSJ2, MRM3

Mitochondrial rRNA (mt-rRNA) methylation regulates ribosome assembly and stability to ensure correct translation of mitochondrial transcripts. One of the enzymes responsible for mt-rRNA methylation is **Mrm2** (yeast), also known as **FTSJ2** (human), ortholog of *E. coli* Ftsj/Rrmj, the rRNA methyltransferase responsible for ribosome stability, particularly under heat stress conditions (Caldas et al., 2000; Rorbacha et al., 2014). FTSJ2 belongs to the FtsJ-like methyltransferase family. The other 2 mt-rRNA Nm writers, **Mrm1** and **Mrm3**, belong to the SpoU methyltransferase family, structurally characterised by a deep threefoil knot (Rorbacha et al., 2014). Human Mrm1 methylates G_{1145} to stabilise the 16S rRNA (K. W. Lee & Bogenhagen, 2014). FTSJ2 and Mrm3 methylate the adjacent residues U_{1369} and G_{1370}, respectively, on the 16S rRNA A-loop, part of the PTC, modulating ribosome assembly and translation, and having therefore an impact on the mitochondrial

respiratory chain (Rorbacha et al., 2014). FTSJ2 is probably the most known among the 3 mitochondrial enzymes. From its bacterial ortholog, human FTSJ2 inherited the sequence and structure of its catalytic centre, as well as the property of heat shock protein as it was found overexpressed upon heat stress in mammals. In rhabdomyosarcoma cells it acts as onco-suppressor, inhibiting cell invasion and migration (Lai et al., 2014). The protein is also conserved in lower Eukaryotes, where it maintained its heat shock properties and methyltransferase functions. Yeast lacking the enzyme are thermosensitive, suggesting that Mrm2 might induce ribosomal conformational changes to adapt to heat stress (Pintard, Bujnicki, et al., 2002). In *Drosophila*, the impaired mitochondrial ribosome biogenesis and translation due to lack of Ftsj2 lead to developmental arrest at the larval stage, with the few flies reaching eclosion not able to complete it or dying immobilised on the food due to weakness (Rebelo-Guiomar et al., 2022).

1.6.2-Nm on small non-coding RNAs and its writers

Nm has been reported at the 3' position of miRNAs and piRNAs where it protects them from the action of 3'→5' exonucleases (Y. Huang et al., 2009). snRNAs also bear Nm, mainly added in the Cajal Body where scaRNAs determine the residue to be methylated. Similar to snoRNAs, these scaRNA contain a C/D box sequence. In addition, they bear a UG-rich motif which is responsible for the Cajal Body localization (Meier, 2017), through the action of the protein TDP-43. This ensures Nm deposition on U1 and U2 snRNAs (Izumikawa et al., 2019), contributing to the fine-tuning of the splicing process. An unmethylated *U2* spliceosomal RNA has been indeed linked to impaired splicing in *Xenopus*, while Nm deposition at the level of a cryptic branch point of a pre-mRNA can also alter its splicing pattern (Ge et al., 2010; Y. T. Yu et al., 1998).

HEN1

Almost twenty years ago, an enzyme methylating the 3'-end of small RNA species was identified in *Arabidopsis thaliana* in the protein HUA ENHANCER 1 (HEN1), and suggested to be involved in miRNAs and siRNAs stability (Bin Yu et al., 2005; J. Li et al., 2005). Afterwards, the orthologs in other animals and flies, as well as bacteria, were identified. *Drosophila* piRNA methyltransferase (Pimet)/Hen1 methylates the 3' terminal ribose of siRNAs and piRNAs, which inhibit the expression of genes and retrotransposons in somatic and germ cells, respectively (Horwich et al., 2007; Saito et al., 2007). This methylation determines the length and stability of siRNAs and piRNAs, by preventing 3'-polyuridylation, and in turn protects them from 3'→5' exonuclease (Horwich et al., 2007). A more recent study associates Hen1-dependent stabilization of miRNAs to aging and neurodegeneration in *Drosophila*. In particular, a correlation was shown between increase in Nm in miRNAs and their loading into Ago2, but not Ago1, during aging. Loss of Hen1 causes destabilization of Ago2-loaded miRNAs, which in turn reduces the lifespan and cause neurodegeneration in *Drosophila* (Abe et al., 2014).

In higher organisms Hen1 functions are narrowed to piRNAs methylation, and consistently the enzyme is only found in ovaries and testis. In mice, it seems to be testis-specific (Kirino & Mourelatos, 2007), while in *Zebrafish* it is essential for female germline maintenance, where Hen1-dependent stabilization of piRNAs correlates with inhibition of retrotransposons (Kamminga et al., 2010).

Bacteria Hen1 functions, on the other hand, differ from the eukaryotic orthologs. In bacteria, Hen1 interacts with Pnkp to participate in the repair mechanism for small RNAs, including tRNAs, for which addition of Nm guarantees increased resistance to future damage at the repaired site (Chan et al., 2009).

Structural information from *Arabidopsis* Hen1 have been provided by Huang et al. in 2009. The enzyme belongs to class I SAM-dependent methyltransferases, containing a seven-stranded β-sheet flanked by α-helices. Beside the methyltransferase domain, other three domains of the enzyme also interact with RNA: double stranded-specific binding domains 1 and 2 (dsRBD1 and dsRBD2) which bind the double stranded portion of pre-miRNAs, and the La-motif containing domain (LCD), that binds the two nucleotides overhanging from the unmethylated strand (the two nucleotides overhanging from the methylated strand are deep into the catalytic pocket). The fifth domain of the enzyme, peptidylprolyl isomerase (PPI)-like domain (PLD), of unknown functions, resembles FK506-binding proteins, suggesting that it might fulfill chaperone functions(Y. Huang et al., 2009) .

1.6.3-Nm on mRNA and its writers

Nm on mRNA is well documented for the first and second position after the cap structure, where it forms the so-called cap 1 (m^7GpppNmRNA) and cap 2 (m^7GpppNmNmRNA). These methylations have important roles in immunity, where they help distinguish “self” vs “non-self” mRNA. Absence of cap1 and cap2 induces interferon I (IFN-I) expression through the cytosolic sensor MDA5 (Züst et al., 2011). Some viruses manage to escape the immune response by getting their RNA methylated, for instance by encoding their own Nm methyltransferase, like the coronavirus (Züst et al., 2011), or by hijacking the host methyltransferase, like the HIV which recruits human Nm writer FTSJ3 to methylate its own RNA (Ringeard et al., 2019). Mechanistically, cap1 and cap2 are important to prevent binding of IFN-induced protein with tetratricopeptide repeats-1 (IFIT1), which would otherwise compete with the translation factor eIF4, and inhibit translation (Abbas et al., 2017). Moreover, Cap1/Cap2 methylation is important for stability, as in its absence mRNAs are bound and degraded by the exonuclease DXO (Picard-Jean et al., 2018).

Nm prevalence on internal positions of mRNA, on the other hand, has been the subject of debate. Attempts to map this modification transcriptome-wide led to the development of Nm-seq, that identified thousands of Nm sites on mRNA, which are predominantly Um (Q. Dai et al., 2017). Controversial about this study is the strong resemblance of the identified consensus motif and the sequence of the adaptor used for library preparation. Another attempt in this direction came from a study in BioRxiv showing how Spb1, a conserved methyltransferase ortholog of human FTSJ3, deposits Nm on hundreds of transcripts in yeast (Bartoli et al., 2018). Some mechanistics insight came from a study in 2018 showing that Nm on mRNA interferes with GTP hydrolysis by elongation factor Tu and causes tRNA rejection from the ribosome A site during the proofreading process (Choi et al., 2018). While the writers for the +1 and +2 position near the cap are stand-alone enzymes, sno(s)RNPs/Fibrillarin complexes use snoRNAs as guide to specifically target internal Nm sites. For example, Nm deposited by Fibrillarin on *Pxdn* mRNA stabilises the mRNA but at the same time inhibits its translation in mammals (Elliott et al., 2019). Beside Fibrillarin, it still remains unclear whether other stand-alone methyltransferases also methylate internal position on mRNA in higher organisms.

CMTr1 and CMTr2

The enzymes involved in these methylations are cap methyltransferases 1 and 2 (CMTr1 and CMTr2), responsible for deposition of cap1 and cap2, respectively. Structural studies show that these enzymes have a typical Rossman-fold catalytic domain, with seven β-sheets and six α-helices (Smietanski et al., 2014). These enzymes, beside playing an essential role in immunity, have been shown to promote translation during *Xenopus* oocyte maturation (Kuge et al., 1998). In *Drosophila*, where the two enzymes can act redundantly to methylate cap1, CMTr1 localises with RNA Pol II, probably for a co-transcriptional methylation, while CMTr2 does not, as it happens to have a selective set of targets mainly involved in synaptic vesicle release and cell adhesion, targets for which cap1 methylation is essential to ensure synaptic localisation and translation and, in turn, proper learning ability (Haussmann et al., 2022).

1.6.4-Nm on tRNA and its writers

Nm is also abundant on tRNAs, for which it increases stability (Prusiner et al., 1974). Several Nm sites on tRNA have a structural role and help in the translation process, for example the conserved Gm_{18} in the D-loop fosters interactions with ψ_{55}, and when missing it causes translation defects in *E. coli* (Urbonavičius et al., 2002; Watanabe et al., 2006). Nm deposited on residues in the anticodon loop of tRNA have been mainly reported to strengthen codon-anticodon interactions with the mRNA during translation, while specifically on the second and third positions of the anticodon are detrimental for codon reading (Satoh et al., 2000). A recent study has shown the importance of Nm for tRNA stability, and how depletion of this modification from the anticodon loop leads to increased tRNA fragmentation in fly gonads and brain (Angelova, Dimitrova,

Da Silva, et al., 2020). While the role of some Nm writers in stability and translation has been proven, their specificity towards one or two sites, compared to the higher Nm abundance, suggests that more writers than we currently know of might contribute to the tRNA Nm methylome. Two of such novel writers, Mettl25 and Mettl25b, have been characterized in this project and are described in Chapter 4.

Trm3/TARBP1

The yeast **Trm3** protein is the Nm writer known to methylate G_{18} on $tRNA^{Ser}$ (Cavaillé et al., 1999). The human ortholog, TAR binding protein 1 (**TARBP1**), owes its name to its antiviral function against HIV-1, as it binds to the HIV-1 regulatory long terminal repeat TAR, leading to RNA Pol II disengagement during the elongation process, thereby blocking HIV-1 genome expression (Wu-Baer et al., 1996). Bacterial Gm_{18} has also been shown to inhibit human Toll-like receptor 7 (TLR7)-mediated interferon (IFN) production, by sequestering TLR7 and hence preventing its interaction with stimulatory molecules (Rimbach et al., 2015). In line with this, antibiotic stress induced in *E.coli* an increase in Gm_{18}, which did not affect translation but further reduced bacterial tRNA immunostimulatory property in human cells (Galvanin et al., 2020). Structurally, TARBP1 contains a Rossman-fold catalytic core, like most methyltransferases. It belongs to the SPOUT superfamily, presents an unusual knot structure at its C-terminus, which is responsible for cofactor binding, and acts as a homodimer (H. Wu et al., 2008). Recently, an increase in DNA methylation at CpG islands of *TARBP1* promoter has been associated with Attention-Deficit/Hyperactivity Disorder (ADHD) (Weiß et al., 2021).

TRM13

Trm13 methylates the acceptor stem in position 4 of $tRNA^{GlyGCC}$, which is normally hypo-methylated. Beside a common Rossman-fold catalytic core, Trm13 does not show any sequence similarity with other methyltransferases; its N-terminus, indeed, represents a structurally independent unit composed by a novel Zn-finger motif (Tkaczuk, 2010; Wilkinson et al., 2007).

TRM44

Trm44 is responsible for methylation of U_{44} in $tRNA^{Ser}$. While highly conserved, from bacteria to metazoans, it is absent in plants, and the main knowledge about the enzyme derives from a study in yeast, according to which Um_{44} is involved in tRNA stability at non permissive temperatures, together with ac^4C_{12} (Kotelawala et al., 2008).

Trm7/FTSJ1

The last tRNA writer, **Trm7** in yeast, methylates the anticodon loop of $tRNA^{Phe}$ on residues C_{32} and G_{34}, with the help of target-specific partners: Trm732 and Trm734, targeting positions 32 and 34, respectively (Pintard, Lecointe, et al., 2002). The structure of this enzyme with its partner Trm734 shows that Trm7 possesses the catalytic activity in a Rossman-fold domain, and its C-terminus binds to Trm734 β-propeller domains (Hirata et al., 2019). Trm7 mutants in *S. cerevisiae* also lack wybutosine (yW) at position G_{37} (Guy & Phizicky, 2015) and display slow growth and translational defects (Pintard, Lecointe, et al., 2002), indicating a function for the anticodon loop methylation in mediating other modifications and in translation efficiency.

In *Drosophila* there are two functional orthologs of yeast Trm7: CG7009 and CG5220, responsible of methylation at positions 34 and 32, respectively, on $tRNA^{Phe}$, $tRNA^{Trp}$ and $tRNA^{Leu}$. Depletion of *CG7009* has been associated with reduced lifespan and increased sensitivity to RNA-virus infections. CG7009 is important for tRNA stability; in its absence a significant increase in tRNA fragments (tRFs) is observed in fly gonads and brain. This increment correlates with reduced post-transcriptional silencing of transposable elements, likely due to Dicer sequestering by tRFs (Angelova, Dimitrova, Da Silva, et al., 2020).

The paralog of Trm7 in higher eukaryotes is known as Ftsj1 (Pintard, Lecointe, et al., 2002). Human **FTSJ1** plays important roles in synaptic morphology and has been associated with X-linked intellectual disability (XLID) (Brazane et al., 2023; Guy et al., 2015; Nagayoshi et al., 2021). At a molecular level, the XLID phenotype is associated with decreased $tRNA^{Phe}$ stability in brain and reduced translation efficiency as well as impaired expression of XLID-related genes and several miRNAs (Brazane et al., 2023; Nagayoshi et al., 2021).

1.7-Mapping methods for Nm

In the 70's, thin layer chromatography allowed the determination of Nm stoichiometry at different sites on rRNA and tRNA in different Eukaryotes (Hughes & Maden, 1978; Vold, 1976; B. N. White, 1975). Following years saw improvements in chromatography and mass spectrometry and the development of new methods which allowed a transcriptome-wide mapping of the modification (Table 2). Reverse phase-high performance liquid chromatography (**RP-HPLC**), based on the separation of molecules according to their hydrophobicity, allowed mapping of the entire yeast rRNA (J. Yang et al., 2016), while **LC-MS**, with the addition of a labelling step for the sample and an *in vitro* transcribed standard, provided the absolute stoichiometry of Nm on rRNA (Taoka et al., 2015). Other methods were developed exploiting the ability of 2'O-methylation to increase RNA stability in alkaline condition and to arrest reverse transcriptase at low magnesium or low deoxyribonucleoside triphosphate (dNTPs) concentration. Primer extension and reverse transcription at low

dNTPs concentration followed by polymerase chain reaction (RTL-P) use low dNTP for site specific Nm quantification. With primer extension the Nm-dependent RT pause can be visualised on gel using a radioactive primer (B. Edward H. Maden, 2001). RTL-P is semi-quantitative as a methylation score can be obtained by comparing samples reverse transcribed at high and low dNTPs concentrations, prior to qPCR quantification (Dong et al., 2012).

Highthroughput methods:

Only in the past few years, the development of several methodologies coupled with next generation sequencing allowed a high-throughput mapping of this modification.

RiboMeth-seq, one of such methods, relies on reduced RNA fragmentation in alkaline conditions at the level of 2'O-methylated riboses. This results in a random fragmentation pattern, with fragments potentially starting and ending with nucleotides from all positions along the RNA molecule, except the 2'O-methylated nucleotide at the 3' end of the fragment, and its adjacent nucleotide (+1), at the 5' end of the fragment. Then, the analysis of the 5' and 3' coverage allows a single nucleotide resolution mapping of this modification (Birkedal et al., 2015; Marchand et al., 2016).

A different approach can be seen with the 2'OMe-seq method, which relies on the reverse transcriptase arrest at Nm sites in presence of low dNTPs (Incarnato et al., 2017).

In addition to these, the more recent development of other two similar methodologies, RibOxi-seq and Nm-seq, relying on the different reactivity of methylated ribonucleotides to periodate cleavage, allowed the mapping also of less abundant RNA species. The two methods use benzonase or fragmentation buffers to produce fragments which are then subjected to cycles of oxidation, in which periodate converts unmethylated nucleotides into dialdehyde, leading to β-elimination, followed by a dephosphorylation step (OED). While unmethylated nucleotides are thus lost during library preparation, methylated fragments get enriched as they can get ligated because they retain their 3' hydroxyl (Q. Dai et al., 2017; Zhu et al., 2017). Very similar to these latter methods, Nm mapping based on RNA exoribonuclease and periodate oxidative reactivity coupled with sequencing (Nm-REP-seq) also uses cycles of oxidation and β-elimination to enrich for Nm ending fragments. The difference is that these cycles follow a *Mycoplasma genitalium* RNaseR (MgR) treatment, which generates fragments ending one nucleotide downstream a Nm site. The combination of MgR with/without periodate treatment guarantees increased efficiency in mapping highly structured non coding RNA (P. Zhang et al., 2023). Other laboratories focused on optimising a RT enzyme that would efficiently produce mutations at Nm sites. The method, called Nm-Mut-seq, uses a modified HIV RT which

leads to Nm→T mutations upon low dNTP concentration (Li Chen et al., 2023). While the enzyme works well and the method mostly confirmed results from other methods, it cannot be used to detect Um and it has limitations in providing reliable stoichiometry information, as the enzyme mutation rate strongly depends on the sequence context in which Nm is located.

Direct sequencing:

As described above, with the Nanopore sequencers, the RNA molecule passes via electrophoresis through a pore where a detector identifies RNA sequence and chemical modification as mean of current intensity change (squiggle) caused by the modification compared to the original sequence. While big step forwards have been done in the field, with the development of softwares like nanoRMS, which extracts the signal intensity, the trace and the dwell time of a signal in the nanopore to call for Nm and provide stoichiometric information, there is still room for improvement as the modification generates different squiggles according to the sequence context, and Cm is still harder to detect than other methylated nucleotides (Begik et al., 2021).

Table 2. Methods for detection and mapping of Nm.

	Technique	Advantages	Disadvantages	References
Biophysical	**LC-MS**	Good detection Absolute stoichiometry	Laborious	Yang et al. 2016
	TL-HPLC/RP-HPLC	Good detection	Laborious	Taoka et al., 2015
Exploiting Nm effects on RT	**Primer extension**	Reliable	Not quantitative Site-specific Radioactivity	Maden, 2001
	RTL-P	Semi-quantitative	Site-specific Hard to detect partially modified site	Dong et al., 2012
	2'Ome-seq	Single nucleotide resolution Quantitative (relative)	Low sensitivity for structured RNA	Incarnato et al., 2017
	Nm-Mut-seq	Single nucleotide resolution Stoichiometry	Stochiometry information not always reliable as the RT activity shows some sequence bias Inability to detect Um	Chen et al., 2023
Exploiting Nm stability	**RiboMeth-seq**	Single nucleotide resolution Absolute quantification	No stochiometry information High coverage required therefore not ideal for rare RNA species	Birkedal et al., 2015 Marchand et al., 2016
	Nm-seq/RibOxi-seq	Single nucleotide resolution High sensitivity for less abundant RNA species	Sensitivity and specificity depend on number of OED cycles High imput required Not quantitative	Dai et al., 2017 Zhu et al., 2017
	Nm-REP-seq	Single nucleotide resolution Detect Nm in structured RNA	High starting material required	Zhang et al., 2023
Direct sequencing	**Nanopore**	Single nucleotide resolution No bias caused by library preparation	Sequence context bias Problems in detecting Cm	Begik et al., 2021

1.8-*Drosophila melanogaster*

Drosophila melanogaster, the "fruit fly", is the most characterised species of the Drosophilidae family. Discovered nearly a century ago, it is nowadays widely used in biology research. Its genome is simple, consisting only of three autosomes (chromosomes 2, 3 and 4) and two sex chromosomes, of which X is present in both and Y determines the male gender. The simple genome has allowed wide use of the CRISPR/Cas9 technology to generate a wide variety of mutant strains, as well as the use of the UAS/Gal4 system which easily permits the overexpression of a gene of interest in a specific tissue or in the whole fly, uncovering the effects of the loss or gain of specific proteins, at a molecular and phenotypic level (Hales et al., 2015). The presence of "balancer" chromosomes permits to keep track of a specific mutation in a strain as the balancer is characterised by inverted segments which impedes recombination with its homolog; moreover, it contains a phenotypic marker which allows identification of heterozygote flies, for example *cyo* that confers a curved shape to the fly's wings, and a lethal allele that makes sure the balancer chromosome is never carried in homozygosis (Hales et al., 2015).

1.8.1-Life cycle of *D. melanogaster*

Flies have become wildly popular in laboratories not only for their simple genome, but because of their small size and short life cycle, which allows to collect large number of flies in a short time and small space. Flies go through four main stages during their lifetime: embryo, larvae, pupae and adult (Fig. 5). The life cycle of *Drosophila* is affected by temperature, with higher temperature shortening it. At 25°C the cycle takes roughly 9-10 days. After fertilization, the developing embryo passes through 17 stages and hatches into larva after approximately one day. The larva is motile, eats and grows, turning into a second instar larvae after 24 hours, and another 24 hours into a third instar larvae. During this stage larvae gain weight and start crawling far from food to reach the pupation after two days. During this stage of metamorphosis, that lasts four days, the body dramatically remodels to hatch into the final form as an adult fly (Hales et al., 2015; Robertson, 1936). An adult fly, maintained at 25°C and 60% humidity can live up to three months.

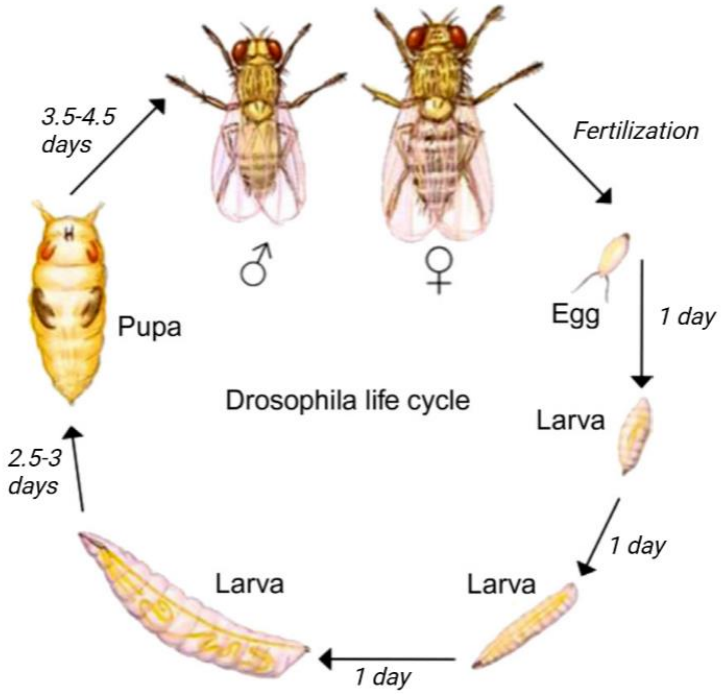

Figure 5. Drosophila melanogaster life cycle.
Figure adapted from [Wangler and Beller (2017)].

1.8.2-Nervous system development of *D. melanogaster*

The fly nervous system starts developing as early as stage 9 of embryonic development, together with the definition of the organ primordia of the future digestive system and epidermis. During this stage until stage 13, the neuronal stem cells, or neuroblasts, divide to give rise to the first neurons and glial cells (Tissot & Stocker, 2000). After differentiation and mitotic arrest of these embryonic neurons, a second wave of neurogenesis begins during larval stages. In the central brain and optic lobe neurogenesis begins already during the first instar larvae, with the mushroom bodies, the region responsible for learning and memory, being the most proliferative. In the thoracic and abdominal regions, neuroblasts start proliferating only during the second and third instar larvae stages, respectively. The first neurons to be born are the large motoneurons, which are mainly produced during the larval neurogenesis and remodelled during the metamorphosis. Another subpopulation of neurons of larval origin, which survives the pupariation, is the interneurons that constitute the mushroom bodies, the so-called Kenyon cells, important in the olfactory pathway (Tissot & Stocker, 2000). While a large number of embryonic neurons are remodelled to adapt to the adult needs, particularly the motoneurons, the remaining set of neurons undergoes programmed cell death, which is either triggered by the metamorphosis process for neurons that are no longer needed (e.g. motoneurons of the abdominal area, whose corresponding larval muscle has degenerated); or by gender-specific stimuli, which spare some larval neurons in one gender and not the other.

Essential for the remodelling and/or cell death of larval neurons is a hormonal control orchestrated by the ecdysteroid 20-hydroxyecdysone (20-HE), produced in 2 major waves during fly development. The first wave is released right before the pupariation and it induces dendritic regression, which starts the cell death pathway in some nest cells.. The second wave of 20-HE is released and ends during metamorphosis, at the end of which reduction of 20-HE triggers the expression of cell death genes in some peptidergic neurons (Tissot & Stocker, 2000).

1.8.3-Nervous system and walking behaviour

Motoneurons are controlled by the ventral cord, which in turn is linked indirectly to the main region of the central nervous system responsible for the coordination of visual stimuli, orientation and locomotion: the so-called **central complex** (Roland Strauss, 2002) (Fig. 6A). The central complex is composed by four components: the protocerebral bridge, responsible for the determination of fly walking speed; the ellipsoid body and the fan-shaped body which guide the formation of short-term memories essential for fly orientation; and finally, the paired noduli, mainly responsible of the fly handedness during exploratory walking; their inhibition increases lateral exploration on both sides and reduces the one-side bias (Buchanan et al., 2015; Roland Strauss, 2002).

The walking behaviour of a fly can be addressed in an assay known as **Buridan paradigm** (Fig. 6B), which consists of recording a fly positioned onto a round platform surrounded by water and by 2 visual landmarks in diametrically opposite positions around the platform. A fly perceives these landmarks as escape paths leading out of the platform and, being deprived of the ability of flying as their wings are cut before the experiment, continues walking on the platform in a straight line between these two landmarks. Deviation from this common behaviour can be analysed and provide information on the fly walking activity (speed, time spent walking) and orientation (angular deviation from the commonly walked straight line) (R. Strauss & Pichler, 1998), providing information on possible behavioural impairments in some fly strains.

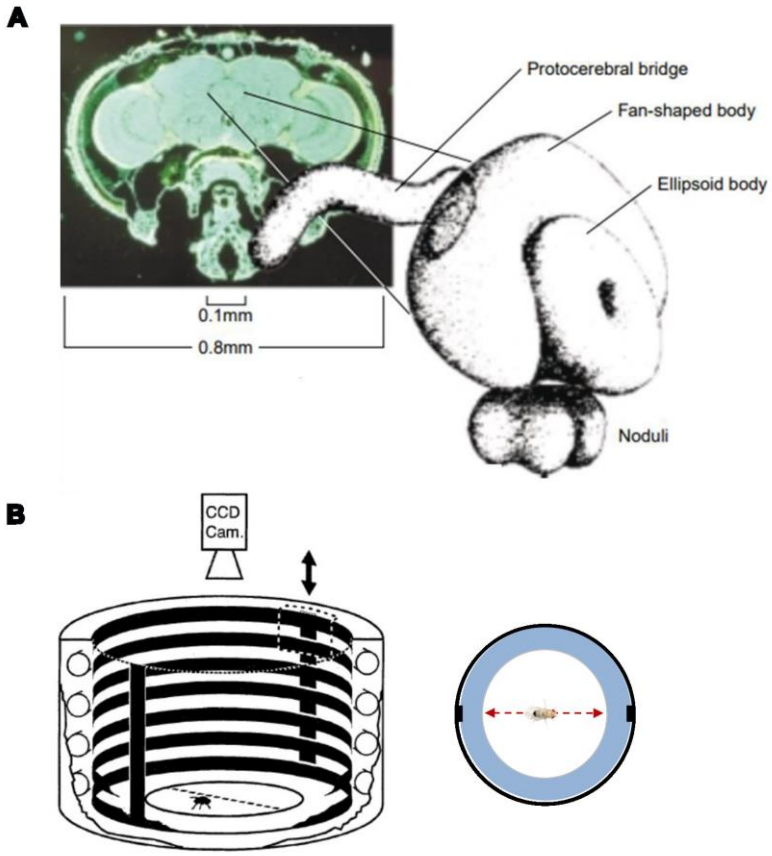

Figure 6. The central complex in the CNS regulates D. melanogaster walking behaviour.
(A) Frontal section of Drosophila head and brain showing at its centre the central complex, enlarged on the right. The complex comprises four regions: the protocerebral bridge, the fan-shaped body, the ellipsoid body and the paired noduli. Figure adapted from [Strauss (2002)].
(B) Setting for the Buridan paradigm. An elevated platform is surrounded by water and by two layers of clear plastic film. The presence of two landmarks along the cylinder determine the walking path of the fly, attracted by them. On top of the cylinder a camera records the fly movements on the platform. Figure from [Strauss and Pichler (1998)]. On the right, cartoon depicting the platform as seen from the top, where the camera is positioned.

2. Aim of the study

The field of epitranscriptomics has experienced an unprecedented interest in the past ten years, proven by the exponentially growing number of publications. Breakthrough discoveries about the most important and abundant mRNA modification, m^6A, deposited by the METTL3 complex, have shown its essential role in the regulation of all mRNA metabolic processes. Another very abundant modification is 2'O-methylation, or Nm, about which its cardinal role in ribosome biogenesis and translational regulation has been demonstrated by pivotal studies on its most known rRNA writer: the Fibrillarin complex.

An important gap in the knowledge still lies in the identification of the enzymes that deposit these modifications on specific RNAs. For instance most of the knowledge on the functions of m^6A comes from studies on the mRNA m^6A writers and little is known about m^6A functions on other RNA classes. Likewise, for Nm most of the knowledge are derived from studies on rRNA. Therefore the aim of my PhD was to expand the knowledge about these two modifications by characterizing novel writers and addressing their functions in development and behaviour in the model organism *Drosophila melanogaster*.

Project I: N6-methyladenosine

- The first goal of my project was to identify and characterize novel m^6A writers, which was achieved with the discovery of the rRNA methyltransferase **Mettl5**. In particular, after the identification of this writer, the objectives of my PhD were to:
  - (A) Identify its target RNAs;
  - (B) Unveil its molecular functions, in particular its direct or indirect influence on transcription and translation, by employing loss of function and state-of-the-art techniques, like IP-MS/MS, RNA-seq, ribo-seq;
  - (C) Discover its physiological role with focus on brain development and functions, using behavioural assays.
- Part of this project aimed at the exploration of a second m^6A writer: the spliceosomal RNA methyltransferase **Mettl16**, for which I aimed at confirming its known targets and understanding its physiological role in flies.

Project II: 2'O-methylation

- With the same premises as for m^6A, my goal for this project was to characterize unknown Nm writers. This was achived with the discovery of two novel Nm methyltransferases targeting tRNAs: **Mettl25** and **Mettl25b**. For this purpose I asked the following questions:

- (A) Do these enzymes deposit Nm on tRNA in flies? And if yes, on which species?
- (B) What is their function in fly development, healthspan and lifespan?
- (C) What are the molecular consequences of their absence, especially at the translational level?

❖ With the same goal, I have generated mutant lines for other Nm writers, and started the characterization of one of these enzymes: the ortholog of human FTSJ3, for which I aimed at identifying its target RNAs and its functions in ribosome biogenesis, as well as its impact on the transcriptome.

Preliminary remarks Part I: m^{6}A

Part of the results of this section have been published in a peer-reviewed journal as research article.

Research article: Leismann J*, Spagnuolo M*, Pradhan M, Wacheul L, Vu MA, Musheev M, Mier P, Andrade-Navarro MA, Graille M, Niehrs C, Lafontaine DL, Roignant JY. The 18S ribosomal RNA m6 A methyltransferase Mettl5 is required for normal walking behavior in Drosophila. EMBO Rep. 2020 Jul 3;21(7):e49443. doi: 10.15252/embr.201949443. Epub 2020 Apr 29. PMID: 32350990; PMCID: PMC7332798.

*Contributed equally

For this project I performed the cloning of Mettl5 and Trmt112 CDS into vectors for their overexpression with FLAG-Myc, HA and eGFP tag, Mettl5 and Trmt112 endogenous promoters into these vectors, and Mettl16 gRNAs for CRISPR/Cas9. I generated Mettl5 overexpression fly line, performed the staining (Fig. 8C), the RNA immunoprecipitation-qPCR (RIP-qPCR; Fig. 9D), the immunoprecipitation (IP) of FLAG-Myc Mettl5, which was followed by mass spectrometry (Fig. 11A), the co-IP western blot (Fig. 11B), the assay to test Trmt112 role on Mettl5 stability (Fig. 11D), RNA-seq, and established the ribo-seq protocol in our lab, performed on Mettl5 mutants (Fig. 13A-D). For the part of the project dedicated to Mettl16 I supervised a master student for the generation and characterization of the Mettl16 mutant line (Fig. 14-15).

Contributions:

Jessica Leissmann (master student Roignant's lab)

Generated the Mettl5 mutant lines, performed the Buridan paradigm and qRT-PCR on fly staging samples. Moreover, she performed the METTL enzymes RNAi screen.

Minh Anh Vu (master student Roignant's lab)

Generated the Mettl16 mutant line and helped with its characterization, learning RIP-qPCR and ovaries dissection. He also helped perform the METTL enzymes RNAi screen.

Prof. Dr. Miguel A. Andrade-Navarro

Performed phylogenetic analyses and generated phylogenetic trees for Mettl5 orthologs.

Mihika Pradhan and Dr. Michael Musheev (Prof. Dr. Christoph Niehrs' lab)

Performed LC-MS/MS quantification of RNA modifications.

Ludivine Wacheul (Prof. Dr. Denis LaFontaine's lab)

Carried out HPLC and the pre-rRNA processing analysis.

Prof. Dr. Marc Graille

Performed the 3D modelling of *D. melanogaster* Mettl5 and Trmt112.

Nastasja Kreim (IMB)

Performed the bioinformatic analysis of Mettl5 RNA-seq data

Dr. Marion Leleu (EPFL, Lausanne)

Performed bioinformatic analysis of Ribo-seq data.

Jiaxuan Chen and Mario Dejung (Proteomics core facility, IMB, Mainz)

Performed quantitative proteomics and data analysis of Mettl5 interactome.

3. Results part I: m^{6}A

3.1. Identification and characterization of a novel m^{6}A writer

3.1.1. Mettl5 controls m^{6}A levels in total RNA

When I started my PhD most of the knowledge about m^{6}A was derived from studies on Mettl3, the methyltransferase responsible for mRNA methylation. In order to identify potential novel m^{6}A methyltransferases, we performed a targeted RNAi screening for 20 genes identified as orthologs of the 32 known human METTLs (Fig. 7A and Supplementary fig. 1). We knocked down their function in S2R+ cells and quantified m^{6}A via mass spectrometry. After 6 days of incubation with dsRNA targeting each of the 20 *Drosophila* orthologs, cells were harvested and RNA was extracted. A fraction of total RNA and a fraction of Poly(A)-enriched RNA were submitted for mass spectrometry measurements. As control, we confirmed that the reduction of the known mRNA methyltransferase Mettl3, and its partner Mettl14, led to a strong decrease in m^{6}A in the poly(A) fraction, while the total RNA remained unaffected. However, the knock down (KD) of *CG7544*, the ortholog of human METTL16 and known m^{6}A writer, did not show any reduction in m^{6}A levels, likely reflecting that few targets are methylated by this enzyme. On the other hand, we noticed significant changes upon *CG9666* KD in the total RNA, but not in the mRNA fractions, suggesting that CG9666 either methylates multiple sites on non-coding RNAs, or it methylates an abundant species like rRNA (Fig. 7B-C). Being the ortholog of human METTL5, we refer to it in this study as Mettl5.

A

Human	Drosophila
METTL1	CG4045
METTL2A	Metl
METTL2B	Metl
METTL3	Mettl3
METTL4	CG14906
METTL5	CG9666
METTL6	CG34195
METTL7A	
METTL7B	
METTL8	
METTL9	CG5339
METTL10	CG9643
METTL11A	
METTL11B	
METTL12	
METTL13	CG2614
METTL14	Mettl14
METTL15	CG14683
METTL16	CG7544
METTL17	CG13126
METTL18	CG17219
METTL19	CG9386
METTL20	
METTL21A	
METTL21B	
METTL21C	
METTL21D	
METTL22	CG10584
METTL23	CG5013
METTL24	
METTL25	CG33964
METTL25B	CG2906
METTL26	CG18661
METTL27	

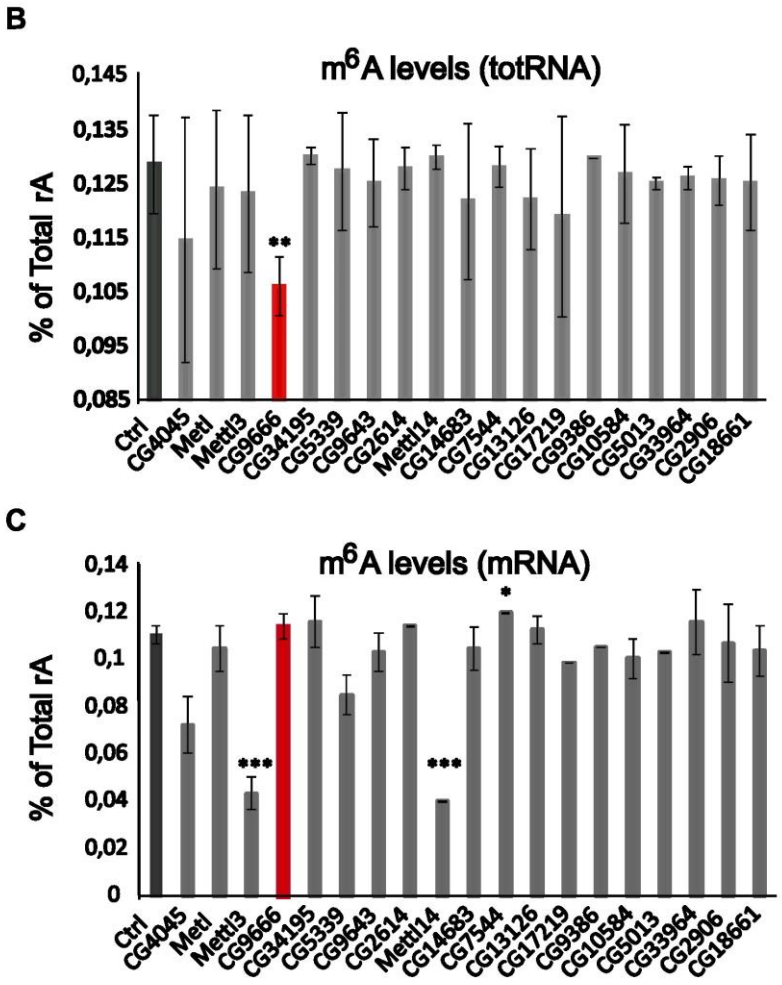

Figure 7. Mettl5 regulates m^{6}A level in total RNA.
Figure from [Leismann, Spagnuolo et al (2020)].
(A) *List of human methyltransferases and their orthologs in Drosophila melanogaster. Empty cells indicate that no ortholog could be identified.*
(B, C) *LC-MS/MS measurements of m6A levels in total RNA (B) or in poly(A) + RNA (C) upon KD of predicted methyltransferases in Drosophila S2R+ cells. m6A abundance in total RNA is significantly reduced when Mettl5 is depleted, while its depletion has no effect on m6A level in mRNA. As expected, the KD of Mettl3 and Mettl14 reduce m6A levels in mRNA. Bar chart represents the mean ± standard deviation of three technical measurements from three biological replicates. *P < 0.05, **P < 0.01, ***P < 0.001 (two-tailed t-test).*

3.1.2. Mettl5 is predominantly cytosolic and enriched in the brain

Mettl5 orthologs are present in all eukaryotic species (with the exception of fungi), as well as in archaea (Pyrococcus and Bathyarchaeota) and bacteria (Acidobacteriales) (Fig. 8A). Interestingly, among eukaryotes there is a high degree of sequence conservation, for example *Arabidopsis, Drosophila* and human share 53% sequence identity, and all the analysed species conserve the typical m^{6}A writers motif NPPF (Fig. 8B and Supplementary fig. 2), suggesting that the catalytic activity must be conserved and important throughout

evolution. The N-terminal sequence resemble the methyltransferase small domain (MTS, PFAM: PF05175), typical of many families of methyltransferases, which in flies spans the amino acid sequence 39-146, while the C-terminal domain is unique.

In order to understand the function of this potential methyltransferase, we checked its expression throughout fly development and its subcellular localization. Differently from human METTL5, which is mainly nucleolar, in *Drosophila* the enzyme, cloned with a FLAG tag and under the control of its endogenous promoter, localises in the cytosol (Fig. 8C), suggesting different targets or timings of m^{6}A deposition for the fly ortholog. During development Mettl5 is highly expressed in embryonic stages and it is maintained at low level from the second half of embryonic develoment until the larval stages, to then mildly increase in pupae and adults (Fig. 8D). Its predominant embryonic expression hints at some role in development, probably in neurogenesis, as results from fly express show that the transcript is mainly enriched in the nervous system (Fig.7E) (http://www.flyexpress.net/search.php?type=image&search=FBgn0036856).

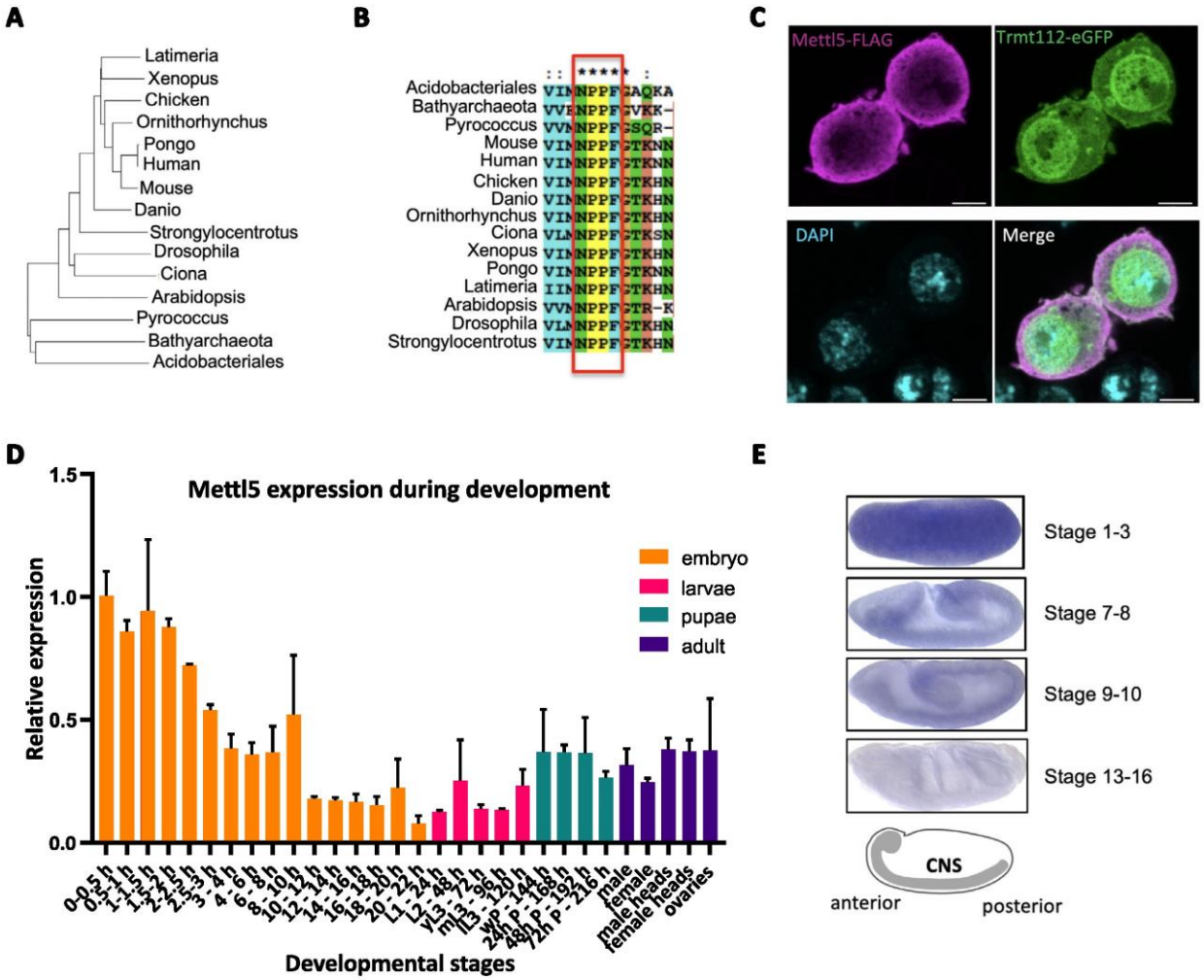

Figure 8. Mettl5 is conserved and enriched in the embryonic central nervous system (CNS) in flies.
Adapted from [Leismann, Spagnuolo et al., (2020)].
(A) *Phylogenetic tree of the alignment of representative Mettl5 orthologs from selected species (see Materials and Methods for details). Prokaryotic sequences from archaea (Pyrococcus, Bathyarchaeota) and bacteria (Acidobacteriales) are included as outliers.*
(B) *Multiple sequence alignment of Mettl5 orthologs showing conservation of the NPPF motif. Asterisks indicate perfect conservation.*
(C) *Subcellular localization of Mettl5-FLAG (purple) and Trmt112-eGFP (green) expressed under the control of their own promoter in S2R+ cells. Nuclei were counterstained with 4′,6-diamidino-2-phyenylindole (DAPI; cyan). Images obtained using confocal microscopy with a 63x objective. Scale bar: 4.47 µm.*
(D) *Developmental expression of Mettl5 transcript assayed by RT–qPCR analysis. The figure shows mean ± standard deviation of three technical measurements from one biological replicate.*
(E) *In situ hybridization of Mettl5 transcript at different embryonic stages. The central nervous system (CNS) is highlighted in the schematics. Data retrieved from FlyExpress 7 (http://www.flyexpress.net/search.php?type=image&search=FBgn0036856*

3.1.3. Mettl5 promotes m^{6}A deposition on 18S rRNA

To address the molecular and physiological functions of Mettl5, we employed the CRISPR/Cas9 methodology to obtain mutant flies, using two guide RNAs (gRNAs) encompassing the predicted methyltransferase domain. In this way, we obtained two mutant alleles (Supplementary fig. 3). The first one is characterised by depletion of two conserved alanines at positions 36 and 37, immediately upstream the methyltransferase domain, and is therefore referred to as Mettl5$^{\Delta 2AA}$ in this study (Fig. 9A, top). The second allele shows an indel mutation of 13 nucleotides upstream the methyltransferase domain and a downstream insertion of 3 nucleotides, resulting in a frameshift at the level of amino acid 36 and a premature stop codon at amino acid 107 (Fig. 9A, bottom), suggesting that this mutation gives rise to a protein with a truncated, non-functional, catalytic domain. This allele is called Mettl5^{fs}. The mutant fly lines are viable and fertile without any obvious morphological defect. We then sought to address whether Mettl5 function as potential m^{6}A writer was conserved *in vivo*. From mass spectrometry measurements we found that Mettl5$^{\Delta 2AA}$ flies showed comparable m^{6}A levels relative to the WT counterpart, while *Mettl5^{fs}* mutants showed a drastic 45% reduction in total RNA (Fig. 9B). As per from our screening in S2R+ cells, m^{6}A levels in mRNA were not affected in neither of the two mutant lines (Supplementary Fig. 4), suggesting that Mettl5 is not methylating mRNA.

Once established that *Drosophila* Mettl5 is an m^{6}A writer, we performed HPLC on purified 18S and 28S rRNAs from WT and mutant flies. RNA from mutant and isogenic control flies was subjected to velocity centrifugation and then digested to nucleosides, before the HPLC measurements. Commercial m^{6}A used as calibrator indicated that the elution time of this methylated adenosine is 48 min. In this way, we could establish that fly Mettl5 is the specific m^{6}A writer targeting the 18S rRNA, as complete loss of this modification was observed in *Mettl5^{fs}* mutant flies (Fig. 9C), while the 28S rRNA remained unaffected

(Supplementary Fig. 5). To understand whether the 18S m^{6}A is a constitutive or plastic modification, contributing or not to ribosome heterogeneity, the stoichiometry of this modification was analysed using the UV254 molar response factor of m^{6}A. In chromatography, this factor is a standard value that depends on the concentration of a given nucleotide and the response of the detector. It is given by the ratio between peak area and concentration of the nucleotide. Dividing the obtained m^{6}A peak from our HPLC by the m^{6}A molar response factor, and comparing it with the same ratio from other unmodified nucleotides on the 18S rRNA, we could conclude that in flies m^{6}A is a constitutive modification present at 100% stoichiometry.

To further strenghten our findings, we transfected S2R+ cells with a UAS plasmid to overexpress FLAG-Myc-tagged Mettl5. Using an anti-FLAG antibody, RNA immunoprecipitation (RIP) was performed in cells transfected with the empty plasmid, and hence expressing only the FLAG-Myc tag (Ctrl sample), versus cells expressing FLAG-Myc-Mettl5 (Mettl5 IP sample). 18S rRNA levels were then quantified via qPCR, showing a significant enrichment of 18S upon Mettl5 IP (Fig. 9D), confirming that this RNA is indeed recognised and bound by Mettl5.

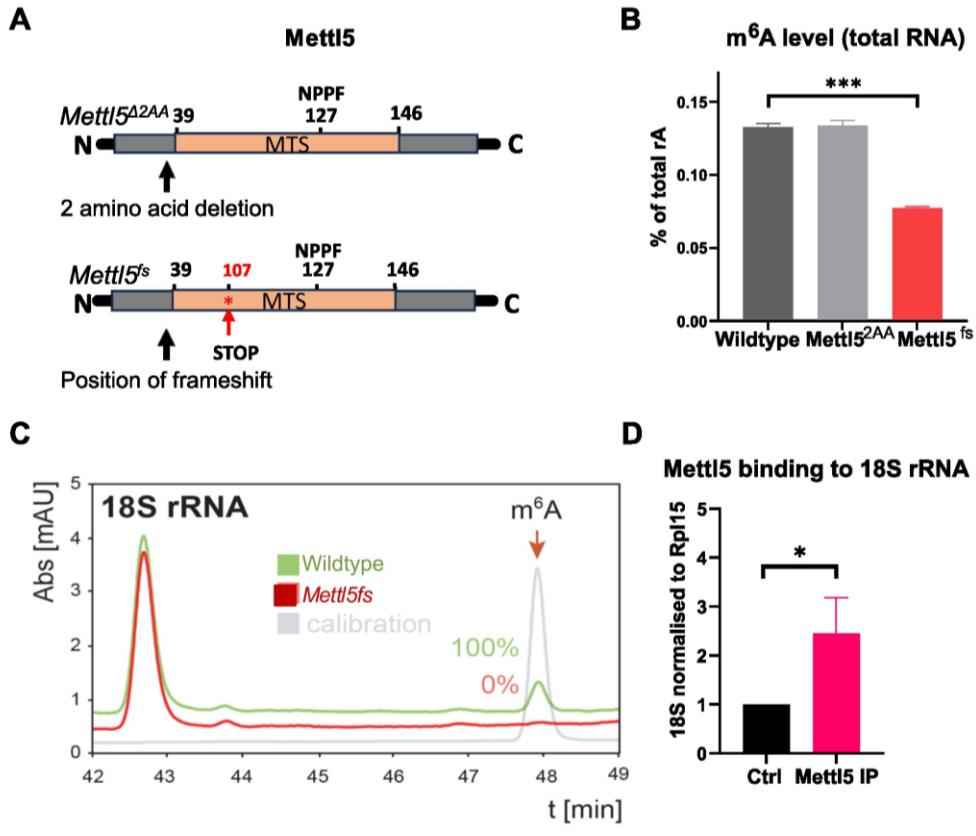

Figure 9 Drosophila Mettl5 is required for m^{6}A deposition on 18S rRNA.
Adapted from [Leismann, Spagnuolo et al. (2020)].
(A) *Representation of the two Mettl5 mutant alleles generated in this work, consisting either of a two amino acid deletion upstream of the methyltransferase domain (top, Mettl5$^{\Delta 2AA}$) or of a frameshift mutation leading to a premature stop codon (bottom, Mettl5^{fs}).*

*(B) LC-MS/MS measurements of m6A levels in total RNA of WT and Mettl5 mutant flies. Bars represent mean ± standard deviation of measurements of three biological replicates. ***P < 0.001 (two-tailed t-test).*
(C) Purified 18S rRNA analyzed for its m6A content by quantitative HPLC. The 18S rRNA was extracted from 40S subunits isolated on sucrose gradients. The calibration control is a commercial source of m6A (in gray). m6A elutes at 48 min.
*(D) RIP-qPCR quantification of 18S rRNA from control (expressing FLAG-Myc) and Mettl5 (expressing FLAG-Myc-tagged Mettl5) samples. Bars represent mean ± standard deviation of measurements of three biological replicates. *P < 0.05 (two-tailed t-test).*

3.1.4. Mettl5-dependent m^{6}A deposition on 18S rRNA is dispensable for rRNA biogenesis

As broadly described in many studies, some rRNA modifications, in particular Nm and Ψ, are essential for rRNA biogenesis (Sloan 2017). In *Drosophila*, a long polycistronic RNA transcribed by RNA Polymerase I is processed to generate the final mature 5.8S, 2S, 18S, 28Sa and 28Sb rRNAs. Two distinct pathways can take place, one starting with the removal of the external transcribed spacer (ETS), upstream of the future 18S rRNA, and then proceeding with the removal of the internal transcribed spacers (ITS), and a second pathway that starts from the separation of the 18S rRNA from the other rRNA molecules and then proceeds with the removal of the remaining ETS and ITSs (Fig. 10A). To address whether Mettl5-dependent m^{6}A is essential for rRNA biogenesis, total RNA from WT and mutant flies, as well as from control and Mettl5 KD S2R+ cells, was extracted and separated on denaturing agarose gel. The ratio between the 28S rRNAs and 18S rRNA shows that the relative content of the molecules between control and Mettl5-depleted samples was comparable (Fig. 10B). Furthermore, northern blot with specific probes against ITS1 or ITS2 showed that accumulation of the pre-rRNA as well as of the intermediate fragments is comparable between Mettl5^{fs} and its isogenic control fly line, suggesting that Mettl5 does not impact biogenesis (Fig. 10C).

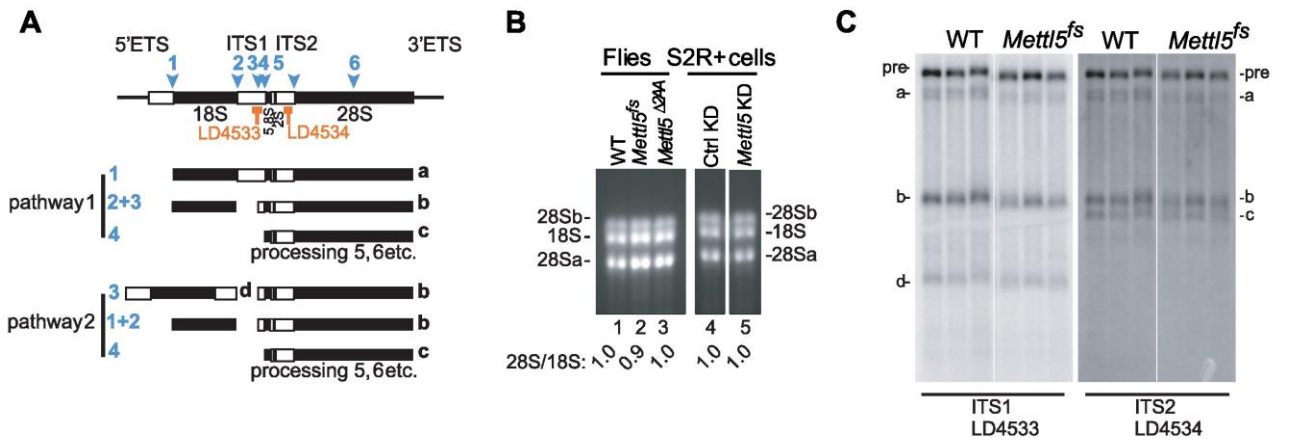

Figure 10. Mettl5 depletion does not impair rRNA biogenesis.
From [Leismann, Spagnuolo et al. (2020)].
(A) Pre-rRNA processing in Drosophila: four mature rRNAs (the small ribosomal subunit 18S, and the large ribosomal subunit 5.8S, 2S, and 28Sa and 28Sb) are produced by sequential RNA cleavage following two alternative pathways, as depicted. Processing sites are indicated (1–6). The major pre-rRNA intermediates (a, b, c, and d) are highlighted.

(B) Mature rRNA analysis on ethidium-stained denaturing agarose gels. The same amounts of total RNA extracted from the indicated flies and from S2R+ cells depleted or not of Mettl5 were loaded. The 28S/18S ratio was established by densitometry.
(C) Analysis of 18S rRNA maturation in WT and mutant flies (Mettl5fs). Total RNA extracted from the indicated animals was resolved on denaturing agarose gels and processed for Northern blotting with specific probes (complementary to ITS1 or ITS2 sequences). The pre-rRNAs detected accumulate to normal levels indicating that processing is unaffected.

3.1.5. Trmt112 is a conserved Mettl5 co-factor

Trmt112 is a known co-factor of several methyltransferases, including Mettl5 in human (Van Tran et al., 2019). In order to verify if this interaction is conserved in flies**,** we performed immunoprecipitation (IP) in S2R+ cells expressing FLAG-Myc-tagged Mettl5, and submitted the samples for mass spectrometry to identify Mettl5 interactors. Beside ribosomal proteins, other 7 proteins were mainly enriched in this pull-down (Fig. 11A), some of which to date uncharacterised. Among the enriched proteins, we found the ortholog of human TRMT112, CG12975, which we named Trmt112. To confirm this interaction, Trmt112 was cloned with a N-terminal HA-tag or with a C-terminal eGFP-tag and co-immunoprecipitation followed by western blot (coIP-WB) was performed. The results show that the two proteins interact, as FLAG-Myc-Mettl5 was identified in Trmt112 pull-down, and Trmt112-eGFP was detected upon Mettl5 pull-down (Fig. 11B). Strenghtening this finding, Trmt112 KD in S2R+ cells led to a mild yet significant reduction in m^{6}A as revealed by mass spectrometry (Fig. 11C). Moreover, like Mettl5, Trmt112 transcript also showed a predominant embryonic expression, suggesting that they work synergistically during development (Supplementary fig 6A).

From Van Tran *et al*. we learnt that human TRMT112 is important for METTL5 stabiity as structural analysis revealed that the interface between TRMT112 and METTL5 protects a core of hydrophobic residues from the cytosolic environment (Van Tran et al., 2019). To test this hypothesis we expressed FLAG-Myc-Mettl5 in S2R+ cells upon *Trmt112* KD and assessed Mettl5 stability by western blot at different time points after translation inhibition by cycloheximide treatment. Compared to the control, in *Trmt112* KD cells Mettl5 showed a faster rate of decay, as a reduction of FLAG-Myc-Mettl5 after 8 and 24 hours of cycloheximide treatment was observed, compared to time 0 (right after cycloheximide addition to the medium) (Fig. 11D and Supplemetary fig. 6B). In line with this, structural prediction based on the sequence conservation between flies and human, confirmed that the residues predicted to occupy the interface between the two enzymes are highly conserved and mainly hdrophobic, and that the structure of the heterodimer should highly resemble the one from the human orthologs (Fig. 11E and supplementary fig. 7).

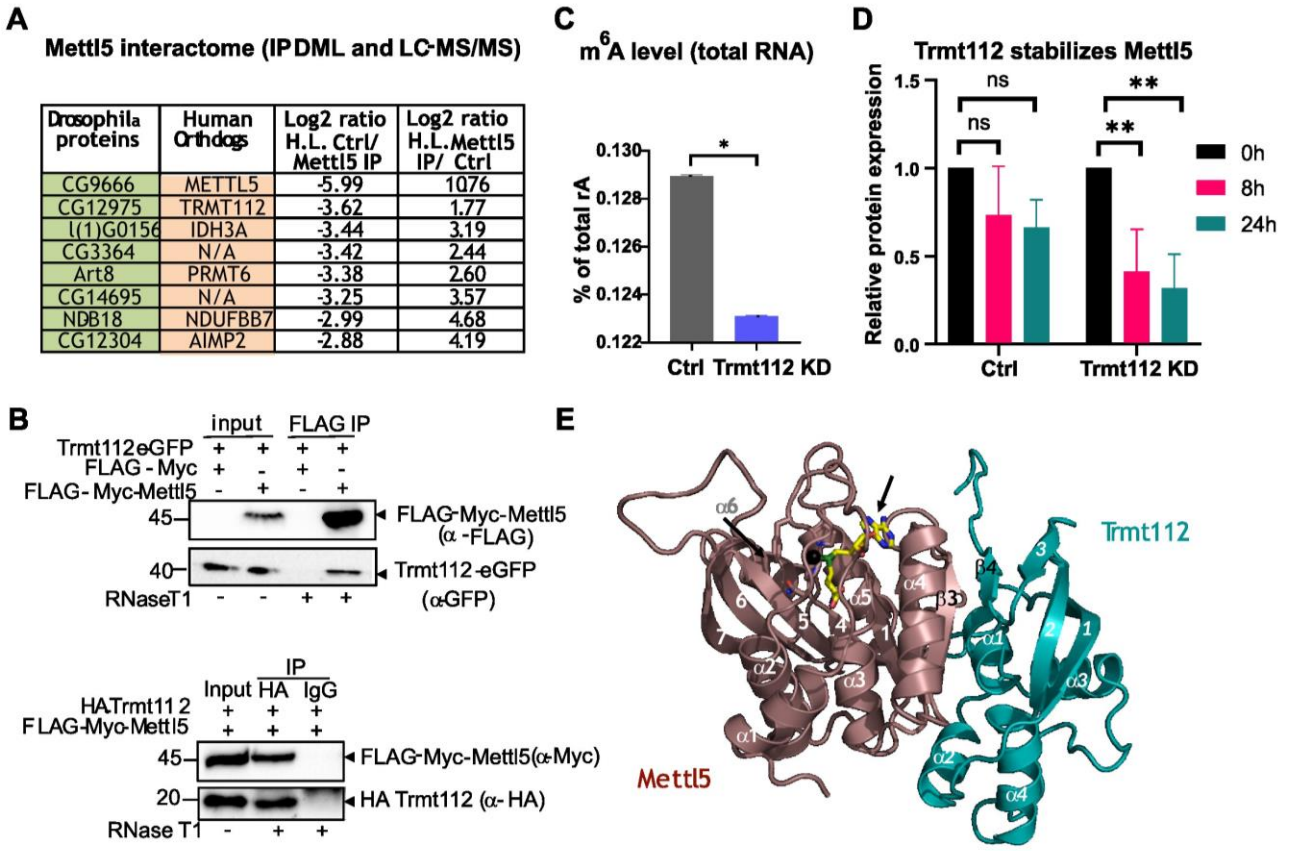

Figure 11. Mettl5 interacts with Trmt112 to install m6A on 18S rRNA.
Adapted from [Leismann, Spagnuolo et al. (2020)].
(A) Mettl5 partners identified as significantly enriched candidates in mass spectrometric analysis of Mettl5-FLAG-Myc affinity purifications (ribosomal proteins not listed for simplicity). Measurements of two biological replicates.
(B) Western blot validation of the co-immunoprecipitated proteins Mettl5-FLAG-Myc and Trmt112, bearing either a N-terminal HA tag (top) or a C-terminal GFP tag (bottom), in S2R+ cells. The arrows point at the indicated proteins. HA-Trmt12 migrates below the antibody light chains (top). Trmt112-eGFP migrates above the heavy chains indicated by an asterisk (bottom).
*(C) Trmt112 depletion reduces m6A levels in total RNA from Drosophila S2R+ cells. Mean ± standard deviation of three technical measurements from three biological replicates. *P < 0.05 (two-tailed t-test).*
*(D) Western blot quantification of Mettl5 at the indicated timepoints (0, 8 and 24h) after cycloheximide treatments in control and upon Trmt112 KD in S2R+ cells. Mean ± standard deviation of three biological replicates. n.s. not significant, **P < 0.01 (two-tailed t-test).*
(E) The sequences of D. melanogaster Mettl5 and Trmt112 were modeled in the experimentally determined atomic resolution structure of the human METTL5-TRM112 complex (based on PDB model 6H2V), revealing high conservation and formation of a parallel b-zipper involving main chain atoms at the complex interface. Mettl5 and Trmt112 are colored light brown and blue, respectively. The NPPF signature, known to co-ordinate planar nitrogen groups to be methylated, is shown as sticks. The S-adenosyl-methionine (SAM) is shown in stick representation (yellow) with the methyl group to be transferred to the 18S rRNA represented as a black sphere. Important secondary structure elements, including b3 on Mettl5 and b4 on Trmt112, are indicated.

3.1.6. Mettl5 is required for locomotion and orientation

As described in chapter 1.3.3. in the subsection "Mettl5 and diseases", *Mettl5* mutant alleles were identified in human patients with autosomal recessive intellectual disabilities, characterized by learning and

behavioural impairments and microcephaly. The mutation in these patients resembled the mutant allele we obtained in *Drosophila*, therefore we decided to address whether it causes behavioural problems in flies. For this, we performed the Buridan assay (described in Chapter 1.5.3.), which assesses the walking behaviour of flies (Fig. 5B and Fig. 12A). As shown in figure 12A and 12B, *Mettl5*^{fs} mutant flies lost orientation within the platform, as they kept changing direction. We also used trans-heterozygote mutants, obtained by crossing Mettl5^{fs} with a decifiency line lacking a large segment of chromosome 3, including the *Mettl5* gene, to strenghten the association of the observed behaviour with the absence of Mettl5. With this line we obtained very similar results as per homozygous Mettl5^{fs} flies. The Mettl5$^{\Delta 2AA}$ mutant line, on the other hand, showed a mild change in the walking behaviour, but still maintained the focus on the 2 landmarks like the WT line, suggesting that the observed phenotype is due to the loss of Mettl5 catalytic activity (Fig. 12A and B). The activity of flies, measured as walking distance, was also mildly reduced in the mutant lines (supplementary fig. 8A). We could confirm that the locomotion defects were not due to blindness, as we measured the time spent in different portion of the platform and observed a significant preference towards the areas marked with the 2 black stripes, compared to a more random distribution, expected in the case of blindness (Supplementary fig. 8B). Lastly, we also measured the brain to body ratio in WT as well as mutant flies, and we noticed a reduction in the latter group compared to the WT counterpart, reminiscent of the microcephaly phenotype observed in human patients affected by METTL5-dependent intellectual disability (Supplementary fig. 8C).

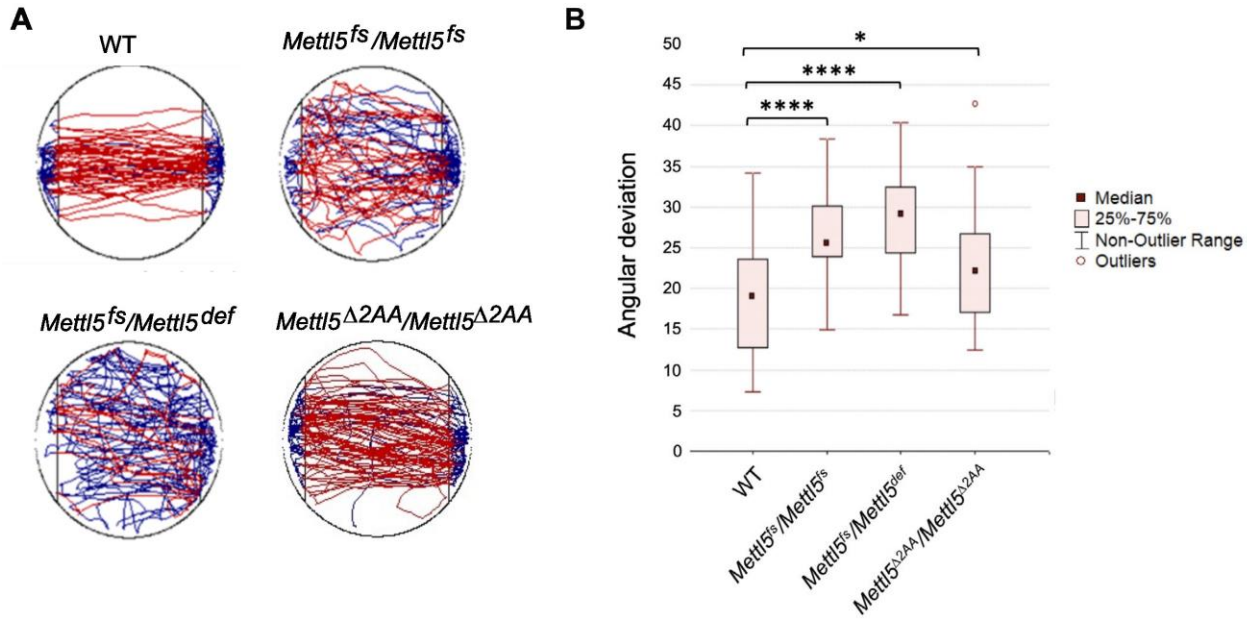

Figure 12. Mettl5 is required for fly orientation.
From [Leisman, Spagnuolo et al. (2020)].
***(A)** Representative trajectories of WT and Mettl5 mutant flies analyzed by Buridan's paradigm. The blue lines indicate when the fly stops and changes direction.*

(B) *Orientation evaluated with the help of Buridan's paradigm for Mettl5 mutant flies. Orientation was measured as the angular deviation from the straight path needed to move from one landmark to another in the arena. Number of flies tested per genotype: 30. Mean standard deviation. Shapiro–Wilk test was used to test for normal distribution in each group. Normally distributed groups were tested by t-test. Due to multiple comparison, Bonferroni correction was applied (*P < 0.05; ****P < 0.0001).*

3.1.7. Mettl5 modulates metabolic processes in fly brain

To address the molecular mechanisms underpinning the observed neuronal phenotypes, we performed RNA-seq and Ribo-seq libraries from WT and Mettl5^{fs} adult fly heads, in order to monitor the transcriptional and translational changes, respectively. Ribo-seq, or ribosome profiling, is a widely used technique which provides information about the mRNAs that are being actively translated (Mcglincy & Ingolia, 2017). The principle behind this method is that mRNAs which are being translated are not fully digested by RNaseI treatment because they are protected by the ribosome for a length of approximately 30 nucleotides, and are therefore called ribosome footprints. In parallel, total RNA libraries are prepared to distinguish changes that occur specifically at the translation level from those that mainly reflect transcriptional changes. The results from these libraries show multiple changes in the transcriptome. In particular, genes involved in carbohydrates metabolism were found upregulated in mutant flies, while the modulation of lipid metabolism, in particular fatty acid synthesis, was significantly impaired (Fig. 13A-B).

At the level of translation, results from the ribo-seq libraries show that glucosidase and oxidoreductase activity are upregulated (Fig. 13C), which is in line with RNA-seq results, and suggests that mutant fly brain might be under oxidative stress. Serine-endopeptidases and hydrolases, which include lipid hydrolases, are instead downregulated in the mutant line (Fig. 13D).

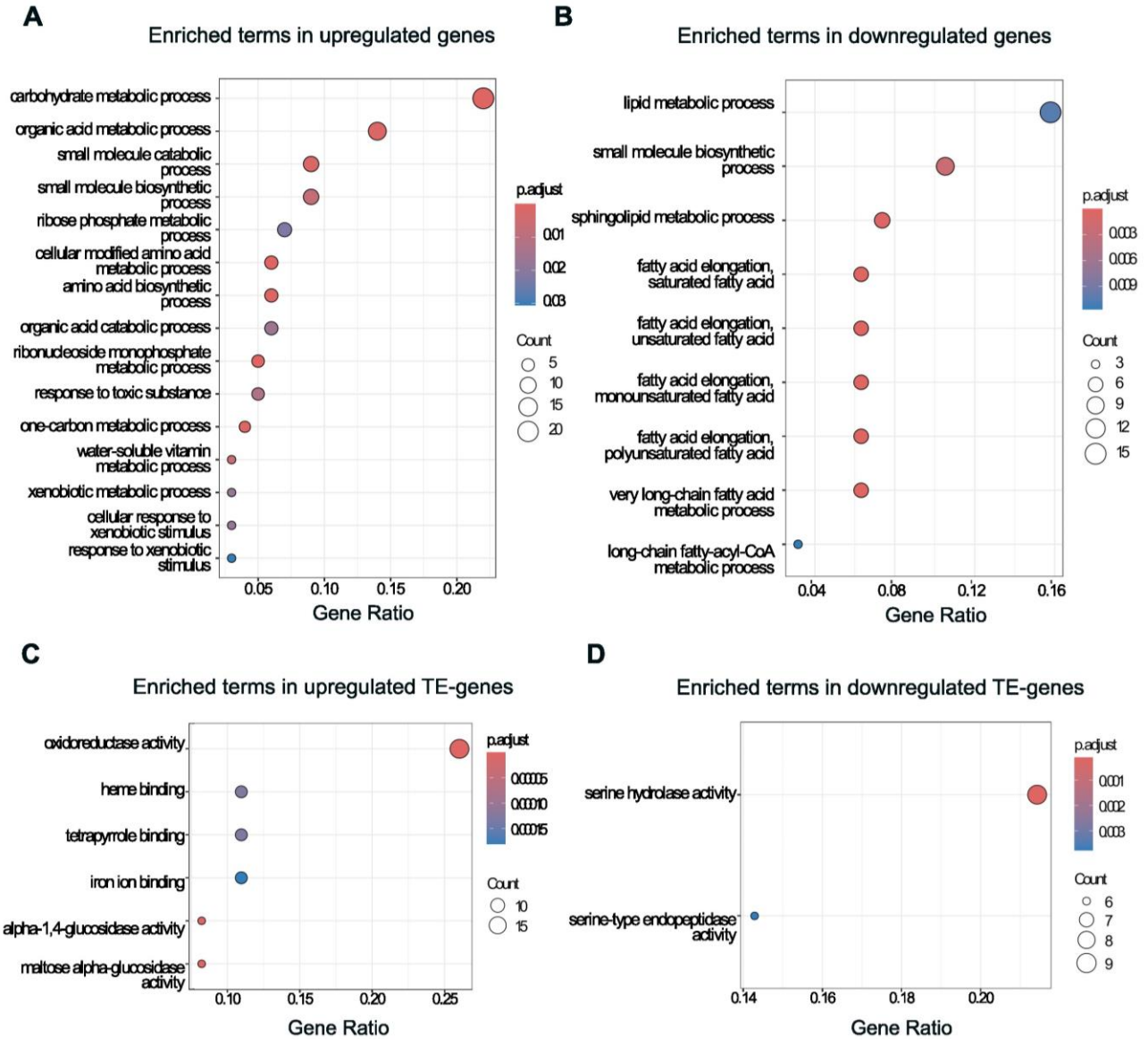

Figure 13. Genes involved in lipid and carbohydrate metabolism are dysregulated upon Mettl5 depletion in fly brain.
(A-B) RNA-seq results showing enriched biological processes in upregulated (A) and downregulated (B) genes (FDR <0.05) in Mettl5fs brain compared to their isogenic control.
(C-D) Ribo-seq resuts showing enriched terms of upregulated (C) and downregulated (D) translated (TE) genes (FDR<0.05) in Mettl5fs brain.

3.2. Characterization of CG7544: the fly ortholog of human METTL16

3.2.1. Mettl16 is predominantly nuclear and highly enriched in ovaries

m^{6}A decorates a plethora of RNA species, but very little is known about its regulation on non-coding RNAs. Mettl16, an m^{6}A writer, has been studied in higher vertebrates, where it was shown to be essential for cellular SAM homeostasis and embryonic development (Mendel et al., 2018; Pendleton et al., 2017). It was also linked to splicing regulation through methylation of the *U6* snRNA and to the modulation of *Mat2A* pre-mRNA splicing (Pendleton et al., 2017; Warda et al., 2017). During evolution, in vertebrates, Mettl16 acquired new C-terminal regions, known as vertebrate conserved regions 1 and 2 (VCR1 and VCR2), which span over 200 amino acids and are responsible of the recruitment of the spliceosome machinery to *Mat2A* transcript (Pendleton et al., 2017). The fly ortholog of human METTL16, CG7544, referred hereafter as Mettl16, consists of 305 amino acids, while the human ortholog, with the acquisition of VCR1 and 2, reaches 562 amino acids. The N-terminal RNA binding domain is conserved, especially the positively charged amino acids responsible for RNA binding (Mendel et al., 2018; Pendleton et al., 2017). The most conserved portion is the methyltransferase domain, which in *Drosophila* is predicted to encompass the region between amino acid 11 and 296 (Fig. 15A) and the catalytic motif, NPPF, is present from bacteria to eukaryotes (Fig 14A) (Mendel et al., 2018). What functions Mettl16 fulfils in invertebrates, lacking the VCRs, and how these functions are accomplished, is not known.

In order to gain insight in fly Mettl16 functions, we checked its expression levels during development via RT-qPCR. Mettl16 levels are high during the first 4 hours of embryonic development and drastically drop for the remaining embryonic stages and throughout larvae and pupae development, as well as in the adult, where it is highly expressed only in the ovaries, suggesting a potential role for this enzyme in fertility (Fig. 14B). Next we cloned *Mettl16* coding sequence in a UAS plasmid backbone with a FLAG-Myc tag in order to visualise its subcellular localization. We found that Mettl16 is mainly nuclear in fly S2R+ cells, even though it could be detected in the cytosol as well (Fig. 14C). This suggests that Mettl16 might also fulfill functions in the cytosol that are different from its nuclear role in splicing regulation. For example, a recent study proposed a role for cytosolic Mettl16 in translation regulation, fulfilled via interaction with eukaryotic initiation factors 3a and b (eIF3a/b) and independent of its catalytic activity (Su et al., 2022).

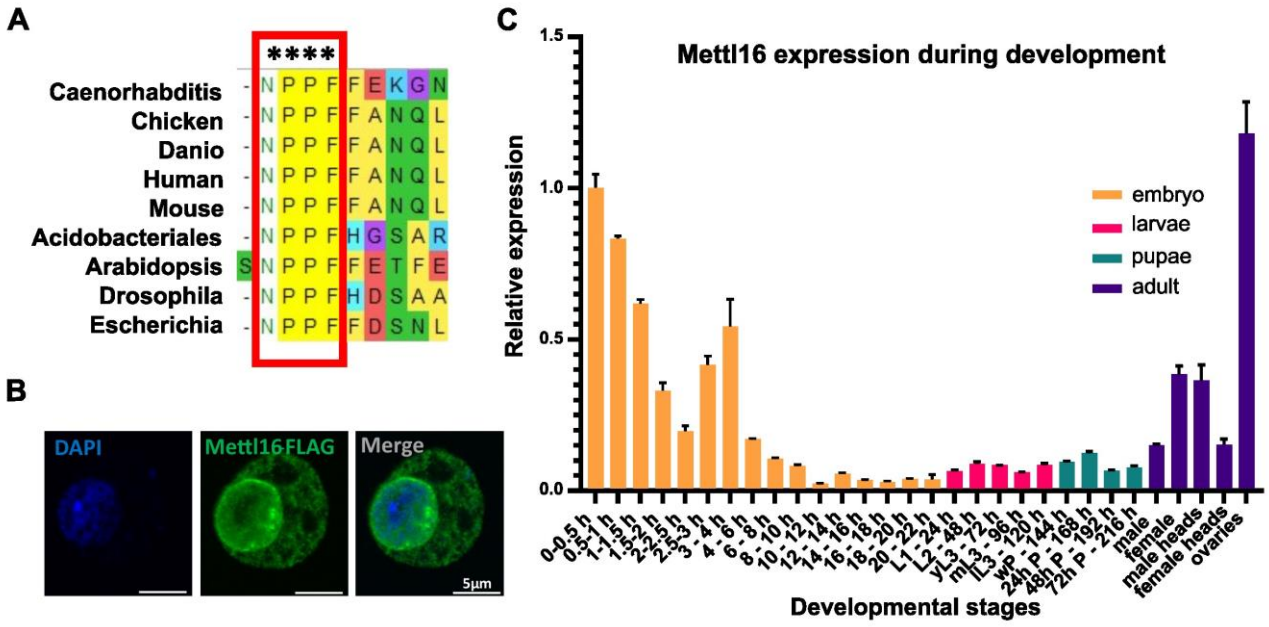

Figure 14.Mettl16 is a conserved nuclear protein highly expressed in fly ovaries and during early embryogenesis.
(A) Multiple sequence alignment of Mettl16 orthologs showing conservation of the NPPF motif. Asterisks indicate perfect conservation.
(B) Subcellular localization of Mettl16-FLAG (green) expressed under the control of a UAS promoter in S2R+ cells. 63× magnified merge of fluorescently labelled S2R+ cells. Scale bar: 5 µm.
(C) Developmental expression of Mettl16 measured via qRT-PCR. Results represent the mean ± standard deviation of three technical replicates from one biological replicate.

3.2.2 Fly Mettl16 binds to *U6* spliceosomal RNA and is essential for ovarian development.

Intrigued by its high expression in ovaries, we decided to address its physiological functions by generating *Mettl16* KO fly lines, to estimate the effects of its depletion on fertility and development. We therefore employed CRISPR-Cas9 system to target Mettl16 catalytic domain with the use of two guide RNAs encompassing this region, and obtained an insertion of two Thymines in the second exon, at position 216, which caused a frameshift and a premature stop codon at amino acid 85, suggesting that the protein, if not degraded, has lost its catalytic functions (Fig. 15A and Supplementary fig. 9). Mutant flies are viable and with no apparent morphological defects. We therefore checked whether fertility was impaired, and crossed homozygotes or heterozygotes mutants of both genders with WT flies. Interestingly, while heterozygotes were having progeny, as we could observe larvae and pupae after 5-6 days from the crossing, homozygote mutants of both genders failed to procreate. The fact that females are infertile is consistent with the high expression found in ovaries. However, it was surprising to find that males also were sterile, as public databases (Thurmond et al., 2019) show low Mettl16 expression in testis, which suggests that Mettl16, even at low levels, might play a role in male germline development.

We then addressed the morphology of the ovaries. WT flies contain a pair of ovaries, formed by 15-20 strings known as ovarioles (Olovnikov & Kalmykova, 2013)(Fig. 15B). Ovarioles host germ cells at increasingly mature stages as they approach the uterus. At the most anterior side of the ovariole lies the germarium made up of primordial germ cells (PGC). PGCs undergo a precise pattern of divisions to produce oocytes or nurse cells, which supply mRNAs and proteins to the developing oocyte (Olovnikov & Kalmykova, 2013). We found that ovaries from WT and heterozygotes flies appeared normal, while those from homozygotes flies are dramatically smaller, suggesting incomplete development (Fig. 15C).

To address how Mettl16 accomplishes these functions at a molecular level, we wondered whether its target specificity is conserved between *Drosophila* and vertebrates, and therefore addressed Mettl16 binding to *U6* and *Mat2A* via RIP experiments.To do so, S2R+ cells transfected with either an empty UAS FLAG-Myc vector or a UAS FLAG-Myc-Mettl16 vector, were lysed and incubated with an anti-FLAG antibody for FLAG pull-down. Levels of *U6* and *Mat2A* transcripts were then quantified in control (expressing FLAG-Myc) and Mettl16 IP (expressing FLAG-Myc-Mettl16) samples via RT-qPCR. Results show an enrichment of both transcripts upon Mettl16 IP, although binding is significant only for *U6,* suggesting that binding to *U6* might be stronger than to *Mat2A* (Fig. 15D). These results hint that fly Mettl16 may work, as its vertebrate orthologs, as a splicing regulator via methylation of *U6* and *Mat2A* RNAs and that impairments due to Mettl16 absence are deleterious for germline maturation and fertility in flies.

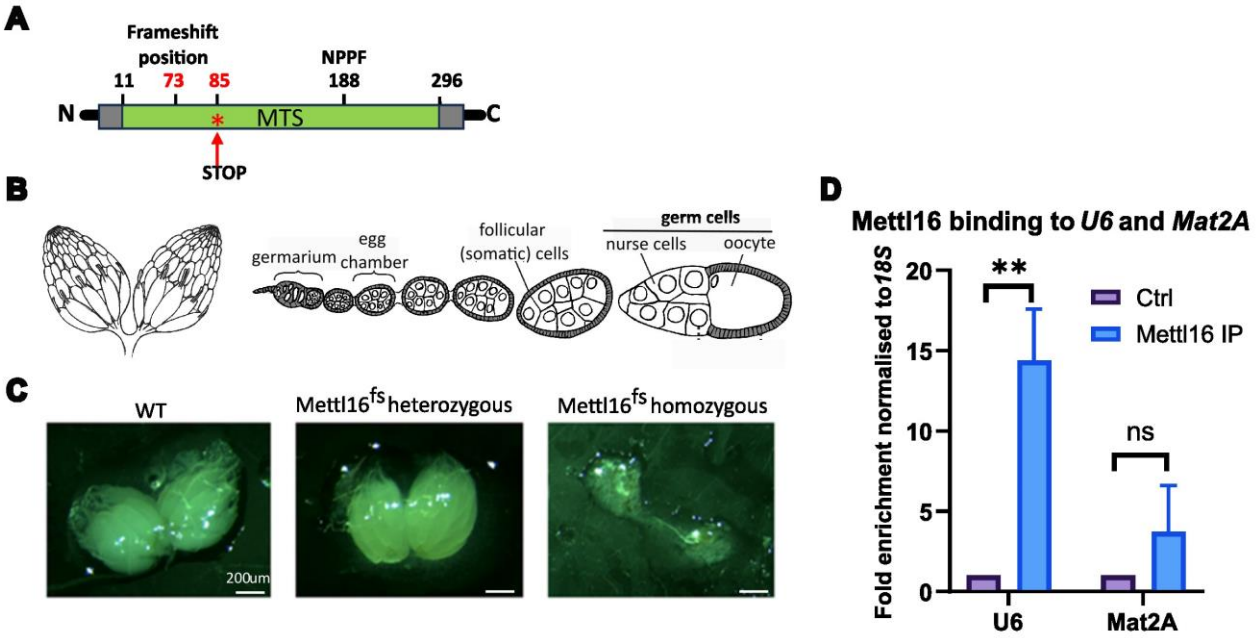

Figure 15. Mettl16 is essential for ovarian development.
(A) Representation of Mettl16 mutant allele (Mettl16fs) consisting in a dinucleotide insertion causing frameshift and a premature stop codon.(B) Representation of fly ovaries. Figure adapted from [Olovnikov (2013)].
(C) From left to right: ovaries from WT, heterozygous and homozygous Mettl16fs mutant, taken at a light microscope.
*(D) Results of RNA immunoprecipitation showing U6 and Mat2A enrichment in a Mettl16 pull-down. Mean ± standard deviation of 3 biological replicates. **P < 0.01*

Preliminary remarks Part II: Nm

For the second part of my thesis I worked on the methyltransferases Mettl25, Mettl25b and Ftsj3. I performed the cloning for their overexpression in S2R+ cells and in flies, and the cloning of the gRNAs for the generation of KO fly lines. I generated the mutant lines (Fig. 17A-B), performed the staining in S2R+ cells (Fig. 16C-D), the qRT-PCR on fly staging samples (Fig. 16A-B; Supplementary fig. 15) and upon aging,(Fig. 18A), the lifespan assay on Mettl25 mutant lines (Fig. 18B, Supplementary fig. 13A,C), the IP to detect Mettl25 interactors (Fig. 19A), the Puromycin incorporation assay on Mettl25 and Mettl25B mutants (Fig. 19B; Supplementary fig. 14) and the RNA-seq and riboseq on Mettl25 mutant lines (Fig. 20A-D). Lastly, I performed RTL-P to verify Ftsj3 target specificity and MRP, 18S and 28S rRNAs expression upon *Ftsj3* and *Fib* KD in S2R+ cells (Fig. 22B-C).

Contributions:

Dr. Tina Lence (Prof. Dr. Jean-Yves Roignant)
Performed *D. melanogaster* staging and prepared the Ftsj3 KD RNA-seq libraries.
Jessica Leismann
Performed the staining for Ftsj3 and the qRT-PCR of Ftsj3 in fly staging samples
Vishwaja Jhaveri (Prof. Dr. Jean-Yves Roignant's lab)
Performed the lifespan assay on Mettl25 OE line
Prof. Dr. Iouri Motorin
Performed RiboMeth-seq to map Mettl25-dependent Nm.
Dr. Athena Sklias (Prof. Dr. Jean-Yves Roignant's lab)
Performed bioinformatic analysis of RNA-seq data and nanopore data.
Dr. Marion Leleu (EPPL; Lausanne)
Performed bioinformatic analysis of Ribo-seq data.
Jiaxuan Chen and Mario Dejung (Proteomics core facility, IMB, Mainz)
Performed quantitative proteomics and data analysis of Mettl25 interactome.
Sonia Cruciani (Prof. Dr. Eva Maria Novoa's lab)
Performed nanopore sequencing.
Michael Wiederkehr (Prof. Dr. Roignant's lab) f
Helped me generate and maintain Mettl25 KO lines in Roignant's laboratory in Lausanne.

4. Results Part II: Nm

4.1. Characterization of Mettl25 and Mettl25b as novel Nm methyltransferases

rRNA and tRNA are the most abundantly methylated molecules on the ribose moiety. While the snoRNA-dependent Fibrillarin complex is responsible for methylation of most of the rRNA sites, for tRNAs several stand-alone methyltransferases come into action to methylate, with different specificities, one or more positions and tRNA isomers (described in Chapter 1.4.4). Therefore, while mapping methodologies are uncovering with increasing precision and sensitivity all the Nm sites, it is challenging to keep up with the pace in the identification of the responsible enzymes for each of these sites. Recently, novel tRNA Nm writers have been identified in vertebrates, in Prof. Dr. Suzuki's laboratory, in the proteins Mettl25 and Mettl25b (data not published; personal communication). The presence of these two orthologs in *Drosophila* (Fig 7A) provided us the possibility to address Nm functions on tRNA and characterize these enzymes at a molecular and physiological level.

4.1.1. Mettl25 and Mettl25b are mainly cytosolic and expressed at low levels throughout development

Mettl25 and Mettl25b are part of the METTL family, including enzymes methylating DNA, RNA and proteins, and enzymes of which functions are still unknown. Evolutionarily, Mettl25 and Mettl25b are the most closely related enzymes of the METTL family, whose common ancestor separated from the ancestor that gave rise to all the other known METTLs, with the exception of the most ancient Mettl15 (Wong and Erin-Lopez, 2021). In *Drosophila*, the orthologs of these 2 enzymes, *CG33964* and *CG2906* (from now on called respectively Mettl25 and Mettl25b) are on the second chromosome, and encode for proteins sharing 26% of amino acid sequence identity. The first exon of Mettl25 transcript encodes for a different protein, CG13175, of unknown functions, and the transcript largest intron encodes for Small ribonucleoprotein particle SmF, involved in the splicing process (Thurmond et al., 2019). Mettl25b has two isoforms, one of which is translated from the end of exon 2 and is therefore shorter (Thurmond et al., 2019).

To gain insight into the functions of these enzymes, we performed RT-qPCR, to check their expression levels during development, as well as immunostaining, to check their subcellular localization. Mettl25 mRNA levels are low from hour 12 of embryonic development, as well as in larvae and pupae. In the adult the expression mildly increases, and reaches its highest peak in the ovaries (Fig. 16A). Mettl25b levels are comparable with

Mettl25, low in embryonic and larval stages. In this case, a mild increase is observed during pupal stages, suggesting that the enzyme might be involved in the regulation of the metamorphosis (Fig. 16B). Concerning their subcellular localisation, in S2R+ cells, overexpression of eGFP-tagged Mettl25 and Mettl25b shows a cytosolic expression, with Mettl25 occupying the nucleus as well (Fig. 16C).

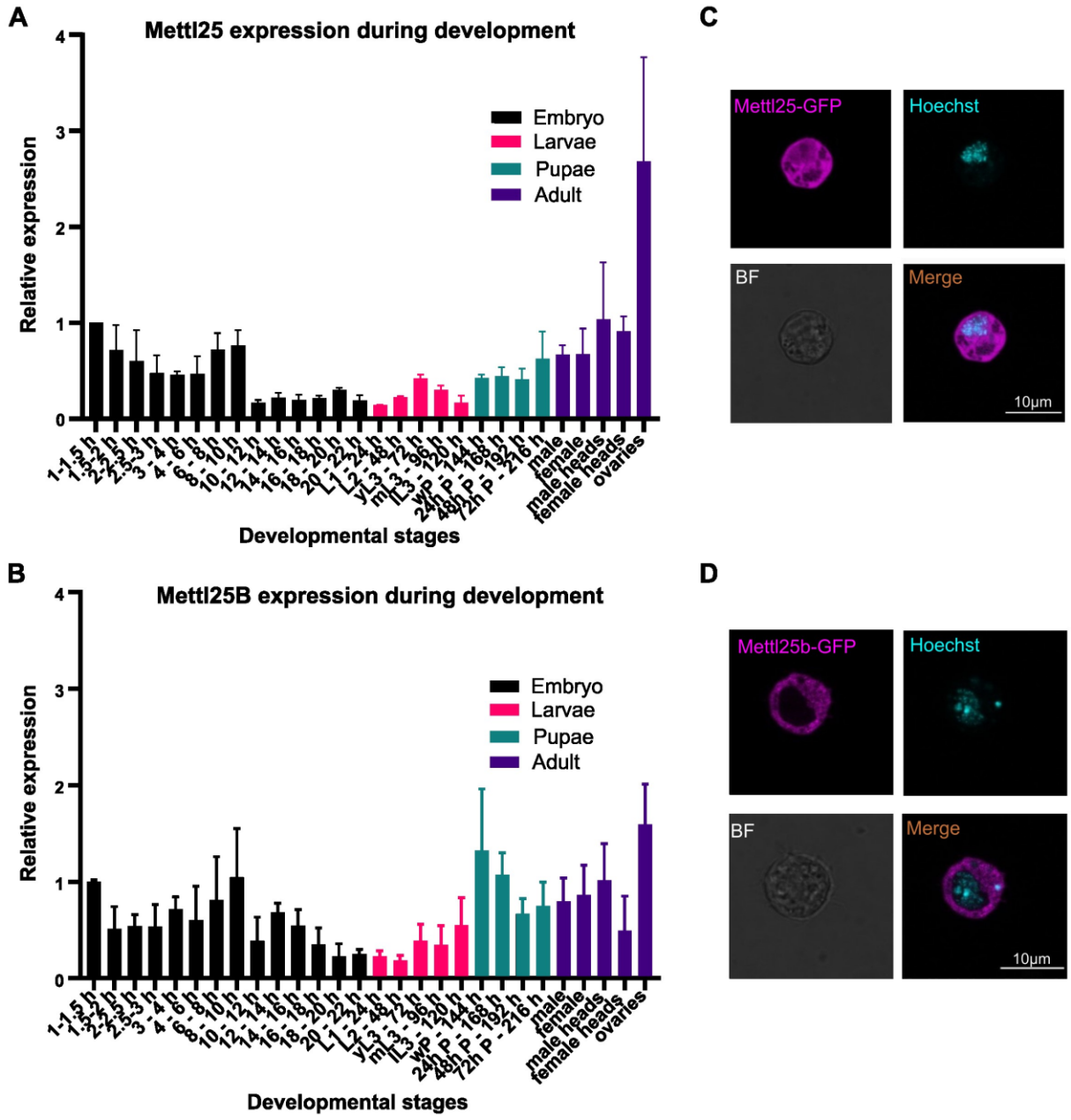

Figure 16. Developmental expression of the cytosolic proteins Mettl25 and Mettl25b.
(A-B) Mettl25 (A) and Mettl25b (B) expression during development measured via RT-qPCR. Results represent mean ± standard deviation of three biological replicates.
(C-D) Subcellular localization of GFF-tagged Mettl25 (C) and Mettl25b (D) in S2R+ cells. Images taken with 63× objective. Scale bar: 10 µm. GFP-tagged protein in purple. BF = bright field.

4.1.2. Mettl25 is responsible of tRNA $^{Gly\text{-}GCC}$ methylation

In order to understand their role, we decided to employ the CRISPR-Cas9 system to generate KO fly lines. Using this system, we obtained 2 mutant alleles for Mettl25, called Mettl25$^{\Delta 2}$ and Mettl25$^{\Delta 4}$, characterized by a deletion of 2 and 4 nucleotides, respectively, upstream the predicted methyltransferase domain. The deletion leads to a frameshift from amino acid 53 and a truncated protein of 68 and 60 amino acids, respectively (Fig. 17A and Supplementary fig. 10). The resulting protein is expected to be not functional. These mutant lines are viable and do not show any visible defect.

For Mettl25b we also obtained 2 mutant alleles, named *Mettl25b$^{\Delta 2}$*, as it is characterized by a 2 nucleotides deletion and premature stop codon, and *Mettl25b$^{\Delta 1kb}$*, where the deletion, spanning over a thousand nucleotides, encompasses the putative methyltransferase domain and is therefore also expected to generate a non-functional protein (Fig. 17B and Supplementary fig. 11). While the Mettl25b$^{\Delta 2}$ line gave rise to a healthy progeny, the *Mettl25b$^{\Delta 1kb}$* allele is lethal and hence flies survive only as heterozygotes, over a *cyo* balancer (heterozygous flies are characterized by curly wings). This could be explained by the fact that the alternative, shorter, isoform of this gene is not affected by the 2 nucleotides deletion of the *Mettl25b$^{\Delta 2}$* allele (Supplementary fig. 11A), suggesting that the shorter isoform accomplishes the functions of the enzyme essential for fly viability. Alternatively, some off-target activity of the gRNA may have occurred.

To verify if Mettl25 and Mettl25b are also tRNA Nm writers in *Drosophila* we collaborated with Prof. Dr. Motorin, who performed RiboMethSeq (RMS) on tRNAs isolated from Mettl25$^{\Delta 4}$ and Mettl25b$^{\Delta 2}$ mutants in young flies. RMS, as described in Chapter 1.4.5., is a high-throughput sequencing method identifying Nm sites based on the 5' and 3'-end read coverage of fragments generated by alkaline hydrolysis, given that an Nm site confers resistance to hydrolysis and therefore is never found at the 3'-end of a fragment generated with the RMS protocol. We found that Mettl25 depletion led to a loss of Nm at position 38 of tRNA$^{Gly\text{-}GCC}$, as identified by the increased 3'-end coverage at this position in the mutant line (Fig. 17C). This confirms that the enzyme is also a novel tRNA Nm writer in flies. RMS was repeated on old flies and ovaries. While the results in old flies were very similar to those obtained in young flies, in ovaries, G38 site was less protected from hydrolysis, suggesting lower methylation (Supplementary fig 12. A-B). This was unexpected since Mettl25 is expressed at a higher level in ovaries.

We also performed RMSon Mettl25b$^{\Delta 2}$ mutant flies. However we did not find any protected site suggesting that Mettl25b is not a tRNA methyltransferase in *Drosophila*. Alternatively, the short isoform that is not altered in this mutant might fulfill this function.

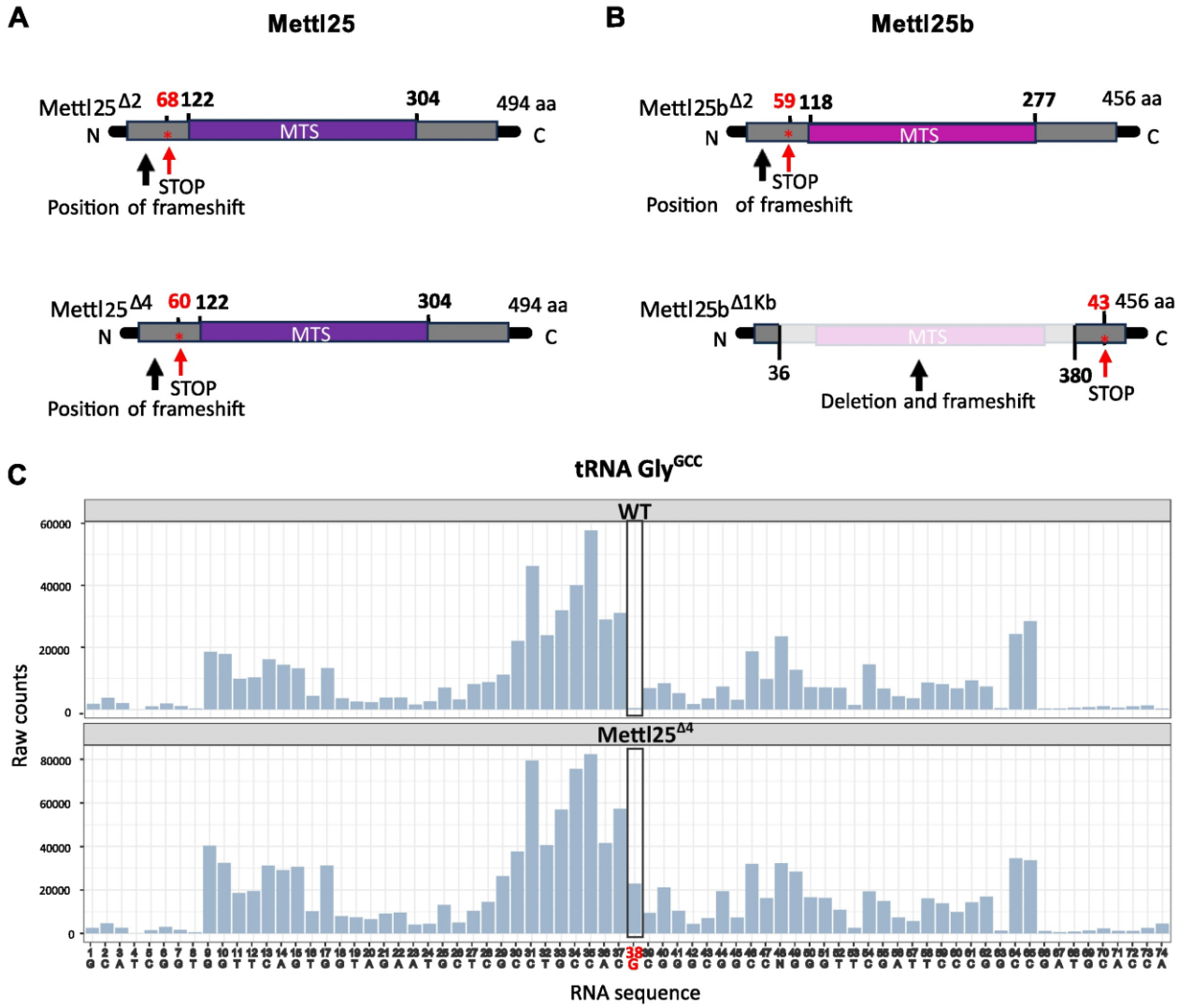

Figure 17. Mettl25 and Mettl25b mutants generation and target identification.
(A) Rappresentation of Mettl25 mutant alleles, consisting of a deletion of 2 or 4 nucleotides which leads to a truncated protein.
(B) Rappresentation of Mettl25b mutant alleles consisting in a 2 nucleotides deletion with subsequent frameshift or in a large 1 kb deletion in which the whole putative methyltransferase domain is lost.
(C) Results of RiboMethSeq (RMS) showing the 3' coverage at different positions along tRNA GlyGCC, of fragments generated in the RMS protocol. While WT flies show no coverage for residue G38, this increases in Mettl25 mutants, indicating loss of Nm at this position in absence of Mettl25. The experiment was repeated on three biological replicates, with the same outcome.

4.1.3. Mettl25 is highly expressed in aging flies and affects lifespan

Considering that these 2 enzymes are not highly expressed during development, we also checked whether their expression is subjected to fluctuations during aging. We collected fly heads on different days during aging starting from young flies up until 69 days old flies, which corresponds to when 80% mortality is reached in our WT population, and performed RT-qPCR. While Mettl25b showed a very mild increase in 69

days old flies, compared to their young counterpart, Mettl25 levels increased 3-fold in 2 months old flies and reached a sharp 5-fold increase in 69 days old flies (Fig. 18A).

Considering this strong expression in old flies, we wondered whether Mettl25 could influence lifespan. Therefore, Mettl25 mutant females and their isogenic controls were collected to perform a lifespan assay. Two hundreds flies per genotype were flipped to new tubes, to avoid accidental death due to the moistened yeast at the bottom of the tube, and dead flies were counted every second day. Mettl25$^{\Delta 4}$ mutant flies showed a significant reduction in lifespan compared to their isogenic control, suggesting an important role of this enzyme during aging (Fig. 18B). Similar results were observed for Mettl25$^{\Delta 2}$ mutants, for which a lower number of flies could be used as homozygotes were not present at a high percentage in the population (Supplementary fig. 13A). In line with these results, overexpressing Mettl25 increased lifespan compared to control flies. Overexpressing (OE) Mettl25, under a UAS promoter, was achieved by crossing the line bearing the *UAS-eGFP-Mettl25* sequence with a TubGal4 line. These 2 lines were used as control in the lifespan assay and compared to the TubGal4>UAS-eGFP-Mettl25 line. While TubGal4 flies are particularly weak and have a shorter lifespan, the second control line, UAS-eGFP-Mettl25, showed only a mild reduction compared to the Mettl25 OE line. This could be partially due to leaky expression of the UAS-driven Mettl25, despite the absence of Gal4 (Supplementary fig. 13B).

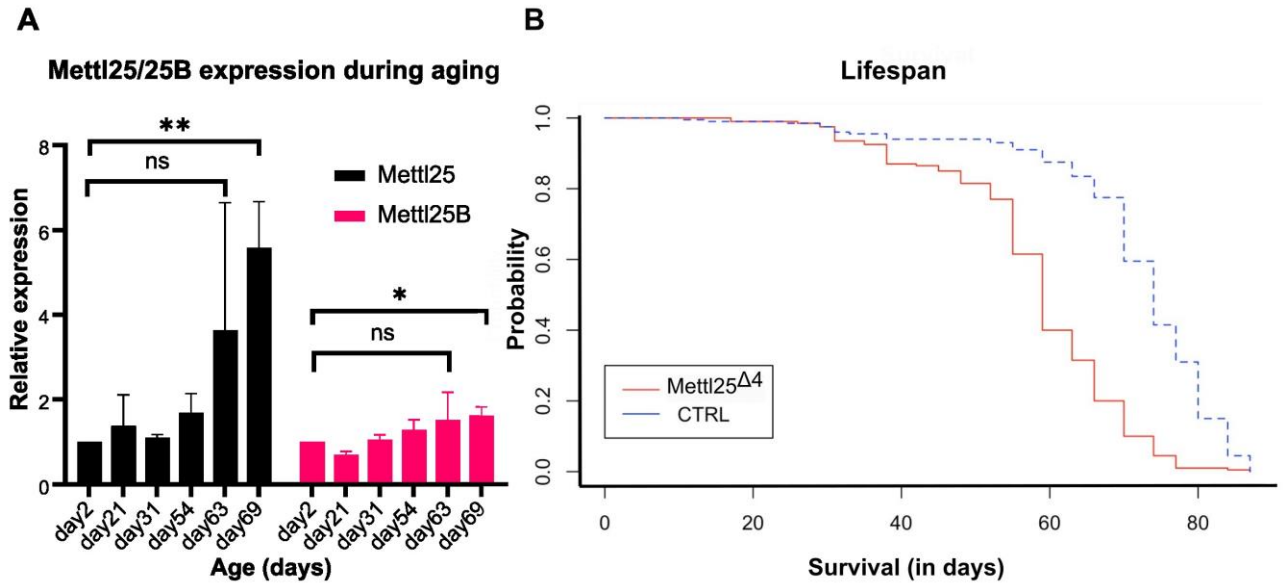

Figure 18. Mettl25 expression during aging is essential for survival.
*(A) RT-qPCR of Mettl25 and Mettl25b during aging. Graph shows the relative expression during aging compared to young flies (2 days old). Results are mean ± standard deviation of 3 biological replicates. *P<0.05, **P<0.01.*
(B) Lifespan assay showing reduced lifespan upon Mettl25 depletion. N Mettl25Δ4 = 200; N CTRL = 200. Logrank test_ P= <2e-16.

4.1.4. Mettl25 interacts with proteins associated with translation and its depletion increases puromycin incorporation in flies

To decipher Mettl25 functions at a molecular level, we aimed at identifying Mettl25 interactors via immunoprecipitation of a GFP-tagged Mettl25 followed by mass spectrometry in transfected S2R+ cells. Among the enriched proteins, beside some ribosomal and uncharacterized factors, proteins involved in lipid synthesis, splicing and stress response were identified (fig. 19A). The most highly enriched protein in the pulldown is CG5726, orthologous of the human cap binding complex dependent translation initiation factor (CTIF; *CG5726 | Drosophila melanogaster gene | Alliance of Genome Resources (alliancegenome.org)*. CG5726 has been suggested as Mextli (mxt) partner, which binds to eIF4E and promotes translational initiation (*CG5726 protein (Drosophila melanogaster) - STRING interaction network (string-db.org);* (Hernández et al., 2013). On the other hand, the human ortholog of CG5726, CTIF, is involved in the regulation of non-sense mediated mRNA decay (NMD) and in cap-binding proteins 80 and 20 (CBP80/20)-mediated translation, responsible of the translation occurring right after mRNA nuclear export, rather than the eIF4E-dependent steady-state translation (Kyoung et al., 2009), suggesting a potential versatile role for Mettl25 in regulating translation via interation with mxt and with CBP80/20.

Given the nature of Mettl25 interactors, we checked if translation was affected in the absence of Mettl25 via puromycin incorporation assay. This assay shows the relative level of nascent proteins as the antibiotic puromycin incorporates in the ribosome A-site during active protein synthesis and causes translational arrest; therefore, the amount of puromycin that is detected via western blot (WB) is directly proportional to the level of active protein synthesis occurring in the moment of sample collection. Flies were fed for 24 hours with a 5% sucrose solution containing 600 µM Puromycin, before being lysed for WB measurements (Supplementary fig 14A). By comparing WT and Mettl25$^{\Delta 4}$ flies, increased puromycin levels were observed in mutant flies, especially in females (Fig. 19B and Supplementary fig. 14B). This could indicate increased translation in Mettl25 mutants.

In contrast, when performing the same assay on Mettl25b$^{\Delta 2}$ line, a reduction in puromycin levels was observed in both genders, suggesting that Mettl25b promotes translation. Since the short isoform containing the methyltransferase domain is still intact in this mutant allele, this suggests that the non-catalytic functions encoded in the N-terminal part are responsible for this translation activation (Supplementary fig. 14B).

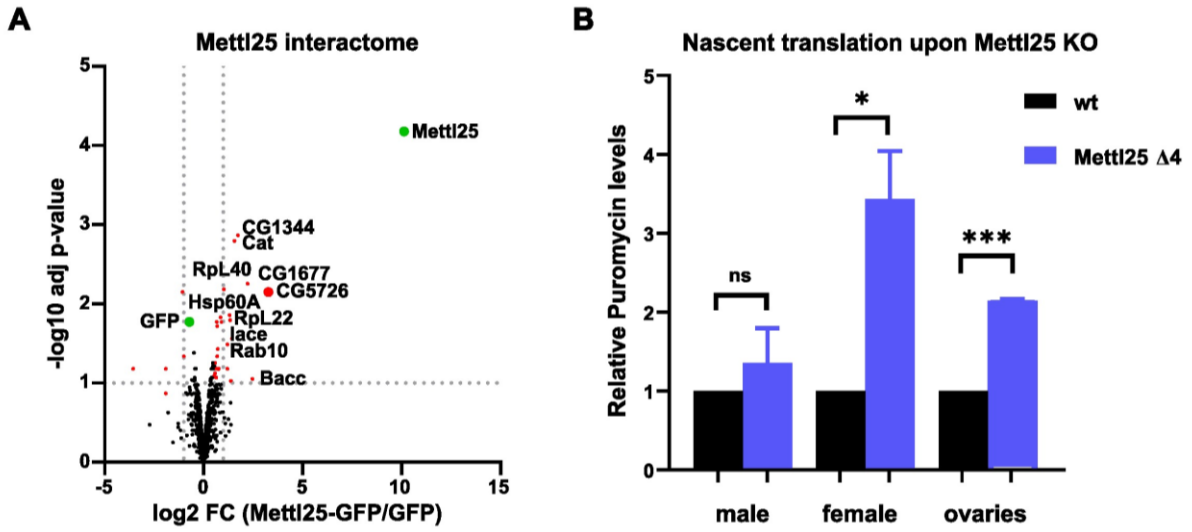

Figure 19. Mettl25 interactome and impact on translation.
(A) Volcano plot of Mettl25 interactome obtained by Mettl25-GFP pulldown in transfected S2R+ cells followed by mass spectrometry in four biological replicates. Fold change cut-off ≥ 2.
*(B) Bar graph showing relative puromycin incorporation in Mettl25 mutant males, females and ovaries and their wt counterpart. The experiment refers to three biological replicates. ns = not significant, *P<0.05, ***P<0.001.*

4.1.5. Mettl25 depletion affects carbohydrate metabolism and translation in flies

To gain some molecular insight on how Mettl25 affects gene expression, ribosome profiling was performed on Mettl25$^{\Delta 4}$ female flies and their wt counterpart. We found that most changes occur at the transcriptional level, with particular increase in transcription of genes involved in carbohydrate metabolism (Fig. 20A-B). However, a proportion of genes is instead exclusively affected at the translational level. Among those, the most affected are genes encoding for ribosomal proteins and translation elongation factors (eEFs), which are downregulated in Mettl25 mutants (Fig. 20A). Gene Ontology (GO) terms are mainly enriched in carbohydrate metabolism for the translationally upregulated genes, reflecting the fact that upregulation mainly occurs at the transcriptional level (Fig. 20C). For the downregulated genes instead, enriched terms include peptide metabolism and ribosome biogenesis, showing an overall translation impairment in this mutant line (Fig. 20D). Interestingly, the decreased synthesis of eEFs suggests impaired elongation, hinting at an increase in ribosome pausing, which could explain the raise in puromycin incorporation observed in Mettl25 KO flies, as paused ribosomes, characterized by reduced A-site occupancy, have been suggested to more easily accommodate puromycin (Starck & Roberts, 2002). Overall, these results suggest that Mettl25 depletion leads to translation impairment due to defects in ribosome biogenesis and translation elongation.

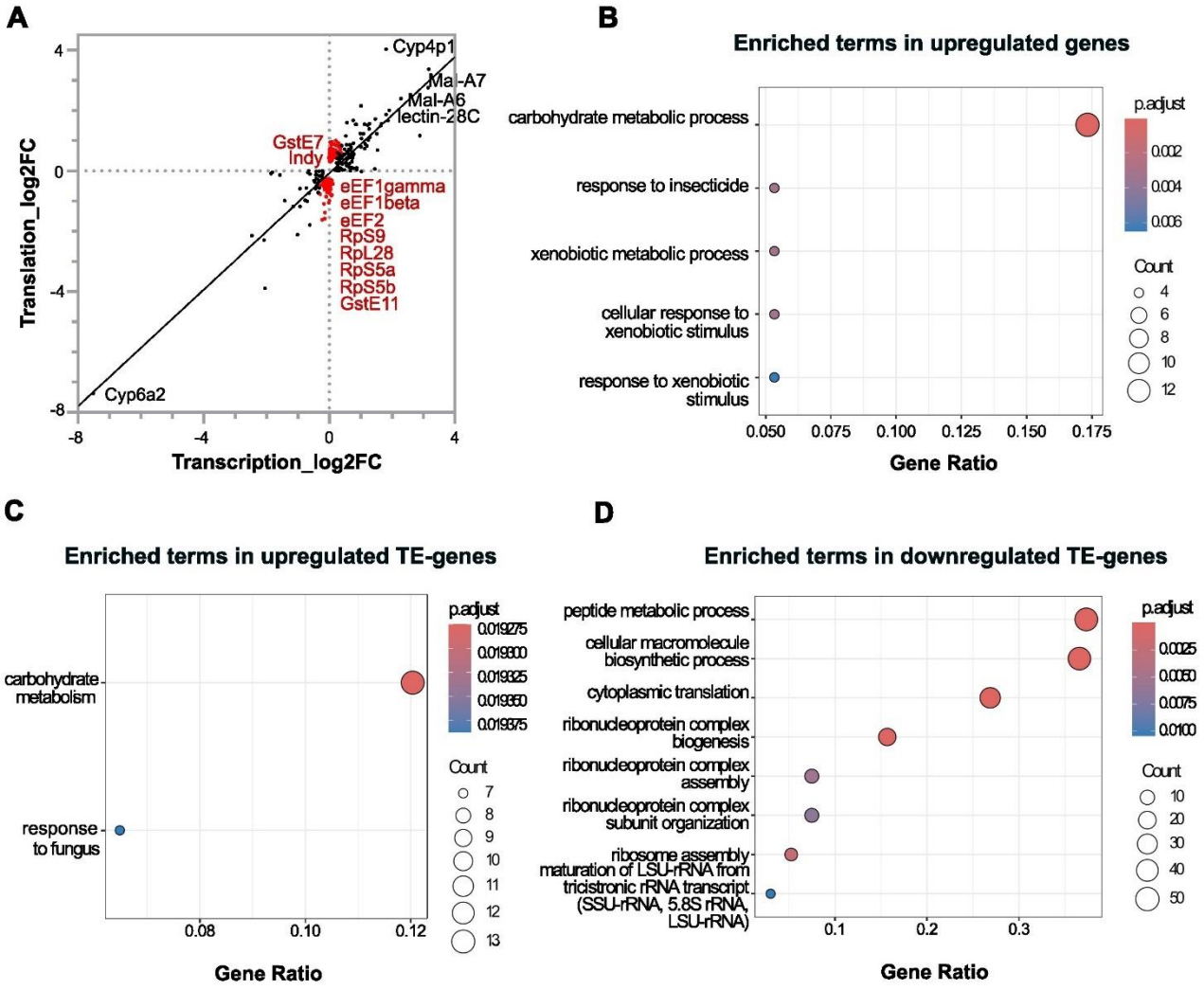

Figure 20. Transcriptional and translational changes upon Mettl25 KO via ribo-seq.
(A) *Differentially transcribed and/or translated genes in Mettl25 mutant flies compared to isogenic control. Black dots along the diagonal indicate genes that are affected both at the transcriptional and translational level. Red dots indicate genes that are affected only at the translational level.*
(B) *Enriched terms of transcriptionally upregulated genes upon Mettl25 KO (FDR < 0.05).*
(C-D) *Enriched terms in upregulated translated (TE) genes (C) and downregulated TE genes (D) in Mettl25 mutant flies (FDR < 0.05).*

4.2. Characterization of CG8939: ortholog of human Ftsj3

4.2.1. Ftsj3 is a nucleolar protein mainly expressed during fly embryonic development

The yeast ortholog of human FTSJ3 is known to methylate guanosine on the pre-rRNA (Lapeyre et al., 2004) and suggested to methylate mRNA especially on uridine residues (Bartoli et al., 2018). In order to study the functions of the fly ortholog of FTSJ3, CG8939, we checked its expression level during development and subcellular localization in S2R+ cells. CG8939, hereafter named Ftsj3, shows a pattern of expression similar to the other rRNA Nm writer Fibrillarin (Supplementary fig. 15), as its highest expression occurs in the early stages of embryonic development and in ovaries, suggesting important functions for early development (Fig. 21 A). When comparing the expression pattern of Ftsj3 with mRNA Nm levels in our WT flies, measured via mass spectrometry, it can be observed that Nm, especially on uridine and guanidine, is more abundant in embryonic stages, and its fluctuactions partially mirror Ftsj3 expression pattern (Fig.21 A). Yet, while Ftsj3 levels are low in the second half of embryonic development, Nm levels on mRNA remains high until the larval stages, suggesting that, if Ftsj3 is involved in mRNA Nm deposition, it is likely not the only writer.

In order to check its subcellular localization, Ftsj3 coding sequence was cloned with a FLAG-tag in a UAS plasmid, and transfected into S2R+ cells together with a plasmid expressing a GFP-tagged version of the cytosolic marker Barentz. Ftsj3 (in red) occupies a small portion of the nucleus, and it is absent from the cytosol, indicating that *Drosophila* Ftsj3, like its human ortholog, is a nucleolar protein, likely involved in rRNA maturation (Fig.21 B).

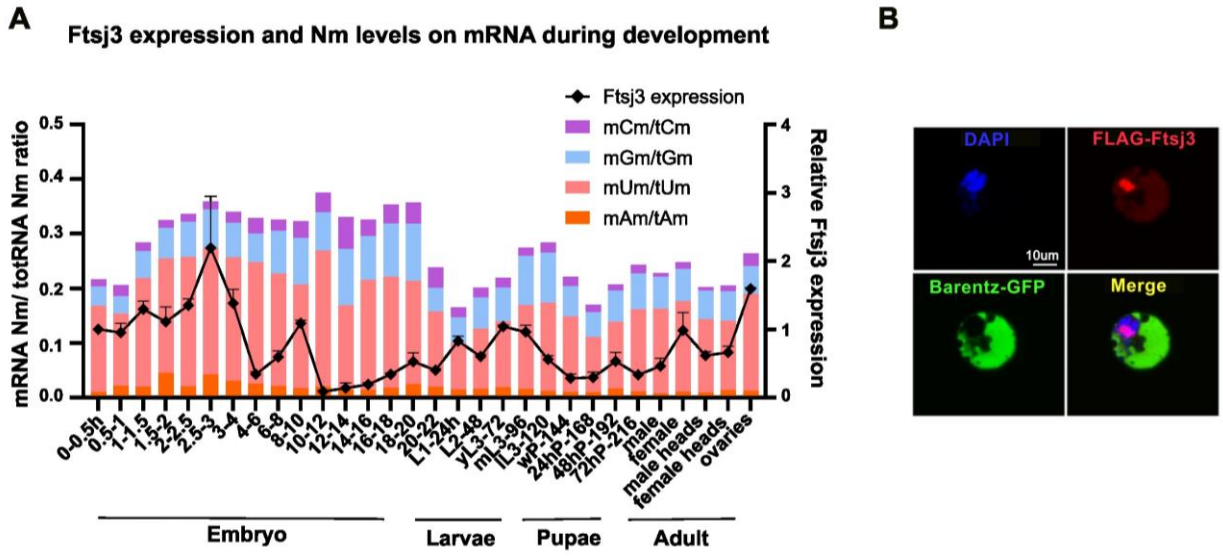

Figure 21. Ftsj3 expression during fly development and bubcellular localization.
(A) *Ratio of Nm levels on mRNA over Nm levels on total RNA during fly development measured via mass spectrometry on all four nucleotides. Ftsj3 expression during Drosophila development, measured via RT-qPCR in three technical replicate sand shown as mean ± standard deviation.*

(B) *Subcellular localization of FLAG-Ftsj3 (red) in immunofluorescently labelled S2R+ cells. Nuclei (blue) were counterstained with DAPI, Barentz, a cytosolic marker, shown in green. Images obtained with confocal microscope using a 63x objective. Scale bar: 10µm.*

4.2.2. Ftsj3 methylates RNase MRP in flies

To address Ftsj3 functions in flies, CRISPR/Cas9 system was employed to generate KO lines. Unfortunately, despite many attempts and the use of multiple gRNAs to target different sequences along the *Ftsj3* gene, a KO allele was not obtained.Therefore, a KD was performed in S2R+ cells and the extracted RNA was analysed in Dr. Novoa's laboratory, expert in nanopore sequencing, to identify potential Ftsj3 target RNAs. If Ftsj3 is the writer responsible for Nm deposition at a specific site, the signal detected from this site significantly differs between control sample and *Ftsj3* KD sample. The difference in this signal between control and KD samples (Δ feature) is the parameter used to identify Nm sites at single nucleotide resolution. Surprisingly, Ftsj3 KD did not unveil any Nm site on rRNAs targeted by Ftsj3. We instead identified a single site on a non-coding RNA important for rRNA maturation: the ribonuclease MRP, responsible for endonucleolitic cleavage of the pre-rRNA between the future 18S and 5.8S RNAs (Lygerou et al., 1996). The Ftsj3-methylated residue identified by nanopore is residue C137, the only site generating a Δ feature significantly raising above the background in two replicates (Fig. 22 A). On the contrary, KD of Fibrillarin generated strong signals revealing the many rRNA sites targeted by the enzyme (Supplementary fig. 16).

To validate the results obtained by nanopore, RTL-P [Reverse Transcription at Low deoxy-ribonucleoside triphosphate (dNTP) concentrations followed by Polymerase chain reaction (PCR)] was performed in control S2R+ cells and *Ftsj3* KD cells. Nm sites constitute a hindrance for reverse transcriptase if reverse transcription is performed at low dNTPs concentration and this can be used to test the methylation status of a specific site via qPCR, using primers aligning near the tested Nm site. Higher PCR amplification upon Ftsj3 KD compared to the control sample indicates that the tested site is methylated by Ftsj3 and methylation is lost upon its depletion. While for well known sites on the 18S and 28S rRNA, of which the Nm writer is Fibrillarin, the results showed a clear difference between control and *Fib* KD sample, for C137 on *MRP* results were less consistent Fig. 22 B). In particular, while 2 replicates showed a clear reduction of Cm137 exclusively upon *Ftsj3* KD and not upon *Fib* KD, the third one did not. Moreover, the double KD of *Fib* and *Ftsj3* showed Nm reduction only in one replicate, and not in the other 2, nor in the previous optimisation attempts.

Several reason could explain these results. *In primis*, the abundance of the tested RNA, as well as the presence of neighbouring Nm sites, can strongly mislead the result interpretation. In fact, optimisation of the protocol to test methylation of the two adjacent sites on the 28S rRNA was more challenging than for the 18S rRNA, due to the presence of Nm on one of the 2 sites and to the fact that Ftsj3 might be able to

compensate for Fib absence and methylate both the neighbouring U3454 and G3455 sites, which correspond to the known yeast U2921-G2922, targeted by Fib and Spb1 (Ftsj3), respectively (Lapeyre & Purushothaman, 2004). Another reason for the inconsistency of the results for *MRP* Nm site validation could be that *MRP* is probably not fully methylated, as it is also suggested by the weakness of the signal obtained by nanopore sequencing for Cm137 (Fig. 22 A). The effects of the depletion of Fib and Ftsj3 on rRNAs and *MRP* levels were checked via qPCR (Fig. 22 C). Interestingly, while the 28S and 18S rRNAs levels were unaffected by the methyltransferases KD, *MRP* expression increased, particularly upon Fib KD, suggesting that incomplete ribosome biogenesis due the lack of Fibrillarin leads to increased expression of *MRP*.

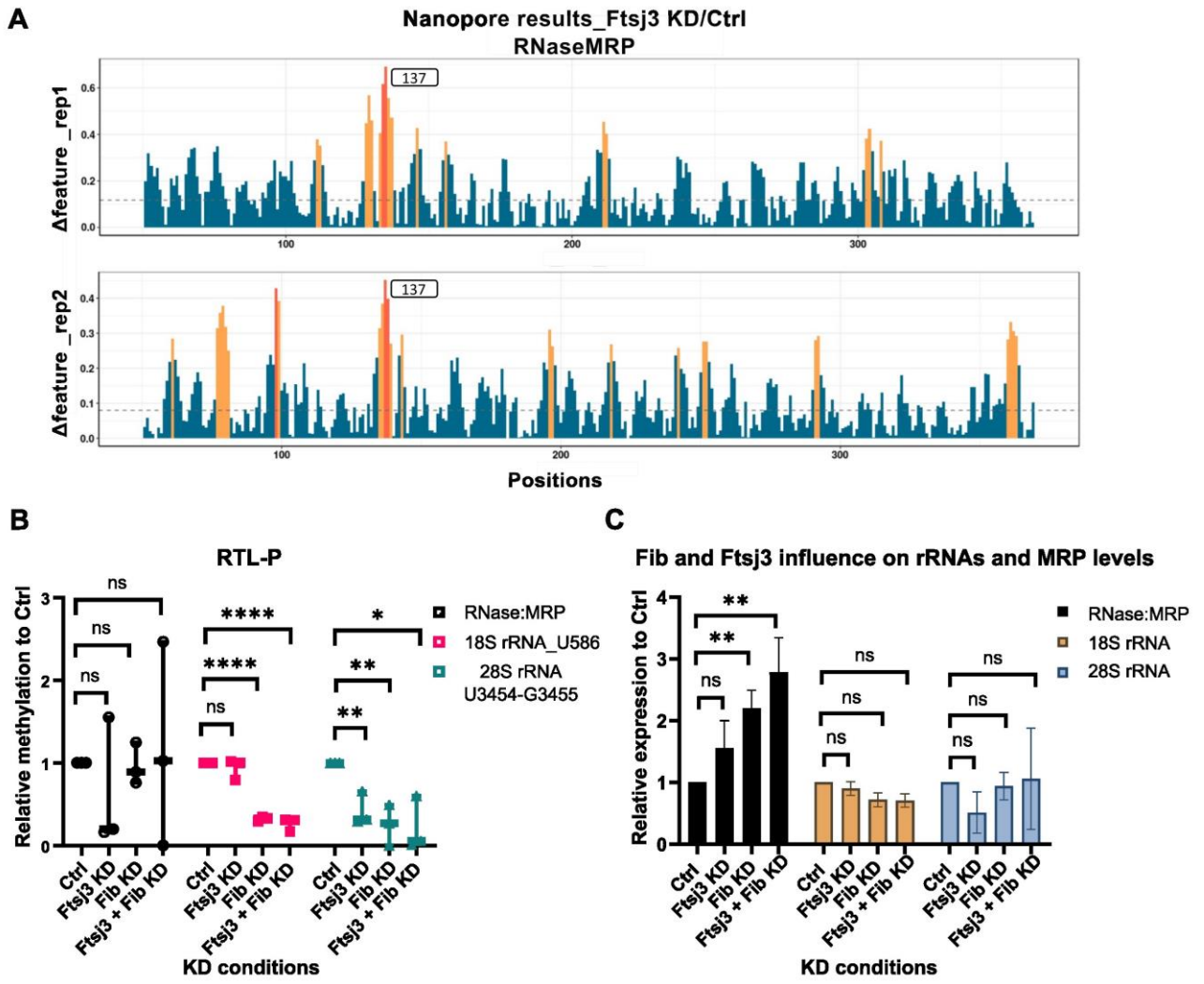

Figure 22. Ftsj3 methylates RNase MRP RNA.
(A) Nanopore sequencing of MRP showing the differences in the signals between control and Ftsj3 KD samples, shown on the Y axes. Positions along the MRP sequence are indicated on the X axes. Positions where the differences between the signals generated by the two samples are significant, indicating lack of Nm upon Ftsj3 KD, are shown in orange, over a blue background.
(B) RTL-P results showing differences in Nm levels at the given sites on MRP, 18S and 28S rRNA upon Fib and /or Ftsj3 KD in S2R+ cells. Results are shown as mean ± standard deviation of three biological replicates.
(C) RT-qPCR measurements of MRP, 18S and 28S rRNA levels upon Ftsj3 and/or Fib KD in S2R+ cells. Results show mean ± standard deviation of three biological replicates.
*ns = not significant; ****P < 0.0001; **P < 0.01; *P < 0.05.*

4.3.3. Ftsj3 depletion fosters transcription of DNA damage repair factors

In order to address the consequences of Ftsj3 absence at a molecular level, RNA-seq libraries were prepared from S2R+ cells subjected to treatment with dsRNA targeting the *Ftsj3* transcript or a control *lacZ*. The results of the analysis show a general metabolic downregulation, especially of carbohydrates and organic acids (Fig. 23 B). In contrast, an upregulation of genes involved in the DNA damage response and terms related to translation like tRNA aminoacylation and translational initiation was observed (Fig. 23 A). Interestingly, a recent paper has shown that in mouse germ cells, during meiosis, pre-rRNA and other associated factors, like ribosomal proteins, some snoRNAs, and the RNase MRP, are located to XY bodies. XY bodies are phase-separated granules that form during meiosis and are enriched with double strand break (DSB) DNA repair factors, which interact with and are probably recruited to the XY bodies by pre-rRNA (Gai et al., 2022). Impaired rRNA biogenesis also impaires phase-separation of DNA repair factors (Gai et al., 2022). It is thus possible that something similar happens in *Drosophila*, and pre-rRNA and its associated factors ensure DNA repair to occur. Therefore, a compromised rRNA biogenesis that would be due to unmethylated MRP could lead to defects in the DNA repair mechanism and fosters further transcription of repair factors. Additional work would be necessary to test this hypothesis.

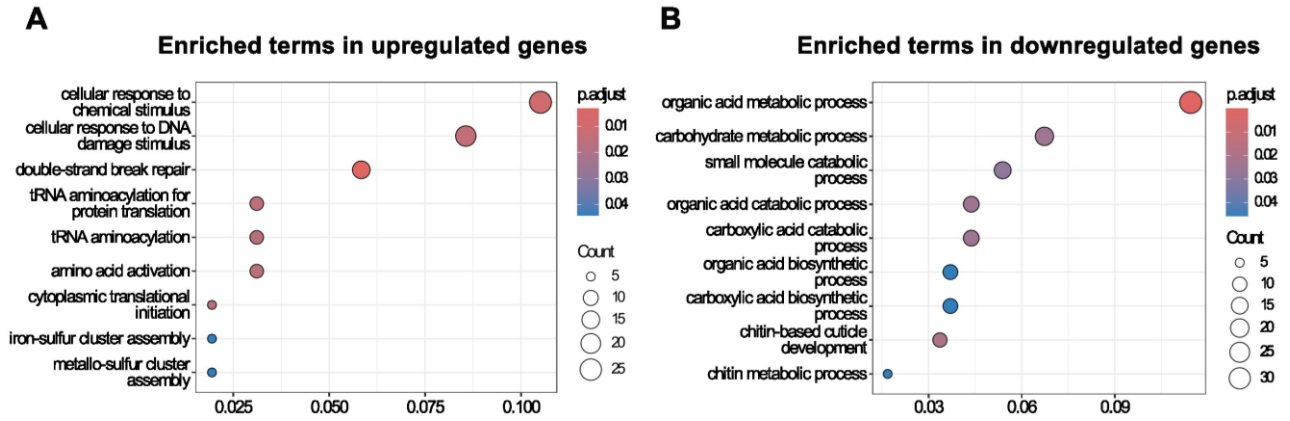

Figure 23. GO-term analysis of RNA-seq results in S2R+ cells.
(A-B) *Enriched terms in upregulated genes (A) and downregulated genes (B) in S2R+ cells upon Ftsj3 KD (FDR < 0.05).*

5. Discussion

Gene expression regulation is at the basis of every biological process: it allows growth, development, reproduction, the ability to adapt to environmental stimuli and to respond to stress. It consists of different layers of regulation, starting in the nucleus where chromatin is organised into hetero and eu-chromatin and modulates DNA accessibility to transcription factors. Several histone modifiers and chromatin remodellers come into play to fine-tune transcription, and the study of their functions has led to the birth of the epigenetic field.

RNA modifications, on the other hand, regulate the RNA fate, and have proven themselves equally important, earning, in the last decade, a new dedicated field, known as epitranscriptomics. Nowadays, more than 170 modifications have been identified on all RNA species in all three kingdoms of life, and some of them have been mapped transcriptome-wide and widely studied. For example, m^6A, the most known mRNA modification, has been shown to play a role in mRNA stability, translation, splicing, nuclear export, and processes like X-chromosome dosage compensation, brain functions and immunity (Chapter 1.3.1). In our lab, novel members of the mRNA m^6A writer complex have been identified in *Drosophila* and their involvement in splicing, sex determination, and neuronal functions has been uncovered (Lence et al., 2016). Moreover, the link between m^6A and a known translational repressor, Fmr1, in brain development has been shown (Worpenberg et al., 2021), contributing to expand the knowledge in the field. A growing number of studies is also focusing on some less known modifications. For example, the importance of the most abundant rRNA modifications, Ψ and Nm, in ribosome biogenesis has been broadly studied. Despite this, the functions of RNA modifications on most of the non-coding species still remains largely unknown.

My PhD project aimed at unveiling the functions of RNA modifications on non-coding species. The first part of my PhD focused on m^6A, with the purpose of identifying novel writers in *Drosophila melanogaster*. This goal was achived with the discovery of the rRNA methyltransferase Mettl5. We addressed its subcellular localization, interactome, target specificity and its impact on gene expression and brain functions in flies. The findings related to its roles are discussed in sections 5.1 to 5.5 of this chapter. Spliceosomal RNAs are also decorated by m^6A. The *U6* snRNA writer Mettl16 is conserved in flies and findings on its physiological role in reproduction are discussed in section 5.6.

The second part of my PhD focused on studying Nm and identifying novel writers in order to unveil new functions of this modification. Nm is a very unique modification. First of all, differently from all the others, it is deposited on the ribose moiety and it can therefore be present on all nucleotides. Secondly, it abolishes

the nucleophylic nature of the ribose 2'-OH group, conferring increased resistance to alkalyne treatment and enzymatic digestion, increasing RNA stability. Moreover, it is present in all RNA species and is abundant on highly structured RNA, in particular rRNA and tRNA, suggesting a role in structural stabilisation and translation. This part of my PhD mainly focused on the characterization of the novel tRNA Nm writer Mettl25, for which we uncovered its methylated target in flies, its interactors and its impact on translation, revealing a role in lifespan determination. These results are discussed in sections 5.8 to 5.11. Finally, efforts into the characterization of other Nm writers, Mettl25b and Ftsj3, are respectively discussed below in sections 5.8 and 5.12-5.14.

5.1 Mettl5 is a novel SAM-dependent rRNA m^{6}A writer stabilised by Trmt112 to methylate the 18S rRNA

Mettl5 is a conserved SAM-dependent methyltransferase, identified in our KD screen as m^{6}A writer in *Drosophila* (Fig. 7). From our pull-down experiments and structural predictions, we observe that its structure is conserved during evolution, and its stability depends on the interaction with Trmt112 (Fig. 11), which was shown to stabilise Mettl5 in archaea and human as well (Van Tran et al., 2019). This interaction allows the formation of an eleven-stranded β-sheet between the two proteins, which protects a conserved core of hydrophobic amino acids from the hydrophylic environment, and it is surrounded by positively charged residues involved in the RNA binding. In collaboration with Prof. Dr. La Fontaine, we established via chromatography, that Mettl5 in flies accomplishes the same molecular functions as its human ortholog: it methylates one single adenosine in the 18S rRNA (Fig. 9C). While the degree of conservation suggests that this modification is highly important, as it is lacking only in bacteria and yeast, it is puzzling that a protein is produced to modify only one residue. Future efforts, in this regard, might be put into addressing the presence of other possible targets of the enzyme, employing individual-nucleotide resolution crosslinking and immunoprecipitation (iCLIP) and methylation iCLIP (miCLIP) to identify respectively Mettl5 binding targets and m^{6}A sites in presence and absence of the enzyme, although results of the latter experiment might be hampered by the presence of many Mettl3-dependent m^{6}A sites on mRNA. A step in this direction has been taken by Ignatova et al., who performed an *in vitro* methylation assay suggesting that Mettl5 could methylate poly(A) RNA (Ignatova et al., 2020), perhaps when structured as helix 44 of the 18S rRNA. Interestingly, Mettl5 RNA binding mechanism resembles that of the DNA binding enzyme *Taq I* from *Thermus aquaticus* (Van Tran et al., 2019), which suggests that Mettl5 might be able to bind and/or methylate DNA. It would not be the first time that an RNA methyltransferase is shown to methylate DNA, as it is the case for Mettl4, which deposits 6mA on DNA to regulate transcription, by helping the maintenance of an histone inhibitory mark (Kweon et al., 2019). This would be an interesting hypothesis to investigate, particularly in

higher eukaryotes, where Mettl5 is mainly nuclear. In our model Mettl5 is cytosolic (Fig. 8C), suggesting that DNA binding is not a feature of the *Drosophila* ortholog, and it might have appeared later in evolution. This does not exclude that Mettl5 in flies might target other cytosolic RNAs or have other functions independent of its catalytic domain. Moreover, the distinct subcellular localisation of Mettl5 in different species might also indicate differences in the timing of rRNA methylation, which could reflect distinct functional outcomes during ribosome biogenesis and/or translation.

5.2- Mettl5 is a potential translational regulator for brain development

While the nuclear localisation of METTL5 in human might hint at a role in rRNA maturation, results show that neither in human nor in our fly model, the lack of m^6A on the 18S rRNA affects its biogenesis (Fig. 10) (Leismann et al., 2020; Van Tran et al., 2019). Structural evidence rather suggest that Mettl5 methylates the 18S rRNA at later stages of ribosomal maturation, after which the helix 44, containing the targeted adenosine, changes conformation and is no longer accessible to other proteins (Van Tran et al., 2019). From our study we also observed that the 18S rRNA is fully methylated implying that this m^6A is a constitutive modification. This suggests that Mettl5-dependent methylation might occur as a checkpoint indicating that maturation can proceed and the ribosome can be translationally active. What has been also suggested is that the 18S rRNA methylation serves to establish stronger connection between the rRNA C_{1703} and m^6A_{1832} sites with the mRNA during translation elongation (Rong et al., 2020), hinting at a role for Mettl5 in translation regulation. In this line, Xing et al. show that presence of m^6A on the 18S rRNA fosters more efficient translation of A/T rich transcripts (Xing et al., 2020). Interestingly, transcripts with codons mainly ending with A/T are more evolutionalrily conserved and co-regulated as they often encode for proteins of the same complex. These transcripts are mainly associated with metabolic processes, RNA and protein modifications, and cell proliferation, while genes enriched in G/C ending codons are mainly involved in cellular differentiation, particularly towards the neuronal lineage (Benisty et al., 2023).

Many studies, including ours, hint at a role for Mettl5 in neuronal differentiation and brain functions, especially during embryonic development. We have observed that Mettl5 in flies is mainly expressed in the embryonic central nervous system (CNS) (Fig. 8D-E) and that adult flies show impairment in their spatial behaviour in absence of Mettl5 (Fig. 12). Recent studies in mice showed loss of pluripotency in stem cells upon Mettl5 depletion, particularly towards the neuronal lineage, and precocious differentiation (Ignatova et al., 2020; L. Wang et al., 2020; Xing et al., 2020). An hypothesis to explain this phenotype, in line with the above-mentioned study linking Mettl5 with increased translation of A/T-rich transcripts, could be that the enzyme, rather than promoting neuronal maturation, is important to determine the **right timing** for stem

cells differentiation. Premature differentiation, particularly during neurogenesis, can lead to the exhaustion of the progenitors pool and therefore to an incomplete brain development. Mettl5 might foster the expression of genes involved in proliferation and metabolism (A/T-rich genes) to maintain the progenitor pool and their pluripotent potential. Other factors might then come into play to favour, at a later stage, the expression of genes promoting differentiation. This correlation of Mettl5 and translation of proliferation genes would apply in the context of cancer as well, where studies have shown a link between Mettl5 and increased proliferation in hepatocellular carcinoma and pancreatic cancer (Hua Huang et al., 2022; Xia et al., 2023), hence providing a new therapeutic target.

5.3 Molecular functions of Mettl5 and brain development

To better understand the molecular underpinnings of Mettl5 involvement in brain functions in flies, we checked the consequences of Mettl5 absence on transcription and translation performing RNA-seq and ribo-seq libraries in fly brain. Results report a massive transcriptional dysregulation showing upregulation of genes involved in carbohydrate metabolism and downregulation of genes involved in lipid metabolism (Fig. 13A-B). Interestingly, lipids are key molecules for brain development and functions and have been linked to intellectual disability. More specifically, in vertebrates, defective lipid metabolism observed upon fatty acid synthase FASN depletion, has been associated to impaired adult hippocampal neural stem/progenitor cells (NSPC) activity. This results in endoplasmic reticulum (ER) stress due to lipid accumulation, with consequences on cell proliferation and on cognitive functions (Bowers et al., 2020). Intriguingly, fatty acid synthase 2 (FASN2), the fly ortholog of the human FASN associated to intellectual disability, is significantly downregulated in Mettl5^{fs} flies (Supplementary fig. 17). Bowers et al. also show that FASN-dependent metabolic disorders impair human NSPCs proliferation in brain organoids, leading to smaller organoids (Bowers et al., 2020), which recalls the reduced brain size of our Mettl5 flies and the microcephaly phenotype observed in Mettl5 patients (Supplementary fig. 8C) (Riazuddin et al., 2017), suggesting a link between the defective lipid metabolism and the impaired brain functions observed in our mutant line. Furthermore, Mettl5-dependent effect on sugar and lipid metabolism is common to several other model organisms, including mice and nematodes (H. Chen, Liu, et al., 2020; Ignatova et al., 2020; Liberman et al., 2020; Rong et al., 2020; Sepich-Poore et al., 2022; L. Wang et al., 2020; Xia et al., 2023; Xing et al., 2020), suggesting that its functions are conserved throughout evolution. In one of these studies it was shown that upon METL-5 depletion in *C.elegans*, an increase in translation of Cyp-29A3 occurs. Cyp-29A3 fosters the production of the lipids eicosanoids, stress signaling molecules, which increase stress resistance and lifespan in *C. elegans* (Liberman et al., 2020).

At a translational level, we observed an upregulation of glucosidase and oxidoreductase activity, which suggests that the brain of Mettl5 KO flies might be under oxidative stress, in line with a possible ER stress response activation, due to lipid accumulation. Serine-endopeptidases and hydrolases, which include lipid hydrolases, are instead downregulated in Mettl5^{fs} flies (Fig. 13C-D). On the whole, our results show that lack of Mettl5 leads to a massive transcriptional dysregulation of metabolic genes, which potentially triggers lipid-dependent ER stress in fly brain and causes impairement in brain functions.

5.4 Molecular functions of Mettl5 in the adult

Interestingly, despite the predominant embryonic expression of Mettl5, the m^{6}A mark decorates the 18S rRNA in adult flies as well. Performing a behavioural assay known as Buridan paradigm, we assessed brain functionality in adult Mettl5 KO flies in terms of walking behaviour, to check whether their activity and orientation were compromised (Fig. 12). Compared to their isogenic control, Mettl5 KO flies showed problems in their orientation, suggesting impaired functionality of the central complex, region of the brain dedicated to the coordination of walking and the formation of short-term memories, essential for flies to get oriented around spatial clues. Although, whether this effect is determined by an impaired brain maturation during early development, or it is a direct effect of Mettl5 absence in the adult fly, is not clear. It would be interesting to dissect the differences between Mettl5 functions in embryo and adult, for which purpose the development of a conditional KO line would help. In our KO line we also observed a smaller brain-to-body ratio compared to WT flies, suggesting that brain development is not fully completed and reminiscent of the microcephaly phenotype observed in patients with similar mutations in the *Mettl5* gene (Richard et al., 2019). With a conditional KO line, Mettl5 could be depleted in the adult, to not compromise CNS embryonic development and therefore address its functions specifically in adult flies.

It would be interesting to address potential context-specific functions of Mettl5 in adults. For example, some studies linked Mettl5 to the regulation of the stress response (H. Chen, Liu, et al., 2020; Liberman et al., 2020). In *C. elegans* this was caused by a Cyp-29A3-dependent increase in lipids eicosanoids upon METL-5 depletion,which in turn increased the nematode stress resistance and lifespan(Liberman et al., 2020). It is interesting that METL-5 acts as a negative regulator of the stress response and reduces lifespan. These findings suggest that METL-5 might be rather required in normal conditions but inhibited upon stress to guarantee translation of Cyp-29A3 and worm survival. The idea of m^{6}A erasers intervening upon stress to demethylate the 18S rRNA is unlikely as no ortholog of ALKBH5 and FTO have been found in *C. elegans* nor in *Drosophila*; moreover the conformation of a mature ribosome would render inaccessible the 18S m^{6}A site to putative erasers. An interesting possibility is that Mettl5 gets post-translationally modified upon stress or has

autoinhibitory functions so that some newly synthesized 18S rRNAs are unmethylated, generating context-specific ribosome heterogeneity and promoting translation of stress-related mRNAs.

5.5 Outlook Mettl5

We have addressed Mettl5 functions in *Drosophila*, identifying the 18S rRNA as its target and showing how the lack of this modification does not affect rRNA biogenesis but impairs lipid metabolism and brain functions. Future efforts should be put into addressing the following open questions:

- Are there other methylated targets by Mettl5?
- Does Mettl5 have catalytically-independent functions?
- What are its functions in the adult brain?
- Is Mettl5 post-translationally modified or inhibited upon stress? Does this lead to hypo-m^6A and hence ribosome heterogeneity?
- Does Mettl5 involvement in brain functions and potentially stress modulation affect fly lifespan?

To identify further targets of Mettl5, iCLIP and miCLIP, as well as *in vitro* methylation assays, could be employed. The development of a catalitically-dead KO line, as well as the possibility of performing rescue experiments with catalytically dead Mettl5, could help address the importance of the methyltransferase domain for its functions. Conditional KO lines or rescue experiments where Mettl5 expression is induced only in the embryo or only in the adult, followed by molecular and behavioural assay, would help address the impact of Mettl5 functions at different developmental stages. Evaluating the stress adaptability and the longevity of Mettl5 mutant flies, employing paraquat assay and lifespan assay, and addressing the levels of m^6A on the 18S rRNA and the translational profile of wt and mutant flies upon stress, would help identify versatile roles of this modification and potentially show another example of ribosome heterogeneity.

5.6 Other m^{6}A writers in *Drosophila*: the role of Mettl16 in ovarian development

In parallel with the study of Mettl5 functions, the role of another m^{6}A writer, Mettl16, in fly development, has been addressed in this study. We have first analysed its expression level during fly development and in the adult, to understand at which stages the enzyme exerts its functions, and found it particularly enriched in fly ovaries and in early embryo, suggesting essential functions during early developmental stages (Fig. 14C). Employing CRISPR-Cas9 system, we have obtained a mutant allele with an insertion that causes a premature stop codon and generates a truncated non-functional protein. This mutant line is viable and healthy but sterile. Female flies carry ovaries completely devoid of proper structure, suggesting incomplete development (Fig. 15C). Surprisingly, both genders are sterile, despite the low expression of *Mettl16* transcript in testis (Thurmond et al., 2019). This suggests that the role of Mettl16 in germline specification is mainly exerted during early embryogenesis, when the level of the enzyme is high in both genders. The high expression observed in ovaries is probably necessary to ensure that high levels of the enzyme are present in the embryo, rather than to modulate fertility.

Mettl16 is known to regulate splicing and SAM homeostasis by methylating the spliceosomal RNA *U6* and the SAM synthetase *Mat2A* transcript in higher eukaryotes. We have verified that binding to these targets is conserved in flies (Fig. 15D), suggesting a conserved function. Although, while in mice Mettl16 absence is lethal, due to the massive transcriptional changes caused by the disrupted SAM homeostasis (Mendel et al., 2018), mutant flies develop normally, with the exception of the reproductive system. This suggests that the epitranscritomic control exerted by Mettl16 on gene expression expanded its functions during evolution. In line with this, Mettl16 sequence in higher eukaryotes has gained two more domains known as vertebrate conserved regions (VCRs), which have been proven responsible for Mettl16 interactions with the spliceosome machinery (Pendleton et al., 2017). Recent studies have also shown that METTL16, initially presented as a nuclear protein, exerts catalytically-independent functions in the cytosol, where it binds to eIF3a/b to modulate translation (Su et al., 2022). It would be interesting to investigate the role of fly Mettl16 independently of its catalytic functions, considering that also in our model Mettl16 occupies both nucleus and cytosol (Fig. 14B).

5.7 Outlook Mettl16

Mettl16 absence is deleterious for fly fertility, and the identification of its conserved targets, *U6* and *Mat2A* transcripts, suggests that Mettl16 could exert its functions in germline specification through the modulation

of splicing and SAM homeostasis. Given its high expression in embryos and ovaries, it would be interesting to address Mettl16 functions in a timely manner. For example, rescue experiments could be conducted to express Mettl16 only in embryos or only in adults and check if the ovary structure and fertility can be rescued. It would be also important to raise an antibody against Mettl16 to specifically address its spatial distribution in early embryos.

A recent study identified thousands of intronic sites methylated by Mettl16 in human cells (Mikutis et al., 2020). It would be important to identify other bound and methylated targets in flies as well, by employing high resolution sequencing techniques like iCLIP and miCLIP. Identifying the specific binding sites of Mettl16 in *Drosophila* would also help us understand the mechanism by which splicing is modulated in invertebrates. For example, a recent study showed that Mettl16 ortholog in *C. elegans*, METT-10, can modulate splicing despite the absence of the VCRs, by methylating the 3' splice site of pre-mRNAs, hence inhibiting binding of the splicing factor U2AF35. At low SAM levels, METT-10 does not methylate the pre-mRNA and splicing occurs (Mendel et al., 2021).

Employing RNA-sequencing and proteomic analysis from WT and Mettl16 KO flies would provide hints about how transcription, splicing and translation are influenced by Mettl16. Moreover, considering the importance of Mat2A in SAM synthesis, the impact of Mettl16 on other epigenetic and epitranscriptomic marks could be addressed via mass spectrometry. Finally, it would be interesting to understand if Mettl16 influences translation and if it requires other factors to fine-tune its activity, with the help of techniques like ribosome profiling and IP-MS, respectively.

5.8 Mettl25 is a novel Nm writer methylating tRNA$^{Gly\text{-}GCC}$ at position 38 in *Drosophila melanogaster*

The second part of my PhD focused on the characterization of the novel Nm methyltransferases Mettl25 and Mettl25b, with a particular focus on Mettl25. To study their role in flies, we generated KO lines with the use of the CRISPR/Cas9 system. The complete deletion of *Mettl25b* is not viable, as homozygous flies do not survive beyond the larval stages, suggesting that Mettl25b might be important for larval development. Mettl25 depletion, on the other hand, led to healthy and fertile flies. In S2R+ cells, a GFP-tagged version of the two enzymes shows that they are cytosolic proteins, suggesting that their methylated targets are cytosolic RNAs. In collaboration with Prof. Dr. Motorin, we performed ribomethseq (RMS) on purified tRNAs from wt and Mettl25 KO flies to determine Mettl25 target specificity. The results identified one targeted guanosine on tRNA$^{Gly\text{-}GCC}$ at position 38. Interestingly, Schaefer et al. pointed out that position 38 of tRNA$^{Asp\text{-}GTC}$, tRNA$^{Gly\text{-}GCC}$ and tRNA$^{Val\text{-}AAC}$ are methylated by Dnmt2 to form m^{5}C and increase their stability (Schaefer et al., 2010). Nevertheless, when checking the sequence of tRNA$^{Gly\text{-}GCC}$ we noticed that the cytosine methylated by Dnmt2 is at position 37, adjacent to G38 methylated by Mettl25, and therefore Dnmt2 is mostly, but not entirely, specific for position 38. Beside tRNA$^{Gly\text{-}GCC}$, no further residues emerged from our sequencing as Mettl25 target. A possibility that could explain this is that Mettl25 and Mettl25b might have some shared functions. To circumvent this situation, we are generating double mutant lines, where both *Mettl25* and *Mettl25b* are mutated, to identify potential common targets. Moreover, for the Mettl25b KO line, larvae are being collected for RMS, as mutants fail to pupate.

5.9 The secret for a long life: a molecular understanding of Mettl25 functions

In order to better understand the function of the enzymes, we checked their expression at different developmental times and upon aging. Interestingly, while their expression was not particularly high during development and in 2 days old flies, Mettl25 levels increased by 5-fold in 2 months old flies. This prompted us to investigate Mettl25 functions during aging. We therefore checked the mortality of Mettl25 mutant flies and their isogenic control with a lifespan assay. Both males (Supplementary fig. 13C) and females showed a significant reduction in lifespan (Fig. 18B) upon Mettl25 depletion. Interestingly, other tRNA modifications have been also associated with lifespan determination. For example, depletion of the m^{5}C writer Dnmt2, led to a shorter lifespan in flies (M. J. Lin et al., 2005), probably dependent on the increased instability of the targeted tRNAs. Schaefer et al show that the absence of Dnmt2 destabilizes the targeted tRNAs, which are

more easily cleaved by angiogenin, and mutant flies are more sensitive to a plethora of stressors (Schaefer et al., 2010), linking an efficient stress response with longevity. This role is probably conserved in higher eukaryotes as Dnmt2 depletion induced stress-dependent apoptosis and inhibited proliferation in mouse and human fibroblasts, respectively (Lewinska et al., 2017, 2018). Also Nm has been linked to lifespan regulation. In particular, depletion of the tRNA Nm writer Trm7 orthologs in *Drosophila* causes tRNA instability, altered Ago2-dependent gene silencing, reduced resistance to virus infections and reduced lifespan (Angelova, Dimitrova, Silva, et al., 2020).

In order to gain more insights into Mettl25 molecular functions, we performed IP followed by mass spectrometry to identify its interactors. Among them, some factors involved in translation and in the stress response were identified (Fig. 19A). In particular, the most enriched protein was CG5726, orthologous of the human cap binding complex dependent translation initiation factor (CTIF), suggesting an involvement of Mettl25 in translation regulation. When we looked at translation levels in wt and mutant flies we observed higher puromycin levels, suggesting that Mettl25 inhibits translation. On the other hand, studies showed that during active translation, the ribosomes that are the most prone to accommodate puromycin are paused ribosomes, as they show reduced A-site occupancy. In one study this was mainly observed for some Glycine codons, particularly when followed by Phenylananine, in the *preprolactine* mRNA and *globin* mRNAs (Starck & Roberts, 2002). This may indicate that in the absence of Mettl25 an increased level of ribosome pausing occurs during translation. While pausing is essential for protein folding, if excessive it can cause ribosome collisions which activate the ribosome-associated quality control (RQC). A recent paper identified in aging *C. elegans* an increase in ribosome pausing specific for Proline, Arginine and Tyrosine (Stein et al., 2022)., This led to an overload of the RQC and nascent protein aggregation, landmark of the decline observed in aging. In line with this, long-lived *C. elegans* were characterized by less ribosome pausing (Stein et al., 2022). It would be interesting to test this hypothesis in Mettl25 mutant flies and check for RQC activity and ribosome collisions. For example a reporter assays could be done with a reporter preceeded or followed by polybasic sequences, and check the protein level of the reporter as way of measuring the level of paused/collided ribosome and therefore failed translation.

5.10 Mettl25 effects on translation

To study the effects of the loss of Mettl25 on gene expression, we performed ribo-seq on wt and Mettl25 mutant female flies, as females show the major changes in the puromycin and the lifespan assays compared to wt flies. The results showed a transcriptional and translational upregulation of genes involved in

carbohydrate metabolism, particularly genes of the maltase family, like Mal-A6, involved in the conversion of maltose into 2 molecules of glucose (Fig. 20 A-B).

From a translational point of view, the most striking changes comprised a significant downregulation of many factors involved in translation regulation, including ribosomal proteins and translation elongation factors (Fig. 20 A, D). This result contradicts the notion of a negative regulation of ribosome synthesis as landmark of longevity, as mutant flies die earlier than wt flies. Long-lived organisms normally reduce ribosome biogenesis, as it is a highly energy-consuming process, and with age they accumulate mutations that would lead to less functional ribosomes, so they are instead recycled through autophagocytosis (Macinnes, 2016). This might indicate that the reduced longevity in the absence of Mettl25 is not aggravated by high ribosomal biogenesis but other causes. For example, the increased puromycin incorporation could indicate higher ribosome stalling and collisions, which lead to an overall decline of proteostasis.

From a Ribo-seq Unit Step Trasnformation (RUST) analysis of our ribo-seq libraries, which shows ribosome footprint density for each codon, an enrichment for alanine (Ala), glutamic acid (Glu), histidine (His), glutamine (Gln) and threonine (Thr) codons was observed. Some of these codons, in particular His, Gln and Thr, were enriched in the ribosome A site, suggesting increased stalling during translation of these codons. It would be interesting to further investigate ribosome stalling and collision events upon aging via ribo-seq from disomes (Supplementary fig. 18).

Interestingly, among the translationally upregulated genes, INDY was found, a trans-membrane transporter of Kreb cycle intermediates (Fig. 20A). As its name suggests, INDY, which stands for “I’m not dead yet”, mutations that reduce INDY protein levels have been reported to increase stress resistance and double *Drosophila* lifespan, probably by favouring a metabolic state that resembles caloric restriction (Rogers & Rogina, 2014; Rogina et al., 2000). This protein is mainly expressed in the fat body, midgut and oenocytes. Upon its depletion, an increased mitochondrial biogenesis and decrease in ROS is observed, and this contributes to intestinal homeostasis, essential for healthy aging (Rogers & Rogina, 2014). The upregulation of INDY, might have therefore contributed in our mutants to a metabolic shift that is not favorable for longevity, and it is probably reflected by the higher expression of maltase genes.

5.11 Outlook Mettl25

Mettl25 has been revealed as a Nm tRNA methyltransferase that increases fly lifespan and modulates the expression of metabolic genes as well as ribosomal components. It has been shown to interact with factors

involved in translation regulation, but it is not clear how Mettl25 mechanistically achieve its functions and extends lifespan. Future efforts should be put into addressing the following open questions:

- Are there other methylated targets for the 2 enzymes?
- What is the effect of Nm absence on tRNA stability?
- Which functions does Mettl25 fulfill independently of its methyltransferase activity? Does it impact stress and translation through its interactors?
- Does Mettl25 absence cause an increase in ribosome collisions?
- Does INDY overexpression explain the extended lifespan? Are mutant flies more resistant to stress? Is this caused by increased mitochondrial activity?

To address these questions, we are currently working on the generation of a Mettl25-Mettl25b double mutant line which will help us with the identification of other possible target RNAs. Attempts to rescue the observed phenotypes with the full length or the catalytically-dead mutant sequence of Mettl25 will tell to which extent the catalytic domain plays a role in translation regulation and lifespan in flies. In the meantime, the interaction of Mettl25 with CG5726 should be validated in S2R+ cells via coIP-WB. Furthermore, it would be interesting to understand the level of protein aggregation during aging in Mettl25 mutants, considering that the ortholog of CG5726, CTIF, plays important functions in the nonsense-mediated decay of mutated transcripts.

The effects of the loss of methylation on tRNA fate will be addressed via Northern blot to detect levels of fragmentation in the mutant line. Preliminary attempts in this direction suggest that Mettl25 does not play a role in $tRNA^{Gly\text{-}GCC}$ stability (data not shown).

A deeper understanding of Mettl25 impact on ribosomal activity could be achieved by optimising the ribosome profiling protocol to sequence footprints from disomes, rather than monosomes, as their presence is often a sign of ribosome collisions.

From a physiological point of view, some behavioural assays like the Buridan paradigm and the Paraquat assay, to assess respectively brain functionality and stress resistance in Mettl25 mutant flies, could be performed.

5.12 The nucleolar Nm writer Ftsj3 methylates the pre-rRNA ribonuclease *Mrp* in *Drosophila melanogaster*

With Mettl25 we have seen how a tRNA Nm methyltransferase can affect translation in flies. Another Nm methyltransferase, Ftsj3, was reported to mediate rRNA biogenesis in yeast and human (Lapeyre & Purushothaman, 2004; Morello et al., 2011) and suggested as an mRNA Nm writer in yeast (Bartoli et al., 2018). We decided to understand whether these functions are conserved in *Drosophila*. In order to understand its role in flies we first checked its expression during development via RT-qPCR and observed higher peaks in embryonic stages, suggesting a function in early development (Fig. 21A). Immunofluorescence of a FLAG-tagged Ftsj3 in transfected S2R+ cells showed that Ftsj3 is occupying the nucleolus, the nuclear compartment where most of the pre-rRNA processing occurs, suggesting that Ftsj3 might be involved in rRNA maturation (Fig. 21B). We then decided to employ nanopore on S2R+ cells depleted of Ftsj3 versus control cells expressing endogenous levels of Ftsj3 to identify its methylated targets. Interestingly, no site on rRNA was identified, but another RNA, the RNase *MRP*, involved in rRNA maturation, was instead modified on residue C_{137}, suggesting a unique way for fly Ftsj3 to partecipate in ribosome biogenesis (Fig. 22A). The mild signal obtained with nanopore, and the fact that this methylation could not be significantly confirmed via RTL-P, suggest that *MRP* is not fully methylated. This could either indicate that its methylation is context-dependent, or that the results were misled because other enzymes might compensate for Ftsj3 absence and still methylate C_{137}. When employing RTL-P, while upon Ftsj3 KD two over three replicates show a clear loss of Nm, suggesting that further optimisation or increasing the amount of replicates might better prove *MRP* methylation status, the reduction in methylation upon double KD, of Ftsj3 and Fibrillarin, could not be observed (Fig. 22B). We therefore checked the effect of the absence of these two enzymes on the expression of rRNAs and *MRP* via RT-qPCR. Interestingly, upon depletion of these enzymes, in particular upon depletion of Fibrillarin, while the 18S and the 28S rRNAs were not affected, *MRP* underwent a significant increase in expression (Fig. 22C). These differences in *MRP* expression levels between control and double KD might perhaps explain why changes in methylation were not easy to prove upon depletion of both enzymes.

5.13 Ftsj3 link with the DNA damage response

Considering that rRNA biogenesis is an essential step for gene expression regulation and might have effects that extend from protein synthesis to transcription regulation, we addressed whether there were significant changes in the transcriptome upon Ftsj3 KD in S2R+ cells. Interestingly, upon depletion of Ftsj3, a significant increase in the expression of genes involved in the DNA damage repair pathway was found (Fig. 23A). This

suggests that Ftsj3 involvement in ribosome biogenesis might take part in the DNA damage response. It has been shown by several studies that the two processes are linked. For example, in mouse germ cells ribosomal factors and pre-rRNA co-colocalise with DSB repair factors during meiosis (Gai et al., 2022). Another study shows that ribosome biogenesis and DNA repair are also linked in some cancer cell lines. In particular, upon decrease of the nucleotide pool, the impaired ribosome biogenesis checkpoint (IRBC), made up of RPL11, RPL5 and the 5S rRNA, stabilises p53 by inhibiting the E3 ubiquitin ligase MDM2, and this causes G1 cell cycle arrest through the activation of p21. This mechanism for cell cycle arrest has been suggested to act as a barrier against DNA damage. Indeed, further depletion of the nucleotide pool, or inhibition of the IRBC, leads to cell cycle progression to the S phase, via proteasome-mediated degradation of p21, and cells encounter more replicative stress and DNA damage (Pelletier et al., 2020). Thus impaired biogenesis can precede the activation of the DNA damage response. Given these premises, it would be interesting to confirm and further investigate this link of Ftsj3 with the DNA damage response.

5.14 Outlook Ftsj3

After our preliminary work on Ftsj3 identifying *MRP* as its methylated target and its connection with the DNA damage response, it would be important to further understand its role in ribosome biogenesis. *In primis*, methylation of *MRP* and the identification of other target RNAs should be addressed. For this, the employment of other mapping methodologies to complement and strenghten the results obtained with nanopore, and the use of iCLIP, could provide reliable results on its methylated targets. Then the effects on rRNA biogenesis should be unveiled, for example via Northen blot, and the activation of the DNA damage response upon Ftsj3 KD could be verified via immunofluorescence to visualise DSB repair factors. A connection between Ftsj3 catalytic activity and the DNA damage response pathway could be verified, for example, by checking the co-localization of methylated and not methylated MRP with DNA damage repair factors. Finally, Ftsj3 IP-MS with the subsequent identification of its interactors might provide more clues towards a better understanding of its functions.

6. CONCLUSIONS

This study aimed at expanding our knowledge about m^6A and Nm and their role on non-coding RNA functions, with a particular focus on the characterization of the rRNA writer Mettl5 and the tRNA writer Mettl25 in *Drosophila melanogaster*. The main findings from this study are summarised below.

Part I : m^6A

Mettl5

- Mettl5 is a conserved m^6A writer methylating the 18S rRNA
- Mettl5 requires binding of Trmt112 for its stability and activity
- Mettl5 does not modulate rRNA biogenesis
- The absence of m^6A on the 18S rRNA impacts the transcriptome causing an impairment in lipid synthesis, important for brain functions
- Mettl5 KO flies show impaired walking behaviour, reflecting defects in brain functions
- Mettl5 KO flies show reduced brain/body ratio, reminiscent of the microcephaly phenotype of Mettl5 patients

Mettl16

- Mettl16 is a conserved m^6A writer in flies, binding to *U6* snRNA and *Mat2A* mRNA
- The absence of Mettl16 impairs ovarian development and causes infertility in both genders

Part II: Nm

Mettl25

- Mettl25 is a cytosolic Nm writer methylating G38 of $tRNA^{Gly\text{-}GCC}$
- Mettl25 is highly expressed upon aging and its depletion shortens lifespan in flies
- Mettl25 interacts with factors involved in the stress response and in the regulation of translation
- Mettl25 depletion leads to the downregulation of ribosomal proteins and translation factors and the upregulation of carbohydrate metabolism
- The absence of Mettl25 seems to cause an increase in ribosome pausing, harbinger of ribosome collisions and loss of proteostasis

- The shortened lifespan observed in Mettl25 mutants might be explained by the metabolic shift caused by the upregulation of the transporter of Krebs cycle intermediates, INDY, and by the increase in ribosome pausing at Gln and Glu codons

Ftsj3

- Ftsj3 is a nucleolar protein potentially methylating the RNase *MRP*, essential for rRNA biogenesis
- The absence of the two Nm writers Ftsj3 and Fib fosters *MRP* expression
- The lack of Ftsj3 leads to the upregulation of DNA damage repair factors, probably as a consequence of impaired ribosome biogenesis

These findings contribute to expand our knowledge about m^6A and Nm, in particular on their importance for rRNA biogenesis and translational regulation, providing a link between RNA modifications and the metabolic and physiological changes observed in mutant flies. In particular, we have shown the importance of m^6A on brain functions, development and fertility, and an interesting correlation between Nm on tRNA and on RNase *MRP*, with longevity and DNA damage, respectively.

7.Supplementary data

Supplementary figure 1

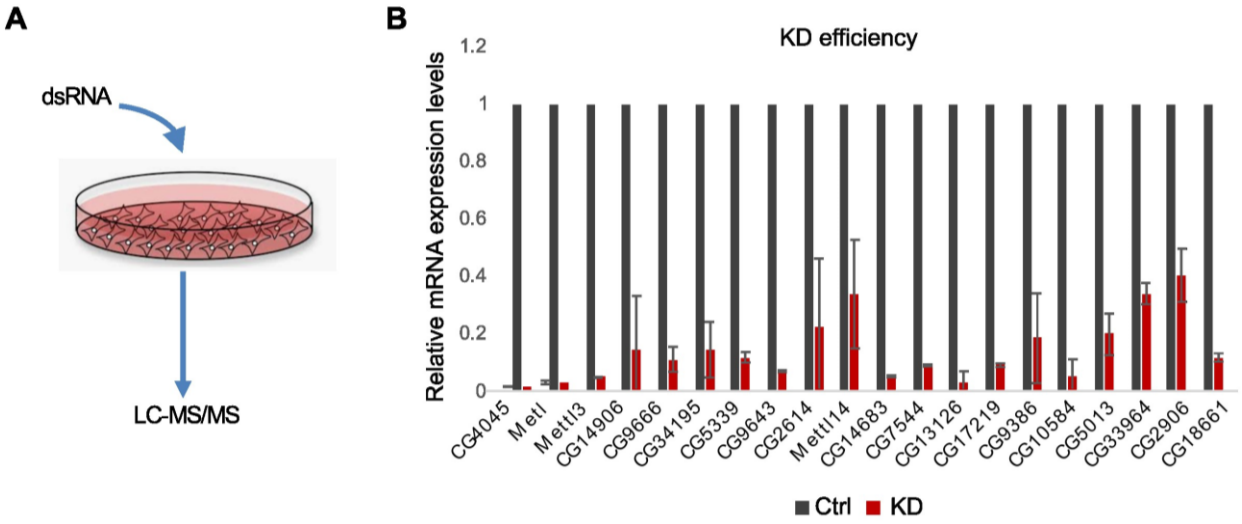

Supplementary figure 1: Design and validation of the candidate-based RNAi screen.
Adapted from [Leissman, Spagnuolo et al. (2020)].
(A) *Experimental scheme of the RNAi screen performed in Drosophila S2R+ dells. After KD prolonged for 6 days, RNA was extracted and submitted to mass spectrometry analysis.*
(B) *Efficiency of the KD quantified by RT-qPCR. Bar chart represents mean ± standard deviation of three technical replicates from three biological replicates.*

Supplementary figure 2

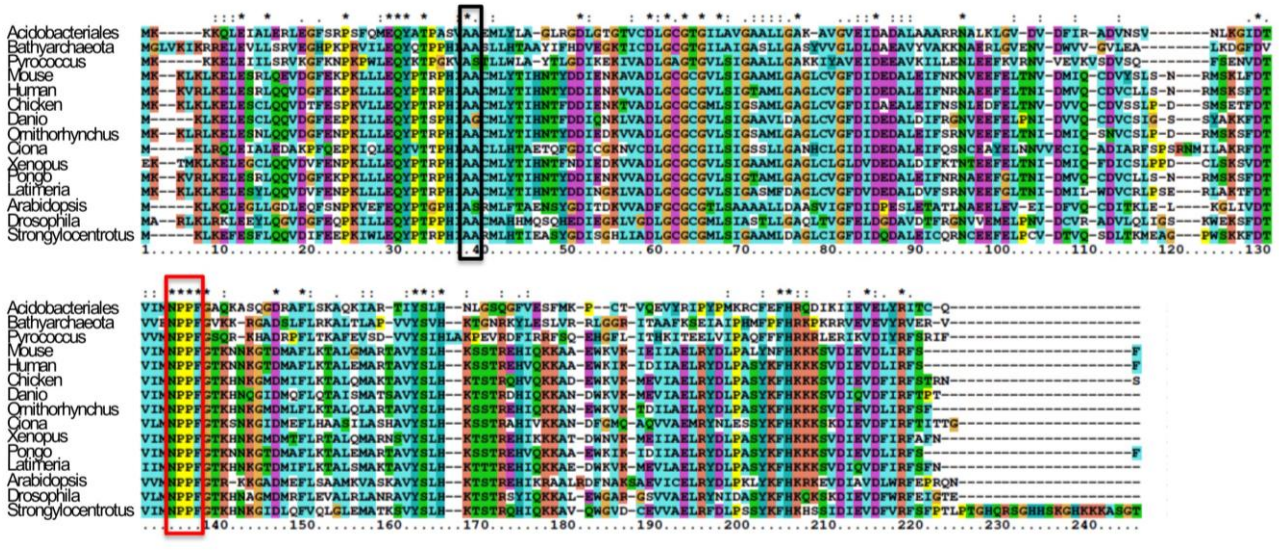

Supplementary figure 2: Phylogenetic analysis.
Adapted from [Leismann, Spagnuolo et al. (2020)]. Multiple sequence analysis of Mettl5 (UniProt: Q8MSW4_DROME) and representative orthologs for selected species (See Materials and Methods for details and sequence identifiers). Prokaryotic exemplary sequences from archaea (Pyrococcus, Bathyarchaeota)and bacteria (Acidobacteriales) are included as outliers. The red rectangles indicates the conserved NPPF motif and the black rectangle the position of the two amino acids deleted in the Mettl5$^{\Delta 2AA}$ allele.

Supplementary figure 3

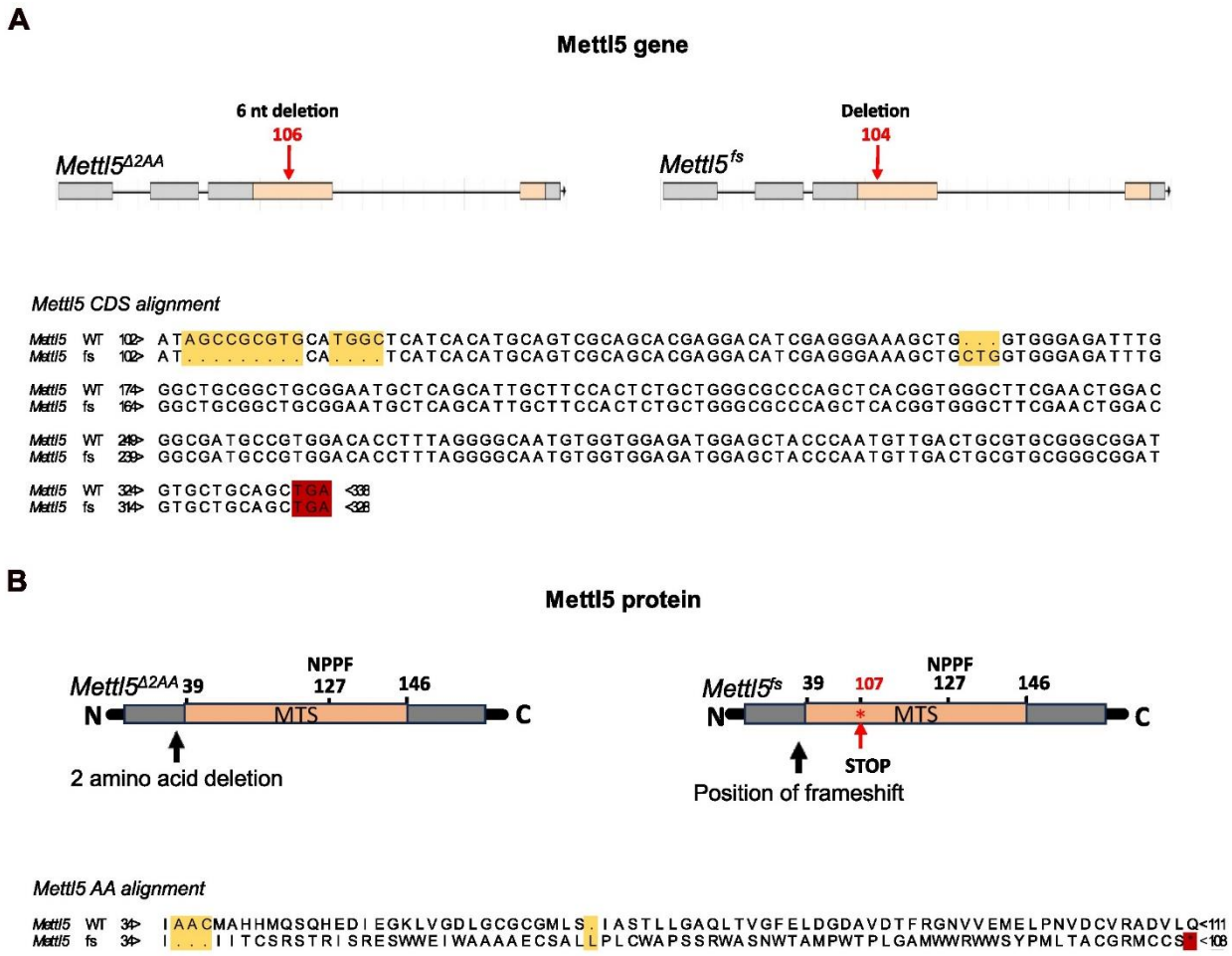

Supplementary figure 3: Description of Mettl5 mutant alleles obtained in this study.
Adapted from [Leismann et al. (2020)].
(A) *Representation of Mettl5$^{\Delta 2AA}$ and Mettl5^{fs} alleles showing the position of the obtained mutations along the gene. Pink squares represent the coding sequence, lines represent the introns. At the bottom, nucleotide alignment of Mettl5^{fs} allele to the WT sequence. Yellow boxes indicate the mutations. Red indicates the stop codon.*
(B) *Representation of the Mettl5 mutant proteins showing the methyltransferase domain (MTS) in pink. At the bottom, the amino acid sequence alignment of Mettl5^{fs} and Mettl5 WT sequence, showing in yellow the changes in the mutant allele and in red the premature stop codon.*

Supplementary figure 4

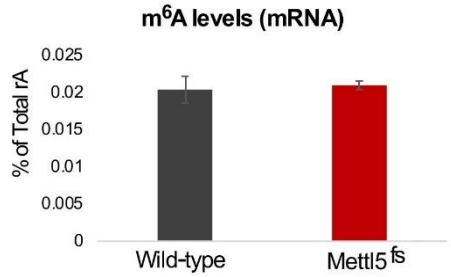

Supplementary figure 4: Methylation levels analysis.
From [Leismann, Spagnuolo et al. (2020)].
LC-MS/MS measurements of m6A levels in mRNA of WT and Mettl5fs mutant flies. Bars represent mean ± standard deviation of measurements of three biological replicates.

Supplementary figure 5

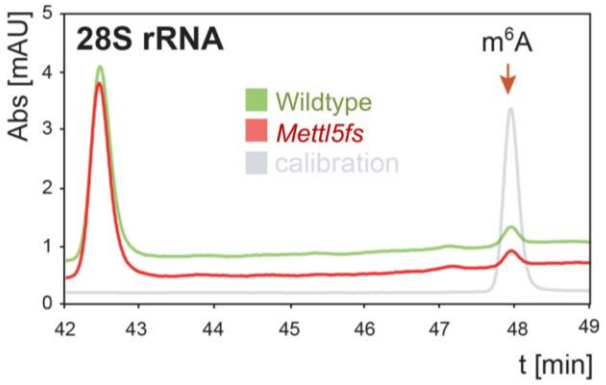

Supplementary figure 5: Analysis of m^6A levels on 28S rRNA by quantitative HPLC.
From [Leismann, Spagnuolo et al. (2020)].Purified 28S rRNA analyzed for it m^6A content by quantitative HPLC. The 28S rRNA was extracted from 60S subunits isolated on sucrose gradients. The calibration control is a commercial source of m6A (in grey). m^6A elutes at 48 min.

Supplementary figure 6

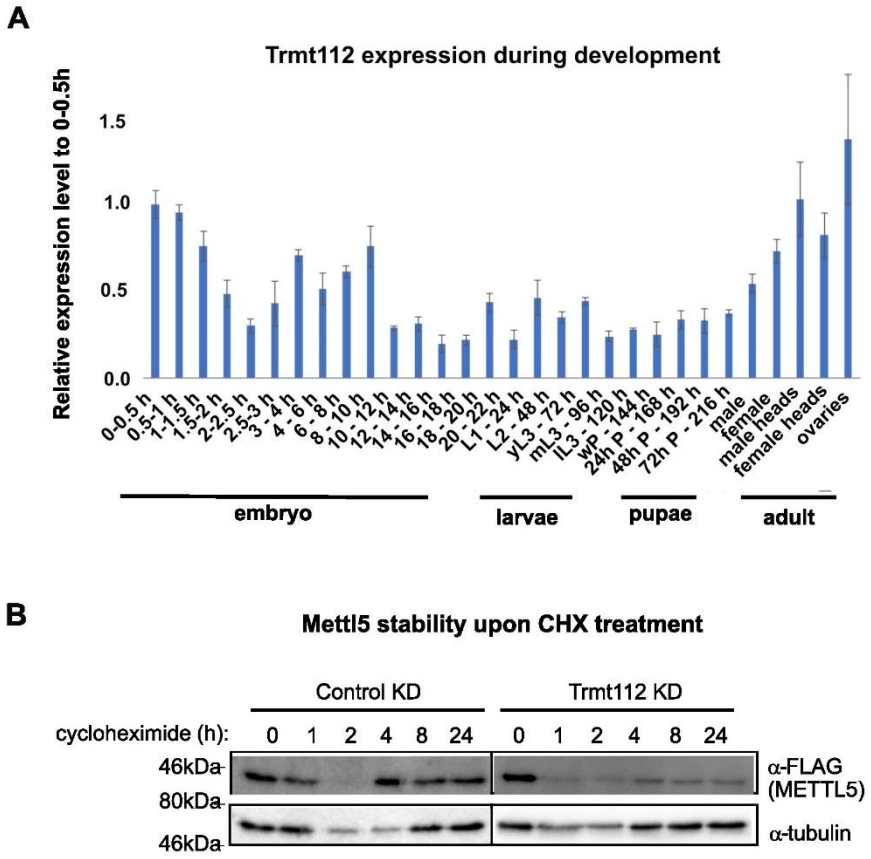

Supplementary figure 6: Trmt112 is important for Mettl5 stability.
Adapted from [Leismann, Spagnuolo et al (2020)]. ***(A)*** *Expression of Trmt112 transcript during development. Bar chart represents mean ± standard deviation of three technical measurements.*
(B) *Mettl5 is less stable upon Trmt112 KD. S2R+ cells were treated with dsRNA against Trmt112 and transfected with a UAS plasmid for Mettl5-FLAG overexpression prior to cycloheximide (CHX) treatment. Cells were lysed for WB measurements of Mettl5 at the indicated time points after CHX treatment.*

Supplementary figure 7

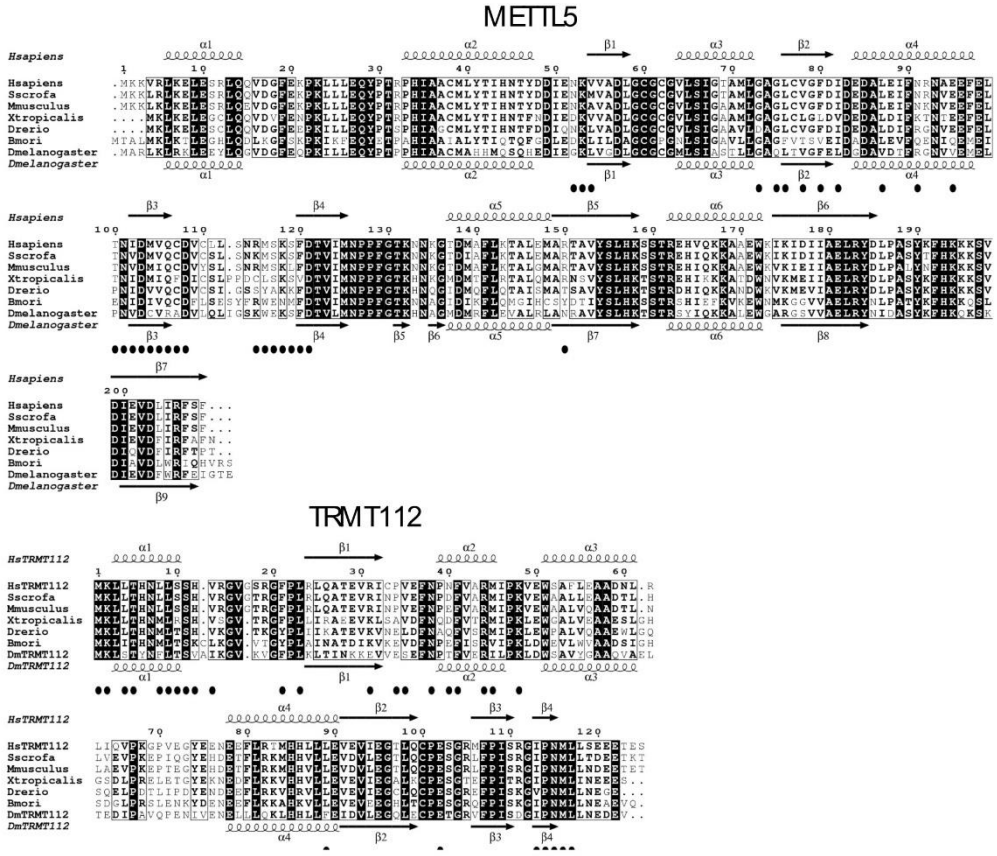

Supplementary figure 7: Secondary structure element analysis of fly Mettl5 and Trmt112.
From [Leismann, Spagnuolo et et al. (2020)]. Strictly conserved residues appear in white font on a black background. Partially conserved amino acids are indicated with a grey font. Secondary structure elements assigned on the basis of the H. sapiens crystal structure and our fly model are indicated above and below the alignment, respectively. Black circles underneath the multiple sequence alignment indicate residues involved in complex formation. Display generated using the ESpript server (Robert & Gouet, 2014).

Supplementary figure 8

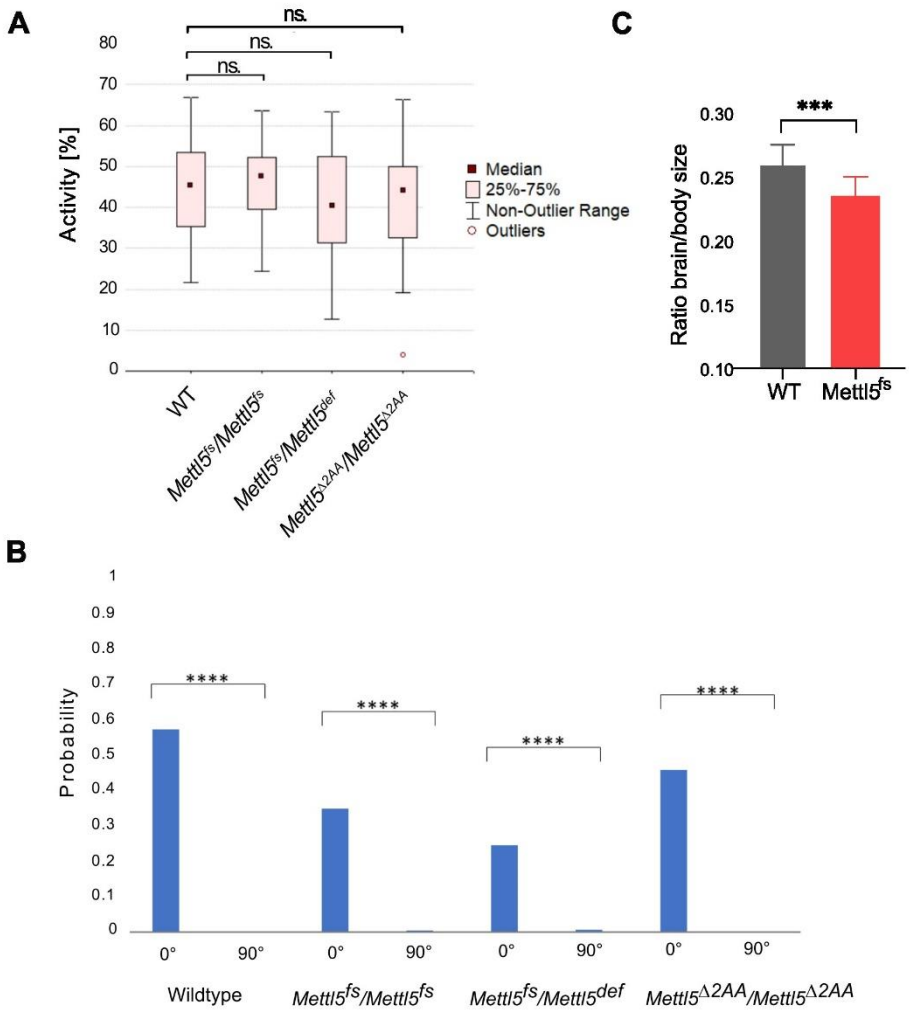

Supplementary figure 8: Statistical analysis of fly activity and brain size.

(A) *Fly activity evaluated with the help of the Buridan's paradigm. Shapiro-Wilk test was used to test for normal distribution in each group. Normally distributed groups were tested by t-test. Due to multiple comparison Bonferroni correction was applied. Number of flies tested: 30 per genotype. (n.s. = not significant).*

(B) *Fixation index analyzed by Buridan's paradigm. 0° indicates area around black stripes, 90° indicates area 90° to the black stripes. Number of flies tested: 30 per genotype. ****P<0.0001 (t-test). (C) Brain to body ratio of wt vs Mettl5 KO flies. ***P<0.001.*

Supplementary figure 9

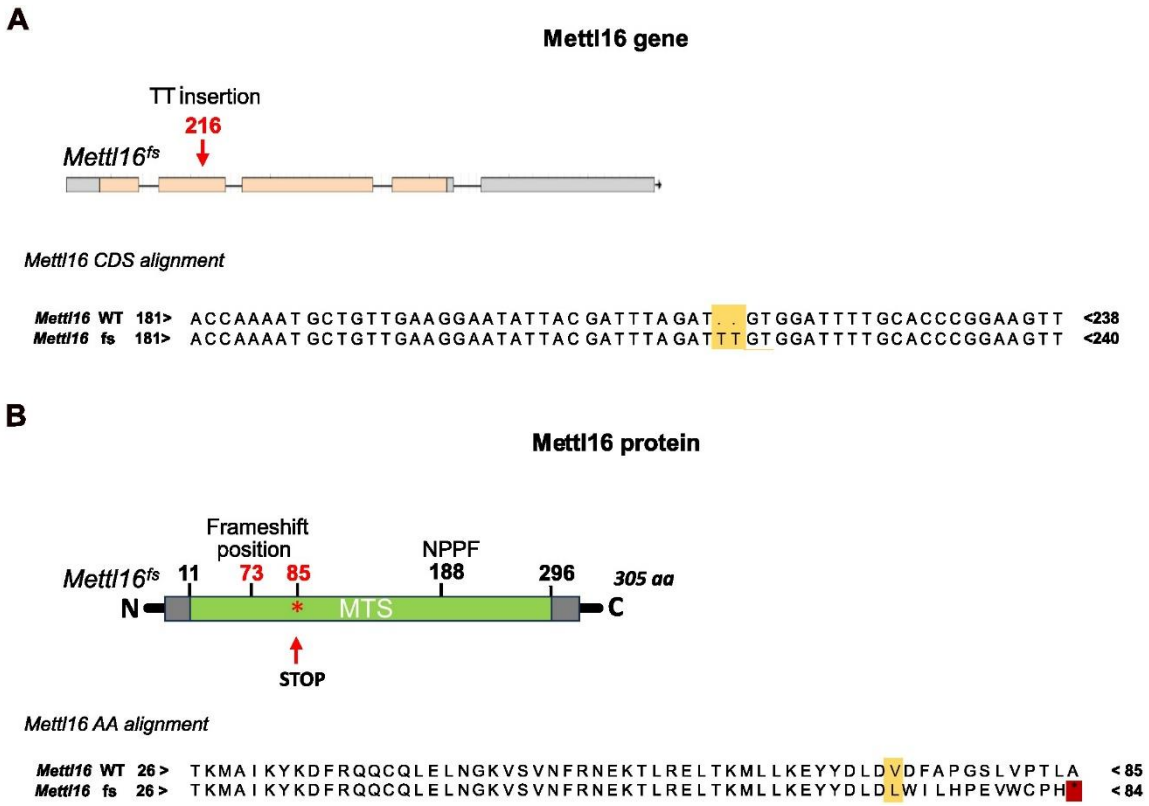

Supplementary figure 9: Description of Mettl16^{fs} mutation.
(A) Representation of Mettl16^{fs} allele showing the position of the obtained insertions on the second exon (pink boxes) of the gene. At the bottom, nucleotide alignment of Mettl16^{fs} allele to the WT sequence. Yellow boxes indicate the mutations.
(B) Representation of the Mettl16^{fs} protein showing the methyltransferase domain (MTS) in green and the position of the mutation, as well as the premature stop codon, in red. At the bottom, the amino acid sequence alignment of Mettl16^{fs} and the WT sequence, showing in yellow the changes in the mutant allele and in red the premature stop codon

Supplementary figure 10

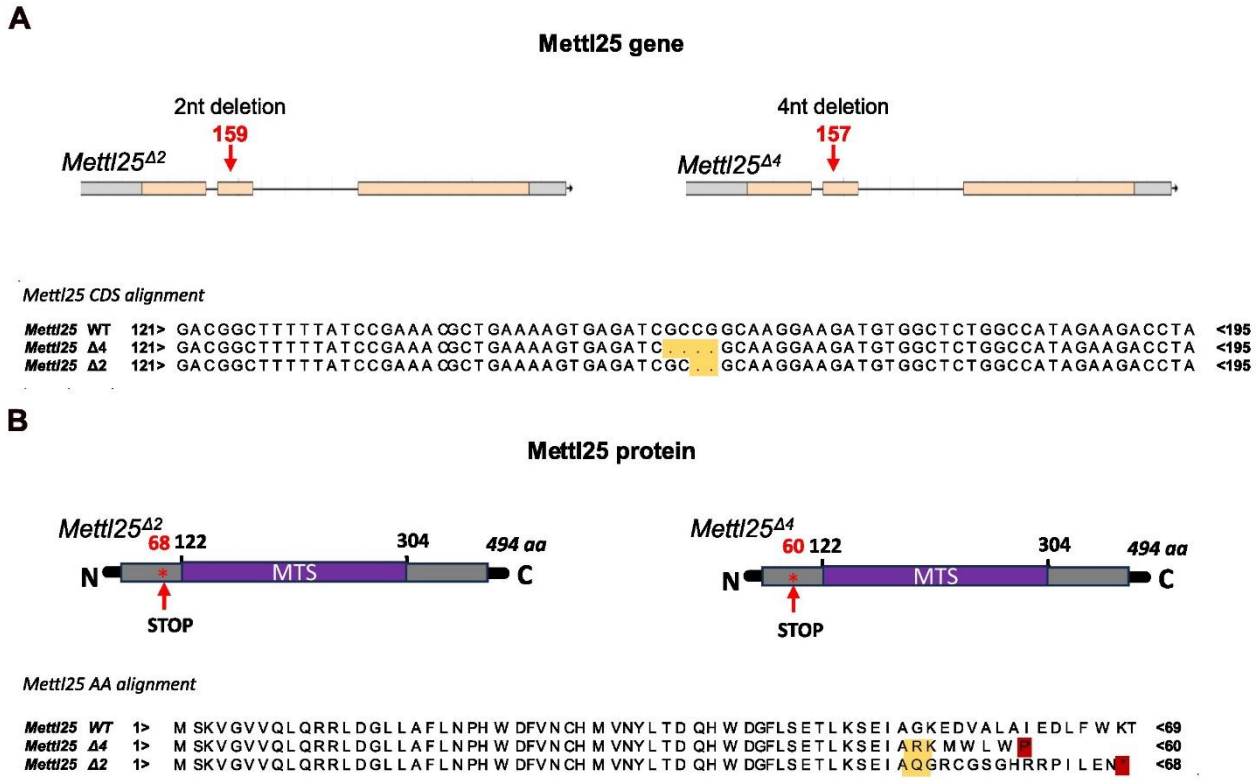

Supplementary figure 10: Description of Mettl25 mutant alleles.
(A) Representation of Mettl25$^{\Delta 2}$ and Mettl25$^{\Delta 4}$ alleles showing the position of the obtained deletions on the second exon (pink boxes) of the gene. At the bottom, nucleotide alignment of the mutant alleles to the WT sequence. Yellow boxes indicate the mutations.
(B) Representation of the Mettl25 proteins generated by the obtained mutant alleles showing the methyltransferase domain (MTS) in violet and the position of the mutation, as well as the premature stop codon, in red. At the bottom, the amino acid sequence alignment showing in yellow the changes in the mutant alleles and in red the premature stop codon.

Supplementary figure 11

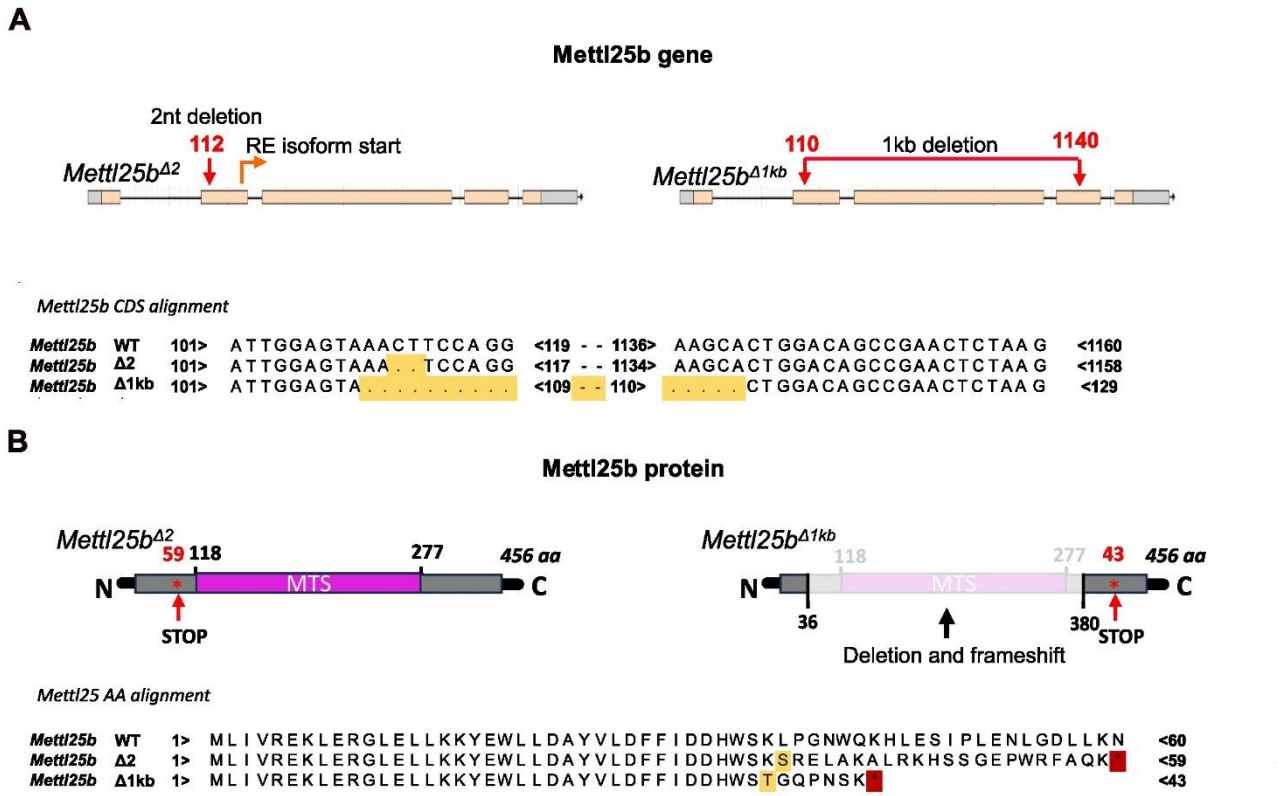

Supplementary figure 11: Description of Mettl25b mutant alleles.
(A) Representation of Mettl25b$^{\Delta 2}$ and Mettl25b$^{\Delta 1kb}$ alleles showing the position of the obtained deletions. Pink boxes represent the coding exons, straight lines are the introns. Orange arrow indicates the start codon of Mettl25b short isoform. At the bottom, nucleotide alignment of the mutant alleles to the WT sequence. Yellow boxes indicate the mutations.
(B) Representation of the Mettl25b proteins generated by the obtained mutant alleles showing the methyltransferase domain (MTS) in purple and the premature stop codon in red. At the bottom, the amino acid sequence alignment showing in yellow the changes in the mutant alleles and in red the premature stop codon.

Supplementary figure 12

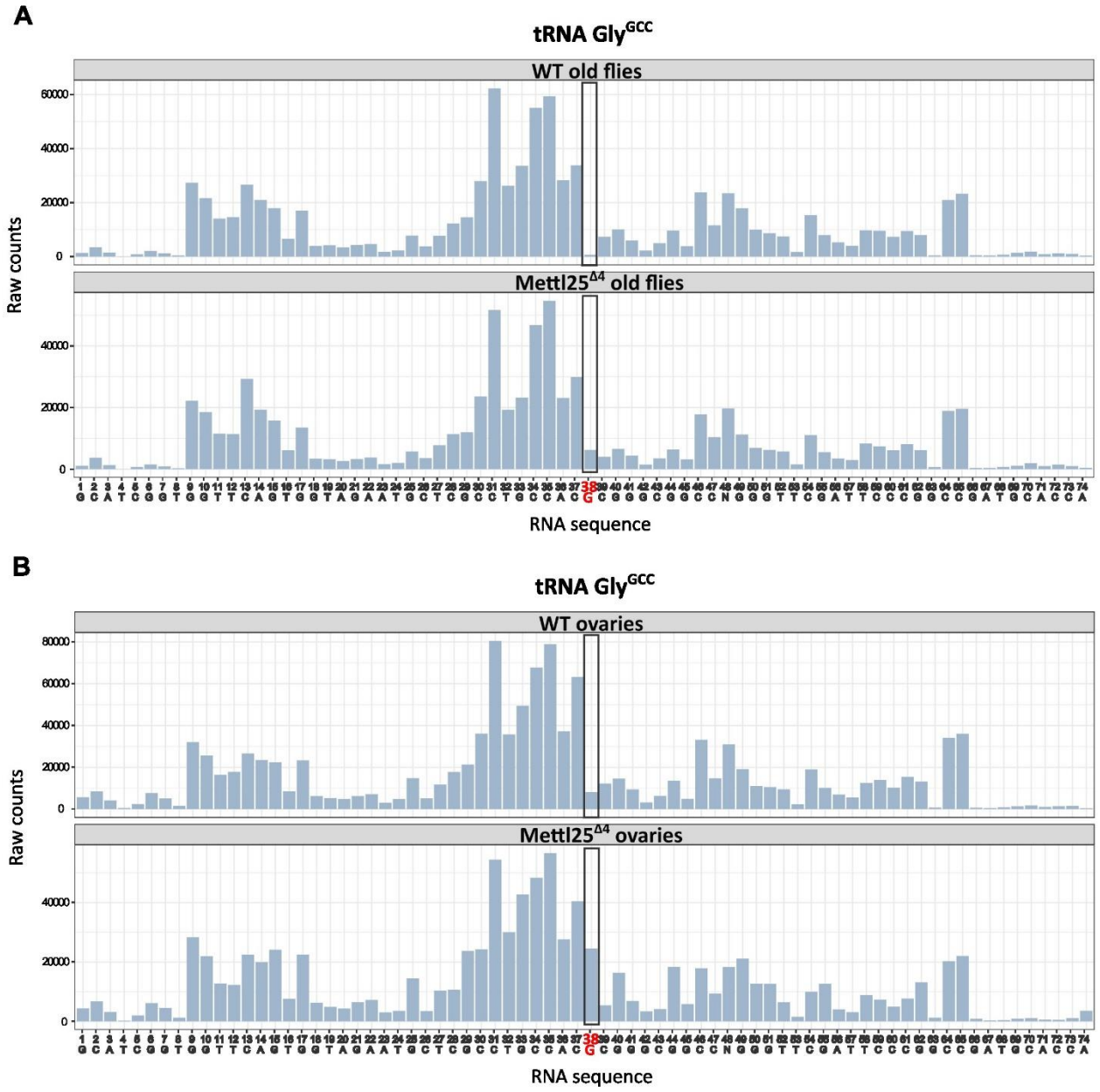

Supplementary figure 12: Loss of Nm in tRNA GlyGCC upon Mettl25 depletion.
Results of RiboMethSeq (RMS) showing the 3' coverage at different positions along tRNA GlyGCC, of fragments generated in the RMS protocol. While WT flies show no coverage for residue G38, this increases in Mettl25 mutants, indicating loss of Nm, in both in aged (69 days old) full flies ***(A)*** *and in ovaries* ***(B).*** *The experiment was repeated on three biological replicates.*

Supplementary figure 13

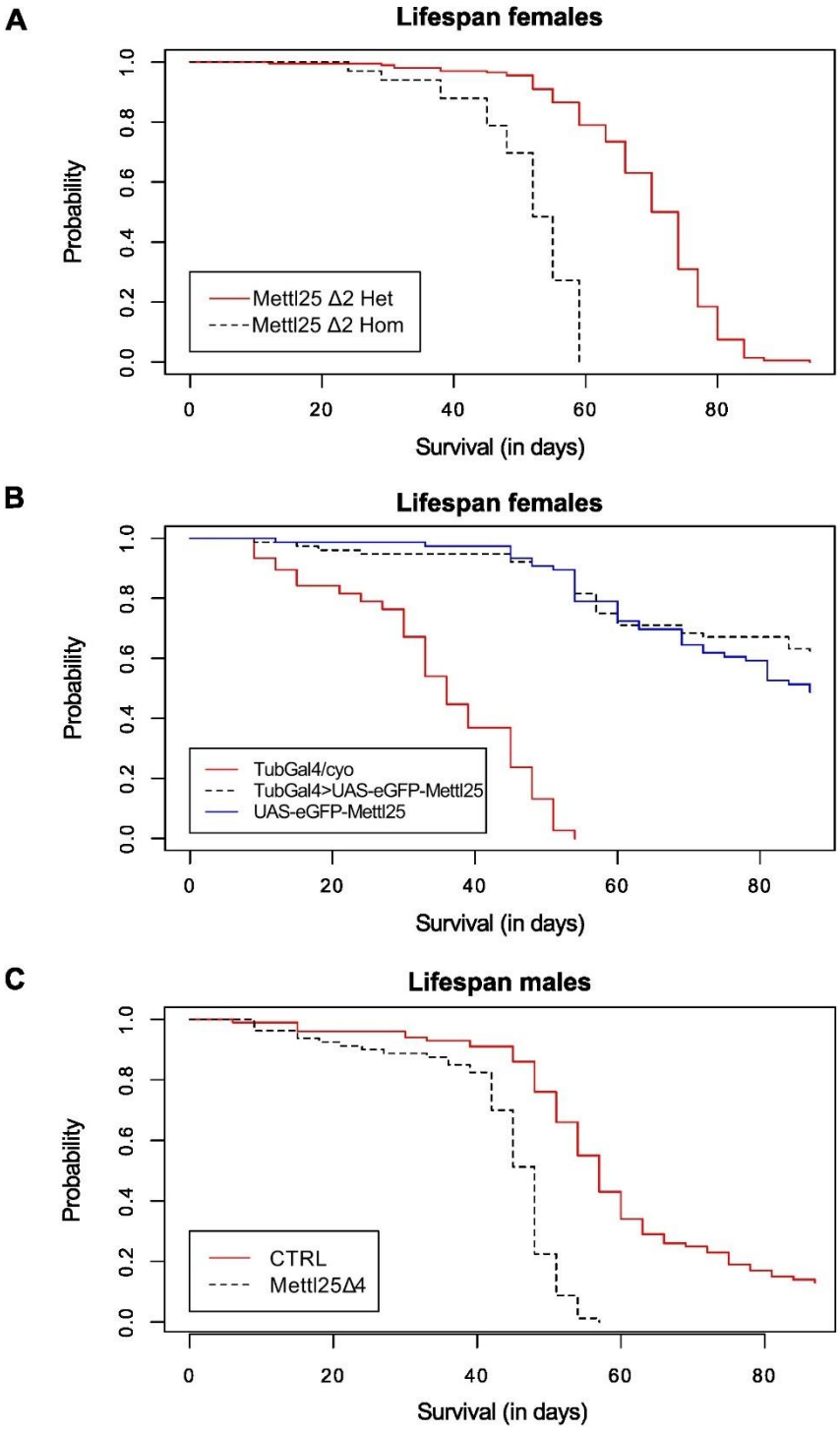

Supplementary figure 13: Mettl25 affects lifespan in flies.
(A) Lifespan assay showing reduced lifespan upon Mettl25 depletion. N Mettl25Δ2 = 33; N Het= 200. Logrank test_ P= 6.537e-09.
(B) Lifespan assay showing extended lifespan upon Mettl25 overexpression. N TubGal4 = 80; N UAS-eGFP-Mettl25 = 100; N TubGal4>UAS-eGFP-Mettl25 = 140. Logrank test_ P<2.2e-16. The assay was carried out for 3 months. At that point, only 39 UAS-eGFP-Mettl25 flies and 30 TubGal4> UAS-eGFP-Mettl25 flies had died.
(C) Lifespan assay carried out on Mettl25Δ4 male flies. N CTRL = 100; N Mettl25Δ4 = 80. Logrank test_ P = 1.019e-12.

Supplementary figure 14

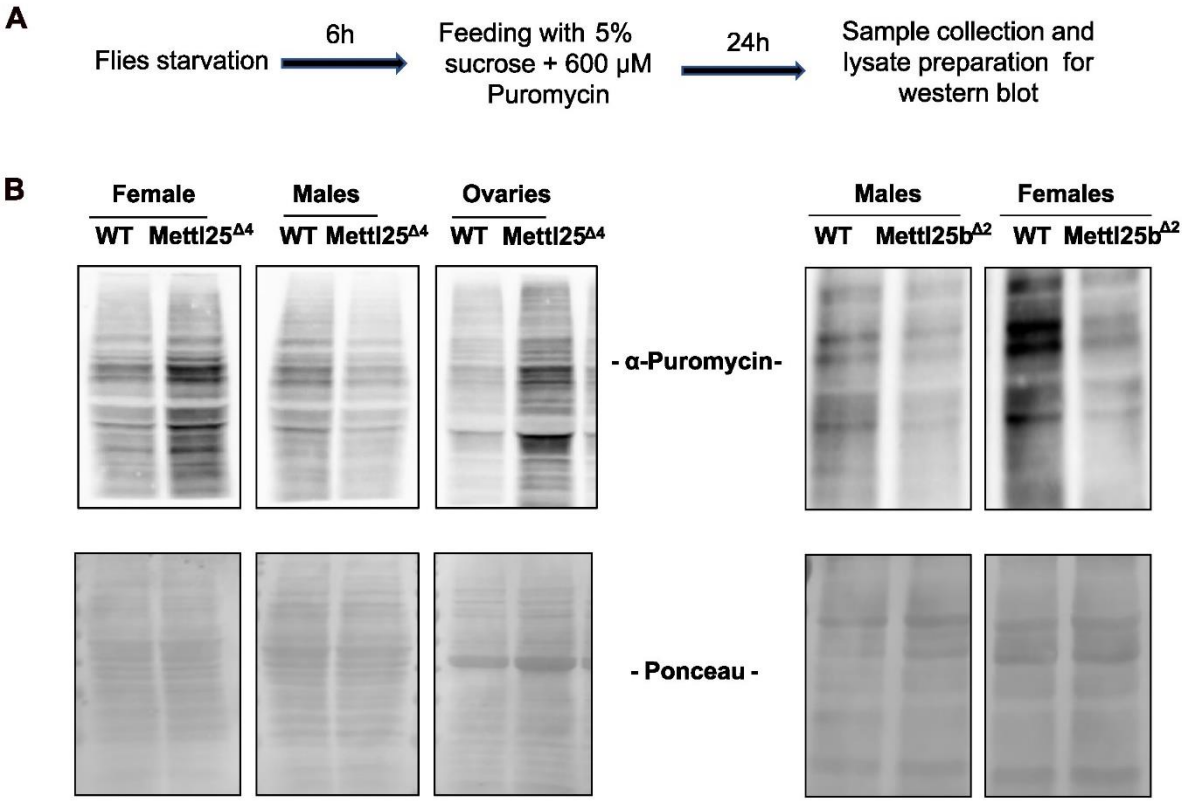

Supplementary figure 14: Mettl25 and Mettl25b impact on translation.
(A) Scheme of the Puromycin incorporation assay.
(B) WB results for Mettl25 (left) and Mettl25b (right) mutant flies showing levels of Puromycin incorporation in comparison with WT flies. Loading control was done by Ponceau staining of the membranes and is shown at the bottom.

Supplementary figure 15

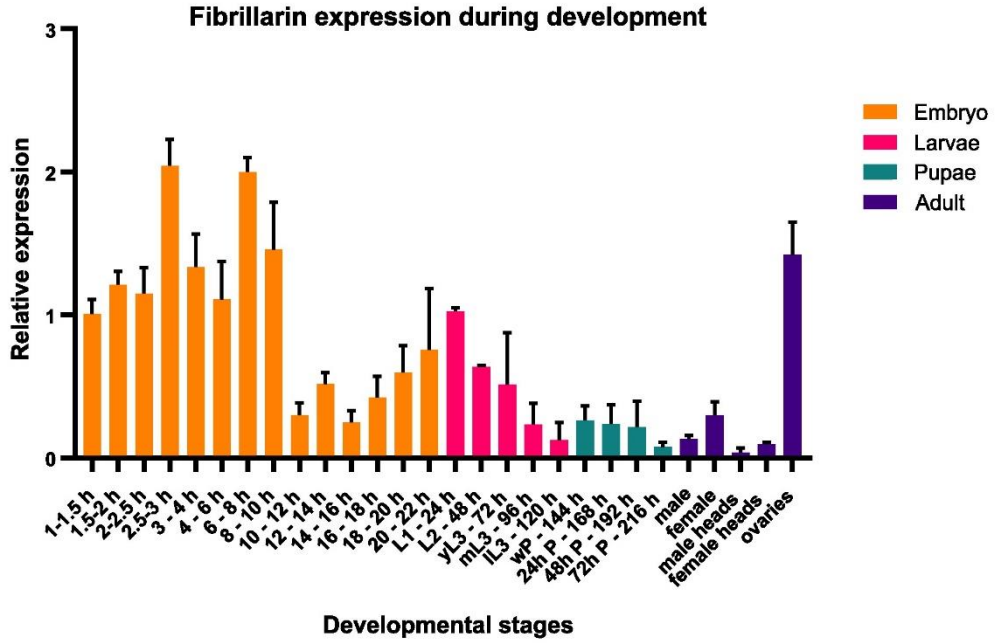

Supplementary figure 15: Developmental expression of Fibrillarin.
RT-qPCR measurements of Fibrillarin expression. Results represent mean ± standard deviation of three biological replicates.

Supplementary figure 16

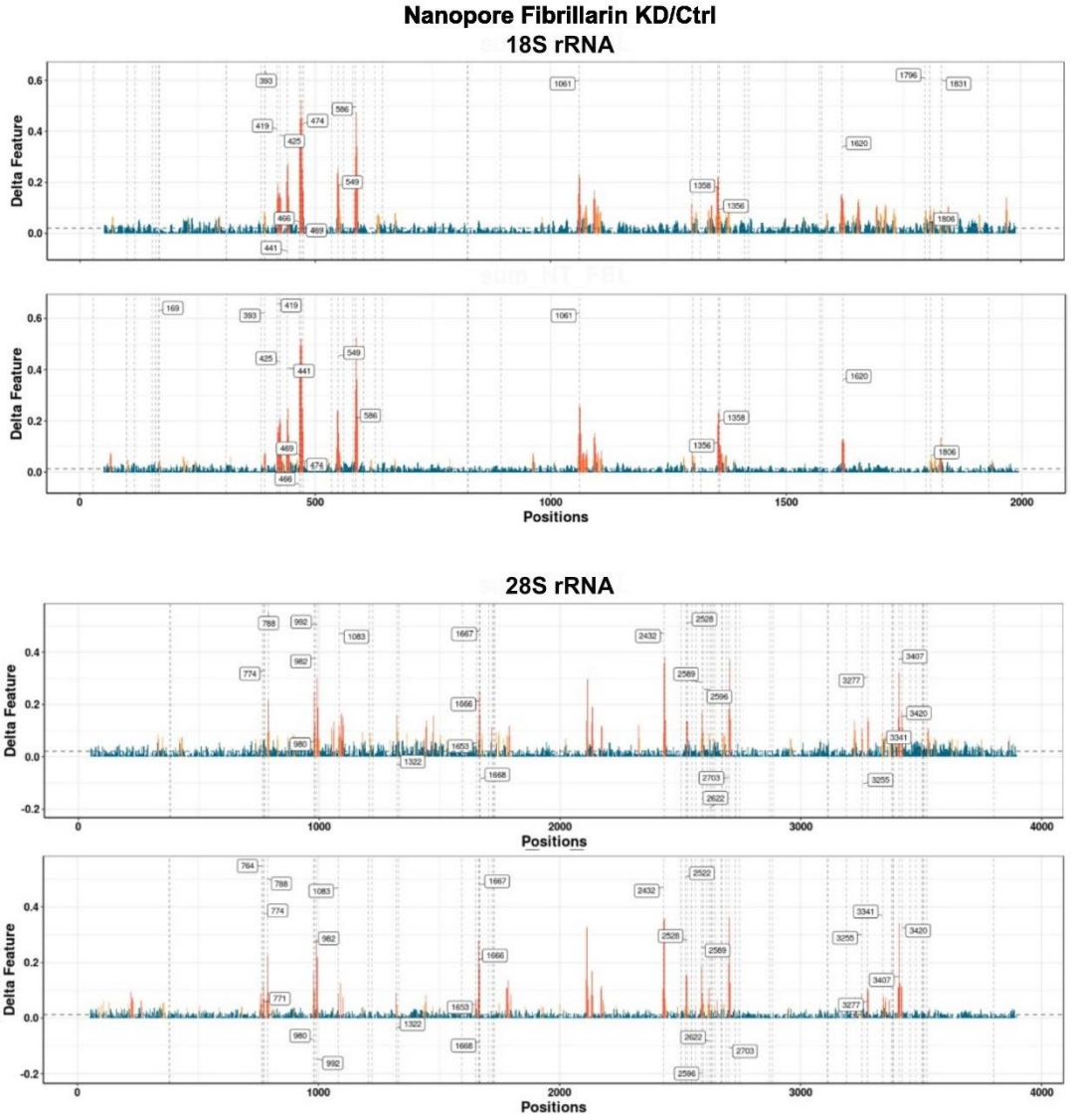

Supplementary figure 16:Methylated sites by Fibrillarin on fly 18S and 28S rRNA.
Nanopore sequencing of 18S and 28S in S2R+ cells upon Fib KD showing the Δfeature between control and Fib KD samples on the Y axes. Positions along the rRNAs sequences are indicated on the X axes. Positions where the difference between the signals generated by the two samples is significant, indicating lack of Nm upon Fib KD, are shown in orange, over a blue background.

Supplementary figure 17

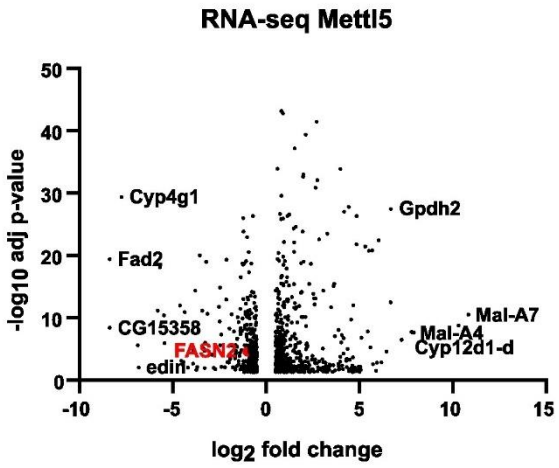

Supplementary figure 17: RNA-seq results upon Mettl5 depletion.
Volcano plot showing transcriptional changes in Mettl5^{fs}flies compared to WT. RNA-seq was performed in 3 biological replicates. FASN2 expression, reported in red, is halved in absence of Mettl5.

Supplementary figure 18

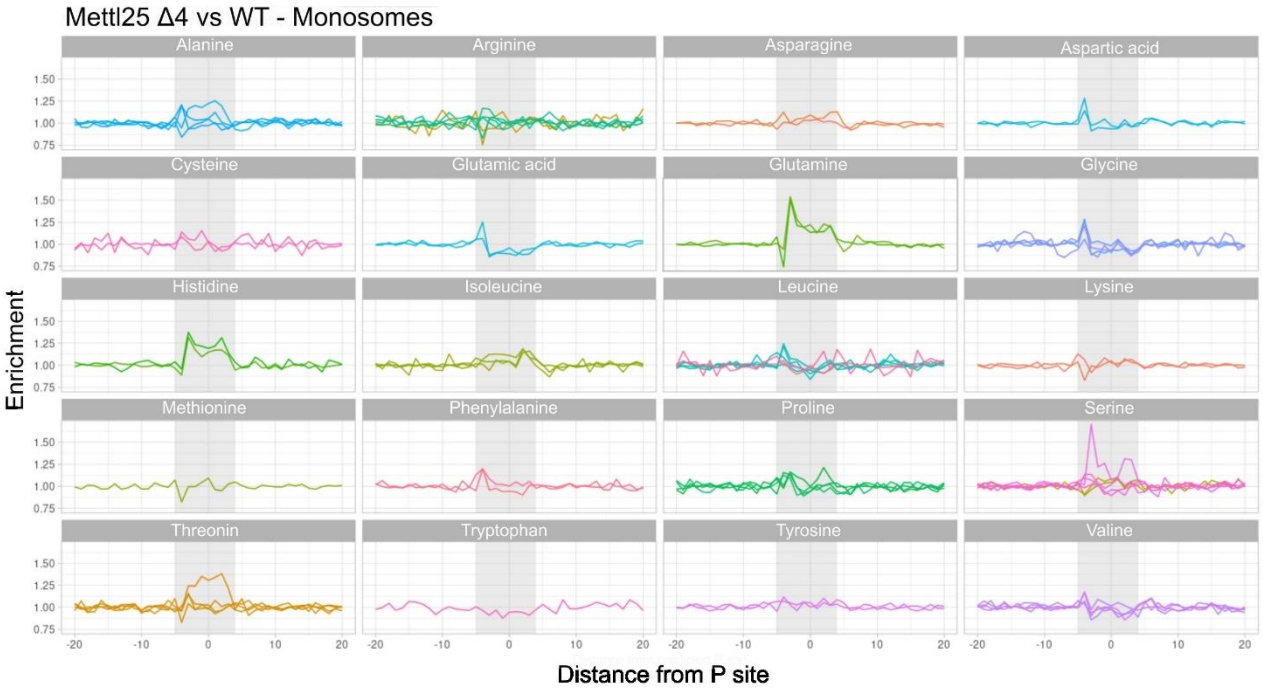

Supplementary figure 18: Mettl25 depletion increases A-site occupancy at specific codons.
RUST analysis of ribo-seq libraries showing the distance from the P site on the X axes and the occupancy of the codons for each amino acid on the Y axes.

8.Materials and methods

Drosophila stocks and genetics

Drosophila melanogaster fly stocks used in this study are reported in table 3. Canton-S with mutant alleles for Mettl5, Mettl16, Mettl25 and Mettl25b were generated using the CRISPR/Cas9 system. Two guide RNAs were designed encompassing the putative methyltransferase domain of the targeted genes, using the crispr fly design tool (www.crisprflydesign.org) and they are listed in table 4. The oligos were then annealed and cloned into the pBFv-U6.2 vector (National Institute of Genetics, Japan), which was injected into embryos of TBX-0002 flies (y1 v1 P{nos-phiC31\int.NLS}X; attP40 (II)). These were further crossed with TBX-0008 flies (y2 cho2 v1/Yhs-hid; Sp/CyO) which allows the identification of the recombinant flies by eye colour marker. Flies bearing the U6-gRNA transgene were crossed with flies expressing Cas9: CAS-0001. After screening the progeny to identify mutations in the targeted gene, flies were crossed with a balancer line for chromosome 2, carrying the marker *cyo* for Mettl16, Mettl25 and Mettl25b mutants, and a baolancer line for chromosome 3, carrying the marker TM6c for Mettl5 mutant lines. Trans-heterozygous Mettl5 fly mutants were producedby crossing Mettl5^{fs} flies with a deficiency fly line for Mettl5 (BL8083-CG9666def, Bloomington Drosophila Stock Center) to exclude possible off-target effects by the CRISPR/Cas9 system. UAS-HA-Mettl5, UAS-eGFP-Mettl25 and UAS-eGFP-Mettl25b lines were generated by injecting pUAST-tag-cDNA. Mettl5 gRNA line and UAS line were generated in house. Injections to generate the other fly lines was performed by FlyORF (Zurich, Switzerland).

Cloning

For the immunostaining and immunoprecipitation the coding sequences of the genes of interest were cloned in the Gateway-based vectors with N-terminal 3XFLAG-6XMyc tag (pPFMW), N-terminal 3XHA tag (pAHW) or C-terminal eGFP tag (pAc5.1b). More specifically, Mettl5, Mettl16 and Ftsj3 coding sequences were cloned into the pPFMW vector, Trmt112 was cloned into both the pAHW and the pAc5.1b vectors, Mettl25 and Mettl25b were cloned into the pAc5.1b vector. Moreover, for the immunofluorescence in S2R+ cells, the UAS promoter of pPFMW and the Actin promoter of pAc5.1b were replaced with the endogenous promoters of Mettl5 and Trmt112, respectively. The oligos used for cloning are listed in table 4, the generated plasmids are in tables 7.

RNA extraction, mRNA purification and qRT-PCR

Total RNA was isolated using TRIzol reagent (Invitrogen) and DNA was digested by DNase I (NEB). mRNA was enriched with three rounds of purification with Dynabeads Oligo(dT)25 (Invitrogen) and the sample quality was then tested by capillary electrophoresis using the Bioanalyzer (Agilent). cDNA for qRT-PCR was prepared using the M-MLV reverse transcriptase (Promega). qPCR was used for the validation of Nm via RTL-P, for KD validation and for checking the expression levels of the genes of interest during fly development. For this,

flies were staged as previously described (Lence et al., 2016). The RT-qPCR was performed using SYBR Green PCR Master Mix (Thermo Fisher Scientific) and the oligos listed in table 5 using the ViiA 7 Real-Time PCR System (Thermo Fisher Scientific).

Cell culture, RNAi and transfection

Drosophila S2R+ cells were grown in Schneider's medium (Gibco), supplemented with 10% FBS (Sigma) and 1% Penicillin and Streptomycin (Sigma). For RNAi experiments, dsRNAs targeting the genes of interestor the bacterial β-galactosidase gene (LacZ) used as control in the KD experiments, were prepared using the T7 megascript Kit (NEB) and the primers listed in table 5. Cells, seeded at a density of 10^6/mL, were treated for 6 hours with FBS-free serum and 7.5 µg/mL dsRNA, after which time, FBS-supplemented medium was added to the cells. The treatment was performed three times at alternate days and samples were collected 24h after the last treatment. For plasmid transfection cells were seeded at a density of 10^6 cells/mL and were transfected using the Effectene Transfection Reagent kit (Qiagen) following manufacturer's protocol. For UAS vectors, co-transfection with an Actin-Gal4 vector was performed to activate the expression of UAS-driven genes.

Immunostaining

Immunostaining was performed in S2R+ cells to visualise the subcellular localization of the studied proteins. For the purpose, S2R+ cells were transfected with a vector in which the coding sequence of the gene of interests was cloned adjacent to a tag (FLAG-Myc, HA or wGFP) and controlled by either a UAS or an Actin promoter. In the case of Mettl5 and Trmt112 constructs, transcription was controlled by their endogenous promoter cloned in place of the original UAS and Actin promoters, respectively. Immunostaining was performed 72 hours after transfection. Cells were incubated with primary antibody (anti-Myc, Enzo 9E19, 1:1000) in 0.2% Triton X-100 PBS (PBST) supplemented with 10% donkey serum overnight at 4°C and secondary antibody (anti-mouse AlexaFluor 568, 1:1,000) and DAPI (1ug/mL, Thermo Fisher Scientific) in 10% donkey serum in PBST for 2h at room temperature (RT). For constructs tagged with eGFP (Mettl25 and Mettl25b) no antibody was used and the nuclei were visualised with Hoechst 33342 (5µg/mL, Thermo Fisher Scientific). Images were taken with Leica SP5 confocal microscope using 63× oil immersion objective.

Co-immunoprecipitation and Western blot analysis

For the immunoprecipitation (IP) assay, S2R+ were cells seeded in 10 cm cell culture dish and co-transfected with FLAG-Myc-Mettl5 vector and HA-Trmt112 or Trmt112-eGFP vector. 72 h post transfection cells were collected, washed with DPBS and pelleted by 5 min centrifugation at 500 g. Cells were then lysed in 1mL lysis buffer (50 mM Tris-HCl pH 7.4, 150 mM NaCl, 0.05 % NP-40) supplemented with protease inhibitors for 30 min at 4°C. After 5 cycles of sonication 30 s ON, 30 s OFF at low power, lysates were centrifuged at 20,000g for 10 min at 4°C to remove the remaining debris and the protein concentration was determined using Bradford reagents (Bio-Rad). 15µL of pre-cleared protein G beads (Thermo Fisher Scientific) were pre-coated

with either mouse anti-FLAG (Sigma-Aldrich, M2-F1804) or mouse anti- HA (clone 12CA5, produced in house) or normal mouse IgG (Santa Cruz Biotechnology, sc-2025) for 30 min and then added to 2mg lysate for 2h head over tail rotation at 4°C. The beads were then washed three times with washing buffer (50 mM Tris–HCl at pH 7.4, 150 mM NaCl) before eluting the samples by incubation with 1x NuPAGE LDS buffer (Thermo Fisher) and 100mM DTT at 70°C for 10 min. Before incubation with antibody, 5% lysate was set aside, to function as input sample. For the Western blot analysis, input and IP samples were separated on a 12% SDS-PAGE gel and transferred to a PVDF membrane (Bio-Rad). After 1h blocking of the membrane with 5%milk in PBST (0.05% Tween in PBS), the membrane was incubated at 4°C overnight in 5% milk PBST with one of the following primary antibodies: mouse anti-Myc (1:2,000; Enzo,9E10), mouse anti-FLAG (1:2,000, Sigma, M2), mouse anti-HA (1:2,000, in-house, 12CA5), and mouse anti-GFP (1:200, Santacruz, B-2). The membrane was washed three times in PBST for 15 min prior incubation with anti-mouse secondary antibody (Jackson ImmunoResearch) for 1 h at room temperature in 5% milk. Protein bands were detected using SuperSignalWest Pico chemiluminescent substrate (Thermo Scientific).

Immunoprecipitation, Dimethyl labelling and proteomic analysis

For analysis of Mettl5 interactors two biological replicates, representing the forward and reverse experiment, were prepared transfecting S2R+ cells with FLAG-Myc empty plasmid and two biological replicates with FLAG-Myc Mettl5 construct. 72h after transfection cells were hasvested and IP was performed as described above in the co-IP section. In this case, IP was performed incubating 15µL of anti-Myc coupled with magnetic beads (Pierce, 9E10) for 2mg of protein lysate. After 2h incubation at 4°C head-over-tail rotation and three rounds of washes of the beads in lysis buffer, immunoprecipitated proteins were eluted at 70°C for 10 min in 1× NuPAGE LDS buffer (Thermo Fisher) supplemented with 100 mM DTT.

Protein lysates were subjected to tryptic digestion, as described by Hsu et al. (Hsu et al., 2003) prior to dimethyl labelling. This was performed by adding formaldehyde-H2 (4% in water, 1 µL) to the control sample and formaldehyde-D2 (4% in water, 1 µL) to the Mettl5 IP sample in the forward experiment, and the opposite combination was done for the reverse experiment. Freshly prepared sodium cyanoborohydride (260 mM, 1 µL) was added. Samples were then vortexed and let rest for 5 min to allow the labelling to occur, as previously described (Hsu et al., 2003). Mass spectrometry measurements were then performed as previously described (Bluhm et al., 2015). MaxQuant (version 1.5.2.8) was used to process to raw file the UniProt database of annotated Drosophila proteins (D. melanogaster: 41,850 entries, downloaded January 8, 2015) was used to identify the enriched proteins.

LC/MS-MS analysis of m^6A and Nm levels

A 0.1-1 µg of RNA was degraded to nucleosides with 0.003 U nuclease P1 (Roche), 0.01 U snake venom phosphodiesterase (Worthington), and 0.1 U alkaline phosphatase (Fermentas). Separation of the nucleosides was performed using with an Agilent 1290 UHPLC system at a flow rate of 0.4 mL/min and

linearly increased to 0.5 mL/mL during first 7 min.This flow was maintained during the washing and reconditioning steps and linearly decreased to 0.4 mL/min in the last minute. The gradients were performed by a gradual increase from 0% to 7% of acetonitrile (Sigma-Aldrich) for 3 min, followed by isocratic elution for 4 min, then switching back to 0% acetonitrile during the next 4 min to recondition the column. Quantitative MS/MS analysis was performed as previously described (Schomacher et al., 2016), using an Agilent 6490 triple quadrupole mass spectrometer in positive electrospray ionization mode. Multiple reaction monitoring (MRM) transitions were 269.2→137.2 (rA, Silantes); 278.2→171.2 (1369-rA, Silantes), 282.1→150.1 (N6mrA, Silantes) and 285.1→153.1 ($^{2}H_{3}$-N6mrA, TRC Inc, Toronto, Canada). For Nm measurements, MRM were 284.1→152.1 (G), 244.1→112.1 (C), 245.1→113.1 (U), 282.1→136.1 (Am), 298.1→152.1 (Gm), 258.1→112.1 (Cm), 259.1→113.1 (Um). The quantification was performed in biological triplicates for all samples. The variances between samples was similar, therefore, two-tailed unpaired Student's t-test was applied.

Phylogenetic analysis

The Protein Path Tracker online tool (PPT) was used as previously described (44 M5 paper) to search for CG9666 orthologs. Identifiers and species names are the following: Q8K1A0, *Mus musculus*; Q9NRN9, *H. sapiens*; F1NZ60, *Gallus gallus*; F1QVR8, *Danio rerio*; F6R9A4, *Ornithorhynchus anatinus*; F6WB92, *Ciona intestinalis*; F7AIW5, *Xenopus tropicalis*; H2P7S0, *Pongo abelli*; H3B2F1, *Latimeria chalumnae*; Q84TF1, *A. thaliana*; Q8MSW4, *D. melanogaster*; and W4YQG0, *Strongylocentrotus purpuratus*. MUSCLE was used as described previously (Edgar, 2004), to perform multiple sequence alignment and ClustalW (Larkin et al., 2007) to produce a phylogenetic tree.

Structural prediction of the *Drosophila melanogaster* Mettl5-Trmt112 complex

The structural prediction of fly Mettl5-Trmt112 complex was based on the crystal structure of the human complex, with which fly Mettl5 and Trmt112 share 59 and 50% sequence identity, respectively. The model was obtained by processing the coordinates of the human crystal structure (Van Tran et al., 2019) and the sequence alignments of the human and fly proteins using the ROBETTA server (Song et al., 2013).The obtained model showed a root-mean-square deviation of only 0.4 A° over 250 Cα atoms compared to the structure of the human complex.

Buridan Paradigm

The assay was performed as previously described (Strauss et al., 1992), to analyse activity and orientation of control and mutant flies. The Canton-S strain was used as control. Wings were cut to 5-day-old flies under cold anaesthesia the evening before the experimenst. The sample size was 30 flies for all genotypes. Shapiro-Wilk test was used to check for the normal distribution of all groups, the Levene's test was used to verify to homogeneity of variances, in which case Student t-test was applied, using Bonferroni correction method due to multiple comparisons.

High-performance liquid chromatography (HPLC) on rRNA

RNA fractionation and HPLC was performed as previously described (Van Tran et al., 2019). In brief, RNA from mutant lines and isogenic controls was loaded on a 10–50% sucrose density gradient in buffer A without protease inhibitor and DTT (buffer A: 0.01 M ammonium phosphate, pH 5.3, 2.5% methanol) and centrifuged at 23 000 × g for 20 h in a Beckman L-90K centrifuge with a SW41Ti. The gradient was fractionated with rotor Isco density gradient fraction collector. Circa 30 µg of 18S rRNA or 60 µg of 28S rRNA was denatured at 95◦C and snap cooled on ice. Using 6 mM sodium acetate/20 mM ZnSO4, pH 5.4 with 2 U of Nuclease P1 (Sigma, #N8630), RNA was digested to single nucleotides for 16 h at 37◦C, followed by 2 h incubation at 37° C after the addition of Tris buffer (o.5 M, pH 8.3) and alkaline phosphatase (Sigma #P4252). Digested nucleotides were analyzed on an Agilent 1220 Infinity LC system with a Supelcosil LC-18S column (Sigma, #58298), using elution buffer A and buffer B (0.01Mammonium phosphate, pH 5.1, 20% methanol) and the elution program. The elution time of the m^6A nucleoside was established with the use of a commercial m^6A (Berry and Associates, #PR 3732).as calibration control.

Pre-rRNA processing analysis

The probes used for the Northern blot are the following: LD4533 (ITS1) and LD4534 (ITS2). For the analysis, 5 µg total RNA was extracted from 10 flies and separated on 1.2% denaturing agarose gel. The Northern blot was performed as previously described (Tafforeau et al., 2013).

Mature rRNAs were visualised by ethidium bromide staining of the gels. Their ratio was measured by densitometry on a ChemiDoc MP (Bio-Rad).

Ribosomal RNA modification analysis

rRNAs were purified on 10-30% sucrose gradient (NaCl 300mM, Tris-HCl pH 8 50 mM, MgCl2 2mM, EGTA 1 mM, Triton-X-100 1%, sodium deoxycholate 0.1%), digested to nucleosides with 2 U of P1 nuclease (Sigma N8630) and 10 µL of alkaline phosphatase (Sigma P4252) and analysed by HPLC as previously described (Sharma et al., 2015).

Effect of Trmt112 on Mettl5 stability

S2R+ cells were subjected to Trmt112 KD by incubation with dsRNA against Trmt112 added in presence of serum-free medium on alternate days. After 6 h Schneider's *Drosophila* medium (Gibco) supplemented with 10% FBS (Sigma-Aldrich), and 100 U/mL penicillin/streptomycin (Sigma-Aldrich) was added. The treament was repeated 3 times. The third time, Trmt112 KD was accompanied by transfection with the pPFMW-Mettl5-FLAG-Myc vector for Mettl5 overexpression, using Effectene reagents (Qiagen) following the manufacturer instructions. A 36 h after transfection, cycloheximide (CHX) was added to the cells, at a concentration of 100µg/mL and cells (Ctrl and Trmt112 KD samples) were harvested at the following timepoints after CHX tratment: 0, 1, 2, 4, 8, 24 h. When collecting the samples, 20% of the cells were used for RNA extraction using TRIzol reagent as previously described, the remaining were incubated in LDS

NuPAGE with 100mM DTT for protein denaturation at 70°C for 10 minutes prior to the electrophoretic run. This was performed on a 12% SDS-PAGE gel and followed by transfer on a PVDF membrane. After blocking of the membrane with 5% milk in PBST, the membrane was incubated with primary antibody in blocking solution over night at 4°C, then washed in PBST 3 times before incubation with the secondary antibody (Jackson Immunoresearch). The primary antibodies used were mouse M2 anti-FLAG (1:2000; Sigma-Aldrich) and mouse anti-β-Tubulin-MMS410P (1:5000; Covance). Protein bands were detected using SuperSignalWest Pico chemiluminescent substrate (Thermo Scientific).

Puromycin incorporation assay

For this assay flies of the indicated genotype were gender separated and collected in vials with a Whatmann filter paper (Merck), where they were starved for 6 h. After starvation, a solution of 5% sucrose supplemented with 600 µM Puromycin was added in the tube and absorbed by the filter to avoid the formation of eccessive liquid in the tube. Flies were fed with this solution before sample collection, for which flies were collected in LDS NuPAGE buffer with 100mM DTT in 1.5mL Eppendorf tubes, homogenized with the use of a pestil and incubated at 70°C for 10 min to denature the proteins. For ovarian samples, ovaries were dissected with forceps and washed in PBS before the addition of LDS buffer. The gel was loaded with equal volume of lysate made from equal number of flies or ovaries. Western blot was performed as previously described. Proteins were separated on a 10% SDS-PAGE gel and transferred on a PVDF membrane. Loading control was performed by Ponceu staining. After 1h of blocking at room temperature in 5% milk in PBST, the membranes were incubated with mouse anti-Puromycin 3RH11 (1:1000, Kerafast) over night at 4°C, washed with PBST 3 times for 10 minutes and incubated with anti-mouse secondary antibody (Jackson ImmunoResearch) in 5% milk. SuperSignalWest Pico chemiluminescent substrate (Thermo Scientific). Was used for signal detection.

Lifespan assay

The lifespan assay was performed on flies lacking or overexpressing *Mettl25* and their respective controls (Mettl25$^{\Delta 4}$/ Mettl25$^{\Delta 4}$; Mettl25$^{\Delta 2}$/ Mettl25$^{\Delta 2}$; TubGal4>UAS-eGFP-Mettl25). Flies were gender-separated and collected in media tubes (20 flies/tube) and the survival rate was monitored over time by counting the flies and transferring them to a new tube every 2 days. Number of flies tested varied from 33 to a maximum of 200 per genotype. For the statistical analysis log-rank test was employed to comapre the survival curve of flies with different genotypes, providing average survival time and P-value.

RNA immunoprecipitation

For RIP experiments, S2R+ transfected cells were washed in PBS and pelleted 72 h after transfection. Lysis buffer (50 mL mM Tris-HCl, pH 7.4, 150 mM NaCl, 0.05 % NP-40) supplemented with protease inhibitors was added to the pellet. After 30 min of incubation, the lysates were spinned at 20,000g for 10 min to remove cellular debris. For the immunoprecipitation, 2mg of proteins were incubated with 2µL of anti-Myc antibody

coupled to protein G magnetic beads (Invitrogen) rotating head-over-tail for 3h at 4°C, after which times the beads were washed three times in lysis buffer. For the elution, 20% of the beads were eluted in NuPage LDS buffer with 100mM DTT for 10 min at 70°C to validate the success of the immunoprecipitation via Western blot. The remaining 80% of beads were resuspended in TRIzol for RNA extraction. Transcript enrichment was analysed via qRT-PCR and normalised to the corresponding input sample and then to a control IP sample.

RNA sequencing and computational analysis

RNA-seq libraries were prepared for S2R+ cells transfected with pPFMW-Ftsj3 vector or with flies for Mettl5 and Mettl25 mutants using the TruSeq Sequencing kit (Illumina) and NebNext Ultra II directional RNA library prep kit for Illumina (NEB), respectively, following the manifacturer's protocol. Sequencing was performed on NextSeq500 with a read length of 85 bp. The data was mapped against Ensembl release 90 of *Drosophila melanogaster* using STAR (v2.6.1b). Counts per gene were derived using htseq-Counts (v.0.9.0). Differential expression analysis was performed using DESeq2 (v. 1.16.1) and filtered for an FDR < 0.01. Bedtools (v.2.27.1), samtools (v.1.5) and kentutils (v.365) were used to generate sequencing depth normalised coverage tracks.

Ribosome profiling

Ribosome profiling was performed following the protocol from McGlingy and Ingolia (McGlingy and Ingolia, 2017) with some adaptations. In brief, *Drosophila* (25 per sample) or *Drosophila* heads (150 per sample) were homogenized with pestils and lysed in lysis buffer (20mM Tris pH 7.5, 150mM NaCl, 5mM $MgCl_2$, 1mM DTT, 1% NP-40, 100µM/mL CHX, Turbo DNase, 1x proteinase inhibitor) for 15 min on ice, centrifuged at 10000g to separate the protein lysate from the fat tissues and other debris, 10% of the volume of each sample was flash frozen in liquid nitrogen and set aside to prepare totRNA library. Samples were then subjected to RNaseI (Ambion, 2295) digestion and purified in S400-HR column (GE healthcare) to isolate the ribosomes through size exclusion chromatography. The extracted RNA was separated and excised from a 15% urea polyacrylamide gel. RNA was extracted from the gel overnight at 4°C on a rotating wheel and then precipitated in isopropanol for 2 h at-20°C. RNA was 3' end repaired using 30U of T4 PNK (Lucigen, P0503K) in PNK buffer (Lucigen) for 1 h at 37° C and ligated to 1µM of a 5'-adenylated DNA adaptor, containing sample barcode and an 8N unique molecular identifier (UMI) (Table 6) using 200 U of T4 RNA Ligase 2 deletion mutant K227Q (NEB, M0451L), 10% PEG 8000 (NEB, B1004SVIAL), 13.3 U/µL of Riboguard (Lucigen, RG90910K). The excess unligated adaptor was removed by incubation with 3 U/µL of 5' deadenylase (NEB, M0331S) and 3 U/µL of RecJ exonuclease (NEB, M0264S)for 1 h at 30°C and 1 h at 37°C. Using Zymo Clean & Concentrator columns (Zymo Research, R1016), samples were purified. After pooling the libraries, ribosomal RNA was depleted using the siTools Biotech rRNA depletion kit (dp-K012-000007) following the manufacturer instructions with the exception of the last purification step, for which Zymo Clean & Concentrator columns were used. Pooled libraries were then subjected to reverse transcription, size

selection, circularization and amplification as previously described (McGlingy and Ingolia, 2017). The libraries were sequenced on a NovaSeq6000 (Illumina).

The data were analysed as previously described (Arpat et al., 2020). In brief, reads were trimmed from the adapter sequences using cutadapt (version 3.5) and quality filtered using fastx_toolkit (version 0.0.14). UMItools (version 1.0.0git) was used to extract the UMI sequences. The reads were the sizeselected (26 to 35 nucleotides long for footprints) and mapped to *Drosophila* database using bowtie2 (version 2.3.5) to filter out rRNA and tRNA sequences. Barcode demultiplexing was performed with UMItools. Chip-seq tools (version 1.5.5) were used to make colleration plots. The occurrences for the predicted A site for each of the 64 codons was counted in each sample and the relative frequencies calculated. The log2 value of the frequency ratios were plotted.

RiboMethseq

RiboMethSeq (RMS) was performed as previouslly described (Marchand et al., 2016).

For each sample, 150 ng of total RNA were used. Samples were subjected to alkaline hydrolysis for 16 min at 96°C prior to ethanol precipitation and end repair of the fragments. Libraries were prepared using the NEBNext Small RNA library preparation kit, quantified, multiplexed and sequenced on a NextSeq2000 instrument with single read method with a length of 50 bp. Trimmomatic v0.39 was used to filter out the adapter sequences before mapping the selected sequences to the D. melanogaster sequences using bowtie2 in End-to-End mode. ScoreMean>0.92 and ScoreA >0.5 and ScoreC (MethScore) were considered to quantify the methylation level.

Nanopore-sequencing and data processing

Samples for Nanopore-sequencing were prepared as described in Sklias et al (Sklias et al., 2024). In brief, S2R+ cells (Ctrl, Ftsj3KD and FibKD), in biological duplicates, were harvested and total RNA extracted. DNase treatment and polyadenylation were performed as previously described (Smith et al., 2020). Ligated RNA was prepared for direct RNA sequencing using the SQK-RNA002 kit following the ONT Direct RNA Sequencing protocol version DRS_9080_v2_revI_14Aug2019, with the exception of the annealing step, for which barcoded oligonucleotides A and B were mixed in annealing buffer (0.01 M Tris-Cl pH 7.5, 0.05M NaCl) to a final concentration of 1.4 µM each, heated at 94°C for 5 min and slowly cooled down to room temperature. Then 200 ng of total RNA were ligated to the preannealed-adaptors, using T4 DNA ligase (NEBM0202T), reverse transcribed at 60°C for 30 min with Maxima H Minus RT (Thermo Scientific). The products were purified using 1.8X Agencourt RNAClean XP beads (Fisher Scientific). 50 ng from each reacions were pooled together and the RMX adapter was ligated to the formed RNA:DNA hybrid. After a purification step, the sample was mixed with RNA Running Buffer (RRB) prior to loading onto a R9.4.1 flowcell and run on MinION sequencing devices.

The sequencing results were analysed as described by Sklias et al. (Sklias et al., 2024). In brief, the raw data were processed with the Master od Pores pipeline (version 1.5), demultiplexed with DeePlexiCon, basecalled with Guppy basecaller v4.0, and mapped with minimap2 v3.17 to *D. melanogaster* sequences obtained from Ensembl.

Basecalling features (base quality, mismatch frequency, insertion frequency and deletion frequency) were extracted using Epinano v1.2 (Liu et al., 2019) and scores for each position, based on mismatch, deletion and insertion frequencies between control and KD samples, were assigned as previously described (Begik et al., 2021). The median of scores per transcript and per replicate was calculated and nucleotides with a score greater than 3x the median score of all positions in the same transcript in both replicates were kept as novel Nm sites.

Reverse Transcription at Low deoxy-ribonucleoside triphosphate (dNTP) concentrations followed by polymerase chain reaction (RTL-P)

RTL-P was performed to address the ribose methylation levels on rRNA and on *MRP* in presence and absence of Ftsj3 and Fib in S2R+ cells, as previously described (Dong et al., 2012). Briefly, primers for reverse transcription (RT) were designed complementary to regions downstream the tested Nm sites on the *18S* and *28S* rRNA and *MRP* RNA. Total RNA was collected from S2R+ cells, subjected to KD of *Ftsj3* or *Fib* or double KD of both enzymes, using TRIzol. Reverse transcription was performed with reverse primers from table 5 for all samples using low (0.1µM) or high (1mM) dNTPs concentration. After RT, cDNA was amplified via qPCR using SYBR green reagents (Thermo Fisher Scientific) in the ViiA 7 Real-Time PCR System (Thermo Fisher Scientific). The oligos used for the qPCR are listed in table 5, and were designed in a way that 2 qPCR reaction would be performed for every RT reaction, one using a forward oligo annealing upstream the tested Nm site, and another one using a forward oligo annealing just downstream the tested Nm site, based on the principle that if Nm is present, there will be more amplification, and hence a lower Ct value, in the qPCR reaction which uses oligos downstream the Nm site compared to the reaction with an upstream forward primer, at low dNTPs. The Ct values from reactions with an upstream forward primer are therefore normalised with the Ct values obtained with the downstream oligos (down-up). An ulterior normalization is then performed between values obtained with low dNTPs and high dNTP concentration (low-high). The un-normalized methylation score is obtained as $2^{-(low-high)}$. The relative changes in Nm level upon the methyltransferases KD is obtained normalizing the methylation scores of the KD conditions to the control sample.

Table 3: List of fly lines generated and used in this study.

Category	Genotype	Chr	Source
Mettl5 gRNAs 1 + 2	Met+G4:G31tl5 gRNA/cyo	II	this study
Mettl16 gRNAs 1 + 2	Mettl16 gRNA/cyo	II	this study
Mettl25 gRNAs 1 + 2	Mettl25 gRNA/cyo	II	this study
Mettl25b gRNAs 1 + 2	Mettl25b gRNA/cyo	II	this study
Mutant line Mettl5fs	Mettl5fs/Sb	III	this study
Mutant line Mettl5Δ2AA	Mettl5Δ2AA/Sb	III	this study
Mutant line Mettl16fs	Mettl16fs/cyo	II	this study
Isogenic control Mettl16fs	Mettl16 fs negative control		this study
Mutant line Mettl25Δ2	Mettl25Δ2/cyo	II	this study (injection by FlyORF)
Isogenic control Mettl25Δ2	Mettl16 fs negative control		this study
Mutant line Mettl25Δ4	Mettl25Δ4/cyo	II	this study (injection by FlyORF)
Isogenic control Mettl25Δ4	Mettl25Δ4 negative control		this study
Mutant line Mettl25bΔ2	Mettl25bΔ2/cyo	II	this study (injection by FlyORF)
Isogenic control Mettl25bΔ2	Mettl25bΔ2 negative control		this study
Mutant line Mettl25bΔ1kb	Mettl25bΔ1kb/cyo	II	this study (injection by FlyORF)
Isogenic control Mettl25Δ1kb	Mettl25bΔ1kb negative control		this study
UASp-Mettl5-FLAGMyc	UAS-CG9666.FM/CyO	II	this study
UASp-Mettl5-3xHA	M{UAS-CG9666.ORF.3xHA}ZH-86Fb	III	FlyORF
UASt-Mettl25-eGFP	UAS-CG33964.eGFP/Sb	III	this study (injection by FlyORF)
UASt-Mettl25b-eGFP	UAS-CG2906.eGFP/Sb	III	this study (injection by FlyORF)
BL8083-Mettl5^{def}	w^{1118}; Df(3L)ED4786, P{w[+mW.Scer\FRT.hs3]=3'.RS5+3.3'}ED4786/TM6C, cu^{1} Sb^{1}	III	Bloomington
BL8085-Mettl5^{def}	w^{1118}; Df(3L)ED4799, P{w[+mW.Scer\FRT.hs3]=3'.RS5+3.3'}ED4799/TM6C, cu^{1} Sb^{1}	III	Bloomington
CRISPR/Cas9 line (CAS-0001)	y^{2} cho^{2} v^{1}; attP40{nos-Cas9}/CyO		NIG-FLY
daGal4/cyoGFP	daGal4/Tm6c	II	Bloomington
ElavGal4/cyoGFP	ElavGal4/FM6; UAS-mcherry/Tm6c	II	Lab stock
Tub-Gal4/cyoGFP	w-; Tubulin Gal4; CyO	II	Bloomington
FM6	FRT 19 Ayn^{8B1}/FM6, w		Bloomington
Cyo, TM6b balancer	Sco/Cyo; MKRS/TM6b	II, III	Lab stock
CRISPR/Cas9 line (TBX-0002)	y^{1} v^{1} P{nos-phiC31\int.NLS}X; attP40	II	National Insitute of Genetics
CRISPR/Cas9 line (TBX-0008)	y^{2} cho^{2} v^{1}/Yhs-hid; Sp/CyO	II	National Insitute of Genetics
CRISPR/Cas9 line (TBX-0010)	y^{2} cho^{2} v^{1}; Pr Dr/TM6C, Sb Tb	III	National Insitute of Genetics
WT w^{1118}	Wildtype w^{1118}		Bloomington
WT-Canton S	wildtype-Canton S		Lab stock

Table 4: List of oligos used for mutant lines generation and overexpression experiments.

Oligos for CRISPR/Cas	Sequence 5' → 3'
Mettl5/CG9666 cris gRNA1 F	CTTCGCCGCACATAGCCGCGTGCA
Mettl5/CG9666 cris gRNA1 R	AAACTGCACGCGGCTATGTGCGGC
Mettl5/CG9666 cris gRNA2 F	CTTCTTCGGCACGAAACACAATGC
Mettl5/CG9666 cris gRNA2 R	AAACGCATTGTGTTTCGTGCCGAAT
Mettl16/CG7544 cris gRNA1 F	CTTC GGAATATTACGATTTAGATG
Mettl16/CG7544 cris gRNA1 R	AAAC CATCTAAATCGTAATATTCC
Mettl16/CG7544 cris gRNA2 F	CTTC GGCCAACGTTCCAAGAATAC
Mettl16/CG7544 cris gRNA2 R	AAAC GTATTCTTGGAACGTTGGCC
Mettl25/CG33964 cris gRNA1 F	CTTCGAAAAGTGAGATCGCCGGCA
Mettl25/CG33964 cris gRNA1 R	AAACTGCCGGCGATCTCACTTTTC
Mettl25/CG33964 cris gRNA2 F	CTTCGCTGAAAAACGAACTGCAGG
Mettl25/CG33964 cris gRNA2 R	AAACCCTGCAGTTCGTTTTTCAGC
Mettl25b/CG2906 cris gRNA1 F	CTTCGATCATTGGAGTAAACTTCC
Mettl25b/CG2906 cris gRNA1 R	AAACGGAAGTTTACTCCAATGATC
Mettl25b/CG2906 cris gRNA2 F	CTTCGGGTACTCGCTTTGAAGCAC
Mettl25b/CG2906 cris gRNA2 R	AAACGTGCTTCAAAGCGAGTACCC
Oligos for CRISPR screening	**Sequence 5' → 3'**
CG9666 cris screenF	GCAGTCGCTTTTTCCCACTC
CG9666 cris screenR	CAAAGCGCCAGAAGTCCACC
CG7544 cris screenF	CAATGGCAAGGTTTCTGTGA
CG7544 cris screenR	CGGCAACTTGTGCTTAGTGA
CG33964 cris screenF	CCTGCAGAGACCAATTCTGTCG
CG33964 cris screenR	TAGAGCAGGCGATCCAGGAG
CG2906 cris screenF	CTCCTGGTACACCTCCTGAATC
CG2906 cris screenR	CTCCACCAGCGGAGCCATC

Oligos used for cloning	Sequence 5' → 3'
Mettl5 / CG9666 FM F	AACGCGGCCGCAATGGCCCGGTTGAAGCT
Mettl5 / CG9666 FM R	AACGGCGCGCCCTATTCCGTGCCGATTTCAAA
Trmt112/CG12975 3X-HA F	AGCGGTACCATGAAACTCAGCACATACAAC
Trmt112/CG12975 3X-HA R	AACGGCGCGCCCTAGACCTCGTCCTCGTTAAG
Trmt112/CG12975 eGFP F	AGCGGTACCATGAAACTCAGCACATACAAC
Trmt112/CG12975 eGFP R	AACGGTACCGACCTCGTCCTCGTTAAG
Mettl5 promoter F	AACAGCGCTCAAAAGGCAATGTGCGC
Mettl5 promoter R	AACGAATTCTGTGGATCCGGCTATTTG
Trmt112 promoter F	AGCAGATCTTGGCCCTCTTTAGCCACC
Trmt112 promoter R	AACGGTACCGACCTCGTCCTCGTTAAG
Mettl16/CG7544 FM F	AACGCGGCCGCAATGGTAAAAA CTAAGGG
Mettl16/CG7544 FM F	AACGGCGCGCCTAGTGGCTCCGAGTGGA
Ftsj3/CG8939 F	AGCACCGGTGGCAAGAAGACGAAAGTTGGA
Ftsj3/CG8939 R	AACGGCGCGCCTTATTTACGCCCCTTCCCCTT
Mettl25/CG33964 eGFP F	CGGGGTACCAAATGTCCAAGGTGGGAGTT
Mettl25/CG33964 eGFP R	CTAGTCTAGATCTAGATTATTGTTGCGTTTGCTGCTTT
Mettl25b/CG2906 eGFP F	CGGGGTACCAAATGTTGATTGTAAGAGAAAAACTCG
Mettl25b/CG2906 eGFP R	CTAGTCTAGATCTAGATTACGGTTTAACGGCCCT

Table 5: List of oligos used for RNAi, qRT-PCR and RTL-P in this study.

Oligos used for RNAi	Sequence	Oligos used for qRT-PCR	Sequence
Mettl1 / CG4045 KD F	TTAATACGACTCACTATAGGGAGACGGAGAGTAGAGCCTGGTTG	Mettl1 / CG4045 qF	GCTTCGACTATCCTGCTCGC
Mettl1 / CG4045 KD R	TTAATACGACTCACTATAGGGAGACTCCATGTACCCAGGCATTC	Mettl1 / CG4045 qR	ACCTTGACGCGGATTTCCAT
Mettl2 / Metl KD F	TTAATACGACTCACTATAGACAGTACAGCTCTGAACCGC	Mettl2 / Metl qF	GAGTTTAACGCCTGGGACCA
Mettl2 / Metl KD R	TTAATACGACTCACTATAGTCTGAATCCACACGCGGTAC	Mettl2 / Metl qR	GGGAACTCCGTAAACAGCCA
Mettl3 / Mettl3 KD F	TTAATACGACTCACTATAGGGAGAAGTCGACGATGTTGATCAGCCACAG	Mettl3 / Mettl3 qF	AAGGAACTCGTTGAGGCTGA
Mettl3 / Mettl3 KD R	TTAATACGACTCACTATAGGGAGAGTTGGTTGGTCTTTACCCAGATGAG	Mettl3 / Mettl3 qR	CACCTGTGTGGAGACAATGG
Mettl4 / CG14906 KD F	TTAATACGACTCACTATAGGGAGACGAAGCATATGACGAATTTAAGC	Mettl4 / CG14906 qF	TGATGGACGAAAGGCTATATGA
Mettl4 / CG14906 KD R	TTAATACGACTCACTATAGGGAGATGGTTGCAATGTTCTACTTTACG	Mettl4 / CG14906 qR	GCGTAGCTAATTTACCTCCTCCT
Mettl5 / CG9666 KD F	TAATACGACTCACTATAGGGGTGAATCCAGACTTCCAGGC	Mettl5 / CG9666 qF	TCGAAGGATATTGAGGTGGA
Mettl5 / CG9666 KD R	TAATACGACTCACTATAGGGCAGAGTGGAAGCAATGCTGA	Mettl5 / CG9666 qR	TGTCCAAAACTAAATGCAACTGA
Mettl6 / CG34195 KD F	TTAATACGACTCACTATAGTTGGACGAGCAAAACAAGCG	Mettl6 / CG34195 qF	CCGGGCAACAAGATAGCAGA
Mettl6 / CG34195 KD R	TTAATACGACTCACTATAGGAAGCAGTCCTCCTGGCTTT	Mettl6 / CG34195 qR	TGACCTCAAAGCCGTTCTCC
Mettl9 / CG5339 KD F	TTAATACGACTCACTATAGTCCGAGGAACAGTTTCGCAA	Mettl9 / CG5339 qF	TCGAGCAGTTGTGGCCTTAG
Mettl9 / CG5339 KD R	TTAATACGACTCACTATAGATCACCCTCGCACAAGTACG	Mettl9 / CG5339 qR	ATCACCCTCGCACAAGTACG
Mettl10 / CG9643 KD F	TTAATACGACTCACTATAGATGGATAGCGAGCTGAACGG	Mettl10 / CG9643 qF	CACATACAAGGTGGCGGACT
Mettl10 / CG9643 KD R	TTAATACGACTCACTATAGACAAACAGGCTGTCAGCAGT	Mettl10 / CG9643 qR	GCAACTTTTCCACCGTGTCC
Mettl13 / CG2614 KD F	TTAATACGACTCACTATAGGGTACGGCGAATACCTGGAG	Mettl13 / CG2614 qF	CTACCTAGCCTGCCAGCATC
Mettl13 / CG2614 KD R	TTAATACGACTCACTATAGGAAAACAGGCAGCGTCAAGG	Mettl13 / CG2614 qR	TCGACGGCCGTTATTCTAGC
Mettl14 / Mettl14 KD F	TAATACGACTCACTATAGGGAGATAATCAGAATGCCGCCACTA	Mettl14 / Mettl14 qF	AAGCGTCGTTTGCTTTTAGC
Mettl14 / Mettl14 KD R	TAATACGACTCACTATAGGGAGATGATCAGTTCCCTCAACTTGG	Mettl14 / Mettl14 qR	GCATTACCCAAAGCCTTTTTC
Mettl15 / CG14683 KD F	TTAATACGACTCACTATAGGAGAAGTGTCCCGAGGCAAA	Mettl15 / CG14683 qF	AAGACCTTCCAAGCCATCCG
Mettl15 / CG14683 KD R	TTAATACGACTCACTATAGCGGATGGCTTGGAAGGTCTT	Mettl15 / CG14683 qR	TCCGTTGATGTGACGCTTCA
Mettl16 / CG7544 KD F	TAATACGACTCACTATAGGGAGAAGTTTGGTGCCCACATTAGC	Mettl16 / CG7544 qF	GCAGCCCGACTATACCAAAA
Mettl16 / CG7544 KD R	TAATACGACTCACTATAGGGAGAGTAGTGGCTCCGAGTGGAAG	Mettl16 / CG7544 qR	CACAGAAACCTTGCCATTGA
Mettl17 / CG13126 KD F	TTAATACGACTCACTATAGTTGGAACCGGTATGTGGGTG	Mettl17 / CG13126 qF	TCTGTCCTCGACTTCGGGAT
Mettl17 / CG13126 KD R	TTAATACGACTCACTATAGTGACGGTCTGCCAAGAAGTC	Mettl17 / CG13126 qR	TGACGGTCTGCCAAGAAGTC
Mettl18 / CG17219 KD F	TTAATACGACTCACTATAGGGAGACGTGAGTCGGGTATCACAAA	Mettl18 / CG17219 qF	TATCAAGGGATGTGGCGAAA
Mettl18 / CG17219 KD R	TTAATACGACTCACTATAGGGAGAGCAGCCACATCCCAAATCTA	Mettl18 / CG17219 qR	TTTAAGCGACCAGCAAAGGT
Mettl19 / CG9386 KD F	TTAATACGACTCACTATAGGGAGATGGAGTCAAACACAATCGGA	Mettl19 / CG9386 qF	GGAATTGTGGATTTTGAGAATTG
Mettl19 / CG9386 KD R	TTAATACGACTCACTATAGGGAGACGCTTGGTGCTTGGTATTTT	Mettl19 / CG9386 qR	CACAAATTCCAACCAGTTGGT
Mettl22 / CG10584 KD F	TTAATACGACTCACTATAGAATGGAACTGGGAGCTGGTG	Mettl22 / CG10584 qF	AATGGAACTGGGAGCTGGTG
Mettl22 / CG10584 KD R	TTAATACGACTCACTATAGGTTGCTTGCAGCGATCGTAC	Mettl22 / CG10584 qR	CCGCGGATCAGCTTCAGTAT
Mettl23 / CG5013 KD F	TTAATACGACTCACTATAGGAGCGCCGACAGACACTG	Mettl23 / CG5013 qF	GGCAGCGAGGACAATGACAT
Mettl23 / CG5013 KD R	TTAATACGACTCACTATAGGATGCGCGTGATCTCCAGAA	Mettl23 / CG5013 qR	GAGTAGGCACCCTGAAGCAG
Mettl25A / CG33964 KD F	TTAATACGACTCACTATAGTGCTATCATTTGCTGCGGGA	Mettl25A / CG33964 qF	ATTGGATGCTCCCTGGTTGG
Mettl25A / CG33964 KD R	TTAATACGACTCACTATAGAGCTGCGTTCATAGCCAAGT	Mettl25A / CG33964 qR	AGCTGCGTTCATAGCCAAGT
Mettl25B / CG2906 KD F	TTAATACGACTCACTATAGGGAGAGCTGTTGGATGCCTATGTACTG	Mettl25B / CG2906 qF	CCGCTGGTGGAGAGCATTAT
Mettl25B / CG2906 KD R	TTAATACGACTCACTATAGGGAGATTCAAAGCGAGTACCCTGTACG	Mettl25B / CG2906 qR	GCCCTGGTGATGTGGTTTCT
Mettl26 / CG18661 KD F	TTAATACGACTCACTATAGGATCGCAATTCGCAACCGAT	Mettl26 / CG18661 qF	AAGGCTATTGGGGCGCTATT
Mettl26 / CG18661 KD R	TTAATACGACTCACTATAGGTCCTTAATGTCGCGAACGC	Mettl26 / CG18661 qR	CTCTCGCTCTGACCACTTGG
Trmt112 / CG12975 KD F	TAATACGACTCACTATAGGGAGAAATCCAACTTTTGTGGAGAG	Trmt112 / CG12975 qF	CTCAGCACATACAACTTCTTGACC
Trmt112 / CG12975 KD R	TAATACGACTCACTATAGGGAGATCCTCGTTAAGGAGCATG	Trmt112 / CG12975 qR	CGCTCTCCACCACTTCCTTT
Ftsj3/CG8939 KD F	TTAATACGACTCACTATAGGGAGAGAAGACGCTCAAGACCAAGG	Ftsj3 / CG8939 qF	CTGCAGGTACAAATGCCAAG
Ftsj3/CG8939 KD R	TTAATACGACTCACTATAGGGAGATTGGTGTTTTTGTCACGGAA	Ftsj3 / CG8939 qR	GTTGAAAGCGTAGCGATTCC
Fib KD F	TTAATACGACTCACTATAGGCGAGAAGATTGAGTACCGC	Fib qF	ATCGTCACGAGGGAGTGTTC
Fib KD R	TTAATACGACTCACTATAGGCCTGCATCTTCTTCACCTC	Fib qR	ATTGGTCTCAACGGAGATGC
Oligos used for RTL-P	**Sequence**	18S end FP qP	GAATTCCCAGTAAGTGTGAG
Mrp preC137 qF	CCTAGGATAGAAAGTATCAAGGTG	18S end RP qP	GGAGACCTCACTAAATAATTC
Mrp postC137 qF	GGTGGGTGGTGCATTC	Actin5C qF	CACACCAAATCTTACAAAATGTG
Mrp qR	GGATTCGGATAAAATCCTCTTC	Actin5C qR	AATCCGGCCTTGCACATG
18S preU586 qF	CAATTGGAGGGCAAGTCTGG	Rpl15 qF	AGGATGCACTTATGGCAAGC
18S postU586 qF	GCGTATATTAAAGTTGTTGCGG	Rpl15 qR	GCGCAATCCAATACGAGTTC
18S U586 qR	CAATTGTAAGTTGTACTACCCG	MAT2A qF	GGCAAGATTGTCAAGGACC
28S preU3454 qF	GATAACTGGCTTGTGGCGGC	MAT2A qR	GTTGTCAATCTCCAGAGGC
28S postU3454 qF	GATCCTTCGATGTCGGCTC	U6 qF	GTTCTTGCTT CGGCAGAAC
28S U3454 qR	CCCTTGCATGGGTGAACAATC	U6 qR	AATGTGGAACGCTTCACG

Table 7: List of oligos required for ribo-seq.

Oligos used for Ribo-seq	Sequence 5' →3'
RT NI-802	/5Phos/RNA GAT CGG AAG AGC GTC GTG TAG GGA AAG AG/iSp18/G TGA CTG GAG TTC AGA CGT GTG CTC
PCR F (i5) AL1	AATGATACGGCGACCACCGAGATCTACACTATAGCCTACACTCTTTCCCTACACGACGCTC
PCR F (i5) AL2	AATGATACGGCGACCACCGAGATCTACACATAGAGGCACACTCTTTCCCTACACGACGCTC
PCR F (i5) AL3	AATGATACGGCGACCACCGAGATCTACACCCTATCCTACACTCTTTCCCTACACGACGCTC
PCR F (i5) AL4	AATGATACGGCGACCACCGAGATCTACACGGCTCTGAACACTCTTTCCCTACACGACGCTC
PCR F (i5) AL5	AATGATACGGCGACCACCGAGATCTACACAGGCGAAGACACTCTTTCCCTACACGACGCTC
PCR F (i5) AL6	AATGATACGGCGACCACCGAGATCTACACTAATCTTAACACTCTTTCCCTACACGACGCTC
PCR R (i7) NI-799	CAA GCA GAA GAC GGC ATA CGA GAT CGT GAT GTG ACT GGA GTT CAG ACG TGT G
PCR R (i7) NI-822	CAA GCA GAA GAC GGC ATA CGA GAT ACA TCG GTG ACT GGA GTT CAG ACG TGT G
PCR R (i7) NI-823	CAA GCA GAA GAC GGC ATA CGA GAT GCC TAA GTG ACT GGA GTT CAG ACG TGT G
PCR R (i7) NI-824	CAA GCA GAA GAC GGC ATA CGA GAT TGG TCA GTG ACT GGA GTT CAG ACG TGT G
PCR R (i7) NI-825	CAA GCA GAA GAC GGC ATA CGA GAT CAC TGT GTG ACT GGA GTT CAG ACG TGT G
PCR R (i7) NI-826	CAA GCA GAA GAC GGC ATA CGA GAT ATT GGC GTG ACT GGA GTT CAG ACG TGT G
linker 8NI-810	/5Phos/NNN NNN NNA TCG TAG ATC GGA AGA GCA CAC GTC TGA A/3ddC/
linker 8NI-811	/5Phos/NNN NNN NNA GCT AAG ATC GGA AGA GCA CAC GTC TGA A/3ddC/
linker 8NI-812	/5Phos/NNN NNN NNC GTA AAG ATC GGA AGA GCA CAC GTC TGA A/3ddC/
linker 8NI-813	/5Phos/NNN NNN NNC TAG AAG ATC GGA AGA GCA CAC GTC TGA A/3ddC/
linker 8NI-814	/5Phos/NNN NNN NNG ATC AAG ATC GGA AGA GCA CAC GTC TGA A/3ddC/
linker 8NI-815	/5Phos/NNN NNN NNG CAT AAG ATC GGA AGA GCA CAC GTC TGA A/3ddC/
linker 8NI-816	/5Phos/NNN NNN NNT AGA CAG ATC GGA AGA GCA CAC GTC TGA A/3ddC/
linker 8NI-817	/5Phos/NNN NNN NNT CTA GAG ATC GGA AGA GCA CAC GTC TGA A/3ddC/
34: RP_upper marker	AUGUACACGGAGUCGAGCUCAACCCGCAACGCGA
26: RP_lower marker	AUGUACACGGAGUCGACCCAACGCGA
20/100 Ladder	Cat. Number: 51-05-15-02 (IDT)
115: RP_lowMarker	AUGUACACGGAGUCGACCCAACGCGAUGUACACGGAGUCGACCCAACGCGAUGUACACGGAGUCGACCCAACGCGAUGUACACG GAGUCGACCCAACGCGAUGUACACGGAGUCA
125: RP_midMarker	AUGUACACGGAGUCGACCCAACGCGAUGUACACGGAGUCGACCCAACGCGAUGUACACGGAGUCGACCCAACGCGAUGUACACG GAGUCGACCCAACGCGAUGUACACGGAGUCGACCCAACGCG
155: RP_highMarker	AUGUACACGGAGUCGACCCAACGCGAUGUACACGGAGUCGACCCAACGCGAUGUACACGGAGUCGACCCAACGCGAUGUACACG GAGUCGACCCAACGCGAUGUACACGGAGUCGACCCAACGCGAUGUAUGUACACGGAGUCGACCCAACGCGA
Low Molecular Weigth (LMW) Ladder	Cat. Number: N3233L (NEB)
25bp ladder	Cat. Number: G4511 (Promega)

Table 8: List of plasmids generated and used in his

Construct name	Plasmid backbone	Promoter	Tag	Experiment
U6.2B-Mettl5gR	pPv-U6.2B	U6	/	CRISPR/Cas9
U6.2B-Mettl16gR	pPv-U6.2B	U6	/	CRISPR/Cas9
U6.2B-Mettl25gR	pPv-U6.2B	U6	/	CRISPR/Cas9
U6.2B-Mettl25bgR	pPv-U6.2B	U6	/	CRISPR/Cas9
U6.2B-Mettl5gR	pPv-U6.2B	U6	/	CRISPR/Cas9
pPFMW-Ctrl	pPFMW	UASp	3XFLAG-6XMyc	Ctrl
pPFMW-Mettl5	pPFMW	UASp	N-term 3XFLAG-6XMyc	OE
pPFMW-Mettl5p	pPFMW	Mettl5 promoter	N-term 3XFLAG-6XMyc	OE
pAHW-Ctrl	pAHW	Actin5c	3XHA	Ctrl
pAHW-Trmt112	pAHW	Actin5c	N-term 3XHA	OE
pAc5.1B-eGFP	pAc5.1B-eGFP	Actin5c	eGFP	Ctrl
pAc5.1B-Trmt112	pAc5.1B-eGFP	Actin5c	C-term eGFP	OE
pAc5.1B-Trmt112p	pAc5.1B-eGFP	Trmt112 promoter	C-term eGFP	OE
pAFW-Ftsj3	pAFW	Actin5c	N-term 3XFLAG	OE
pUAST-eGFP-attB	pUAST-eGFP-attB	UASt	eGFP	Ctrl
pUAST-eGFP-Mettl25	pUAST-eGFP-attB	UASt	N-term eGFP	OE
pUAST-eGFP-Mettl25b	pUAST-eGFP-attB	UASt	N-term eGFP	OE
Actin-Gal4	pPac	Actin5c	/	Gal4 expression
GFP-Barentz	pPGW	UASp	N-term eGFP	OE

9.References

Abbas, Y. M., Laudenbach, B. T., Martínez-Montero, S., Cencic, R., Habjan, M., Pichlmair, A., Damha, M. J., Pelletier, J., & Nagar, B. (2017). Structure of human IFIT1 with capped RNA reveals adaptable mRNA binding and mechanisms for sensing N1 and N2 ribose 2?-O methylations. *Proceedings of the National Academy of Sciences of the United States of America*, *114*(11), E2106–E2115. https://doi.org/10.1073/pnas.1612444114

Abe, M., Naqvi, A., Hendriks, G. J., Feltzin, V., Zhu, Y., Grigoriev, A., & Bonini, N. M. (2014). Impact of age-associated increase in 2'-O-methylation of miRNAs on aging and neurodegeneration in Drosophila. *Genes and Development*, *28*(1), 44–57. https://doi.org/10.1101/gad.226654.113

Agrawal, N., Dasaradhi, P. V. N., Mohmmed, A., Malhotra, P., Bhatnagar, R. K., & Mukherjee, S. K. (2003). RNA Interference: Biology, Mechanism, and Applications. *Microbiology and Molecular Biology Reviews*, *67*(4), 657–685. https://doi.org/10.1128/mmbr.67.4.657-685.2003

Akichika, S., Hirano, S., Shichino, Y., Suzuki, T., Nishimasu, H., Ishitani, R., Sugita, A., Hirose, Y., Iwasaki, S., Nureki, O., & Suzuki, T. (2019). Cap-specific terminal N 6 -methylation of RNA by an RNA polymerase II–associated methyltransferase. *Science*, *363*(6423), 1–8. https://doi.org/10.1126/science.aav0080

Alazami, A. M., Al-Owain, M., Alzahrani, F., Shuaib, T., Al-Shamrani, H., Al-Falki, Y. H., Al-Qahtani, S. M., Alsheddi, T., Colak, D., & Alkuraya, F. S. (2012). Loss of function mutation in LARP7, chaperone of 7SK ncRNA, causes a syndrome of facial dysmorphism, intellectual disability, and primordial dwarfism. *Human Mutation*, *33*(10), 1429–1434. https://doi.org/10.1002/humu.22175

Alexandrov, A., Chernyakov, I., Gu, W., Hiley, S. L., Hughes, T. R., Grayhack, E. J., & Phizicky, E. M. (2006). Rapid tRNA decay can result from lack of nonessential modifications. *Molecular Cell*, *21*(1), 87–96. https://doi.org/10.1016/j.molcel.2005.10.036

Alexandrov, A., Martzen, M. R., & Phizicky, E. M. (2002). Two proteins that form a complex are required for 7-methylguanosine modification of yeast tRNA. *Rna*, *8*(10), 1253–1266. https://doi.org/10.1017/S1355838202024019

Alings, F., Sarin, L. P., Fufezan, C., Drexler, H. C. A., & Leidel, S. A. (2015). An evolutionary approach uncovers a diverse response of tRNA 2-thiolation to elevated temperatures in yeast. *Rna*, *21*(2), 202–212. https://doi.org/10.1261/rna.048199.114

Anderson, J., Phan, L., Cuesta, R., Carlson, B. A., Pak, M., Asano, K., Björk, G. R., Tamame, M., & Hinnebusch, A. G. (1998). The essential Gcd10p-Gcd14p nuclear complex 15 required for 1- methyladenosine modification and maturation of initiator methionyl-tRNA. *Genes and Development*, *12*(23), 3650–3662. https://doi.org/10.1101/gad.12.23.3650

Anderson, J., Phan, L., & Hinnebusch, A. G. (2000). The Gcd10p/Gcd14p complex is the essential two-subunit tRNA(1-methyladenosine) methyltransferase of Saccharomyces cerevisiae. *Proceedings of the National Academy of Sciences of the United States of America*, *97*(10), 5173–5178. https://doi.org/10.1073/pnas.090102597

Angelova, M. T., Dimitrova, D. G., Da Silva, B., Marchand, V., Jacquier, C., Achour, C., Brazane, M., Goyenvalle, C., Bourguignon-Igel, V., Shehzada, S., Khouider, S., Lence, T., Guerineau, V., Roignant, J. Y., Antoniewski, C., Teysset, L., Bregeon, D., Motorin, Y., Schaefer, M. R., & Carré, C. (2020). TRNA 2′-O-methylation by a duo of TRM7/FTSJ1 proteins modulates small RNA silencing in Drosophila. *Nucleic Acids Research*, *48*(4), 2050–2072. https://doi.org/10.1093/nar/gkaa002

Angelova, M. T., Dimitrova, D. G., Silva, B. Da, Marchand, V., Jacquier, C., Achour, C., Brazane, M., Goyenvalle, C., Shehzada, S., Khouider, S., Lence, T., Guerineau, V., Roignant, J., Antoniewski, C., Teysset, L., Bregeon, D., Motorin, Y., & Schaefer, M. R. (2020). *tRNA 2 -O-*

methylation by a duo of TRM7 / FTSJ1 proteins modulates small RNA silencing in Drosophila Carr e. *48*(4), 2050–2072. https://doi.org/10.1093/nar/gkaa002

Aoyama, T., Yamashita, S., & Tomita, K. (2020). Mechanistic insights into m6A modification of U6 snRNA by human METTL16. *Nucleic Acids Research*, *48*(9), 5157–5168. https://doi.org/10.1093/nar/gkaa227

Arai, T., Ishiguro, K., Kimura, S., Sakaguchi, Y., Suzuki, T., & Suzuki, T. (2015). Single methylation of 23S rRNA triggers late steps of 50S ribosomal subunit assembly. *Proceedings of the National Academy of Sciences of the United States of America*, *112*(34), E4707–E4716. https://doi.org/10.1073/pnas.1506749112

Arango, D., Sturgill, D., Alhusaini, N., Dillman, A. A., Sweet, T. J., Hanson, G., Hosogane, M., Sinclair, W. R., Nanan, K. K., Mandler, M. D., Fox, S. D., Zengeya, T. T., Andresson, T., Meier, J. L., Coller, J., & Oberdoerffer, S. (2018). Acetylation of Cytidine in mRNA Promotes Translation Efficiency. *Cell*, *175*(7), 1872-1886.e24. https://doi.org/10.1016/j.cell.2018.10.030

Arango, D., Sturgill, D., Yang, R., Kanai, T., Bauer, P., Roy, J., Wang, Z., Hosogane, M., Schiffers, S., & Oberdoerffer, S. (2022). Direct epitranscriptomic regulation of mammalian translation initiation through N4-acetylcytidine. *Molecular Cell*, *82*(15), 2797-2814.e11. https://doi.org/10.1016/j.molcel.2022.05.016

Aubert, M., O'donohue, M. F., Lebaron, S., & Gleizes, P. E. (2018). Pre-ribosomal RNA processing in human cells: From mechanisms to congenital diseases. *Biomolecules*, *8*(4). https://doi.org/10.3390/biom8040123

Babaian, A., Rothe, K., Girodat, D., Minia, I., Djondovic, S., Milek, M., Spencer Miko, S. E., Wieden, H. J., Landthaler, M., Morin, G. B., & Mager, D. L. (2020). Loss of m1acp3Ψ Ribosomal RNA Modification Is a Major Feature of Cancer. *Cell Reports*, *31*(5), 107611. https://doi.org/10.1016/j.celrep.2020.107611

Bagni, C., & Zukin, R. S. (2019). A Synaptic Perspective of Fragile X Syndrome and Autism Spectrum Disorders. *Neuron*, *101*(6), 1070–1088. https://doi.org/10.1016/j.neuron.2019.02.041

Barbieri, I., & Kouzarides, T. (2020). Role of RNA modifications in cancer. *Nature Reviews Cancer*, *20*(6), 303–322. https://doi.org/10.1038/s41568-020-0253-2

Barros-Silva, D., Klavert, J., Jenster, G., Jerónimo, C., Lafontaine, D. L. J., & Martens-Uzunova, E. S. (2021). The role of OncoSnoRNAs and Ribosomal RNA 2'-O-methylation in Cancer. *RNA Biology*, *18*(S1), 61–74. https://doi.org/10.1080/15476286.2021.1991167

Bartoli, K. M., Schaening, C., Carlile, T., & Gilbert, W. V. (2018). Conserved Methyltransferase Spb1 Targets mRNAs for Regulated Modification with 2′-O-Methyl Ribose. *BioRxiv*, 271916. https://www.biorxiv.org/content/10.1101/271916v2

Baskin, F., & Dekker, C. A. (1967). A rapid and specific assay for sugar methylation in ribonucleic acid. *Journal of Biological Chemistry*, *242*(22), 5447–5449. https://doi.org/10.1016/s0021-9258(18)99445-7

Bass, B. L., & Weintraub, H. (1988). An unwinding activity that covalently modifies its double-stranded RNA substrate. *Cell*, *55*(6), 1089–1098. https://doi.org/10.1016/0092-8674(88)90253-X

Baudin-baillieu, A., Fabret, C., Liang, X. H., Piekna-Przybylska, D., Fournier, M. J., & Rousset, J. P. (2009). Nucleotide modifications in three functionally important regions of the Saccharomyces cerevisiae ribosome affect translation accuracy. *Nucleic Acids Research*, *37*(22), 7665–7677. https://doi.org/10.1093/nar/gkp816

Bawankar, P., Lence, T., Paolantoni, C., Haussmann, I. U., Kazlauskiene, M., Jacob, D., Heidelberger, J. B., Richter, F. M., Nallasivan, M. P., Morin, V., Kreim, N., Beli, P., Helm, M., Jinek, M., Soller, M., & Roignant, J. Y. (2021). Hakai is required for stabilization of core components of the m6A mRNA methylation machinery. *Nature Communications*, *12*(1), 1–15. https://doi.org/10.1038/s41467-021-23892-5

Begik, O., Lucas, M. C., Pryszcz, L. P., Ramirez, J. M., Medina, R., Milenkovic, I., Cruciani, S., Liu, H., Vieira, H. G. S., Sas-Chen, A., Mattick, J. S., Schwartz, S., & Novoa, E. M. (2021). Quantitative profiling of pseudouridylation dynamics in native RNAs with nanopore sequencing. *Nature Biotechnology*, *39*(10), 1278–1291. https://doi.org/10.1038/s41587-021-00915-6

Benisty, H., Hernandez-Alias, X., Weber, M., Anglada-Girotto, M., Mantica, F., Radusky, L., Senger, G., Calvet, F., Weghorn, D., Irimia, M., Schaefer, M. H., & Serrano, L. (2023). Genes enriched in A/T-ending codons are co-regulated and conserved across mammals. *Cell Systems*, *14*(4), 312-323.e3. https://doi.org/10.1016/j.cels.2023.02.002

Bin Yu, Zhiyong Yang, Li†, J., Svetlana Minakhina, Maocheng Yang, Richard W. Padgett, Ruth Steward, & Chen, X. (2005). Methylation as a Crucial Step in Plant microRNA Biogenesis Bin. *Science*, *307*(30), 932–935. https://doi.org/10.1126/science.1107130.Methylation

Birkedal, U., Christensen-Dalsgaard, M., Krogh, N., Sabarinathan, R., Gorodkin, J., & Nielsen, H. (2015). Profiling of ribose methylations in RNA by high-throughput sequencing. *Angewandte Chemie - International Edition*, *54*(2), 451–455. https://doi.org/10.1002/anie.201408362

Blanc, V., Park, E., Schaefer, S., Miller, M., Lin, Y., Kennedy, S., Billing, A. M., Hamidane, H. Ben, Graumann, J., Mortazavi, A., Nadeau, J. H., & Davidson, N. O. (2014). *Genome-wide identification and functional analysis of Apobec-1-mediated C-to-U RNA editing in mouse small intestine and liver*. *15*(6), 1–17. https://doi.org/10.1186/gb-2014-15-6-r79

Blanco, S., Bandiera, R., Popis, M., Hussain, S., Lombard, P., Aleksic, J., Sajini, A., Tanna, H., Cortés-Garrido, R., Gkatza, N., Dietmann, S., & Frye, M. (2016). Stem cell function and stress response are controlled by protein synthesis. *Nature*, *534*(7607), 335–340. https://doi.org/10.1038/nature18282

Blanco, S., Dietmann, S., Flores, J. V, Hussain, S., Kutter, C., Humphreys, P., Lukk, M., Lombard, P., Treps, L., Popis, M., Kellner, S., Hölter, S. M., Garrett, L., Wurst, W., Becker, L., Klopstock, T., Fuchs, H., Gailus-Durner, V., Hrabě de Angelis, M., … Frye, M. (2014). Aberrant methylation of t RNA s links cellular stress to neuro-developmental disorders . *The EMBO Journal*, *33*(18), 2020–2039. https://doi.org/10.15252/embj.201489282

Boccaletto, P., MacHnicka, M. A., Purta, E., Pitkowski, P., Baginski, B., Wirecki, T. K., De Crécy-Lagard, V., Ross, R., Limbach, P. A., Kotter, A., Helm, M., & Bujnicki, J. M. (2018). MODOMICS: A database of RNA modification pathways. 2017 update. *Nucleic Acids Research*, *46*(D1), D303–D307. https://doi.org/10.1093/nar/gkx1030

Boccaletto, P., Stefaniak, F., Ray, A., Cappannini, A., Mukherjee, S., Purta, E., Kurkowska, M., Shirvanizadeh, N., Destefanis, E., Groza, P., Avşar, G., Romitelli, A., Pir, P., Dassi, E., Conticello, S. G., Aguilo, F., & Bujnicki, J. M. (2022). MODOMICS: A database of RNA modification pathways. 2021 update. *Nucleic Acids Research*, *50*(D1), D231–D235. https://doi.org/10.1093/nar/gkab1083

Bohnsack, K. E., Höbartner, C., & Bohnsack, M. T. (2019). Eukaryotic 5-methylcytosine (M 5 C) RNA methyltransferases: Mechanisms, cellular functions, and links to disease. *Genes*, *10*(2). https://doi.org/10.3390/genes10020102

Bohnsack, M. T., & Sloan, K. E. (2018). Modifications in small nuclear RNAs and their roles in spliceosome assembly and function. *Biological Chemistry*, *399*(11), 1265–1276. https://doi.org/10.1515/hsz-2018-0205

Boo, S. H., & Kim, Y. K. (2020). The emerging role of RNA modifications in the regulation of mRNA stability. *Experimental and Molecular Medicine*, *52*(3), 400–408. https://doi.org/10.1038/s12276-020-0407-z

Borges, F., & Martienssen, R. A. (2015). The expanding world of small RNAs in plants. *Nature Reviews Molecular Cell Biology*, *16*(12), 727–741. https://doi.org/10.1038/nrm4085

Boulias, K., Toczydłowska-Socha, D., Hawley, B. R., Liberman, N., Takashima, K., Zaccara, S., Guez, T., Vasseur, J. J., Debart, F., Aravind, L., Jaffrey, S. R., & Greer, E. L. (2019). Identification of the m6Am Methyltransferase PCIF1 Reveals the Location and Functions of m6Am in the Transcriptome. *Molecular Cell*, *75*(3), 631-643.e8. https://doi.org/10.1016/j.molcel.2019.06.006

Bousquet-Antonelli, C., Vanrobays, E., Gélugne, J. P., Caizergues-Ferrer, M., & Henry, Y. (2000). Rrp8p is a yeast nucleolar protein functionally linked to Gar1p and involved in pre-rRNA cleavage at site A2. *Rna*, *6*(6), 826–843.

https://doi.org/10.1017/S1355838200992288

Bowers, M., Liang, T., Gonzalez-Bohorquez, D., Zocher, S., Jaeger, B. N., Kovacs, W. J., Röhrl, C., Cramb, K. M. L., Winterer, J., Kruse, M., Dimitrieva, S., Overall, R. W., Wegleiter, T., Najmabadi, H., Semenkovich, C. F., Kempermann, G., Földy, C., & Jessberger, S. (2020). FASN-Dependent Lipid Metabolism Links Neurogenic Stem/Progenitor Cell Activity to Learning and Memory Deficits. *Cell Stem Cell*, *27*(1), 98-109.e11. https://doi.org/10.1016/j.stem.2020.04.002

Brand, R. C., Klootwijk, J., Planta, R. J., & Maden, B. E. H. (1978). Biosynthesis of a hypermodified nucleotide in Saccharomyces carlsbergensis 17S and HeLa-cell 18S ribosomal ribonucleic acid. *Biochemical Journal*, *169*(1), 71–77. https://doi.org/10.1042/bj1690071

Brault, M. E., Lauzon, C., & Autexier, C. (2013). Dyskeratosis congenita mutations in dyskerin SUMOylation consensus sites lead to impaired telomerase RNA accumulation and telomere defects. *Human Molecular Genetics*, *22*(17), 3498–3507. https://doi.org/10.1093/hmg/ddt204

Brazane, M., Dimitrova, D. G., Pigeon, J., Paolantoni, C., Ye, T., Marchand, V., Silva, B. Da, Schaefer, E., Angelova, M. T., Stark, Z., Delatycki, M., Dudding-Byth, T., Gecz, J., Plaçais, P. Y., Teysset, L., Préat, T., Piton, A., Hassan, B. A., Roignant, J. Y., … Carré, C. (2023). The ribose methylation enzyme FTSJ1 has a conserved role in neuron morphology and learning performance. *Life Science Alliance*, *6*(4), 1–23. https://doi.org/10.26508/lsa.202201877

Brown, J. A., Kinzig, C. G., Degregorio, S. J., & Steitz, J. A. (2016). Methyltransferase-like protein 16 binds the 3'-terminal triple helix of MALAT1 long noncoding RNA. *Proceedings of the National Academy of Sciences of the United States of America*, *113*(49), 14013–14018. https://doi.org/10.1073/pnas.1614759113

Brūmele, B., Mutso, M., Telanne, L., Õunap, K., Spunde, K., Abroi, A., & Kurg, R. (2021). Human trmt112-methyltransferase network consists of seven partners interacting with a common co-factor. *International Journal of Molecular Sciences*, *22*(24). https://doi.org/10.3390/ijms222413593

Buchanan, S. M., Kain, J. S., & De Bivorta, B. L. (2015). Neuronal control of locomotor handedness in Drosophila. *Proceedings of the National Academy of Sciences of the United States of America*, *112*(21), 6700–6705. https://doi.org/10.1073/pnas.1500804112

Buchhaupt, M., Sharma, S., Kellner, S., Oswald, S., Paetzold, M., Peifer, C., Watzinger, P., Schrader, J., Helm, M., & Entian, K. D. (2014). Partial methylation at Am100 in 18S rRNA of Baker's yeast reveals ribosome heterogeneity on the level of eukaryotic rRNA modification. *PLoS ONE*, *9*(2). https://doi.org/10.1371/journal.pone.0089640

Bügl, H., Fauman, E. B., Staker, B. L., Zheng, F., Kushner, S. R., Saper, M. A., Bardwell, J. C. A., & Jakob, U. (2000). RNA methylation under heat shock control. *Molecular Cell*, *6*(2), 349–360. https://doi.org/10.1016/S1097-2765(00)00035-6

Bujnicki, J. M. (2001). In silico analysis of the tRNA:m1A58 methyltransferase family: Homology-based fold prediction and identification of new members from Eubacteria and Archaea. *FEBS Letters*, *507*(2), 123–127. https://doi.org/10.1016/S0014-5793(01)02962-3

Burke, M. F., Logan, M. K., & Hebert, M. D. (2018). Identification of additional regulatory RNPs that impact rRNA and U6 snRNA methylation. *Biology Open*, *7*(8), 1–11. https://doi.org/10.1242/bio.036095

Caldas, T., Binet, E., Bouloc, P., Costa, A., Desgres, J., & Richarme, G. (2000). The FtsJ/RrmJ heat shock protein of Escherichia coli is a 23 S ribosomal RNA methyltransferase. *Journal of Biological Chemistry*, *275*(22), 16414–16419. https://doi.org/10.1074/jbc.M001854200

Carlile, T. M., Rojas-Duran, M. F., Zinshteyn, B., Shin, H., Bartoli, K. M., & Gilbert, W. V. (2014). Pseudouridine profiling reveals regulated mRNA pseudouridylation in yeast and human cells. *Nature*, *515*(7525), 143–146. https://doi.org/10.1038/nature13802

Cavaillé, J., Chetouani, F., & Bachellerie, J. P. (1999). The yeast Saccharomyces cerevisiae YDL112w ORF encodes the putative 2'- O-ribose methyltransferase catalyzing the formation of Gm18 in tRNAs. *Rna*, *5*(1), 66–81.

https://doi.org/10.1017/S1355838299981475

Chan, C. M., Zhou, C., & Huang, R. H. (2009). Reconstituting bacterial RNA repair and modification in vitro. *Science*, *326*(5950), 247. https://doi.org/10.1126/science.1179480

Chang, G., Shi, L., Ye, Y., Shi, H., Zeng, L., Tiwary, S., Huse, J. T., Huo, L., Ma, L., Ma, Y., Zhang, S., Zhu, J., Xie, V., Li, P., Han, L., He, C., & Huang, S. (2020). YTHDF3 Induces the Translation of m6A-Enriched Gene Transcripts to Promote Breast Cancer Brain Metastasis. *Cancer Cell*, *38*(6), 857-871.e7. https://doi.org/10.1016/j.ccell.2020.10.004

Chen, C., Yuan, W., Zhou, Q., Shao, B., Guo, Y., Wang, W., Yang, S., Guo, Y., Zhao, L., Dang, Q., Yang, X., Wang, G., Kang, Q., Ji, Z., Liu, J., & Sun, Z. (2021). N6-methyladenosine-induced circ1662 promotes metastasis of colorectal cancer by accelerating YAP1 nuclear localization. *Theranostics*, *11*(9), 4298–4315. https://doi.org/10.7150/thno.51342

Chen, H., Gu, L., Orellana, E. A., Wang, Y., Guo, J., Liu, Q., Wang, L., Shen, Z., Wu, H., Gregory, R. I., Xing, Y., & Shi, Y. (2020). METTL4 is an snRNA m6Am methyltransferase that regulates RNA splicing. *Cell Research*, *30*(6), 544–547. https://doi.org/10.1038/s41422-019-0270-4

Chen, H., Liu, Q., Yu, D., Natchiar, K., Zhou, C., Hsu, C., Hsu, P.-H., Zhang, X., Klaholz, B., Gregory, R. I., Cheng, X., & Shi, Y. (2020). METTL5, an 18S rRNA-specific m6A methyltransferase, modulates expression of stress response genes. *BioRxiv*, *617*, 2020.04.27.064162. https://www.biorxiv.org/content/10.1101/2020.04.27.064162v2%0Ahttps://www.biorxiv.org/content/10.1101/2020.04.27.064162v2.abstract

Chen, K., Luo, G. Z., & He, C. (2015). High-Resolution Mapping of N6-Methyladenosine in Transcriptome and Genome Using a Photo-Crosslinking-Assisted Strategy. In *Methods in Enzymology* (1st ed., Vol. 560). Elsevier Inc. https://doi.org/10.1016/bs.mie.2015.03.012

Chen, Li, Zhang, L. S., Ye, C., Zhou, H., Liu, B., Gao, B., Deng, Z., Zhao, C., He, C., & Dickinson, B. C. (2023). Nm-Mut-seq: a base-resolution quantitative method for mapping transcriptome-wide 2′-O-methylation. *Cell Research*, *33*(9), 727–730. https://doi.org/10.1038/s41422-023-00836-w

Chen, Liutao, Fu, Y., Hu, Z., Deng, K., Song, Z., Liu, S., Li, M., Ou, X., Wu, R., Liu, M., Li, R., Gao, S., Cheng, L., Chen, S., & Xu, A. (2022). Nuclear m 6 A reader YTHDC1 suppresses proximal alternative polyadenylation sites by interfering with the 3′ processing machinery . *EMBO Reports*, *23*(11), 1–18. https://doi.org/10.15252/embr.202254686

Chen, Y. G., Chen, R., Ahmad, S., Verma, R., Kasturi, S. P., Amaya, L., Broughton, J. P., Kim, J., Cadena, C., Pulendran, B., Hur, S., & Chang, H. Y. (2019). N6-Methyladenosine Modification Controls Circular RNA Immunity. *Molecular Cell*, *76*(1), 96-109.e9. https://doi.org/10.1016/j.molcel.2019.07.016

Chen, Y. S., Yang, W. L., Zhao, Y. L., & Yang, Y. G. (2021). Dynamic transcriptomic m5C and its regulatory role in RNA processing. *Wiley Interdisciplinary Reviews: RNA*, *12*(4), 1–23. https://doi.org/10.1002/wrna.1639

Chernoff, Y. O., Newnam, G. P., & Liebman, S. W. (1996). The translational function of nucleotide C1054 in the small subunit rRNA is conserved throughout evolution: Genetic evidence in yeast. *Proceedings of the National Academy of Sciences of the United States of America*, *93*(6), 2517–2522. https://doi.org/10.1073/pnas.93.6.2517

Choe, J., Lin, S., Zhang, W., Liu, Q., Wang, L., Ramirez-Moya, J., Du, P., Kim, W., Tang, S., Sliz, P., Santisteban, P., George, R. E., Richards, W. G., Wong, K. K., Locker, N., Slack, F. J., & Gregory, R. I. (2018). mRNA circularization by METTL3–eIF3h enhances translation and promotes oncogenesis. *Nature*, *561*(7724), 556–560. https://doi.org/10.1038/s41586-018-0538-8

Choi, J., Indrisiunaite, G., Demirci, H., Ieong, K. W., Wang, J., Petrov, A., Prabhakar, A., Rechavi, G., Dominissini, D., He, C., Ehrenberg, M., & Puglisi, J. D. (2018). 2′-O-methylation in mRNA disrupts tRNA decoding during translation elongation. *Nature Structural and Molecular Biology*, *25*(3), 208–216. https://doi.org/10.1038/s41594-018-0030-z

Cohn, W. E. (1960). Pseudouridine, a carbon-carbon linked ribonucleoside in ribonucleic acids: isolation, structure,

and chemical characteristics. *The Journal of Biological Chemistry*, *235*(5), 1488–1498. https://doi.org/10.1016/s0021-9258(18)69432-3

Cohn, Waldo E., & Volkin, E. (1951). Nucleoside-S'-Phosphates from Ribonucleic Acid. *Nature*, *1*(1), 109–111. https://doi.org/10.1021/jf60001a611

Copela, L. A., Chakshusmathi, G., Sherrer, R. L., & Wolin, S. L. (2006). The La protein functions redundantly with tRNA modification enzymes to ensure tRNA structural stability. *Rna*, *12*(4), 644–654. https://doi.org/10.1261/rna.2307206

D'Orazio, K. N., Wu, C. C.-C., Sinha, N., Loll-Krippleber, R., Brown, G. W., & Green, R. (2019). The endonuclease Cue2 cleaves mRNAs at stalled ribosomes during No Go Decay. *ELife*, *8*, 1–27. https://doi.org/10.7554/elife.49117

D'Souza, M. N., Gowda, N. K. C., Tiwari, V., Babu, R. O., Anand, P., Dastidar, S. G., Singh, R., James, O. G., Selvaraj, B., Pal, R., Ramesh, A., Chattarji, S., Chandran, S., Gulyani, A., Palakodeti, D., & Muddashetty, R. S. (2018). FMRP Interacts with C/D Box snoRNA in the Nucleus and Regulates Ribosomal RNA Methylation. *IScience*, *9*, 399–411. https://doi.org/10.1016/j.isci.2018.11.007

Dai, Q., Moshitch-Moshkovitz, S., Han, D., Kol, N., Amariglio, N., Rechavi, G., Dominissini, D., & He, C. (2017). Nm-seq maps 2′-O-methylation sites in human mRNA with base precision. *Nature Methods*, *14*(7), 695–698. https://doi.org/10.1038/nmeth.4294

Dai, X., Wang, T., Gonzalez, G., & Wang, Y. (2018). Identification of YTH Domain-Containing Proteins as the Readers for N1-Methyladenosine in RNA. *Analytical Chemistry*, *90*(11), 6380–6384. https://doi.org/10.1021/acs.analchem.8b01703

Dai, Y. zhang, Liu, Y. da, Li, J., Chen, M. ting, Huang, M., Wang, F., Yang, Q. song, Yuan, J. hang, & Sun, S. han. (2022). METTL16 promotes hepatocellular carcinoma progression through downregulating RAB11B-AS1 in an m6A-dependent manner. *Cellular and Molecular Biology Letters*, *27*(1). https://doi.org/10.1186/s11658-022-00342-8

de Brouwer, A. P. M., Abou Jamra, R., Körtel, N., Soyris, C., Polla, D. L., Safra, M., Zisso, A., Powell, C. A., Rebelo-Guiomar, P., Dinges, N., Morin, V., Stock, M., Hussain, M., Shahzad, M., Riazuddin, S., Ahmed, Z. M., Pfundt, R., Schwarz, F., de Boer, L., … Schwartz, S. (2018). Variants in PUS7 Cause Intellectual Disability with Speech Delay, Microcephaly, Short Stature, and Aggressive Behavior. *American Journal of Human Genetics*, *103*(6), 1045–1052. https://doi.org/10.1016/j.ajhg.2018.10.026

Dedon, P. C., & Begley, T. J. (2014). Cellular stress response at the level of translation. *Chemical Research in Toxicology*, *27*, 330–337.

Delatte, B., Wang, F., Ngoc, L. V., Collignon, E., Bonvin, E., Deplus, R., Calonne, E., Hassabi, B., Putmans, P., Awe, S., Wetzel, C., Kreher, J., Soin, R., Creppe, C., Limbach, P. A., Gueydan, C., Kruys, V., Brehm, A., Minakhina, S., … Fuks, F. (2016). Transcriptome-wide distribution and function of RNA hydroxymethylcytosine. *Science*, *351*(6270), 282–285. https://doi.org/10.1126/science.aac5253

Desrosiers, R., Friderici, K., & Rottman, F. (1974). Identification of methylated nucleosides in messenger RNA from Novikoff hepatoma cells. *Proceedings of the National Academy of Sciences of the United States of America*, *71*(10), 3971–3975. https://doi.org/10.1073/pnas.71.10.3971

Dominissini, D., Moshitch-Moshkovitz, S., Schwartz, S., Salmon-Divon, M., Ungar, L., Osenberg, S., Cesarkas, K., Jacob-Hirsch, J., Amariglio, N., Kupiec, M., Sorek, R., & Rechavi, G. (2012). Topology of the human and mouse m6A RNA methylomes revealed by m6A-seq. *Nature*, *485*(7397), 201–206. https://doi.org/10.1038/nature11112

Dominissini, D., Nachtergaele, S., Moshitch-moshkovitz, S., Peer, E., Kol, N., Ben-haim, M. S., Dai, Q., Segni, A. Di, Clark, W. C., Zheng, G., Pan, T., Solomon, O., Eyal, E., Han, D., Amariglio, N., Rechavi, G., He, C., Sheba, C., & Gan, R. (2016). The dynamic N1-methyladenosine methylome in eukaryotic messenger RNA. *Nature*, *530*(7591), 441–446. https://doi.org/10.1038/nature16998.The

Dong, Z. W., Shao, P., Diao, L. T., Zhou, H., Yu, C. H., & Qu, L.

H. (2012). RTL-P: A sensitive approach for detecting sites of 2′-O-methylation in RNA molecules. *Nucleic Acids Research*, *40*(20). https://doi.org/10.1093/nar/gks698

Doxtader, K. A., Wang, P., Scarborough, A. M., Seo, D., Conrad, N. K., & Nam, Y. (2018). Structural Basis for Regulation of METTL16, an S-Adenosylmethionine Homeostasis Factor. *Molecular Cell*, *71*(6), 1001-1011.e4. https://doi.org/10.1016/j.molcel.2018.07.025

Edens, B. M., Vissers, C., Su, J., Arumugam, S., Xu, Z., Shi, H., Miller, N., Rojas Ringeling, F., Ming, G. li, He, C., Song, H., & Ma, Y. C. (2019). FMRP Modulates Neural Differentiation through m6A-Dependent mRNA Nuclear Export. *Cell Reports*, *28*(4), 845-854.e5. https://doi.org/10.1016/j.celrep.2019.06.072

El Hassouni, B., Sarkisjan, D., Vos, J. C., Giovannetti, E., & Peters, G. J. (2018). Targeting the Ribosome Biogenesis Key Molecule Fibrillarin to Avoid Chemoresistance. *Current Medicinal Chemistry*, *26*(33), 6020–6032. https://doi.org/10.2174/092986732666618120313333 2

El Kazzi, P., Rabah, N., Chamontin, C., Poulain, L., Ferron, F., Debart, F., Canard, B., Misse, D., Coutard, B., Nisole, S., & Decroly, E. (2023). Internal RNA 2′O-methylation in the HIV-1 genome counteracts ISG20 nuclease-mediated antiviral effect. *Nucleic Acids Research*, *51*(6), 2501–2515. https://doi.org/10.1093/nar/gkac996

Elliott, B. A., Ho, H. T., Ranganathan, S. V., Vangaveti, S., Ilkayeva, O., Abou Assi, H., Choi, A. K., Agris, P. F., & Holley, C. L. (2019). Modification of messenger RNA by 2′-O-methylation regulates gene expression in vivo. *Nature Communications*, *10*(1), 1–9. https://doi.org/10.1038/s41467-019-11375-7

Erales, J., Marchand, V., Panthu, B., Gillot, S., Belin, S., Ghayad, S. E., Garcia, M., Laforêts, F., Marcel, V., Baudin-Baillieu, A., Bertin, P., Couté, Y., Adrait, A., Meyer, M., Therizols, G., Yusupov, M., Namy, O., Ohlmann, T., Motorin, Y., … Diaz, J. J. (2017). Evidence for rRNA 2′-O-methylation plasticity: Control of intrinsic translational capabilities of human ribosomes. *Proceedings of the National Academy of Sciences of the United States of America*, *114*(49), 12934–12939. https://doi.org/10.1073/pnas.1707674114

Fu, L., Guerrero, C. R., Zhong, N., Amato, N. J., Liu, Y., Liu, S., Cai, Q., Ji, D., Jin, S. G., Niedernhofer, L. J., Pfeifer, G. P., Xu, G. L., & Wang, Y. (2014). Tet-mediated formation of 5-hydroxymethylcytosine in RNA. *Journal of the American Chemical Society*, *136*(33), 11582–11585. https://doi.org/10.1021/ja505305z

Furuichi, Y. (1974). "Methylation-coupled" transcription by virus-associated transcriptase of cytoplasmic polyhedrosis virus containing double-stranded RNA. *Nucleic Acids Research*, *1*, 809–822.

Gai, X., Xin, D., Wu, D., Wang, X., Chen, L., Wang, Y., Ma, K., Li, Q., Li, P., & Yu, X. (2022). Pre-ribosomal RNA reorganizes DNA damage repair factors in nucleus during meiotic prophase and DNA damage response. *Cell Research*, *32*(3), 254–268. https://doi.org/10.1038/s41422-021-00597-4

Galvanin, A., Vogt, L. M., Grober, A., Freund, I., Ayadi, L., Bourguignon-Igel, V., Bessler, L., Jacob, D., Eigenbrod, T., Marchand, V., Dalpke, A., Helm, M., & Motorin, Y. (2020). Bacterial tRNA 2′-O-methylation is dynamically regulated under stress conditions and modulates innate immune response. *Nucleic Acids Research*, *48*(22), 12833–12844. https://doi.org/10.1093/nar/gkaa1123

Garcia-Campos, M. A., Edelheit, S., Toth, U., Safra, M., Shachar, R., Viukov, S., Winkler, R., Nir, R., Lasman, L., Brandis, A., Hanna, J. H., Rossmanith, W., & Schwartz, S. (2019). Deciphering the "m6A Code" via Antibody-Independent Quantitative Profiling. *Cell*, *178*(3), 731-747.e16. https://doi.org/10.1016/j.cell.2019.06.013

Garus, A., & Autexier, C. (2021). Dyskerin: an essential pseudouridine synthase with multifaceted roles in ribosome biogenesis, splicing, and telomere maintenance. *Rna*, *27*(12), 1441–1458. https://doi.org/10.1261/rna.078953.121

Ge, J., Liu, H., & Yu, Y. T. (2010). Regulation of pre-mRNA splicing in Xenopus oocytes by targeted 2′-O-methylation. *Rna*, *16*(5), 1078–1085. https://doi.org/10.1261/rna.2060210

Gigova, A., Duggimpudi, S., Pollex, T., Schaefer, M., & Koš, M.

(2014). A cluster of methylations in the domain IV of 25S rRNA is required for ribosome stability. *Rna*, *20*(10), 1632–1644. https://doi.org/10.1261/rna.043398.113

Goh, Y. T., Koh, C. W. Q., Sim, D. Y., Roca, X., & Goh, W. S. S. (2020). METTL4 catalyzes m6Am methylation in U2 snRNA to regulate pre-mRNA splicing. *Nucleic Acids Research*, *48*(16), 9250–9261. https://doi.org/10.1093/nar/gkaa684

Goyal, B., Yadav, S. R. M., Awasthee, N., Gupta, S., Kunnumakkara, A. B., & Gupta, S. C. (2021). Diagnostic, prognostic, and therapeutic significance of long non-coding RNA MALAT1 in cancer. *Biochimica et Biophysica Acta - Reviews on Cancer*, *1875*(2), 188502. https://doi.org/10.1016/j.bbcan.2021.188502

Gramates, L. S., Agapite, J., Attrill, H., Calvi, B. R., Crosby, M. A., dos Santos, G., Goodman, J. L., Goutte-Gattat, D., Jenkins, V. K., Kaufman, T., Larkin, A., Matthews, B. B., Millburn, G., & Strelets, V. B. (2022). FlyBase: a guided tour of highlighted features. *Genetics*, *220*(4). https://doi.org/10.1093/genetics/iyac035

Graziadei, A., Masiewicz, P., Lapinaite, A., & Carlomagno, T. (2016). Archaea box C/D enzymes methylate two distinct substrate rRNA sequences with different efficiency. *Rna*, *22*(5), 764–772. https://doi.org/10.1261/rna.054320.115

Greer, E. L., Blanco, M. A., Gu, L., Sendinc, E., Liu, J., Aristizábal-Corrales, D., Hsu, C. H., Aravind, L., He, C., & Shi, Y. (2015). DNA methylation on N6-adenine in C. elegans. *Cell*, *161*(4), 868–878. https://doi.org/10.1016/j.cell.2015.04.005

Grosjean, H., Sprinzl, M., & Steinberg, S. (1995). Posttranscriptionally modified nucleosides in transfer RNA: Their locations and frequencies. *Biochimie*, *77*, 139–141.

Grozhik, A. V., Olarerin-George, A. O., Sindelar, M., Li, X., Gross, S. S., & Jaffrey, S. R. (2019). Antibody cross-reactivity accounts for widespread appearance of m1A in 5'UTRs. *Nature Communications*, *10*(1), 1–13. https://doi.org/10.1038/s41467-019-13146-w

Gu, J., Patton, J. R., Shimba, S., & Reddy, R. (1996). Localization of modified nucleotides in Schizosaccharomyces pombe spliceosomal small nuclear RNAs: modified nucleotides are clustered in functionally important regions. *RNA (New York, N.Y.)*, *2*(9), 909–918. https://rnajournal.cshlp.org/content/2/9/909.long

Gu, L., Wang, L., Chen, H., Hong, J., Shen, Z., Dhall, A., Lao, T., Liu, C., Wang, Z., Xu, Y., Tang, H. W., Chakraborty, D., Chen, J., Liu, Z., Rogulja, D., Perrimon, N., Wu, H., & Shi, Y. (2020). CG14906 (mettl4) mediates m6A methylation of U2 snRNA in Drosophila. *Cell Discovery*, *6*(1), 4–7. https://doi.org/10.1038/s41421-020-0178-7

Guy, M. P., & Phizicky, E. M. (2015). Conservation of an intricate circuit for crucial modifications of the tRNAPhe anticodon loop in eukaryotes. *Rna*, *21*(1), 61–74. https://doi.org/10.1261/rna.047639.114

Guy, M. P., Shaw, M., Weiner, C. L., Hobson, L., Stark, Z., Rose, K., Kalscheuer, V. M., Gecz, J., & Phizicky, E. M. (2015). Defects in tRNA anticodon loop 2'-O-methylation are implicated in non-syndromic X-linked intellectual disability due to mutations in FTSJ1. *Human Mutation*, *36*(12), 1176–1187. https://doi.org/10.1002/humu.22897.Defects

Guzzi, N., Cieśla, M., Ngoc, P. C. T., Lang, S., Arora, S., Dimitriou, M., Pimková, K., Sommarin, M. N. E., Munita, R., Lubas, M., Lim, Y., Okuyama, K., Soneji, S., Karlsson, G., Hansson, J., Jönsson, G., Lund, A. H., Sigvardsson, M., Hellström-Lindberg, E., … Bellodi, C. (2018). Pseudouridylation of tRNA-Derived Fragments Steers Translational Control in Stem Cells. *Cell*, *173*(5), 1204-1216.e26. https://doi.org/10.1016/j.cell.2018.03.008

Hales, K. G., Korey, C. A., Larracuente, A. M., & Roberts, D. M. (2015). Genetics on the fly: A primer on the drosophila model system. *Genetics*, *201*(3), 815–842. https://doi.org/10.1534/genetics.115.183392

Han, L., Diao, L., Yu, S., Xu, X., Li, J., Zhang, R., Yang, Y., Werner, H. M. J., Eterovic, A. K., Yuan, Y., Li, J., Nair, N., Minelli, R., Tsang, Y. H., Cheung, L. W. T., Jeong, K. J., Roszik, J., Ju, Z., Woodman, S. E., … Liang, H. (2015). The Genomic Landscape and Clinical Relevance of A-to-I RNA Editing in Human Cancers. *Cancer Cell*, *28*(4), 515–528. https://doi.org/10.1016/j.ccell.2015.08.013

Han, Y., Du, T., Guo, S., Wang, L., Dai, G., Long, T., Xu, T., Zhuang, X., Liu, C., Li, S., Zhang, D., Liao, X., Dong, Y., Lui, K. O., Tan, X., Lin, S., Chen, Y., & Huang, Z. P. (2022). Loss of m6A Methyltransferase METTL5 Promotes Cardiac Hypertrophy Through Epitranscriptomic Control of SUZ12 Expression. *Frontiers in Cardiovascular Medicine*, *9*(February), 1–13. https://doi.org/10.3389/fcvm.2022.852775

Hasler, D., Meduri, R., Bąk, M., Lehmann, G., Heizinger, L., Wang, X., Li, Z. T., Sement, F. M., Bruckmann, A., Dock-Bregeon, A. C., Merkl, R., Kalb, R., Grauer, E., Kunstmann, E., Zavolan, M., Liu, M. F., Fischer, U., & Meister, G. (2020). The Alazami Syndrome-Associated Protein LARP7 Guides U6 Small Nuclear RNA Modification and Contributes to Splicing Robustness. *Molecular Cell*, *77*(5), 1014-1031.e13. https://doi.org/10.1016/j.molcel.2020.01.001

Haussmann, I. U., Wu, Y., Nallasivan, M. P., Archer, N., Bodi, Z., Hebenstreit, D., Waddell, S., Fray, R., & Soller, M. (2022). CMTr cap-adjacent 2′-O-ribose mRNA methyltransferases are required for reward learning and mRNA localization to synapses. *Nature Communications*, *13*(1), 1–13. https://doi.org/10.1038/s41467-022-28549-5

He, P. C., & He, C. (2021). m 6 A RNA methylation: from mechanisms to therapeutic potential . *The EMBO Journal*, *40*(3), 1–15. https://doi.org/10.15252/embj.2020105977

Hellmuth, K., Grosjean, H., Motorin, Y., Deinert, K., Hurt, E., & Simos, G. (2000). Cloning and characterization of the Schizosaccharomyces pombe tRNA: Pseudouridine synthase Pus1p. *Nucleic Acids Research*, *28*(23), 4604–4610. https://doi.org/10.1093/nar/28.23.4604

Helm, M., & Alfonzo, J. D. (2014). Post-transcriptional RNA modifications: Playing metabolic games in a cell's chemical legoland. *Chem Biol*, *21*(2), 174–185. https://doi.org/10.1016/j.chembiol.2013.10.015.Post-transcriptional

Helm, M., Giegé, R., & Florentz, C. (1999). A Watson-Crick base-pair-disrupting methyl group (m1A9) is sufficient for cloverleaf folding of human mitochondrial tRNA(Lys). *Biochemistry*, *38*(40), 13338–13346. https://doi.org/10.1021/bi991061g

Helm, M., & Motorin, Y. (2017). Detecting RNA modifications in the epitranscriptome: Predict and validate. *Nature Reviews Genetics*, *18*(5), 275–291. https://doi.org/10.1038/nrg.2016.169

Hernández, G., Miron, M., Han, H., Liu, N., Magescas, J., Tettweiler, G., Frank, F., Siddiqui, N., Sonenberg, N., & Lasko, P. (2013). Mextli Is a Novel Eukaryotic Translation Initiation Factor 4E-Binding Protein That Promotes Translation in Drosophila melanogaster . *Molecular and Cellular Biology*, *33*(15), 2854–2864. https://doi.org/10.1128/mcb.01354-12

Higa-Nakamine, S., Suzuki, T., Uechi, T., Chakraborty, A., Nakajima, Y., Nakamura, M., Hirano, N., Suzuki, T., & Kenmochi, N. (2012). Loss of ribosomal RNA modification causes developmental defects in zebrafish. *Nucleic Acids Research*, *40*(1), 391–398. https://doi.org/10.1093/nar/gkr700

Hirata, A., Okada, K., Yoshii, K., Shiraishi, H., Saijo, S., Yonezawa, K., Shimizu, N., & Hori, H. (2019). Structure of tRNA methyltransferase complex of Trm7 and Trm734 reveals a novel binding interface for tRNA recognition. *Nucleic Acids Research*, *47*(20), 10942–10955. https://doi.org/10.1093/nar/gkz856

Hogg, M., Paro, S., Keegan, L. P., & O'Connell, M. A. (2011). RNA Editing by Mammalian ADARs. In *Advances in Genetics* (1st ed., Vol. 73, Issue C). Elsevier Inc. https://doi.org/10.1016/B978-0-12-380860-8.00003-3

Horiuchi, K., Kawamura, T., Iwanari, H., Ohashi, R., Naito, M., Kodama, T., & Hamakubo, T. (2013). Identification of Wilms' tumor 1-associating protein complex and its role in alternative splicing and the cell cycle. *Journal of Biological Chemistry*, *288*(46), 33292–33302. https://doi.org/10.1074/jbc.M113.500397

Horwich, M. D., Li, C., Matranga, C., Vagin, V., Farley, G., Wang, P., & Zamore, P. D. (2007). The Drosophila RNA Methyltransferase, DmHen1, Modifies Germline piRNAs and Single-Stranded siRNAs in RISC. *Current Biology*, *17*(14), 1265–1272. https://doi.org/10.1016/j.cub.2007.06.030

House, A. E., & Lynch, K. W. (2008). Regulation of alternative splicing: More than just the ABCs. *Journal of Biological*

Chemistry, *283*(3), 1217–1221. https://doi.org/10.1074/jbc.R700031200

Hu, J., Frömel, T., & Fleming, I. (2018). Angiogenesis and vascular stability in eicosanoids and cancer. *Cancer and Metastasis Reviews*, *37*(2–3), 425–438. https://doi.org/10.1007/s10555-018-9732-2

Hu, L., Liu, S., Peng, Y., Ge, R., Su, R., Senevirathne, C., Harada, B. T., Dai, Q., Wei, J., Zhang, L., Hao, Z., Luo, L., Wang, H., Wang, Y., Luo, M., Chen, M., Chen, J., & He, C. (2022). m6A RNA modifications are measured at single-base resolution across the mammalian transcriptome. *Nature Biotechnology*, *40*(8), 1210–1219. https://doi.org/10.1038/s41587-022-01243-z

Huang, Hua, Li, H., Pan, R., Wang, S., Khan, A. A., Zhao, Y., Zhu, H., & Liu, X. (2022). Ribosome 18S m6A methyltransferase METTL5 promotes pancreatic cancer progression by modulating c-Myc translation. *International Journal of Oncology*, *60*(1), 1–10. https://doi.org/10.3892/ijo.2021.5299

Huang, Huilin, Weng, H., Sun, W., Qin, X., Shi, H., Wu, H., Zhao, B. S., Mesquita, A., Liu, C., Yuan, C. L., Hu, Y. C., Hüttelmaier, S., Skibbe, J. R., Su, R., Deng, X., Dong, L., Sun, M., Li, C., Nachtergaele, S., … Chen, J. (2018). Recognition of RNA N 6 -methyladenosine by IGF2BP proteins enhances mRNA stability and translation. *Nature Cell Biology*, *20*(3), 285–295. https://doi.org/10.1038/s41556-018-0045-z

Huang, L., Ashraf, S., Wang, J., & Lilley, D. M. (2017). Control of box C/D snoRNP assembly by N 6 -methylation of adenine . *EMBO Reports*, *18*(9), 1631–1645. https://doi.org/10.15252/embr.201743967

Huang, Y., Ji, L., Huang, Q., Vassylyev, D. G., Chen, X., & Ma, J. B. (2009). Structural insights into mechanisms of the small RNA methyltransferase HEN1. *Nature*, *461*(7265), 823–827. https://doi.org/10.1038/nature08433

Hughes, D. G., & Maden, E. H. (1978). The pseudouridine contents of the ribosomal ribonucleic acids of three vertebrate species. Numerical correspondence between pseudouridine residues and 2'-0-methyl groups is not always conserved. *Biochemical Journal*, *171*(3), 781–786. https://doi.org/10.1042/bj1710781

Hussain, S., Sajini, A. A., Blanco, S., Dietmann, S., Lombard, P., Sugimoto, Y., Paramor, M., Gleeson, J. G., Odom, D. T., Ule, J., & Frye, M. (2013). NSun2-mediated cytosine-5 methylation of vault noncoding RNA determines its processing into regulatory small RNAs. *Cell Reports*, *4*(2), 255–261. https://doi.org/10.1016/j.celrep.2013.06.029

Ignatova, V. V., Stolz, P., Kaiser, S., Gustafsson, T. H., Lastres, P. R., Sanz-Moreno, A., Cho, Y. L., Amarie, O. V., Aguilar-Pimentel, A., Klein-Rodewald, T., Calzada-Wack, J., Becker, L., Marschall, S., Kraiger, M., Garrett, L., Seisenberger, C., Hölter, S. M., Borland, K., de Logt, E. Van, … Schneider, R. (2020). The rRNA m6A methyltransferase METTL5 is involved in pluripotency and developmental programs. *Genes and Development*, *34*(9–10), 715–729. https://doi.org/10.1101/gad.333369.119

Incarnato, D., Anselmi, F., Morandi, E., Neri, F., Maldotti, M., Rapelli, S., Parlato, C., Basile, G., & Oliviero, S. (2017). High-throughput single-base resolution mapping of RNA 2-O-methylated residues. *Nucleic Acids Research*, *45*(3), 1433–1441. https://doi.org/10.1093/nar/gkw810

Ishigami, Y., Ohira, T., Isokawa, Y., Suzuki, Y., & Suzuki, T. (2021). A single m6A modification in U6 snRNA diversifies exon sequence at the 5' splice site. *Nature Communications*, *12*(1). https://doi.org/10.1038/s41467-021-23457-6

Ishii, T., Hayakawa, H., Igawa, T., Sekiguchi, T., & Sekiguchi, M. (2018). Specific binding of PCBP1 to heavily oxidized RNA to induce cell death. *Proceedings of the National Academy of Sciences of the United States of America*, *115*(26), 6715–6720. https://doi.org/10.1073/pnas.1806912115

Ishii, T., Hayakawa, H., Sekiguchi, T., Adachi, N., & Sekiguchi, M. (2015). Role of Auf1 in elimination of oxidatively damaged messenger RNA in human cells. *Free Radical Biology and Medicine*, *79*, 109–116. https://doi.org/10.1016/j.freeradbiomed.2014.11.018

Ito, S., Akamatsu, Y., Noma, A., Kimura, S., Miyauchi, K., Ikeuchi, Y., Suzuki, T., & Suzuki, T. (2014). A single acetylation of 18 S rRNA is essential for biogenesis of

the small ribosomal subunit in saccharomyces cerevisiae. *Journal of Biological Chemistry*, *289*(38), 26201–26212. https://doi.org/10.1074/jbc.M114.593996

Ito, S., Horikawa, S., Suzuki, T., Kawauchi, H., Tanaka, Y., Suzuki, T., & Suzuki, T. (2014). Human NAT10 is an ATP-dependent rna acetyltransferase responsible for N4-acetylcytidine formation in 18 S ribosomal RNA (rRNA). *Journal of Biological Chemistry*, *289*(52), 35724–35730. https://doi.org/10.1074/jbc.C114.602698

Iyer, L. M., Zhang, D., & Aravind, L. (2016). Adenine methylation in eukaryotes: Apprehending the complex evolutionary history and functional potential of an epigenetic modification. *BioEssays*, *38*(1), 27–40. https://doi.org/10.1002/bies.201500104

Izumikawa, K., Nobe, Y., Ishikawa, H., Yamauchi, Y., Taoka, M., Sato, K., Nakayama, H., Simpson, R. J., Isobe, T., & Takahashi, N. (2019). TDP-43 regulates site-specific 2-O-methylation of U1 and U2 snRNAs via controlling the Cajal body localization of a subset of C/D scaRNAs. *Nucleic Acids Research*, *47*(5), 2487–2505. https://doi.org/10.1093/nar/gkz086

Jansson, M. D., Häfner, S. J., Altinel, K., Tehler, D., Krogh, N., Jakobsen, E., Andersen, J. V., Andersen, K. L., Schoof, E. M., Ménard, P., Nielsen, H., & Lund, A. H. (2021). Regulation of translation by site-specific ribosomal RNA methylation. *Nature Structural and Molecular Biology*, *28*(11), 889–899. https://doi.org/10.1038/s41594-021-00669-4

Ji, L., & Chen, X. (2012). Regulation of small RNA stability: Methylation and beyond. *Cell Research*, *22*(4), 624–636. https://doi.org/10.1038/cr.2012.36

Jia, G., Fu, Y., Zhao, X., Dai, Q., Zheng, G., Yang, Y., Yi, C., Lindahl, T., Pan, T., Yang, Y., He, C., Group, S., Genomics, D., District, C., Laboratories, C. H., & Mimms, S. (2012). *N6-Methyladenosine in Nuclear RNA is a Major Substrate of the Obesity-Associated FTO*. *7*(12), 885–887. https://doi.org/10.1038/nchembio.687.N

Johansson, M. J. O., & Byström, A. S. (2004). The Saccharomyces cerevisiae TAN1 gene is required for N 4-acetylcytidine formation in tRNA. *Rna*, *10*(4), 712–719. https://doi.org/10.1261/rna.5198204

Jonkhout, N., Tran, J., Smith, M. A., Schonrock, N., Mattick, J. S., & Novoa, E. M. (2017). The RNA modification landscape in human disease. *Rna*, *23*(12), 1754–1769. https://doi.org/10.1261/rna.063503.117

Kadaba, S., Krueger, A., Trice, T., Krecic, A. M., Hinnebusch, A. G., & Anderson, J. (2004). Nuclear surveillance and degradation of hypomodified initiator tRNA Met in S. cerevisiae. *Genes and Development*, *18*(11), 1227–1240. https://doi.org/10.1101/gad.1183804

Kamminga, L. M., Luteijn, M. J., Den Broeder, M. J., Redl, S., Kaaij, L. J. T., Roovers, E. F., Ladurner, P., Berezikov, E., & Ketting, R. F. (2010). Hen1 is required for oocyte development and piRNA stability in zebrafish. *EMBO Journal*, *29*(21), 3688–3700. https://doi.org/10.1038/emboj.2010.233

Kempfer, R., & Pombo, A. (2020). Methods for mapping 3D chromosome architecture. *Nature Reviews Genetics*, *21*(4), 207–226. https://doi.org/10.1038/s41576-019-0195-2

Kendall, A. C., & Nicolaou, A. (2013). Bioactive lipid mediators in skin inflammation and immunity. *Progress in Lipid Research*, *52*(1), 141–164. https://doi.org/10.1016/j.plipres.2012.10.003

Khoddami, V., & Cairns, B. R. (2013). Identification of direct targets and modified bases of RNA cytosine methyltransferases. *Nature Biotechnology*, *31*(5), 458–464. https://doi.org/10.1038/nbt.2566

King, T. H., Liu, B., McCully, R. R., & Fournier, M. J. (2003). Ribosome structure and activity are altered in cells lacking snoRNPs that form pseudouridines in the peptidyl transferase center. *Molecular Cell*, *11*(2), 425–435. https://doi.org/10.1016/S1097-2765(03)00040-6

Kirino, Y., & Mourelatos, Z. (2007). Mouse Piwi-interacting RNAs are 2′-O-methylated at their 3′ termini. *Nature Structural and Molecular Biology*, *14*(4), 347–348. https://doi.org/10.1038/nsmb1218

Kiss-László, Z., Henry, Y., Bachellerie, J. P., Caizergues-Ferrer, M., & Kiss, T. (1996). Site-specific ribose methylation of preribosomal RNA: A novel function for small nucleolar RNAs. *Cell*, *85*(7), 1077–1088.

https://doi.org/10.1016/S0092-8674(00)81308-2

Knuckles, P., Lence, T., Haussmann, I. U., Jacob, D., Kreim, N., Carl, S. H., Masiello, I., Hares, T., Villaseñor, R., Hess, D., Andrade-Navarro, M. A., Biggiogera, M., Helm, M., Soller, M., Bühler, M., & Roignant, J. Y. (2018). Zc3h13/Flacc is required for adenosine methylation by bridging the mRNA-binding factor RbM15/spenito to the m6 a machinery component Wtap/Fl(2)d. *Genes and Development*, *32*(5–6), 415–429. https://doi.org/10.1101/gad.309146.117

Koh, C. W. Q., Goh, Y. T., & Goh, W. S. S. (2019). Atlas of quantitative single-base-resolution N 6-methyl-adenine methylomes. *Nature Communications*, *10*(1). https://doi.org/10.1038/s41467-019-13561-z

Koš, M., & Tollervey, D. (2010). Yeast Pre-rRNA Processing and Modification Occur Cotranscriptionally. *Molecular Cell*, *37*(6), 809–820. https://doi.org/10.1016/j.molcel.2010.02.024

Kotelawala, L., Grayhack, E. J., & Phizicky, E. M. (2008). Identification of yeast tRNA Um44 2′-O-methyltransferase (Trm44) and demonstration of a Trm44 role in sustaining levels of specific tRNASer species. *Rna*, *14*(1), 158–169. https://doi.org/10.1261/rna.811008

Kressler, D., Rojo, M., Linder, P., & De La Cruz, J. (1999). Spb1p is a putative methyltransferase required for 60S ribosomal subunit biogenesis in Saccharomyces cerevisiae. *Nucleic Acids Research*, *27*(23), 4598–4608. https://doi.org/10.1093/nar/27.23.4598

Krogh, N., Jansson, M. D., Häfner, S. J., Tehler, D., Birkedal, U., Christensen-Dalsgaard, M., Lund, A. H., & Nielsen, H. (2016). Profiling of 2′-O-Me in human rRNA reveals a subset of fractionally modified positions and provides evidence for ribosome heterogeneity. *Nucleic Acids Research*, *44*(16), 7884–7895. https://doi.org/10.1093/nar/gkw482

Krogh, N., Kongsbak-Wismann, M., Geisler, C., & Nielsen, H. (2017). Substoichiometric ribose methylations in spliceosomal snRNAs. *Organic and Biomolecular Chemistry*, *15*(42), 8872–8876. https://doi.org/10.1039/c7ob02317k

Kruppa, J., & Zachau, H. G. (1972). MULTIPLICITY OF SERINE-SPECIFIC TRANSFER RNAs OF BREWER'S AND BAKER'S YEAST. *Biochimica et Biophysica Acta (BBA)*, *277*, 499–512.

Kuge, H., Brownlee, G. G., Gershon, P. D., & Richter, J. D. (1998). Cap ribose methylation of c-mos mRNA stimulates translation and oocyte maturation in Xenopus laevis. *Nucleic Acids Research*, *26*(13), 3208–3214. https://doi.org/10.1093/nar/26.13.3208

Kumar, P., Kuscu, C., & Dutta, A. (2016). Biogenesis and function of transfer RNA related fragments (tRFs). *Trends Biochem*, *41*(8), 679–689. https://doi.org/10.1016/j.tibs.2016.05.004

Kweon, S. M., Chen, Y., Moon, E., Kvederaviciutė, K., Klimasauskas, S., & Feldman, D. E. (2019). An Adversarial DNA N6-Methyladenine-Sensor Network Preserves Polycomb Silencing. *Molecular Cell*, *74*(6), 1138-1147.e6. https://doi.org/10.1016/j.molcel.2019.03.018

Kyoung, M. K., Cho, H., Choi, K., Kim, J., Kim, B. W., Ko, Y. G., Sung, K. J., & Yoon, K. K. (2009). A new MIF4G domain-containing protein, CTIF, directs nuclear cap-binding protein CBP80/20-dependent translation. *Genes and Development*, *23*(17), 2033–2045. https://doi.org/10.1101/gad.1823409

Lafontaine, D. L., Vandenhaute, J., & Tollervey, D. (1995). *The 18s rRNA dimethvlase Diml~ is required for pre-ribo~omal RNA processing in yeast*. *9*, 2470–2481.

Lai, C. W., Chen, H. L., Lin, K. Y., Liu, F. C., Chong, K. Y., Cheng, W. T. K., & Chen, C. M. (2014). FTSJ2, a heat shock-inducible mitochondrial protein, suppresses cell invasion and migration. *PLoS ONE*, *9*(3). https://doi.org/10.1371/journal.pone.0090818

Lapeyre, B., & Purushothaman, S. K. (2004). Spb1p-directed formation of Gm2922 in the ribosome catalytic center occurs at a late processing stage. *Molecular Cell*, *16*(4), 663–669. https://doi.org/10.1016/j.molcel.2004.10.022

Lapinaite, A., Simon, B., Skjaerven, L., Rakwalska-Bange, M., Gabel, F., & Carlomagno, T. (2013). The structure of the box C/D enzyme reveals regulation of RNA methylation. *Nature*, *502*(7472), 519–523. https://doi.org/10.1038/nature12581

Lee, K. W., & Bogenhagen, D. F. (2014). Assignment of 2′-O-methyltransferases to modification sites on the mammalian mitochondrial large subunit 16 S ribosomal RNA (rRNA). *Journal of Biological Chemistry*, *289*(36), 24936–24942. https://doi.org/10.1074/jbc.C114.581868

Lee, S. H., Singh, I., Tisdale, S., Abdel-Wahab, O., Leslie, C. S., & Mayr, C. (2018). Widespread intronic polyadenylation inactivates tumour suppressor genes in leukaemia. *Nature*, *561*(7721), 127–131. https://doi.org/10.1038/s41586-018-0465-8

Leismann, J., Spagnuolo, M., Pradhan, M., Wacheul, L., Vu, M. A., Musheev, M., Mier, P., Andrade-Navarro, M. A., Graille, M., Niehrs, C., Lafontaine, D. L., & Roignant, J. (2020). The 18S ribosomal RNA m 6 A methyltransferase Mettl5 is required for normal walking behavior in Drosophila . *EMBO Reports*, *21*(7), 1–12. https://doi.org/10.15252/embr.201949443

Lence, T., Akhtar, J., Bayer, M., Schmid, K., Spindler, L., Ho, C. H., Kreim, N., Andrade-Navarro, M. A., Poeck, B., Helm, M., & Roignant, J. Y. (2016). M6A modulates neuronal functions and sex determination in Drosophila. *Nature*, *540*(7632), 242–247. https://doi.org/10.1038/nature20568

Lence, T., Paolantoni, C., Worpenberg, L., & Roignant, J. Y. (2019). Mechanistic insights into m 6 A RNA enzymes. *Biochimica et Biophysica Acta - Gene Regulatory Mechanisms*, *1862*(3), 222–229. https://doi.org/10.1016/j.bbagrm.2018.10.014

Létoquart, J., Huvelle, E., Wacheul, L., Bourgeois, G., Zorbas, C., Graille, M., Heurgué-Hamard, V., & Lafontaine, D. L. J. (2014). Structural and functional studies of Bud23-Trm112 reveal 18S rRNA N7-G1575 methylation occurs on late 40S precursor ribosomes. *Proceedings of the National Academy of Sciences of the United States of America*, *111*(51), E5518–E5526. https://doi.org/10.1073/pnas.1413089111

Leulliot, N., Bohnsack, M. T., Graille, M., Tollervey, D., & Van tilbeurgh, H. (2008). The yeast ribosome synthesis factor Emg1 is a novel member of the superfamily of alpha/beta knot fold methyltransferases. *Nucleic Acids Research*, *36*(2), 629–639. https://doi.org/10.1093/nar/gkm1074

Lewinska, A., Adamczyk-Grochala, J., Kwasniewicz, E., Deregowska, A., Semik, E., Zabek, T., & Wnuk, M. (2018). Reduced levels of methyltransferase DNMT2 sensitize human fibroblasts to oxidative stress and DNA damage that is accompanied by changes in proliferation-related miRNA expression. *Redox Biology*, *14*(July 2017), 20–34. https://doi.org/10.1016/j.redox.2017.08.012

Lewinska, A., Adamczyk-Grochala, J., Kwasniewicz, E., & Wnuk, M. (2017). Downregulation of methyltransferase Dnmt2 results in condition-dependent telomere shortening and senescence or apoptosis in mouse fibroblasts. *Journal of Cellular Physiology*, *232*(12), 3714–3726. https://doi.org/10.1002/jcp.25848

Li, J., Yang, Z., Yu, B., Liu, J., & Chen, X. (2005). Methylation Protects miRNAs and siRNAs from a 3′-End Uridylation Activity in Arabidopsis. *Current Biology*, *15*(16), 1501–1507. https://doi.org/10.1016/j.cub.2005.07.029.Methylation

Li, X., Xiong, X., Wang, K., Wang, L., Shu, X., Ma, S., & Yi, C. (2016). Transcriptome-wide mapping reveals reversible and dynamic N1-methyladenosine methylome. *Nature Chemical Biology*, *12*(5), 311–316. https://doi.org/10.1038/nchembio.2040

Li, X., Xiong, X., Zhang, M., Wang, K., Chen, Y., Zhou, J., Mao, Y., Lv, J., Yi, D., Chen, X. W., Wang, C., Qian, S. B., & Yi, C. (2017). Base-Resolution Mapping Reveals Distinct m1A Methylome in Nuclear- and Mitochondrial-Encoded Transcripts. *Molecular Cell*, *68*(5), 993-1005.e9. https://doi.org/10.1016/j.molcel.2017.10.019

Li, X., Zhu, P., Ma, S., Song, J., Bai, J., Sun, F., & Yi, C. (2015). Chemical pulldown reveals dynamic pseudouridylation of the mammalian transcriptome. *Nature Chemical Biology*, *11*(8), 592–597. https://doi.org/10.1038/nchembio.1836

Li, Z., Yang, H. Y., Dai, X. Y., Zhang, X., Huang, Y. Z., Shi, L., Wei, J. F., & Ding, Q. (2021). Circmettl3, upregulated in a m6a-dependent manner, promotes breast cancer progression. *International Journal of Biological*

Sciences, *17*(5), 1178–1190. https://doi.org/10.7150/ijbs.57783

Liang, X. H., Liu, Q., & Fournier, M. J. (2009). Loss of rRNA modifications in the decoding center of the ribosome impairs translation and strongly delays pre-rRNA processing. *Rna*, *15*(9), 1716–1728. https://doi.org/10.1261/rna.1724409

Liberman, N., O'Brown, Z. K., Earl, A. S., Boulias, K., Gerashchenko, M. V., Wang, S. Y., Fritsche, C., Fady, P. E., Dong, A., Gladyshev, V. N., & Greer, E. L. (2020). N6-adenosine methylation of ribosomal RNA affects lipid oxidation and stress resistance. *Science Advances*, *6*(17). https://doi.org/10.1126/sciadv.aaz4370

Licht, K., Hartl, M., Amman, F., Anrather, D., Janisiw, M. P., & Jantsch, M. F. (2019). Inosine induces context-dependent recoding and translational stalling. *Nucleic Acids Research*, *47*(1), 3–14. https://doi.org/10.1093/nar/gky1163

Lin, M. J., Tang, L. Y., Reddy, M. N., & Shen, C. K. J. (2005). DNA methyltransferase gene dDnmt2 and longevity of Drosophila. *Journal of Biological Chemistry*, *280*(2), 861–864. https://doi.org/10.1074/jbc.C400477200

Lin, X., Chai, G., Wu, Y., Li, J., Chen, F., Liu, J., Luo, G., Tauler, J., Du, J., Lin, S., He, C., & Wang, H. (2019). RNA m6A methylation regulates the epithelial mesenchymal transition of cancer cells and translation of Snail. *Nature Communications*, *10*(1). https://doi.org/10.1038/s41467-019-09865-9

Lin, Y., & Kielkopf, C. L. (2008). X-ray Structures of U2 snRNA - Branchpoint Duplexes Containing Conserved Pseudouridines. *Biochemistry*, *47*(20), 5503–5514. https://www.ncbi.nlm.nih.gov/pmc/articles/PMC3624763/pdf/nihms412728.pdf%0Ahttps://www.ncbi.nlm.nih.gov/pmc/articles/PMC2688697/pdf/nihms-110443.pdf

Linder, B., Grozhik, A. V, Olarerin-george, A. O., Meydan, C., Mason, C. E., & Jaffrey, S. R. (2015). Single-nucleotide resolution mapping of m6A and m6Am throughout the transcriptome. *Nature Methods*, *12*(8), 767–772. https://doi.org/10.1038/nmeth.3453.Single-nucleotide

Liu, C., Sun, H., Yi, Y., Shen, W., Li, K., Xiao, Y., Li, F., Li, Y., Hou, Y., Lu, B., Liu, W., Meng, H., Peng, J., Yi, C., & Wang, J. (2023). Absolute quantification of single-base m6A methylation in the mammalian transcriptome using GLORI. *Nature Biotechnology*, *41*(3), 355–366. https://doi.org/10.1038/s41587-022-01487-9

Liu, F., Clark, W., Luo, G., Wang, X., Fu, Y., Wei, J., Wang, X., Hao, Z., Dai, Q., Zheng, G., Ma, H., Han, D., Evans, M., Klungland, A., Pan, T., & He, C. (2016). ALKBH1-Mediated tRNA Demethylation Regulates Translation. *Cell*, *167*(3), 816–828. https://doi.org/10.1016/j.cell.2016.09.038

Liu, J., Yue, Y., Liu, J., Cui, X., Cao, J., Luo, G., Zhang, Z., Cheng, T., Gao, M., Shu, X., Ma, H., Wang, F., Wang, X., Shen, B., Wang, Y., Feng, X., & He, C. (2018). VIRMA mediates preferential m6A mRNA methylation in 3'UTR and near stop codon and associates with alternative polyadenylation. *Cell Discovery*, *4*(1). https://doi.org/10.1038/s41421-018-0019-0

Liu, K., Santos, D. A., Hussmann, J. A., Wang, Y., Sutter, B. M., Weissman, J. S., & Tu, B. P. (2021). Regulation of translation by methylation multiplicity of 18S rRNA. *Cell Reports*, *34*(10). https://doi.org/10.1016/j.celrep.2021.108825

Liu, N., Dai, Q., Zheng, G., He, C., Parisien, M., & Pan, T. (2015). N6 -methyladenosine-dependent RNA structural switches regulate RNA-protein interactions. *Nature*, *518*(7540), 560–564. https://doi.org/10.1038/nature14234

Liu, N., Parisien, M., Dai, Q., Zheng, G., He, C., & Pan, T. (2013). Probing N6-methyladenosine RNA modification status at single nucleotide resolution in mRNA and long noncoding RNA. *Rna*, *19*(12), 1848–1856. https://doi.org/10.1261/rna.041178.113

Lorenz, C., Lünse, C. E., & Mörl, M. (2017). Trna modifications: Impact on structure and thermal adaptation. *Biomolecules*, *7*(2). https://doi.org/10.3390/biom7020035

Louloupi, A., Ntini, E., Conrad, T., & Ørom, U. A. V. (2018). Transient N-6-Methyladenosine Transcriptome Sequencing Reveals a Regulatory Role of m6A in Splicing Efficiency. *Cell Reports*, *23*(12), 3429–3437. https://doi.org/10.1016/j.celrep.2018.05.077

Luo, Q., Mo, J., Chen, H., Hu, Z., Wang, B., Wu, J., Liang, Z.,

Xie, W., Du, K., Peng, M., Li, Y., Li, T., Zhang, Y., Shi, X., Shen, W. H., Shi, Y., Dong, A., Wang, H., & Ma, J. (2022). Structural insights into molecular mechanism for N 6-adenosine methylation by MT-A70 family methyltransferase METTL4. *Nature Communications*, *13*(1), 1–11. https://doi.org/10.1038/s41467-022-33277-x

Lygerou, Z., Allmang, C., Tollervey, D., & Seraphin, B. (1996). *Accurate Processing of a Eukaryotic Precursor Ribosomal RNA by Ribonuclease MRP in Vitro*. *272*(April), 268–270.

Ma, H., Wang, X., Cai, J., Dai, Q., Natchiar, S. K., Lv, R., Chen, K., Lu, Z., Chen, H., Shi, Y. G., Lan, F., Fan, J., Klaholz, B. P., Pan, T., Shi, Y., & He, C. (2019). N 6-Methyladenosine methyltransferase ZCCHC4 mediates ribosomal RNA methylation. *Nature Chemical Biology*, *15*(1), 88–94. https://doi.org/10.1038/s41589-018-0184-3

Ma, Shaoqian, & Zhang, Y. (2020). Profiling chromatin regulatory landscape: insights into the development of ChIP-seq and ATAC-seq. *Molecular Biomedicine*, *1*(1), 1–13. https://doi.org/10.1186/s43556-020-00009-w

Ma, Shuai, Chen, C., Ji, X., Liu, J., Zhou, Q., Wang, G., Yuan, W., Kan, Q., & Sun, Z. (2019). The interplay between m6A RNA methylation and noncoding RNA in cancer. *Journal of Hematology and Oncology*, *12*(1), 1–15. https://doi.org/10.1186/s13045-019-0805-7

Machnicka, M. A., Milanowska, K., Oglou, O. O., Purta, E., Kurkowska, M., Olchowik, A., Januszewski, W., Kalinowski, S., Dunin-Horkawicz, S., Rother, K. M., Helm, M., Bujnicki, J. M., & Grosjean, H. (2013). MODOMICS: A database of RNA modification pathways - 2013 update. *Nucleic Acids Research*, *41*(D1), 262–267. https://doi.org/10.1093/nar/gks1007

Macinnes, A. W. (2016). The role of the ribosome in the regulation of longevity and lifespan extension. *Wiley Interdisciplinary Reviews: RNA*, *7*(2), 198–212. https://doi.org/10.1002/wrna.1325

Maden, B. E.H. (1986). Identification of the locations of the methyl groups in 18 S ribosomal RNA from Xenopus laevis and man. *Journal of Molecular Biology*, *189*(4), 681–699. https://doi.org/10.1016/0022-2836(86)90498-5

Maden, B. Edward H. (2001). Mapping 2′-O-methyl groups in ribosomal RNA. *Methods*, *25*(3), 374–382. https://doi.org/10.1006/meth.2001.1250

Malbec, L., Zhang, T., Chen, Y. S., Zhang, Y., Sun, B. F., Shi, B. Y., Zhao, Y. L., Yang, Y., & Yang, Y. G. (2019). Dynamic methylome of internal mRNA N 7-methylguanosine and its regulatory role in translation. *Cell Research*, *29*(11), 927–941. https://doi.org/10.1038/s41422-019-0230-z

Manley, J. L. (1988). *Department of Biological Sciences, Columbia Unioersity, New York, N Y (U.S.A.)*. *950*, 1–12.

Manning, M., Jiang, Y., Wang, R., Liu, L., Rode, S., Bonahoom, M., Kim, S., & Yang, Z. Q. (2020). Pan-cancer analysis of RNA methyltransferases identifies FTSJ3 as a potential regulator of breast cancer progression. *RNA Biology*, *17*(4), 474–486. https://doi.org/10.1080/15476286.2019.1708549

Marchand, V., Ayadi, L., Ernst, F. G. M., Hertler, J., Bourguignon-Igel, V., Galvanin, A., Kotter, A., Helm, M., Lafontaine, D. L. J., & Motorin, Y. (2018). AlkAniline-Seq: Profiling of m7G and m3C RNA Modifications at Single Nucleotide Resolution. *Angewandte Chemie - International Edition*, *57*(51), 16785–16790. https://doi.org/10.1002/anie.201810946

Marchand, V., Blanloeil-Oillo, F., Helm, M., & Motorin, Y. (2016). Illumina-based RiboMethSeq approach for mapping of 2′-O-Me residues in RNA. *Nucleic Acids Research*, *44*(16). https://doi.org/10.1093/nar/gkw547

Mauer, J., Luo, X., Blanjoie, A., Jiao, X., Grozhik, A. V., Patil, D. P., Linder, B., Pickering, B. F., Vasseur, J. J., Chen, Q., Gross, S. S., Elemento, O., Debart, F., Kiledjian, M., & Jaffrey, S. R. (2017). Reversible methylation of m6 Am in the 5′ cap controls mRNA stability. *Nature*, *541*(7637), 371–375. https://doi.org/10.1038/nature21022

Mcglincy, N. J., & Ingolia, N. T. (2017). Transcriptome-wide measurement of translation by ribosome profiling. *Methods*, *126*, 112–129. https://doi.org/10.1016/j.ymeth.2017.05.028.Transcriptome-wide

Meier, U. T. (2017). RNA modification in Cajal bodies. *RNA*

Biology, *14*(6), 693–700. https://doi.org/10.1080/15476286.2016.1249091

Mendel, M., Chen, K. M., Homolka, D., Gos, P., Pandey, R. R., McCarthy, A. A., & Pillai, R. S. (2018). Methylation of Structured RNA by the m6A Writer METTL16 Is Essential for Mouse Embryonic Development. *Molecular Cell*, *71*(6), 986-1000.e11. https://doi.org/10.1016/j.molcel.2018.08.004

Mendel, M., Delaney, K., Pandey, R. R., Chen, K. M., Wenda, J. M., Vågbø, C. B., Steiner, F. A., Homolka, D., & Pillai, R. S. (2021). Splice site m6A methylation prevents binding of U2AF35 to inhibit RNA splicing. *Cell*, *184*(12), 3125-3142.e25. https://doi.org/10.1016/j.cell.2021.03.062

Mer Wei, C., & Moss, B. (1974). Methylation of newly synthesized viral messenger RNA by an enzyme in vaccinia virus. *Proceedings of the National Academy of Sciences of the United States of America*, *71*(8), 3014–3018. https://doi.org/10.1073/pnas.71.8.3014

Meyer, B., Wurm, J. P., Kötter, P., Leisegang, M. S., Schilling, V., Buchhaupt, M., Held, M., Bahr, U., Karas, M., Heckel, A., Bohnsack, M. T., Wöhnert, J., & Entian, K. D. (2011). The Bowen-Conradi syndrome protein Nep1 (Emg1) has a dual role in eukaryotic ribosome biogenesis, as an essential assembly factor and in the methylation of Ψ1191 in yeast 18S rRNA. *Nucleic Acids Research*, *39*(4), 1526–1537. https://doi.org/10.1093/nar/gkq931

Meyer, K. D. (2019). DART-seq: an antibody-free method for global m6A detection. *Nature Methods*, *16*(12), 1275–1280. https://doi.org/10.1038/s41592-019-0570-0

Meyer, K. D., & Jaffrey, S. R. (2017). *Annual Review of Cell and Developmental Biology Rethinking m 6 A Readers, Writers, and Erasers*. *July*, 1–24. https://doi.org/10.1146/annurev-cellbio-100616-

Meyer, K. D., Saletore, Y., Zumbo, P., Elemento, O., Mason, C. E., & Jaffrey, S. R. (2012). Comprehensive analysis of mRNA methylation reveals enrichment in 3′ UTRs and near stop codons. *Cell*, *149*(7), 1635–1646. https://doi.org/10.1016/j.cell.2012.05.003

Mikutis, S., Gu, M., Sendinc, E., Hazemi, M. E., Kiely-Collins, H., Aspris, D., Vassiliou, G. S., Shi, Y., Tzelepis, K., & Bernardes, G. J. L. (2020). MeCLICK-Seq, a Substrate-Hijacking and RNA Degradation Strategy for the Study of RNA Methylation. *ACS Central Science*, *6*(12), 2196–2208. https://doi.org/10.1021/acscentsci.0c01094

Miura, K., Ishii, T., Sugita, Y., & Bannai, S. (1992). Cystine uptake and glutathione level in endothelial cells exposed to oxidative stress. *American Journal of Physiology - Cell Physiology*, *262*(1 31-1). https://doi.org/10.1152/ajpcell.1992.262.1.c50

Molinie, B., Wang, J., Lim, K.-S., Hillebrand, R., Lu, Z., Van Wittenberghe, N., Howard, B. D., Daneshvar, K., Mullen, A. C., Dedon, P., Xing, Y. C. C., & Giallourakis, C. C. (2016). m6A level and isoform characterization sequencing (m6A-LAIC-seq) reveals the census and complexity of the m6A epitranscriptome. *Nature Methods*, *13*(8), 692–698. https://doi.org/10.1038/nmeth.3898.m

Morello, L. G., Coltri, P. P., Quaresma, A. J. C., Simabuco, F. M., Silva, T. C. L., Singh, G., Nickerson, J. A., Oliveira, C. C., Moore, M. J., & Zanchin, N. I. T. (2011). The human nucleolar protein FTSJ3 associates with NIP7 and functions in pre-rRNA processing. *PLoS ONE*, *6*(12). https://doi.org/10.1371/journal.pone.0029174

Morrison, O., & Thakur, J. (2021). Molecular complexes at euchromatin, heterochromatin and centromeric chromatin. *International Journal of Molecular Sciences*, *22*(13). https://doi.org/10.3390/ijms22136922

Motorin, Y., & Helm, M. (2010). TRNA stabilization by modified nucleotides. *Biochemistry*, *49*(24), 4934–4944. https://doi.org/10.1021/bi100408z

Nagayoshi, Y., Chujo, T., Hirata, S., Nakatsuka, H., Chen, C. W., Takakura, M., Miyauchi, K., Ikeuchi, Y., Carlyle, B. C., Kitchen, R. R., Suzuki, T., Katsuoka, F., Yamamoto, M., Goto, Y., Tanaka, M., Natsume, K., Nairn, A. C., Suzuki, T., Tomizawa, K., & Wei, F. Y. (2021). Loss of Ftsj1 perturbs codon-specific translation efficiency in the brain and is associated with X-linked intellectual disability. *Science Advances*, *7*(13). https://doi.org/10.1126/sciadv.abf3072

Nance, D. J., Satterwhite, E. R., Bhaskar, B., Misra, S., Carraway, K. R., & Mansfield, K. D. (2020). Characterization of METTL16 as a cytoplasmic RNA

binding protein. *PLoS ONE*, *15*(1), 1–18. https://doi.org/10.1371/journal.pone.0227647

Noma, A., Kirino, Y., Ikeuchi, Y., & Suzuki, T. (2006). Biosynthesis of wybutosine, a hyper-modified nucleoside in eukaryotic phenylalanine tRNA. *EMBO Journal*, *25*(10), 2142–2154. https://doi.org/10.1038/sj.emboj.7601105

Norris, K., Hopes, T., & Aspden, J. L. (2021). Ribosome heterogeneity and specialization in development. *Wiley Interdisciplinary Reviews: RNA*, *12*(4), 1–23. https://doi.org/10.1002/wrna.1644

Ohashi, Z., Murao, K., Yahagi, T., Von Minden, D. L., McCloskey, J. A., & Nishimura, S. (1972). Characterization of C+ located in the first position of the anticodon of Escherichia coli tRNAMet as N4-acetylcytidine. *BBA Section Nucleic Acids And Protein Synthesis*, *262*(2), 209–213. https://doi.org/10.1016/0005-2787(72)90234-1

Olovnikov, I. A., & Kalmykova, A. I. (2013). PiRNA clusters as a main source of small RNAs in the animal germline. *Biochemistry (Moscow)*, *78*(6), 572–584. https://doi.org/10.1134/S0006297913060035

Orgebin, E., Lamoureux, F., Isidor, B., Charrier, C., Ory, B., Lézot, F., & Baud'huin, M. (2020). Ribosomopathies: New Therapeutic Perspectives. *Cells*, *9*(9), 1–21. https://doi.org/10.3390/cells9092080

Ozanick, S., Krecic, A., Andersland, J., & Anderson, J. T. (2005). The bipartite structure of the tRNA m1A58 methyltransferase from S. cerevisiae is conserved in humans. *Rna*, *11*(8), 1281–1290. https://doi.org/10.1261/rna.5040605

Patil, D. P., Chen, C.-K., Pickering, B. F., Chow, A., Jackson, C., Guttman, M., & Jaffrey, S. R. (2016). m6A RNA methylation promotes XIST-mediated transcriptional repression. *Nature*, *437*(7620), 369–373. https://doi.org/10.1038/nature19342.m

Patton, J. R., Bykhovskaya, Y., Mengesha, E., Bertolotto, C., & Fischel-Ghodsian, N. (2005). Mitochondrial myopathy and sideroblastic anemia (MLASA): Missense mutation in the pseudouridine synthase 1 (PUS1) gene is associated with the loss of tRNA pseudouridylation. *Journal of Biological Chemistry*, *280*(20), 19823–19828. https://doi.org/10.1074/jbc.M500216200

Peifer, C., Sharma, S., Watzinger, P., Lamberth, S., Kötter, P., & Entian, K. D. (2013). Yeast Rrp8p, a novel methyltransferase responsible for m1A 645 base modification of 25S rRNA. *Nucleic Acids Research*, *41*(2), 1151–1163. https://doi.org/10.1093/nar/gks1102

Peixoto, P., Cartron, P., & Serandour, A. (2020). *From 1957 to Nowadays : A Brief History of Epigenetics*.

Pelletier, J., Riaño-Canalias, F., Almacellas, E., Mauvezin, C., Samino, S., Feu, S., Menoyo, S., Domostegui, A., Garcia-Cajide, M., Salazar, R., Cortés, C., Marcos, R., Tauler, A., Yanes, O., Agell, N., Kozma, S. C., Gentilella, A., & Thomas, G. (2020). Nucleotide depletion reveals the impaired ribosome biogenesis checkpoint as a barrier against DNA damage . *The EMBO Journal*, *39*(13), 1–19. https://doi.org/10.15252/embj.2019103838

Pendleton, K. E., Chen, B., Liu, K., Hunter, O. V., Xie, Y., Tu, B. P., & Conrad, N. K. (2017). The U6 snRNA m6A Methyltransferase METTL16 Regulates SAM Synthetase Intron Retention. *Cell*, *169*(5), 824-835.e14. https://doi.org/10.1016/j.cell.2017.05.003

Peng, W., Li, J., Chen, R., Gu, Q., Yang, P., Qian, W., Ji, D., Wang, Q., Zhang, Z., Tang, J., & Sun, Y. (2019). Upregulated METTL3 promotes metastasis of colorectal Cancer via miR-1246/SPRED2/MAPK signaling pathway. *Journal of Experimental and Clinical Cancer Research*, *38*(1), 1–16. https://doi.org/10.1186/s13046-019-1408-4

Perry, R. P., & Kelley, D. E. (1974). Existence of methylated messenger RNA in mouse L cells. *Cell*, *1*(1), 37–42. https://doi.org/10.1016/0092-8674(74)90153-6

Picard-Jean, F., Brand, C., Tremblay-Létourneau, M., Allaire, A., Beaudoin, M. C., Boudreault, S., Duval, C., Rainville-Sirois, J., Robert, F., Pelletier, J., Geiss, B. J., & Bisaillon, M. (2018). 2'-O-methylation of the mRNA cap protects RNAs from decapping and degradation by DXO. *PLoS ONE*, *13*(3), 1–14. https://doi.org/10.1371/journal.pone.0193804

Piekna-Przybylska, D. D., Decatur, W. A., & Fournier, M. J. (2008). The 3D rRNA modification maps database:

With interactive tools for ribosome analysis. *Nucleic Acids Research*, *36*(SUPPL. 1), 178–183. https://doi.org/10.1093/nar/gkm855

Ping, X. L., Sun, B. F., Wang, L., Xiao, W., Yang, X., Wang, W. J., Adhikari, S., Shi, Y., Lv, Y., Chen, Y. S., Zhao, X., Li, A., Yang, Y., Dahal, U., Lou, X. M., Liu, X., Huang, J., Yuan, W. P., Zhu, X. F., … Yang, Y. G. (2014). Mammalian WTAP is a regulatory subunit of the RNA N6-methyladenosine methyltransferase. *Cell Research*, *24*(2), 177–189. https://doi.org/10.1038/cr.2014.3

Pintard, L., Bujnicki, J. M., Lapeyre, B., & Bonnerot, C. (2002). MRM2 encodes a novel yeast mitochondrial 21s rRNA methyltransferase. *EMBO Journal*, *21*(5), 1139–1147. https://doi.org/10.1093/emboj/21.5.1139

Pintard, L., Kressler, D., & Lapeyre, B. (2000). Spb1p Is a Yeast Nucleolar Protein Associated with Nop1p and Nop58p That Is Able To Bind S -Adenosyl- l -Methionine In Vitro . *Molecular and Cellular Biology*, *20*(4), 1370–1381. https://doi.org/10.1128/mcb.20.4.1370-1381.2000

Pintard, L., Lecointe, F., Bujnicki, J. M., Bonnerot, C., Grosjean, H., & Lapeyre, B. (2002). Trm7p catalyses the formation of two 2′-O-methylriboses in yeast tRNA anticodon loop. *EMBO Journal*, *21*(7), 1811–1820. https://doi.org/10.1093/emboj/21.7.1811

Pinto, R., Vågbø, C. B., Jakobsson, M. E., Kim, Y., Baltissen, M. P., O'Donohue, M. F., Guzmán, U. H., Małecki, J. M., Wu, J., Kirpekar, F., Olsen, J. V., Gleizes, P. E., Vermeulen, M., Leidel, S. A., Slupphaug, G., & Falnes, P. O. (2020). The human methyltransferase ZCCHC4 catalyses N6-methyladenosine modification of 28S ribosomal RNA. *Nucleic Acids Research*, *48*(2), 830–846. https://doi.org/10.1093/nar/gkz1147

Poole, A. R., Vicino, I., Adachi, H., Yu, Y. T., & Hebert, M. D. (2017). Regulatory RNPs: A novel class of ribonucleoproteins that potentially contribute to ribosome heterogeneity. *Biology Open*, *6*(9), 1342–1354. https://doi.org/10.1242/bio.028092

Prusiner, P., Yathindra, N., & Sundaralingam, M. (1974). Effect of ribose O(2′)-methylation on the conformation of nucleosides and nucleotides. *BBA Section Nucleic Acids And Protein Synthesis*, *366*(2), 115–123. https://doi.org/10.1016/0005-2787(74)90325-6

Ramanathan, A., Robb, G. B., & Chan, S. H. (2016). mRNA capping: Biological functions and applications. *Nucleic Acids Research*, *44*(16), 7511–7526. https://doi.org/10.1093/nar/gkw551

Rebelo-Guiomar, P., Pellegrino, S., Dent, K. C., Sas-Chen, A., Miller-Fleming, L., Garone, C., Van Haute, L., Rogan, J. F., Dinan, A., Firth, A. E., Andrews, B., Whitworth, A. J., Schwartz, S., Warren, A. J., & Minczuk, M. (2022). A late-stage assembly checkpoint of the human mitochondrial ribosome large subunit. *Nature Communications*, *13*(1), 1–14. https://doi.org/10.1038/s41467-022-28503-5

Ren, W., Lu, J., Huang, M., Gao, L., Li, D., Greg Wang, G., & Song, J. (2019). Structure and regulation of ZCCHC4 in m6A-methylation of 28S rRNA. *Nature Communications*, *10*(1). https://doi.org/10.1038/s41467-019-12923-x

Renda, M. J., Rosenblatt, J. D., Klimatcheva, E., Demeter, L. M., Bambara, R. A., & Planelles, V. (2001). Mutation of the Methylated tRNA3Lys Residue A58 Disrupts Reverse Transcription and Inhibits Replication of Human Immunodeficiency Virus Type 1. *Journal of Virology*, *75*(20), 9671–9678. https://doi.org/10.1128/jvi.75.20.9671-9678.2001

Riazuddin, S., Hussain, M., Razzaq, A., Iqbal, Z., Shahzad, M., Polla, D. L., Song, Y., Van Beusekom, E., Khan, A. A., Tomas-Roca, L., Rashid, M., Zahoor, M. Y., Wissink-Lindhout, W. M., Basra, M. A. R., Ansar, M., Agha, Z., Van Heeswijk, K., Rasheed, F., Van De Vorst, M., … Van Bokhoven, H. (2017). Exome sequencing of Pakistani consanguineous families identifies 30 novel candidate genes for recessive intellectual disability. *Molecular Psychiatry*, *22*(11), 1604–1614. https://doi.org/10.1038/mp.2016.109

Richard, E. M., Polla, D. L., Assir, M. Z., Contreras, M., Shahzad, M., Khan, A. A., Razzaq, A., Akram, J., Tarar, M. N., Blanpied, T. A., Ahmed, Z. M., Abou Jamra, R., Wieczorek, D., van Bokhoven, H., Riazuddin, S., & Riazuddin, S. (2019). Bi-allelic Variants in METTL5 Cause Autosomal-Recessive Intellectual Disability and Microcephaly. *American Journal of Human Genetics*,

105(4), 869–878. https://doi.org/10.1016/j.ajhg.2019.09.007

Rimbach, K., Kaiser, S., Helm, M., Dalpke, A. H., & Eigenbrod, T. (2015). 2'-O-Methylation within Bacterial RNA Acts as Suppressor of TLR7/TLR8 Activation in Human Innate Immune Cells. *Journal of Innate Immunity*, *7*(5), 482–493. https://doi.org/10.1159/000375460

Rimer, J. M., Lee, J., Holley, C. L., Crowder, R. J., Chen, D. L., Hanson, P. I., Ory, D. S., & Schaffer, J. E. (2018). Long-range function of secreted small nucleolar RNAs that direct 2-O-methylation. *Journal of Biological Chemistry*, *293*(34), 13284–13296. https://doi.org/10.1074/jbc.RA118.003410

Ringeard, M., Marchand, V., Decroly, E., Motorin, Y., & Bennasser, Y. (2019). FTSJ3 is an RNA 2'-O-methyltransferase recruited by HIV to avoid innate immune sensing. *Nature*, *565*(7740), 500–504. https://doi.org/10.1038/s41586-018-0841-4

Robertson, C. W. (1936). The metamorphosis of Drosophila melanogaster, including an accurately timed account of the principal morphological changes. *Journal of Morphology*, *59*(2), 351–399. https://doi.org/10.1002/jmor.1050590207

Rogers, R. P., & Rogina, B. (2014). Increased mitochondrial biogenesis preserves intestinal stem cell homeostasis and contributes to longevity in Indy mutant flies. *Aging*, *6*(4), 335–350. https://doi.org/10.18632/aging.100658

Rogina, B., Reenan, R. A., Nilsen, S. P., & Helfand, S. L. (2000). Extended life-span conferred by cotransporter gene mutations in Drosophila. *Science*, *290*(5499), 2137–2140. https://doi.org/10.1126/science.290.5499.2137

Roignant, J. Y., & Soller, M. (2017). m6A in mRNA: An Ancient Mechanism for Fine-Tuning Gene Expression. *Trends in Genetics*, *33*(6), 380–390. https://doi.org/10.1016/j.tig.2017.04.003

Rong, B., Zhang, Q., Wan, J., Xing, S., Dai, R., Li, Y., Cai, J., Xie, J., Song, Y., Chen, J., Zhang, L., Yan, G., Zhang, W., Gao, H., Han, J. D. J., Qu, Q., Ma, H., Tian, Y., & Lan, F. (2020). Ribosome 18S m6A Methyltransferase METTL5 Promotes Translation Initiation and Breast Cancer Cell Growth. *Cell Reports*, *33*(12), 108544. https://doi.org/10.1016/j.celrep.2020.108544

Rorbacha, J., Boesch, P., Gammage, P. A., Nicholls, T. J. J., Pearce, S. F., Patel, D., Hauser, A., Perocchi, F., & Minczuk, M. (2014). MRM2 and MRM3 are involved in biogenesis of the large subunit of the mitochondrial ribosome. *Molecular Biology of the Cell*, *25*(17), 2542–2555. https://doi.org/10.1091/mbc.E14-01-0014

Roundtree, I. A., Evans, M. E., Pan, T., & He, C. (2017). Dynamic RNA Modifications in Gene Expression Regulation. *Cell*, *169*(7), 1187–1200. https://doi.org/10.1016/j.cell.2017.05.045

Roundtree, I. A., Luo, G. Z., Zhang, Z., Wang, X., Zhou, T., Cui, Y., Sha, J., Huang, X., Guerrero, L., Xie, P., He, E., Shen, B., & He, C. (2017). YTHDC1 mediates nuclear export of N6-methyladenosine methylated mRNAs. *ELife*, *6*, 1–28. https://doi.org/10.7554/eLife.31311

Ruszkowska, A., Ruszkowski, M., Dauter, Z., & Brown, J. A. (2018). Structural insights into the RNA methyltransferase domain of METTL16. *Scientific Reports*, *8*(1), 1–13. https://doi.org/10.1038/s41598-018-23608-8

Růžička, K., Zhang, M., Campilho, A., Bodi, Z., Kashif, M., Saleh, M., Eeckhout, D., El-Showk, S., Li, H., Zhong, S., Jaeger, G. De, Mongan, N. P., Hejátko, J., Helariutta, Y., & Fray, R. G. (2017). Identification of factors required for m6A mRNA methylation in Arabidopsis reveals a role for the conserved E3 ubiquitin ligase HAKAI. *New Phytologist*, *215*(1), 157–172. https://doi.org/10.1111/nph.14586

Safra, M., Sas-Chen, A., Nir, R., Winkler, R., Nachshon, A., Bar-Yaacov, D., Erlacher, M., Rossmanith, W., Stern-Ginossar, N., & Schwartz, S. (2017). The m1A landscape on cytosolic and mitochondrial mRNA at single-base resolution. *Nature*, *551*(7679), 251–255. https://doi.org/10.1038/nature24456

Saito, K., Sakaguchi, Y., Suzuki, T., Suzuki, T., Siomi, H., & Siomi, M. C. (2007). Pimet, the Drosophila homolog of HEN1, mediates 2'-O-methylation of Piwi-interacting RNAs at their 3' ends. *Genes and Development*, *21*(13), 1603–1608. https://doi.org/10.1101/gad.1563607

Satoh, A., Takai, K., Ouchi, R., Yokoyamaand, S., & Takaku, H. (2000). Effects of anticodon 2'-O-methylations on

tRNA codon recognition in an Escherichia coli cell-free translation. *Rna*, *6*(5), 680–686. https://doi.org/10.1017/S1355838200000029

Schaefer, M., Pollex, T., Hanna, K., Tuorto, F., Meusburger, M., Helm, M., & Lyko, F. (2010). RNA methylation by Dnmt2 protects transfer RNAs against stress-induced cleavage. *Genes and Development*, *24*(15), 1590–1595. https://doi.org/10.1101/gad.586710

Schöller, E., Marks, J., Marchand, V., Bruckmann, A., Powell, C. A., Reichold, M., Mutti, C. D., Dettmer, K., Feederle, R., Hüttelmaier, S., Helm, M., Oefner, P., Minczuk, M., Motorin, Y., Hafner, M., & Meister, G. (2021). Balancing of mitochondrial translation through METTL8-mediated m3C modification of mitochondrial tRNAs. *Molecular Cell*, *81*(23), 4810-4825.e12. https://doi.org/10.1016/j.molcel.2021.10.018

Schosserer, M., Minois, N., Angerer, T. B., Amring, M., Dellago, H., Harreither, E., Calle-Perez, A., Pircher, A., Gerstl, M. P., Pfeifenberger, S., Brandl, C., Sonntagbauer, M., Kriegner, A., Linder, A., Weinhäusel, A., Mohr, T., Steiger, M., Mattanovich, D., Rinnerthaler, M., … Grillari, J. (2015). Methylation of ribosomal RNA by NSUN5 is a conserved mechanism modulating organismal lifespan. *Nature Communications*, *6*. https://doi.org/10.1038/ncomms7158

Schwartz, S., Bernstein, D. A., Mumbach, M. R., Jovanovic, M., Herbst, R. H., León-Ricardo, B. X., Engreitz, J. M., Guttman, M., Satija, R., Lander, E. S., Fink, G., & Regev, A. (2014). Transcriptome-wide mapping reveals widespread dynamic-regulated pseudouridylation of ncRNA and mRNA. *Cell*, *159*(1), 148–162. https://doi.org/10.1016/j.cell.2014.08.028

Sekulski, K., Cruz, V. E., Weirich, C. S., & Erzberger, J. P. (2023). rRNA methylation by Spb1 regulates the GTPase activity of Nog2 during 60S ribosomal subunit assembly. *Nature Communications*, *14*(1), 1–11. https://doi.org/10.1038/s41467-023-36867-5

Selmi, T., Hussain, S., DIetmann, S., Heiß, M., Borland, K., Flad, S., Carter, J. M., Dennison, R., Huang, Y. L., Kellner, S., Bornelöv, S., & Frye, M. (2021). Sequence-And structure-specific cytosine-5 mRNA methylation by NSUN6. *Nucleic Acids Research*, *49*(2), 1006–1022. https://doi.org/10.1093/nar/gkaa1193

Sendinc, E., Valle-Garcia, D., Dhall, A., Chen, H., Henriques, T., Navarrete-Perea, J., Sheng, W., Gygi, S. P., Adelman, K., & Shi, Y. (2019). PCIF1 Catalyzes m6Am mRNA Methylation to Regulate Gene Expression. *Molecular Cell*, *75*(3), 620-630.e9. https://doi.org/10.1016/j.molcel.2019.05.030

Sepich-Poore, C., Zheng, Z., Schmitt, E., Wen, K., Zhang, Z. S., Cui, X. L., Dai, Q., hu, A. C., Zhang, L., Castillo, A. S., Tan, H., Peng, J., Zhuang, X., He, C., & Nachtergaele, S. (2022). The METTL5-TRMT112 N6-methyladenosine methyltransferase complex regulates mRNA translation via 18S rRNA methylation. *Journal of Biological Chemistry*, *298*(3), 101590. https://doi.org/10.1016/j.jbc.2022.101590

Sergiev, P. V., Serebryakova, M. V., Bogdanov, A. A., & Dontsova, O. A. (2008). The ybiN Gene of Escherichia coli Encodes Adenine-N6 Methyltransferase Specific for Modification of A1618 of 23 S Ribosomal RNA, a Methylated Residue Located Close to the Ribosomal Exit Tunnel. *Journal of Molecular Biology*, *375*(1), 291–300. https://doi.org/10.1016/j.jmb.2007.10.051

Shang, R., Lee, S., Senavirathne, G., & Lai, E. C. (2023). microRNAs in action: biogenesis, function and regulation. *Nature Reviews Genetics*, *24*(12), 816–833. https://doi.org/10.1038/s41576-023-00611-y

Sharma, S., Hartmann, J. D., Watzinger, P., Klepper, A., Peifer, C., Kötter, P., Lafontaine, D. L. J., & Entian, K. D. (2018). A single N1-methyladenosine on the large ribosomal subunit rRNA impacts locally its structure and the translation of key metabolic enzymes. *Scientific Reports*, *8*(1), 1–16. https://doi.org/10.1038/s41598-018-30383-z

Sharma, S., & Lafontaine, D. L. J. (2015). "View From A Bridge": A New Perspective on Eukaryotic rRNA Base Modification. *Trends in Biochemical Sciences*, *40*(10), 560–575. https://doi.org/10.1016/j.tibs.2015.07.008

Sharma, S., Langhendries, J. L., Watzinger, P., Kotter, P., Entian, K. D., & Lafontaine, D. L. J. (2015). Yeast Kre33 and human NAT10 are conserved 18S rRNA cytosine acetyltransferases that modify tRNAs assisted by the

adaptor Tan1/THUMPD1. *Nucleic Acids Research*, *43*(4), 2242–2258. https://doi.org/10.1093/nar/gkv075

Sharma, S., Marchand, V., Motorin, Y., & Lafontaine, D. L. J. (2017). Identification of sites of 2′-O-methylation vulnerability in human ribosomal RNAs by systematic mapping. *Scientific Reports*, *7*(1), 1–15. https://doi.org/10.1038/s41598-017-09734-9

Sharma, S., Watzinger, P., Kötter, P., & Entian, K. D. (2013). Identification of a novel methyltransferase, Bmt2, responsible for the N-1-methyl-adenosine base modification of 25S rRNA in Saccharomyces cerevisiae. *Nucleic Acids Research*, *41*(10), 5428–5443. https://doi.org/10.1093/nar/gkt195

Shatkin, A. J. (1974). Methylated messenger RNA synthesis in vitro by purified reovirus. *Proceedings of the National Academy of Sciences of the United States of America*, *71*(8), 3204–3207. https://doi.org/10.1073/pnas.71.8.3204

Shi, H., Wei, J., & He, C. (2019). Where, When, and How: Context-Dependent Functions of RNA Methylation Writers, Readers, and Erasers. *Molecular Cell*, *74*(4), 640–650. https://doi.org/10.1016/j.molcel.2019.04.025

Shu, X., Cao, J., Cheng, M., Xiang, S., Gao, M., Li, T., Ying, X., Wang, F., Yue, Y., Lu, Z., Dai, Q., Cui, X., Ma, L., Wang, Y., He, C., Feng, X., & Liu, J. (2020). A metabolic labeling method detects m6A transcriptome-wide at single base resolution. *Nature Chemical Biology*, *16*(8), 887–895. https://doi.org/10.1038/s41589-020-0526-9

Shubina, M. Y., Musinova, Y. R., & Sheval, E. V. (2016). Nucleolar methyltransferase fibrillarin: Evolution of structure and functions. *Biochemistry (Moscow)*, *81*(9), 941–950. https://doi.org/10.1134/S0006297916090030

Simabuco, F. M., Morello, L. G., Aragaão, A. Z. B., Leme, A. F. P., & Zanchin, N. I. T. (2012). Proteomic characterization of the human FTSJ3 preribosomal complexes. *Journal of Proteome Research*, *11*(6), 3112–3126. https://doi.org/10.1021/pr201106n

Sklias, A., Cruciani, S., Marchand, V., Spagnuolo, M., Lavergne, G., Bour, V., Brambilla, A., Dreos, R., Marygold, S. J., Novoa, E. M., Motorin, Y., & Roignant, J. (2024). Comprehensive map of ribosomal 2 -O-methylation and C / D box snoRNAs in Drosophila melanogaster. *Nucleic Acids Research*, 1–17. https://doi.org/10.1093/nar/gkae139

Sloan, K. E., Leisegang, M. S., Doebele, C., Ramírez, A. S., Simm, S., Safferthal, C., Kretschmer, J., Schorge, T., Markoutsa, S., Haag, S., Karas, M., Ebersberger, I., Schleiff, E., Watkins, N. J., & Bohnsack, M. T. (2015). The association of late-acting snoRNPs with human pre-ribosomal complexes requires the RNA helicase DDX21. *Nucleic Acids Research*, *43*(1), 553–564. https://doi.org/10.1093/nar/gku1291

Sloan, K. E., Warda, A. S., Sharma, S., Entian, K. D., Lafontaine, D. L. J., & Bohnsack, M. T. (2017). Tuning the ribosome: The influence of rRNA modification on eukaryotic ribosome biogenesis and function. *RNA Biology*, *14*(9), 1138–1152. https://doi.org/10.1080/15476286.2016.1259781

Smietanski, M., Werner, M., Purta, E., Kaminska, K. H., Stepinski, J., Darzynkiewicz, E., Nowotny, M., & Bujnicki, J. M. (2014). Structural analysis of human 2′-O-ribose methyltransferases involved in mRNA cap structure formation. *Nature Communications*, *5*, 1–10. https://doi.org/10.1038/ncomms4004

Squires, J. E., Patel, H. R., Nousch, M., Sibbritt, T., Humphreys, D. T., Parker, B. J., Suter, C. M., & Preiss, T. (2012). Widespread occurrence of 5-methylcytosine in human coding and non-coding RNA. *Nucleic Acids Research*, *40*(11), 5023–5033. https://doi.org/10.1093/nar/gks144

Starck, S. R., & Roberts, R. W. (2002). Puromycin oligonucleotides reveal steric restrictions for ribosome entry and multiple modes of translation inhibition. *Rna*, *8*(7), 890–903. https://doi.org/10.1017/S1355838202022069

Stein, K. C., Morales-Polanco, F., van der Lienden, J., Rainbolt, T. K., & Frydman, J. (2022). Ageing exacerbates ribosome pausing to disrupt cotranslational proteostasis. *Nature*, *601*(7894), 637–642. https://doi.org/10.1038/s41586-021-04295-4

Stern, L., & Schulman, L. H. (1978). The role of the minor base N4-acetylcytidine in the function of the Escherichia coli

noninitiator methionine transfer RNA. *Journal of Biological Chemistry*, *253*(17), 6132–6139. https://doi.org/10.1016/s0021-9258(17)34590-8

Strauss, R., & Pichler, J. (1998). Persistence of orientation toward a temporarily invisible landmark in Drosophila melanogaster. *Journal of Comparative Physiology - A Sensory, Neural, and Behavioral Physiology*, *182*(4), 411–423. https://doi.org/10.1007/s003590050190

Strauss, Roland. (2002). The central complex and the genetic dissection of locomotor behaviour. *Current Opinion in Neurobiology*, *12*(6), 633–638. https://doi.org/10.1016/S0959-4388(02)00385-9

Su, R., Dong, L., Li, Y., Gao, M., He, P. C., Liu, W., Wei, J., Zhao, Z., Gao, L., Han, L., Deng, X., Li, C., Prince, E., Tan, B., Qing, Y., Qin, X., Shen, C., Xue, M., Zhou, K., … Chen, J. (2022). METTL16 exerts an m6A-independent function to facilitate translation and tumorigenesis. In *Nature Cell Biology* (Vol. 24, Issue 2). Springer US. https://doi.org/10.1038/s41556-021-00835-2

Sun, L., Fazal, F. M., Li, P., Broughton, J. P., Lee, B., Tang, L., Huang, W., Kool, E. T., Chang, H. Y., & Zhang, Q. C. (2019). RNA structure maps across mammalian cellular compartments. *Nature Structural and Molecular Biology*, *26*(4), 322–330. https://doi.org/10.1038/s41594-019-0200-7

Suzuki, T., & Suzuki, T. (2014). *A complete landscape of post-transcriptional modifications in mammalian mitochondrial tRNAs*. *42*(11), 7346–7357. https://doi.org/10.1093/nar/gku390

Suzuki, T., Yashiro, Y., Kikuchi, I., Ishigami, Y., Saito, H., Matsuzawa, I., Okada, S., Mito, M., Iwasaki, S., Ma, D., Zhao, X., Asano, K., Lin, H., Kirino, Y., Sakaguchi, Y., & Suzuki, T. (2020). Complete chemical structures of human mitochondrial tRNAs. *Nature Communications*, *11*(1), 1–15. https://doi.org/10.1038/s41467-020-18068-6

Taoka, M., Nobe, Y., Hori, M., Takeuchi, A., Masaki, S., Yamauchi, Y., Nakayama, H., Takahashi, N., & Isobe, T. (2015). A mass spectrometry-based method for comprehensive quantitative determination of post-transcriptional RNA modifications: The complete chemical structure of Schizosaccharomyces pombe ribosomal RNAs. *Nucleic Acids Research*, *43*(18). https://doi.org/10.1093/nar/gkv560

Taoka, M., Nobe, Y., Yamaki, Y., Sato, K., Ishikawa, H., Izumikawa, K., Yamauchi, Y., Hirota, K., Nakayama, H., Takahashi, N., & Isobe, T. (2018). Landscape of the complete RNA chemical modifications in the human 80S ribosome. *Nucleic Acids Research*, *46*(18), 9289–9298. https://doi.org/10.1093/nar/gky811

Tessarz, P., Santos-Rosa, H., Robson, S. C., Sylvestersen, K. B., Nelson, C. J., Nielsen, M. L., & Kouzarides, T. (2014). Glutamine methylation in histone H2A is an RNA-polymerase-I-dedicated modification. *Nature*, *505*(7484), 564–568. https://doi.org/10.1038/nature12819

Thompson, J., Schmidt, F., & Cundliffe, E. (1982). Site of action of a ribosomal RNA methylase conferring resistance to thiostrepton. *Journal of Biological Chemistry*, *257*(14), 7915–7917. https://doi.org/10.1016/s0021-9258(18)34268-6

Thüring, K., Schmid, K., Keller, P., & Helm, M. (2017). *RNA Methylation (book) Chapter I: LC-MS analysis of methylated RNA* (Vol. 1562). http://link.springer.com/10.1007/978-1-4939-6807-7

Thurmond, J., Goodman, J. L., Strelets, V. B., Attrill, H., Gramates, L. S., Marygold, S. J., Matthews, B. B., Millburn, G., Antonazzo, G., Trovisco, V., Kaufman, T. C., Calvi, B. R., Perrimon, N., Gelbart, S. R., Agapite, J., Broll, K., Crosby, L., Dos Santos, G., Emmert, D., … Baker, P. (2019). FlyBase 2.0: The next generation. *Nucleic Acids Research*, *47*(D1), D759–D765. https://doi.org/10.1093/nar/gky1003

Tian, B., Pan, Z., & Ju, Y. L. (2007). Widespread mRNA polyadenylation events in introns indicate dynamic interplay between polyadenylation and splicing. *Genome Research*, *17*(2), 156–165. https://doi.org/10.1101/gr.5532707

Tissot, M., & Stocker, R. F. (2000). Metamorphosis in Drosophila and other insects: The fate of neurons throughout the stages. *Progress in Neurobiology*, *62*(1), 89–111. https://doi.org/10.1016/S0301-0082(99)00069-6

Tkaczuk, K. L. (2010). Trm13p, the tRNA:Xm4 modification

enzyme from Saccharomyces cerevisiae is a member of the Rossmann-fold MTase superfamily: Prediction of structure and active site. *Journal of Molecular Modeling*, *16*(3), 599–606. https://doi.org/10.1007/s00894-009-0570-6

Torun, D., Arslan, M., Çavdarlı, B., Akar, H., & Cram, D. S. (2022). Three Afghani siblings with a novel homozygous variant and further delineation of the clinical features of METTL5 related intellectual disability syndrome. *Turkish Journal of Pediatrics*, *64*(5), 956–963. https://doi.org/10.24953/turkjped.2020.3992

Tuorto, F., Liebers, R., Musch, T., Schaefer, M., Hofmann, S., Kellner, S., Frye, M., Helm, M., Stoecklin, G., & Lyko, F. (2012). RNA cytosine methylation by Dnmt2 and NSun2 promotes tRNA stability and protein synthesis. *Nature Structural and Molecular Biology*, *19*(9), 900–905. https://doi.org/10.1038/nsmb.2357

Urbonavičius, J., Droogmans, L., Armengaud, J., & Grosjean, H. (2009). Deciphering the complex enzymatic pathway for biosynthesis of wyosine derivatives in anticodon of tRNAPhe - Madame Curie Bioscience Database - NCBI Bookshelf. *DNA and RNA Modification Enzymes: Structure, Mechanism, Function and Evolution*, *January*. https://www.ncbi.nlm.nih.gov/books/NBK6080/

Urbonavičius, J., Durand, J. M. B., & Björk, G. R. (2002). Three modifications in the D and T arms of tRNA influence translation in Escherichia coli and expression of virulence genes in Shigella flexneri. *Journal of Bacteriology*, *184*(19), 5348–5357. https://doi.org/10.1128/JB.184.19.5348-5357.2002

Van Tran, N., Ernst, F. G. M., Hawley, B. R., Zorbas, C., Ulryck, N., Hackert, P., Bohnsack, K. E., Bohnsack, M. T., Jaffrey, S. R., Graille, M., & Lafontaine, D. L. J. (2019). The human 18S rRNA m6A methyltransferase METTL5 is stabilized by TRMT112. *Nucleic Acids Research*, *47*(15), 7719–7733. https://doi.org/10.1093/nar/gkz619

Vilardo, E., Amman, F., Toth, U., Kotter, A., Helm, M., & Rossmanith, W. (2021). Functional characterization of the human tRNA methyltransferases TRMT10A and TRMT10B. *Nucleic Acids Research*, *48*(11), 6157–6169. https://doi.org/10.1093/NAR/GKAA353

Vilardo, E., Nachbagauer, C., Buzet, A., Taschner, A., Holzmann, J., & Rossmanith, W. (2018). Erratum: A subcomplex of human mitochondrial RNase P is a bifunctional methyltransferase - extensive moonlighting in mitochondrial tRNA biogenesis (Nucleic Acids Research 40:22 (11583-11593) DOI: 10.1093/nar/gks910). *Nucleic Acids Research*, *46*(20), 11126–11127. https://doi.org/10.1093/nar/gky931

Vilfan, I. D., Tsai, Y. C., Clark, T. A., Wegener, J., Dai, Q., Yi, C., Pan, T., Turner, S. W., & Korlach, J. (2013). Analysis of RNA base modification and structural rearrangement by single-molecule real-time detection of reverse transcription. *Journal of Nanobiotechnology*, *11*(1), 1. https://doi.org/10.1186/1477-3155-11-8

Vold, B. (1976). Modified nucleosides of Bacillus subtilis transfer ribonucleic acids. *Journal of Bacteriology*, *127*(1), 258–267. https://doi.org/10.1128/jb.127.1.258-267.1976

Waas, W. F., Druzina, Z., Hanan, M., & Schimmel, P. (2007). Role of a tRNA base modification and its precursors in frameshifting in eukaryotes. *Journal of Biological Chemistry*, *282*(36), 26026–26034. https://doi.org/10.1074/jbc.M703391200

Wang, H., Deng, Q., Lv, Z., Ling, Y., Hou, X., Chen, Z., Dinglin, X., Ma, S., Li, D., Wu, Y., Peng, Y., Huang, H., & Chen, L. (2019). N6-methyladenosine induced miR-143-3p promotes the brain metastasis of lung cancer via regulation of VASH1. *Molecular Cancer*, *18*(1), 1–17. https://doi.org/10.1186/s12943-019-1108-x

Wang, L., Liang, Y., Lin, R., Xiong, Q., Yu, P., Ma, J., Cheng, M., Han, H., Wang, X., Wang, G., Liang, F., Pei, Z., Chen, D., Yuan, Q., Jiang, Y. Z., & Lin, S. (2020). Mettl5 mediated 18S rRNA N6-methyladenosine (m6A) modification controls stem cell fate determination and neural function. *Genes and Diseases*, *9*(1), 268–274. https://doi.org/10.1016/j.gendis.2020.07.004

Wang, S., Lv, W., Li, T., Zhang, S., Wang, H., Li, X., Wang, L., Ma, D., Zang, Y., Shen, J., Xu, Y., & Wei, W. (2022). Dynamic regulation and functions of mRNA m6A modification. *Cancer Cell International*, *22*(1), 1–12.

https://doi.org/10.1186/s12935-022-02452-x

Wang, Xiang, Feng, J., Xue, Y., Guan, Z., Zhang, D., Liu, Z., Gong, Z., Wang, Q., Huang, J., Tang, C., Zou, T., & Yin, P. (2016). Structural basis of N6-adenosine methylation by the METTL3-METTL14 complex. *Nature*, *534*(7608), 575–578. https://doi.org/10.1038/nature18298

Wang, Xiao, Lu, Z., Gomez, A., Hon, G. C., Yue, Y., Han, D., Fu, Y., Parisien, M., Dai, Q., Jia, G., Ren, B., Pan, T., & He, C. (2014). N 6-methyladenosine-dependent regulation of messenger RNA stability. *Nature*, *505*(7481), 117–120. https://doi.org/10.1038/nature12730

Wang, Y., Xiao, Y., Dong, S., Yu, Q., & Jia, G. (2020). Antibody-free enzyme-assisted chemical approach for detection of N 6-methyladenosine. *Nature Chemical Biology*, *16*(8), 896–903. https://doi.org/10.1038/s41589-020-0525-x

Wang, Z. W., Pan, J. J., Hu, J. F., Zhang, J. Q., Huang, L., Huang, Y., Liao, C. Y., Yang, C., Chen, Z. W., Wang, Y. D., Shen, B. Y., Tian, Y. F., & Chen, S. (2022). SRSF3-mediated regulation of N6-methyladenosine modification-related lncRNA ANRIL splicing promotes resistance of pancreatic cancer to gemcitabine. *Cell Reports*, *39*(6), 110813. https://doi.org/10.1016/j.celrep.2022.110813

Warda, A. S., Kretschmer, J., Hackert, P., Lenz, C., Urlaub, H., Höbartner, C., Sloan, K. E., & Bohnsack, M. T. (2017). Human METTL16 is a N 6 -methyladenosine (m 6 A) methyltransferase that targets pre-mRNAs and various non-coding RNAs . *EMBO Reports*, *18*(11), 2004–2014. https://doi.org/10.15252/embr.201744940

Watabe, E., Togo-Ohno, M., Ishigami, Y., Wani, S., Hirota, K., Kimura-Asami, M., Hasan, S., Takei, S., Fukamizu, A., Suzuki, Y., Suzuki, T., & Kuroyanagi, H. (2021). m 6 A-mediated alternative splicing coupled with nonsense-mediated mRNA decay regulates SAM synthetase homeostasis . *The EMBO Journal*, *40*(14), 1–19. https://doi.org/10.15252/embj.2020106434

Watanabe, K., Nureki, O., Fukai, S., Endo, Y., & Hori, H. (2006). Functional categorization of the conserved basic amino acid residues in TrmH (tRNA (Gm18) methyltansferase) enzymes. *Journal of Biological Chemistry*, *281*(45), 34630–34639. https://doi.org/10.1074/jbc.M606141200

Watkins, N. J., & Bohnsack, M. T. (2012). The box C/D and H/ACA snoRNPs: Key players in the modification, processing and the dynamic folding of ribosomal RNA. *Wiley Interdisciplinary Reviews: RNA*, *3*(3), 397–414. https://doi.org/10.1002/wrna.117

Wei, J., Liu, F., Lu, Z., Fei, Q., Ai, Y., He, P. C., Shi, H., Cui, X., Su, R., Klungland, A., Jia, G., Chen, J., & He, C. (2018). Differential m 6 A, m 6 A m , and m 1 A Demethylation Mediated by FTO in the Cell Nucleus and Cytoplasm. *Molecular Cell*, *71*(6), 973-985.e5. https://doi.org/10.1016/j.molcel.2018.08.011

Weiß, A. L., Meijer, M., Budeus, B., Pauper, M., Hakobjan, M., Groothuismink, J., Shi, Y., Neveling, K., Buitelaar, J. K., Hoogman, M., Franke, B., & Klein, M. (2021). DNA methylation associated with persistent ADHD suggests TARBP1 as novel candidate. *Neuropharmacology*, *184*(October 2020). https://doi.org/10.1016/j.neuropharm.2020.108370

Wen, S., Wei, Y., Zen, C., Xiong, W., Niu, Y., & Zhao, Y. (2020). Long non-coding RNA NEAT1 promotes bone metastasis of prostate cancer through N6-methyladenosine. *Molecular Cancer*, *19*(1), 1–18. https://doi.org/10.1186/s12943-020-01293-4

White, B. N. (1975). Studies on lysine, glutamine and glutamic acid tRNAs from Drosophila. *Biochimica et Biophysica Acta (BBA) - Nucleic Acids and Protein Synthesis*, *395*(3), 322–328. https://doi.org/10.1016/0005-2787(75)90203-8

White, J., Li, Z., Sardana, R., Bujnicki, J. M., Marcotte, E. M., & Johnson, A. W. (2008). Bud23 Methylates G1575 of 18S rRNA and Is Required for Efficient Nuclear Export of Pre-40S Subunits. *Molecular and Cellular Biology*, *28*(10), 3151–3161. https://doi.org/10.1128/mcb.01674-07

Wilkinson, M. L., Crary, S. M., Jackman, J. E., Grayhack, E. J., & Phizicky, E. M. (2007). The 2′-O-methyltransferase responsible for modification of yeast tRNA at position 4. *Rna*, *13*(3), 404–413. https://doi.org/10.1261/rna.399607

Worpenberg, L., Jakobi, T., Dieterich, C., & Roignant, J.

(2019). Epitranscriptomics Book chapter 3: Identification of Methylated Transcripts Using the TRIBE Approach. In *Methods in Molecular Biology*. http://link.springer.com/10.1007/978-1-4939-8808-2

Worpenberg, L., Paolantoni, C., Longhi, S., Mulorz, M. M., Lence, T., Wessels, H., Dassi, E., Aiello, G., Sutandy, F. X. R., Scheibe, M., Edupuganti, R. R., Busch, A., Möckel, M. M., Vermeulen, M., Butter, F., König, J., Notarangelo, M., Ohler, U., Dieterich, C., … Roignant, J. (2021). Ythdf is a N6-methyladenosine reader that modulates Fmr1 target mRNA selection and restricts axonal growth in Drosophila . *The EMBO Journal*, *40*(4), 1–20. https://doi.org/10.15252/embj.2020104975

Wu-Baer, F., Lane, W. S., & Gaynor, R. B. (1996). Identification of a group of cellular cofactors that stimulate the binding of RNA polymerase II and TRP-185 to human immunodeficiency virus 1 TAR RNA. *Journal of Biological Chemistry*, *271*(8), 4201–4208. https://doi.org/10.1074/jbc.271.8.4201

Wu, G., Xiao, M., Yang, C., & Yu, Y. T. (2011). U2 snRNA is inducibly pseudouridylated at novel sites by Pus7p and snR81 RNP. *EMBO Journal*, *30*(1), 79–89. https://doi.org/10.1038/emboj.2010.316

Wu, H., Min, J., Zeng, H., & Plotnikov, A. N. (2008). Crystal structure of the methyltransferase domain of human TARBP1. *Proteins: Structure, Function and Genetics*, *72*(1), 519–525. https://doi.org/10.1002/prot.22065

Wu, Y., Yang, X., Chen, Z., Tian, L., Jiang, G., Chen, F., Li, J., An, P., Lu, L., Luo, N., Du, J., Shan, H., Liu, H., & Wang, H. (2019). M 6 A-induced lncRNA RP11 triggers the dissemination of colorectal cancer cells via upregulation of Zeb1. *Molecular Cancer*, *18*(1), 1–16. https://doi.org/10.1186/s12943-019-1014-2

Wurm, J. P., Meyer, B., Bahr, U., Held, M., Frolow, O., Kötter, P., Engels, J. W., Heckel, A., Karas, M., Entian, K. D., & Wöhnert, J. (2010). The ribosome assembly factor Nep1 responsible for Bowen-Conradi syndrome is a pseudouridine-N1-specific methyltransferase. *Nucleic Acids Research*, *38*(7), 2387–2398. https://doi.org/10.1093/nar/gkp1189

Xia, P., Zhang, H., Lu, H., Xu, K., Jiang, X., Jiang, Y., Gongye, X., Chen, Z., Liu, J., Chen, X., Ma, W., Zhang, Z., & Yuan, Y. (2023). METTL5 stabilizes c-Myc by facilitating USP5 translation to reprogram glucose metabolism and promote hepatocellular carcinoma progression. *Cancer Communications*, *43*(3), 338–364. https://doi.org/10.1002/cac2.12403

Xiao, W., Adhikari, S., Dahal, U., Chen, Y. S., Hao, Y. J., Sun, B. F., Sun, H. Y., Li, A., Ping, X. L., Lai, W. Y., Wang, X., Ma, H. L., Huang, C. M., Yang, Y., Huang, N., Jiang, G. Bin, Wang, H. L., Zhou, Q., Wang, X. J., … Yang, Y. G. (2016). Nuclear m6A Reader YTHDC1 Regulates mRNA Splicing. *Molecular Cell*, *61*(4), 507–519. https://doi.org/10.1016/j.molcel.2016.01.012

Xiao, Y. L., Liu, S., Ge, R., Wu, Y., He, C., Chen, M., & Tang, W. (2023). Transcriptome-wide profiling and quantification of N 6-methyladenosine by enzyme-assisted adenosine deamination. *Nature Biotechnology*, *41*(7), 993–1003. https://doi.org/10.1038/s41587-022-01587-6

Xiao, Y., Wang, Y., Tang, Q., Wei, L., Zhang, X., & Jia, G. (2018). An Elongation- and Ligation-Based qPCR Amplification Method for the Radiolabeling-Free Detection of Locus-Specific N6-Methyladenosine Modification. *Angewandte Chemie - International Edition*, *57*(49), 15995–16000. https://doi.org/10.1002/anie.201807942

Xing, M., Liu, Q., Mao, C., Zeng, H., Zhang, X., Zhao, S., Chen, L., Liu, M., Shen, B., Guo, X., Ma, H., Chen, H., & Zhang, J. (2020). The 18S rRNA m 6 A methyltransferase METTL 5 promotes mouse embryonic stem cell differentiation . *EMBO Reports*, *21*(10), 1–15. https://doi.org/10.15252/embr.201949863

Xu, Liu, & Seki, M. (2020). Recent advances in the detection of base modifications using the Nanopore sequencer. *Journal of Human Genetics*, *65*(1), 25–33. https://doi.org/10.1038/s10038-019-0679-0

Xu, Luang, Liu, X., Sheng, N., Oo, K. S., Liang, J., Chionh, Y. H., Xu, J., Ye, F., Gao, Y. G., Dedon, P. C., & Fu, X. Y. (2017). Three distinct 3-methylcytidine (m3C) methyltransferases modify tRNA and mRNA in mice and humans. *Journal of Biological Chemistry*, *292*(35), 14695–14703. https://doi.org/10.1074/jbc.M117.798298

Yan, L. L., & Zaher, H. S. (2019). How do cells cope with RNA damage and its consequences? *Journal of Biological Chemistry*, *294*(41), 15158–15171. https://doi.org/10.1074/jbc.REV119.006513

Yang, J., Sharma, S., Watzinger, P., Hartmann, J. D., Kötter, P., & Entian, K. D. (2016). Mapping of complete set of ribose and base modifications of yeast rRNA by RP-HPLC and mung bean nuclease assay. *PLoS ONE*, *11*(12), 1–18. https://doi.org/10.1371/journal.pone.0168873

Yang, Xiao, Zhang, S., He, C., Xue, P., Zhang, L., He, Z., Zang, L., Feng, B., Sun, J., & Zheng, M. (2020). METTL14 suppresses proliferation and metastasis of colorectal cancer by down-regulating oncogenic long non-coding RNA XIST. *Molecular Cancer*, *19*(1), 1–16. https://doi.org/10.1186/s12943-020-1146-4

Yang, Xin, Yang, Y., Sun, B. F., Chen, Y. S., Xu, J. W., Lai, W. Y., Li, A., Wang, X., Bhattarai, D. P., Xiao, W., Sun, H. Y., Zhu, Q., Ma, H. L., Adhikari, S., Sun, M., Hao, Y. J., Zhang, B., Huang, C. M., Huang, N., … Yang, Y. G. (2017). 5-methylcytosine promotes mRNA export-NSUN2 as the methyltransferase and ALYREF as an m 5 C reader. *Cell Research*, *27*(5), 606–625. https://doi.org/10.1038/cr.2017.55

Yang, Y., Fan, X., Mao, M., Song, X., Wu, P., Zhang, Y., Jin, Y., Yang, Y., Chen, L. L., Wang, Y., Wong, C. C. L., Xiao, X., & Wang, Z. (2017). Extensive translation of circular RNAs driven by N 6 -methyladenosine. *Cell Research*, *27*(5), 626–641. https://doi.org/10.1038/cr.2017.31

Yang, Z., Lin, J., & Ye, K. (2016). Box C/D guide RNAs recognize a maximum of 10 nt of substrates. *Proceedings of the National Academy of Sciences of the United States of America*, *113*(39), 10878–10883. https://doi.org/10.1073/pnas.1604872113

Yang, Z., Wang, J., Huang, L., Lilley, D. M. J., & Ye, K. (2020). Functional organization of box C/D RNA-guided RNA methyltransferase. *Nucleic Acids Research*, *48*(9), 5094–5105. https://doi.org/10.1093/nar/gkaa247

Yin, H., Chen, L., Piao, S., Wang, Y., Li, Z., Lin, Y., Tang, X., Zhang, H., Zhang, H., & Wang, X. (2023). M6A RNA methylation-mediated RMRP stability renders proliferation and progression of non-small cell lung cancer through regulating TGFBR1/SMAD2/SMAD3 pathway. *Cell Death and Differentiation*, *30*(3), 605–617. https://doi.org/10.1038/s41418-021-00888-8

Yu, C. T., & Allen, F. W. (1959). Studies of an isomer of uridine isolated from ribonucleic acids. *BBA - Biochimica et Biophysica Acta*, *32*(C), 393–406. https://doi.org/10.1016/0006-3002(59)90612-2

Yu, Y. T., Shu, M. Di, & Steitz, J. A. (1998). Modifications of U2 snRNA are required for snRNP assembly and pre-mRNA splicing. *EMBO Journal*, *17*(19), 5783–5795. https://doi.org/10.1093/emboj/17.19.5783

Zaccara, S., & Jaffrey, S. R. (2020). A Unified Model for the Function of YTHDF Proteins in Regulating m6A-Modified mRNA. *Cell*, *181*(7), 1582–1595. https://doi.org/10.1016/j.cell.2020.05.012.A

Zachau, H. G., Diitting, D., & Fieldmann, H. (1966). The structures of two serine transfer ribonucleic acids. *Hoppe-Seyler's Zeitschrift Fur Physiologische Chemie*, *347*(1), 212–235. https://doi.org/10.1515/bchm2.1966.347.1.212

Zeng, X., Zhao, F., Cui, G., Zhang, Y., Deshpande, R. A., Chen, Y., Deng, M., Kloeber, J. A., Shi, Y., Zhou, Q., Zhang, C., Hou, J., Kim, W., Tu, X., Yan, Y., Xu, Z., Chen, L., Gao, H., Guo, G., … Lou, Z. (2022). METTL16 antagonizes MRE11-mediated DNA end resection and confers synthetic lethality to PARP inhibition in pancreatic ductal adenocarcinoma. *Nature Cancer*, *3*(9), 1088–1104. https://doi.org/10.1038/s43018-022-00429-3

Zhang, Feiran, Kang, Y., Wang, M., Li, Y., Xu, T., Yang, W., Song, H., Wu, H., Shu, Q., & Jin, P. (2018). Fragile X mental retardation protein modulates the stability of its m6A-marked messenger RNA targets. *Human Molecular Genetics*, *27*(22), 3936–3950. https://doi.org/10.1093/hmg/ddy292

Zhang, Feng, Yoon, K., Zhang, D. Y., Kim, N. S., Ming, G. li, & Song, H. (2023). Epitranscriptomic regulation of cortical neurogenesis via Mettl8-dependent mitochondrial tRNA m3C modification. *Cell Stem Cell*, *30*(3), 300-311.e11. https://doi.org/10.1016/j.stem.2023.01.007

Zhang, L. S., Liu, C., Ma, H., Dai, Q., Sun, H. L., Luo, G., Zhang, Z., Zhang, L., Hu, L., Dong, X., & He, C. (2019).

Transcriptome-wide Mapping of Internal N7-Methylguanosine Methylome in Mammalian mRNA. *Molecular Cell*, *74*(6), 1304-1316.e8. https://doi.org/10.1016/j.molcel.2019.03.036

Zhang, P., Huang, J., Zheng, W., Chen, L., Liu, S., Liu, A., Ye, J., Zhou, J., Chen, Z., Huang, Q., Liu, S., Zhou, K., Qu, L., Li, B., & Yang, J. (2023). Single-base resolution mapping of 2′-O-methylation sites by an exoribonuclease-enriched chemical method. *Science China Life Sciences*, *66*(4), 800–818. https://doi.org/10.1007/s11427-022-2210-0

Zhang, Z., Chen, L., Zhao, Y., Yang, C., Ian, A., Zhang, Z., Ren, J., Xie, W., & He, C. (2019). Single-base mapping of m 6 A by an antibody-independent method. *Science Advances*, *5*(7).

Zheng, G., Dahl, J. A., Niu, Y., Fedorcsak, P., Huang, C. M., Li, C. J., Vågbø, C. B., Shi, Y., Wang, W. L., Song, S. H., Lu, Z., Bosmans, R. P. G., Dai, Q., Hao, Y. J., Yang, X., Zhao, W. M., Tong, W. M., Wang, X. J., Bogdan, F., … He, C. (2013). ALKBH5 Is a Mammalian RNA Demethylase that Impacts RNA Metabolism and Mouse Fertility. *Molecular Cell*, *49*(1), 18–29. https://doi.org/10.1016/j.molcel.2012.10.015

Zhou, C., Molinie, B., Daneshvar, K., Pondick, J. V., Wang, J., Van Wittenberghe, N., Xing, Y., Giallourakis, C. C., & Mullen, A. C. (2017). Genome-Wide Maps of m6A circRNAs Identify Widespread and Cell-Type-Specific Methylation Patterns that Are Distinct from mRNAs. *Cell Reports*, *20*(9), 2262–2276. https://doi.org/10.1016/j.celrep.2017.08.027

Zhou, F., Liu, Y., Rohde, C., Pauli, C., Gerloff, D., Köhn, M., Misiak, D., Bäumer, N., Cui, C., Göllner, S., Oellerich, T., Serve, H., Garcia-Cuellar, M. P., Slany, R., Maciejewski, J. P., Przychodzen, B., Seliger, B., Klein, H. U., Bartenhagen, C., … Müller-Tidow, C. (2017). AML1-ETO requires enhanced C/D box snoRNA/RNP formation to induce self-renewal and leukaemia. *Nature Cell Biology*, *19*(7), 844–855. https://doi.org/10.1038/ncb3563

Zhu, Y., Pirnie, S. P., & Carmichael, G. G. (2017). High-throughput and site-specific identification of 2′-O-methylation sites using ribose oxidation sequencing (RibOxi-seq). *Rna*, *23*(8), 1303–1314. https://doi.org/10.1261/rna.061549.117

Zorbas, C., Nicolas, E., Wacheul, L., Huvelle, E., Heurgué-Hamard, V., & Lafontaine, D. L. J. (2015). The human 18S rRNA base methyltransferases DIMT1L and WBSCR22-TRMT112 but not rRNA modification are required for ribosome biogenesis. *Molecular Biology of the Cell*, *26*(11), 2080–2095. https://doi.org/10.1091/mbc.E15-02-0073

Züst, R., Cervantes-Barragan, L., Habjan, M., Maier, R., Neuman, B. W., Ziebuhr, J., Szretter, K. J., Baker, S. C., Barchet, W., Diamond, M. S., Siddell, S. G., Ludewig, B., & Thiel, V. (2011). Ribose 2′-O-methylation provides a molecular signature for the distinction of self and non-self mRNA dependent on the RNA sensor Mda5. *Nature Immunology*, *12*(2), 137–143. https://doi.org/10.1038/ni.1979

10. Appendix Research article

Leismann J*, Spagnuolo M*, Pradhan M, Wacheul L, Vu MA, Musheev M, Mier P, Andrade-Navarro MA, Graille M, Niehrs C, Lafontaine DL, Roignant JY. The 18S ribosomal RNA m6 A methyltransferase Mettl5 is required for normal walking behavior in Drosophila. EMBO Rep. 2020 Jul 3;21(7):e49443. doi: 10.15252/embr.201949443. Epub 2020 Apr 29. PMID: 32350990; PMCID: PMC7332798.

*Contributed equally

Report

TRANSPARENT PROCESS

EMBO reports

The 18S ribosomal RNA m^{6}A methyltransferase Mettl5 is required for normal walking behavior in *Drosophila*

Jessica Leismann[1,†], Mariangela Spagnuolo[1,†], Mihika Pradhan[1], Ludivine Wacheul[2], Minh Anh Vu[1], Michael Musheev[1], Pablo Mier[3], Miguel A Andrade-Navarro[3], Marc Graille[4], Christof Niehrs[1,5], Denis LJ Lafontaine[2,*] & Jean-Yves Roignant[1,6,**]

Abstract

RNA modifications have recently emerged as an important layer of gene regulation. N6-methyladenosine (m^{6}A) is the most prominent modification on eukaryotic messenger RNA and has also been found on noncoding RNA, including ribosomal and small nuclear RNA. Recently, several m^{6}A methyltransferases were identified, uncovering the specificity of m^{6}A deposition by structurally distinct enzymes. In order to discover additional m^{6}A enzymes, we performed an RNAi screen to deplete annotated orthologs of human methyltransferase-like proteins (METTLs) in *Drosophila* cells and identified CG9666, the ortholog of human METTL5. We show that CG9666 is required for specific deposition of m^{6}A on 18S ribosomal RNA via direct interaction with the *Drosophila* ortholog of human TRMT112, CG12975. Depletion of CG9666 yields a subsequent loss of the 18S rRNA m^{6}A modification, which lies in the vicinity of the ribosome decoding center; however, this does not compromise rRNA maturation. Instead, a loss of CG9666-mediated m^{6}A impacts fly behavior, providing an underlying molecular mechanism for the reported human phenotype in intellectual disability. Thus, our work expands the repertoire of m^{6}A methyltransferases, demonstrates the specialization of these enzymes, and further addresses the significance of ribosomal RNA modifications in gene expression and animal behavior.

Keywords behavior; *Drosophila*; m^{6}A; Mettl5; ribosome; RNA methyltransferase

Subject Categories Neuroscience; Post-translational Modifications & Proteolysis; RNA Biology

DOI 10.15252/embr.201949443 | Received 8 October 2019 | Revised 2 April 2020 | Accepted 7 April 2020

EMBO Reports (2020) e49443

Introduction

N6-methyladenosine (m^{6}A) was discovered on mammalian mRNA in the last seventies [1,2]. The recent development of transcriptome-wide modification mapping approaches and identification of the m^{6}A mRNA machinery sparked new interest in the field. Mapping approaches revealed the prevalence of m^{6}A within thousands of mRNAs and long noncoding RNAs (lncRNAs) [3,4], while genetic manipulation of m^{6}A players revealed its diverse roles in development and diseases through regulation of mRNA fate [5].

Deposition of m^{6}A is catalyzed by a subfamily of methyltransferases characterized by the conserved catalytic motif [D/N/S/H]PP [Y/F/W] [6]. In mRNA, the methylation is installed on adenosine within a conserved consensus sequence context, DRACH (where D = A/G/U, R = A/G and H = A/C/U), by a multi-subunit methyltransferase complex. In mammals, methyltransferase-like 3 (METTL3) is the catalytic subunit and forms a stable heterodimer with METTL14, which facilitates binding to mRNA substrates [7–9]. The role of other subunits, which include Wilms tumor 1-associated protein (WTAP), Vir-like m^{6}A methyltransferase associated (VIRMA) [10], RNA binding motif 15 (RBM15) [11], Zinc-finger CCH domain-containing protein (ZC3H13) [12–14], and HAKAI [10,15], is less understood. This complex is highly conserved from insects to mammals but is only partially present in the yeast *Saccharomyces cerevisiae* and absent in the worm *Caenorhabditis elegans* [16–18].

In addition to its well-characterized occurrence on mRNA, m^{6}A is also known to occur on circular RNAs, small nuclear RNAs (snRNAs), microRNAs (miRNAs), long noncoding RNAs (lncRNAs), and ribosomal RNAs (rRNAs), whereas its presence on transfer RNAs (tRNAs) was only reported in bacteria so far [18]. Recent

1 Institute of Molecular Biology (IMB), Mainz, Germany
2 RNA Molecular Biology, ULB Cancer Research Center (U-CRC), Centre for Microscopy and Molecular Imaging (CMMI), Fonds de la Recherche Scientifique (F.R.S.-FNRS), Université Libre de Bruxelles (ULB), Charleroi-Gosselies, Belgium
3 Faculty of Biology, Johannes-Gutenberg Universität Mainz, Mainz, Germany
4 BIOC, CNRS, Ecole Polytechnique, IP Paris, Palaiseau, France
5 Division of Molecular Embryology, DKFZ-ZMBH Alliance, Heidelberg, Germany
6 Center for Integrative Genomics, Faculty of Biology and Medicine, University of Lausanne, Lausanne, Switzerland
*Corresponding author. Tel: +32 2650 9771; E-mail: denis.lafontaine@ulb.ac.be
**Corresponding author. Tel: +41 21 692 3965; E-mail: jean-yves.roignant@unil.ch
†These authors contributed equally to this work

reports found that METTL16 binds a subset of mRNAs and adds m^6A on *MAT2A* transcripts, as well as on U6 snRNA [19–22]. In contrast, m^6A deposition on rRNA is less understood. rRNAs are the second most heavily modified class of RNAs, after tRNAs, with ~ 2% of rRNA nucleotides bearing post-transcriptional modifications [23]. 2′-*O*-methylation of the sugar backbone and pseudouridylation are the most abundant modifications, while base modifications represent only about 5% of total rRNA modifications in yeast and humans [24]. Among these, m^6A is reported to be present on human 18S and 28S rRNA at positions 1832 and 4220, respectively [25]. In a recent report, ZCCHC4 was shown to generate m^6A on the 28S rRNA; impacting ribosome subunit distribution, global translation, and cancer cell proliferation [26]. This study, along with others [27–30], demonstrated that base modifications on rRNA may play important roles in gene expression.

In order to identify additional m^6A methyltransferases, we carried out a screen in *Drosophila* S2R + cells, in which we knocked down all annotated orthologs of human methyltransferase-like proteins (METTLs) and assessed the effect on global m^6A levels on total and messenger RNAs. Our screen identified the previously uncharacterized *Drosophila* gene: *CG9666*, the ortholog of *METTL5*. We show that CG9666 contains the conserved catalytic "asparagine-proline-proline-phenylalanine" ("NPPF") motif found in most m^6A methyltransferase enzymes and that it is required for m^6A deposition on 18S rRNAs. In addition, a proteomic screen identified the ortholog of human TRMT112, CG12975, as a co-factor of CG9666. In yeast and archaea, TRMT112 homologs were shown to bind and activate several methyltransferases (Bud23, Trm9, Trm11, and Mtq2) [31]. Here, we found that CG12975 forms a stable and conserved complex with CG9666. This is consistent with a recent report in human cells showing the importance of the METTL5-TRMT112 interaction for m^6A deposition on 18S RNA [23]. The lack of m^6A modification on 18S rRNA does not affect rRNA processing, yet flies lacking this modification display impaired orientation in walking behavioral assays. Interestingly, recent exome sequencing in Pakistani and Yemenite families identified *METTL5* as a novel gene associated with recessive intellectual disability [30]. Altogether, these findings demonstrate the importance of m^6A modification on 18S rRNA for normal behavior and suggest that this function is conserved from flies to human.

Results and Discussion

Mettl5 controls m^6A levels in total RNA

In order to identify novel enzymes required for m^6A deposition on RNA, we conducted a targeted RNAi screen in *Drosophila* S2R + cells followed by m^6A quantification using mass spectrometry. Candidates were selected based on their sequence homology with annotated human METTLs (Fig 1A). Out of the 32 annotated human METTL enzymes, 20 have a *Drosophila* ortholog. Most of these enzymes are not related to each other by sequence homology. Few candidates were predicted to catalyze m^6A modification based on characteristics of their catalytic domain. These include the already known mRNA m^6A methyltransferase, Mettl3, and uncharacterized homologs of METTL4 (CG14906), METTL5 (CG9666), and METTL16 (CG7544). We generated double-stranded RNA for the 20 *Drosophila* genes and incubated S2R + cells for a total period of 6 days, to ensure sufficient depletion (Appendix Fig S1A and B). Total and poly(A)$^+$ RNA were then purified and subjected to mass spectrometry analysis. As expected, the knock down (KD) of *Mettl3* and *Mettl14* resulted in a substantially decreased m^6A level within the mRNA fraction, but had no effect on total RNA (Fig 1B and C and Appendix Fig S1C). In contrast, the KD of *CG9666* led to a reduction of m^6A on total RNA, but did not alter the abundance of m^6A on mRNA. KD of other predicted methyltransferases did not significantly affect m^6A levels, suggesting that they are involved in different types of enzymatic reactions or that they regulate only a subset of m^6A sites. The latter case is likely true for CG7544, as the vertebrate ortholog METTL16 has only few confirmed m^6A targets. Similarly, human METTL4 was recently shown to specifically catalyze m^6A on U2 snRNA [24]. Thus, our screen identified CG9666, hereafter named Mettl5, as a potential new m^6A methyltransferase in *Drosophila*.

Mettl5 is predominantly expressed in the cytoplasm and is enriched in the brain

Sequence analysis shows that Mettl5 is probably an ancient protein with full-length orthologs detected in all eukaryotic genomes (except fungi), but also in all completely sequenced archaeal species examined. The presence of orthologs in a few species of bacteria and phylogenetic analysis (Fig 2A and Appendix Fig S2) suggests horizontal transfer from archaea to bacteria. Conservation is high across eukarya (e.g., 53% identity between human, plant *Arabidopsis thaliana*, and fly sequences). The protein harbors N-terminal signatures characteristics of methyltransferase enzymes (amino acid co-ordinates in the fly sequence 39–146) with homology to many families (PFAM domain PF05175; MTS; methyltransferase small domain) and a C-terminal part (aa 147–213), which is unique to this family. Of note, all orthologs contain the characteristic NPPF motif, indicating that the catalytic activity is likely conserved throughout evolution (Fig 2B).

To get more insight into Mettl5 function, we examined its subcellular distribution and its expression during fly development. We found that Mettl5-FLAG expressed under its own regulatory promoter accumulates predominantly in the cytoplasm (Fig 2C). This is in sharp contrast with the localization of Mettl5 in human cells where it is predominantly localized to the nucleolus [23]. *Mettl5* is expressed at high level in early embryo, and its expression gradually decreases and remains low in the larval stages (Fig 2D). A mild increase is observed at metamorphosis, and this level remains constant in the adult phase. According to fly express (http://www.flyexpress.net/search.php?type=image&search=FBgn0036856), *Mettl5* is broadly expressed during embryogenesis and displays some enrichment in the nervous system (Fig 2E).

Mettl5 promotes m^6A deposition on *Drosophila* 18S rRNA

In order to get deeper insights into the molecular and functional role of Mettl5 *in vivo*, we generated loss-of-function alleles using the CRISPR/Cas9 methodology. Two guide RNAs encompassing the methyltransferase domain were designed. Using this approach, we obtained two distinct mutations (Fig 3A). The first allele ($Mettl5^{\Delta 2AA}$) lacks six nucleotides, resulting in a two amino acid deletion just upstream the predicted methyltransferase signatures

A

Human	Drosophila
METTL1	CG4045
METTL2A	Metl
METTL2B	Metl
METTL3	Mettl3
METTL4	CG14906
METTL5	CG9666
METTL6	CG34195
METTL7A	
METTL7B	
METTL8	
METTL9	CG5339
METTL10	CG9643
METTL11A	
METTL11B	
METTL12	
METTL13	CG2614
METTL14	Mettl14
METTL15	CG14683
METTL16	CG7544
METTL17	CG13126
METTL18	CG17219
METTL19	CG9386
METTL20	
METTL21A	
METTL21B	
METTL21C	
METTL21D	
METTL22	CG10584
METTL23	CG5013
METTL24	
METTL25	CG33964
METTL25B	CG2906
METTL26	CG18661
METTL27	

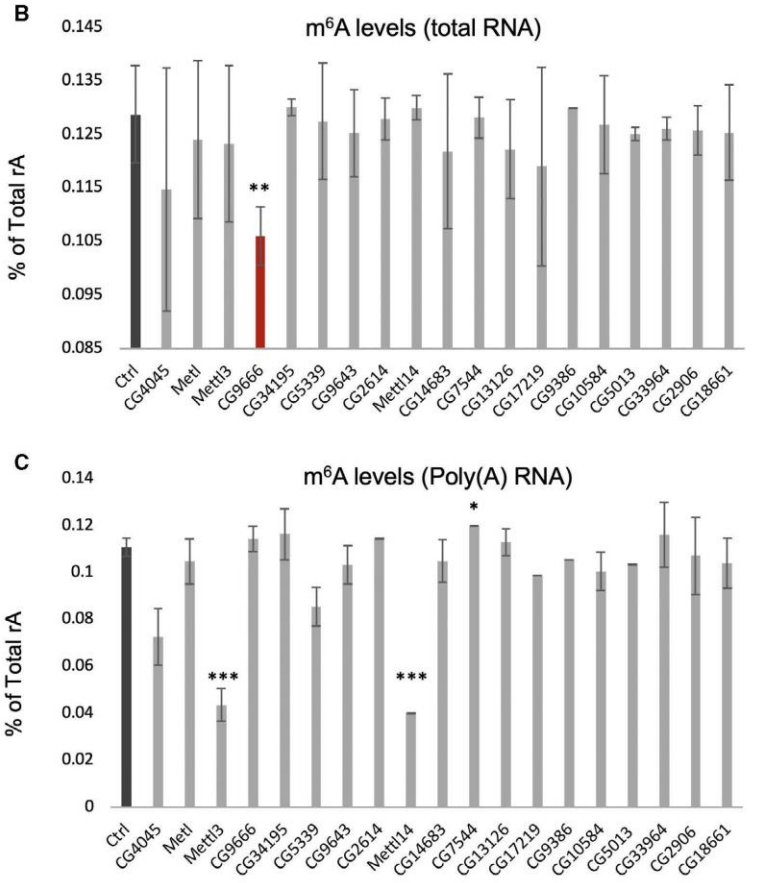

Figure 1. Mettl5 regulates m^{6}A level in total RNA.

A List of human methyltransferases and their orthologs in *Drosophila melanogaster*. Empty cells indicate that no ortholog could be identified (see Material and Methods for details).

B, C LC-MS/MS measurements of m^{6}A levels in total RNA (B) or in poly(A) $^+$ RNA (C) upon KD of predicted methyltransferases in *Drosophila* S2R+ cells. m^{6}A abundance in total RNA is significantly reduced when *Mettl5* is depleted, while its depletion has no effect on m^{6}A level in mRNA. As expected, the KD of *Mettl3* and *Mettl14* reduce m^{6}A levels in mRNA. Bar chart represents the mean ± standard deviation of three technical measurements from three biological replicates. $^*P < 0.05$, $^{**}P < 0.01$, $^{***}P < 0.001$ (two-tailed *t*-test).

(at positions 36 and 37; the AA in PHIAACMAH). These two amino acids are conserved from flies to human (Appendix Fig S2). The second allele (*Mettl5^{fs}*) is an insertion–deletion (indel) mutation consisting of a deletion of thirteen nucleotides combined with an insertion of three nucleotides (Appendix Fig S3). This indel mutation results in a frameshift at the amino acid position 36 and in a premature stop codon after amino acid 107, indicating that if the resulting mRNA is not eliminated by the nonsense-mediated mRNA decay pathway, only a truncated protein lacking the full methyltransferase domain is produced.

We found that both mutations give rise to viable and fertile flies with no obvious defect at the morphological level. In order to address their impact on m^{6}A levels, RNA was isolated from whole flies and analyzed by mass spectrometry. We found that the level of m^{6}A from *Mettl5$^{\Delta 2AA}$* flies is similar to wild type (WT) on both total and poly(A) RNA. However, a 45% decrease in total RNA of *Mettl5^{fs}* flies was observed, consistent with a reduction of rRNA methylation, while the level on mRNA remained unchanged (Fig 3B and Appendix Fig S4). This is in agreement with our experiments in S2R+ cells indicating that Mettl5 is required for proper m^{6}A levels. Furthermore, this suggests that *Mettl5^{fs}* is a strong loss-of-function allele, while *Mettl5$^{\Delta 2AA}$* has little to no impact on Mettl5 methyltransferase activity.

Recently, METTL5 was identified as a m^{6}A methyltransferase for 18S human rRNA [23]. To address whether this function is

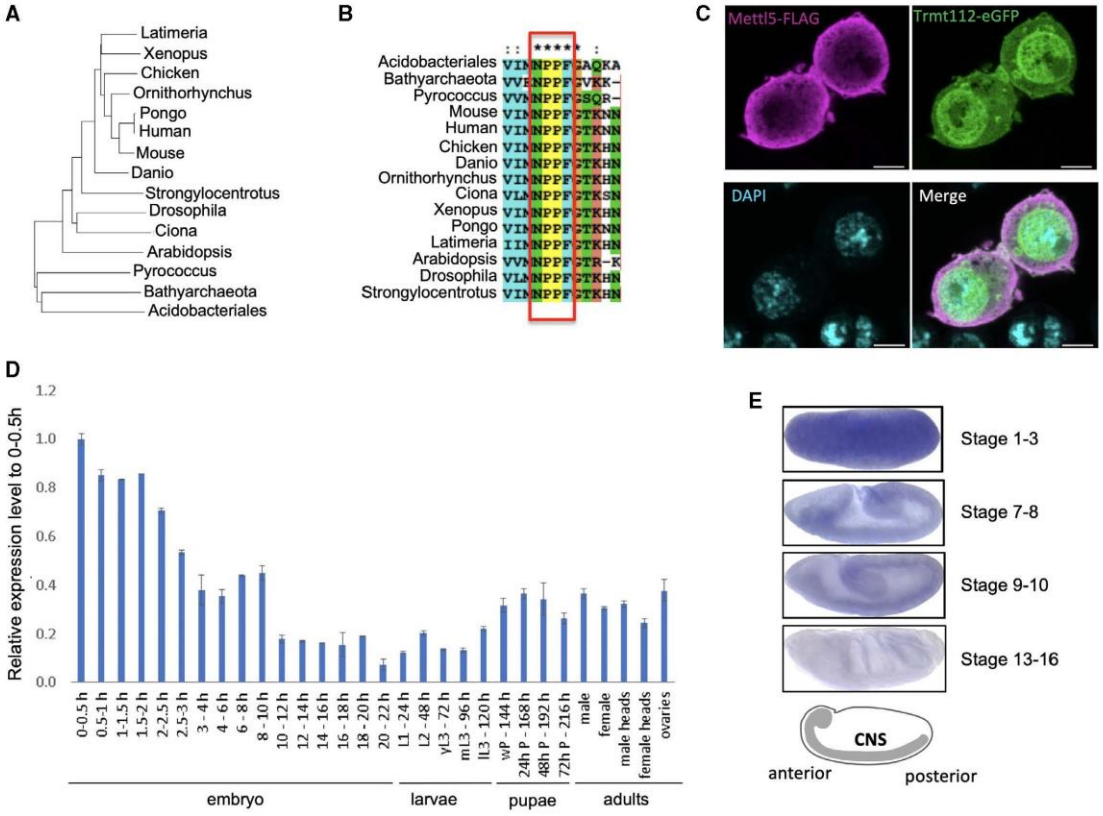

Figure 2. Phylogenetic and expression analyses of Mettl5.

A Phylogenetic tree of the alignment of representative Mettl5 orthologs from selected species (see Materials and Methods for details). Prokaryotic sequences from archaea (Pyrococcus, Bathyarchaeota) and bacteria (Acidobacteriales) are included as outliers.

B Multiple sequence alignment of Mettl5 orthologs showing conservation of the NPPF motif. Asterisks indicate perfect conservation.

C Subcellular localization of Mettl5-FLAG (purple) and Trmt112-eGFP (green) expressed under the control of their own promoter in S2R+ cells. 63× magnified merge of immunofluorescently labeled S2R+ cells. Scale bar: 4.47 μm.

D Developmental expression of *Mettl5* transcript assayed by RT–qPCR analysis. The figure shows mean ± standard deviation of three technical measurements from three biological replicates.

E In situ hybridization of *Mettl5* transcript at different embryonic stages. The central nervous system (CNS) is highlighted in the schematics. Data retrieved from FlyExpress 7 (http://www.flyexpress.net/search.php?type=image&search=FBgn0036856).

conserved in flies, the 18S and 28S rRNAs were individually isolated from mutant and isogenic control flies by velocity centrifugation, digested to nucleosides, and analyzed by HPLC (Fig 3C and Appendix Fig S5). Using commercial m^6A as calibration control, we established that this modified nucleoside elutes at 48 min (Fig 3C and Appendix Fig S5, gray). Analysis of purified 18S rRNA from flies confirmed the presence of the modification in wild-type animals, as expected, and revealed its absence in the *Mettl5*^{fs} mutant (Fig 3C). In contrast, the level of m^6A on 28S rRNA was not substantially affected (Appendix Fig S5). These results indicate that Mettl5 is required for m^6A deposition on 18S rRNA in *Drosophila*, which is consistent with the activity of human METTL5 [23].

Since another ribosomal RNA modification, 2′-*O*-methylation, was recently shown to occur substoichiometrically at specific positions [32,33,34], we wondered whether m^6A on 18S rRNA might also be partially modified. To address this question, we used the standard molar response factor on HPLC profiles ([28]). We made use of the UV_{254} molar response factors (M_r) of unmodified nucleosides (A, C, G, and U) and of selected modified (ac^4C and m^6A) nucleosides. The M_r values of A, C, G, U, ac^4C, and m^6A are, respectively, of: 431, 215, 463, 290, 172, and 340 (ref. [35]). The number of A, C, G, U, ac^4C, and m^6A nucleosides on fly 18S rRNA is, respectively, of: 564, 376, 473, 583, 2, and 1. For each nucleoside, the peak area was established on four independent HPLC profiles using four independent RNA preparations. Each

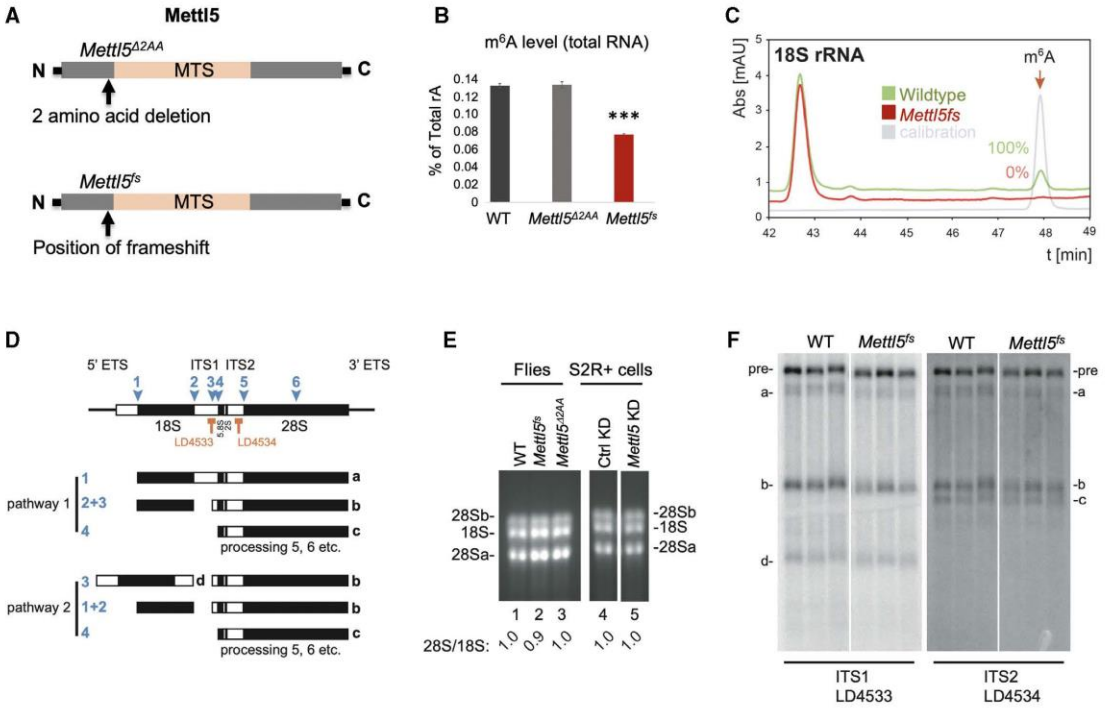

Figure 3. *Drosophila* Mettl5 is required for m^{6}A deposition on 18S rRNA.

A Representation of the two *Mettl5* mutant alleles generated in this work, consisting either of a two amino acid deletion upstream of the methyltransferase domain (top, *Mettl5*$^{\Delta 2AA}$) or of a frameshift mutation leading to a premature stop codon (bottom, *Mettl5*^{fs}).

B LC-MS/MS measurements of m^{6}A levels in total RNA of WT and *Mettl5* mutant flies. Bars represent mean ± standard deviation of measurements of three biological replicates. ***$P < 0.001$ (two-tailed *t*-test).

C Purified 18S rRNA analyzed for its m^{6}A content by quantitative HPLC. The 18S rRNA was extracted from 40S subunits isolated on sucrose gradients. The calibration control is a commercial source of m^{6}A (in gray). m^{6}A elutes at 48 min.

D Pre-rRNA processing in *Drosophila*: four mature rRNAs (the small ribosomal subunit 18S, and the large ribosomal subunit 5.8S, 2S, and 28Sa and 28Sb) are produced by sequential RNA cleavage following two alternative pathways, as depicted. Processing sites are indicated (1–6). The major pre-rRNA intermediates (a, b, c, and d) are highlighted.

E Mature rRNA analysis on ethidium-stained denaturing agarose gels. The same amounts of total RNA extracted from the indicated flies and from S2R+ cells depleted or not of *Mettl5* were loaded. The 28S/18S ratio was established by densitometry.

F Analysis of 18S rRNA maturation in WT and mutant flies (*Mettl5*^{fs}). Total RNA extracted from the indicated animals was resolved on denaturing agarose gels and processed for Northern blotting with specific probes (complementary to ITS1 or ITS2 sequences). The pre-rRNAs detected accumulate to normal levels indicating that processing is unaffected.

peak area was divided by its respective standard molar response factor. The levels of m^{6}A were estimated by comparing the value obtained for m^{6}A with that of ac^{4}C or of each of the unmodified nucleosides. In each case, the level of m^{6}A modification was estimated to be of 100%. This indicates that m^{6}A on fly 18S rRNA is fully methylated and does not appear to be regulated, at least in the conditions tested.

To test whether Mettl5-mediated 18S rRNA m^{6}A modification is required for ribosome biogenesis, we analyzed mature rRNA steady-state levels and pre-rRNA processing in the *Mettl5*^{fs} and control flies. In *Drosophila*, five mature rRNAs (the 18S, 5.8S, 2S, 28Sa, and 28Sb —the 28S rRNA is fragmented in fly following cleavage at site 6) are produced from a long polycistronic transcript synthesized by RNA polymerase I (see Fig 3D). Total RNA was extracted from *Mettl5*^{fs} and from control wild-type and *Mettl5*$^{\Delta 2AA}$ flies, resolved on denaturing agarose gels, and processed for Northern blotting with probes specific to major pre-rRNA intermediates. First, we analyzed the steady-state accumulation of the large mature rRNAs (18S, 28Sa, and 28Sb) by ethidium bromide staining (Fig 3E). The ratio of 28S/18S was unaffected in the *Mettl5*^{fs} mutant flies. This was also the case in S2R+ cells depleted for Mettl5 (Fig 3E). Next, we analyzed the levels of individual pre-rRNA intermediates (Fig 3F). We found that *Mettl5*^{fs} mutant flies do not display any qualitative difference in pre-rRNA processing. Altogether, we conclude that the Mettl5-mediated m^{6}A site is not required for pre-rRNA processing or 18S rRNA production (Fig 3E and F).

A

Mettl5 interactome (IP DML and LC-MS/MS)

Drosophila proteins	Human Orthologs	Log2 ratio H.L. Ctrl/ Mettl5 IP	Log2 ratio H.L. Mettl5 IP/ Ctrl
CG9666	METTL5	-5.99	10.76
CG12975	TRMT112	-3.62	1.77
l(1)G0156	IDH3A	-3.44	3.19
CG3364	N/A	-3.42	2.44
Art8	PRMT6	-3.38	2.60
CG14695	N/A	-3.25	3.57
ND-B18	NDUFBB7	-2.99	4.68
CG12304	AIMP2	-2.88	4.19

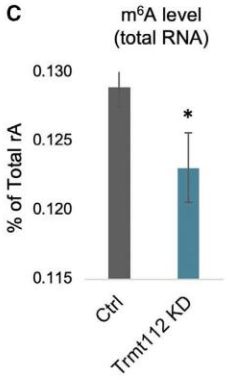

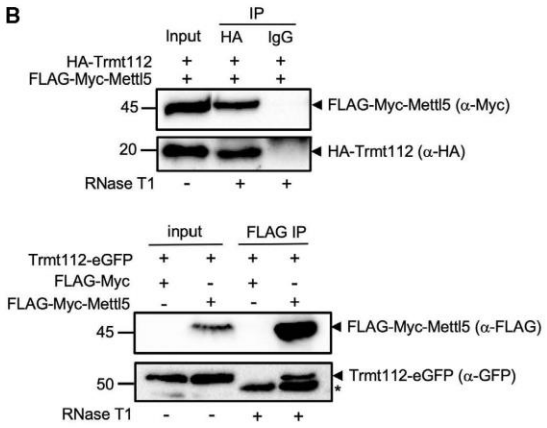

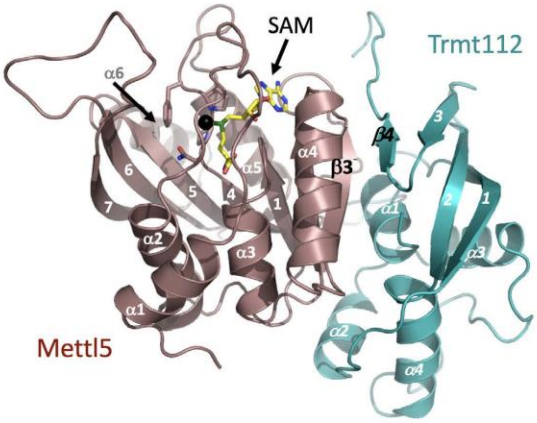

Figure 4. Mettl5 interacts with Trmt112 to install m^{6}A on 18S rRNA.

A Mettl5 partners identified as significantly enriched candidates in mass spectrometric analysis of Mettl5-FLAG-Myc affinity purifications (ribosomal proteins not listed for simplicity). Measurements of two biological replicates.

B Western blot validation of the co-immunoprecipitated proteins Mettl5-FLAG-Myc and Trmt112, bearing either a N-terminal HA tag (top) or a C-terminal GFP tag (bottom), in S2R+ cells. The arrows point at the indicated proteins. HA-Trmt12 migrates below the antibody light chains (top). Trmt112-eGFP migrates above the heavy chains indicated by an asterisk (bottom).

C *Trmt112* depletion reduces m^{6}A levels in total RNA from *Drosophila* S2R+ cells. Mean ± standard deviation of three technical measurements from three biological replicates. *$P < 0.05$ (two-tailed *t*-test).

D The sequences of *D. melanogaster* Mettl5 and Trmt112 were modeled in the experimentally determined atomic resolution structure of the human METTL5-TRM112 complex (based on PDB model 6H2V), revealing high conservation and formation of a parallel β-zipper involving main chain atoms at the complex interface. Mettl5 and Trmt112 are colored light brown and blue, respectively. The NPPF signature, known to co-ordinate planar nitrogen groups to be methylated, is shown as sticks. The *S-adenosyl-methionine* (SAM) is shown in stick representation (yellow) with the methyl group to be transferred to the 18S rRNA represented as a black sphere. Important secondary structure elements, including β3 on Mettl5 and β4 on Trmt112, are indicated.

Trmt112 is a conserved Mettl5 co-factor

In human cells, METTL5 has recently been shown to act as an m^{6}A 18S rRNA methyltransferase in concert with the noncatalytic co-activator, TRMT112 [36]. To test whether this mode of action is conserved in fly, we immunoprecipitated FLAG-Myc-tagged Mettl5 from S2R+ cells and submitted the co-precipitated proteins to mass spectrometry analysis. We found that seven proteins were significantly enriched in the pull-down fraction (omitting the ribosomal proteins; Fig 4A and Table EV1). Among them, we found the homolog of TRMT112, the previously uncharacterized CG12975. To validate this interaction, we cloned *CG12975* (hereafter called Trmt112) along with the HA epitope in the N-terminal region. Immunoprecipitation of HA-Trmt112 pulled down FLAG-Myc-Mettl5, revealing that both proteins are in the same complex, independently of RNA (the interaction pertains in the presence of RNase T1; Fig 4B). Reciprocally, this was confirmed by immunoprecipitating FLAG-Myc-Mettl5 and blotting the eluates with anti-GFP that revealed Trmt112-eGFP (Fig 4B). Consistent with a role of Mettl5 in regulating m^{6}A on ribosomal RNA, we found that

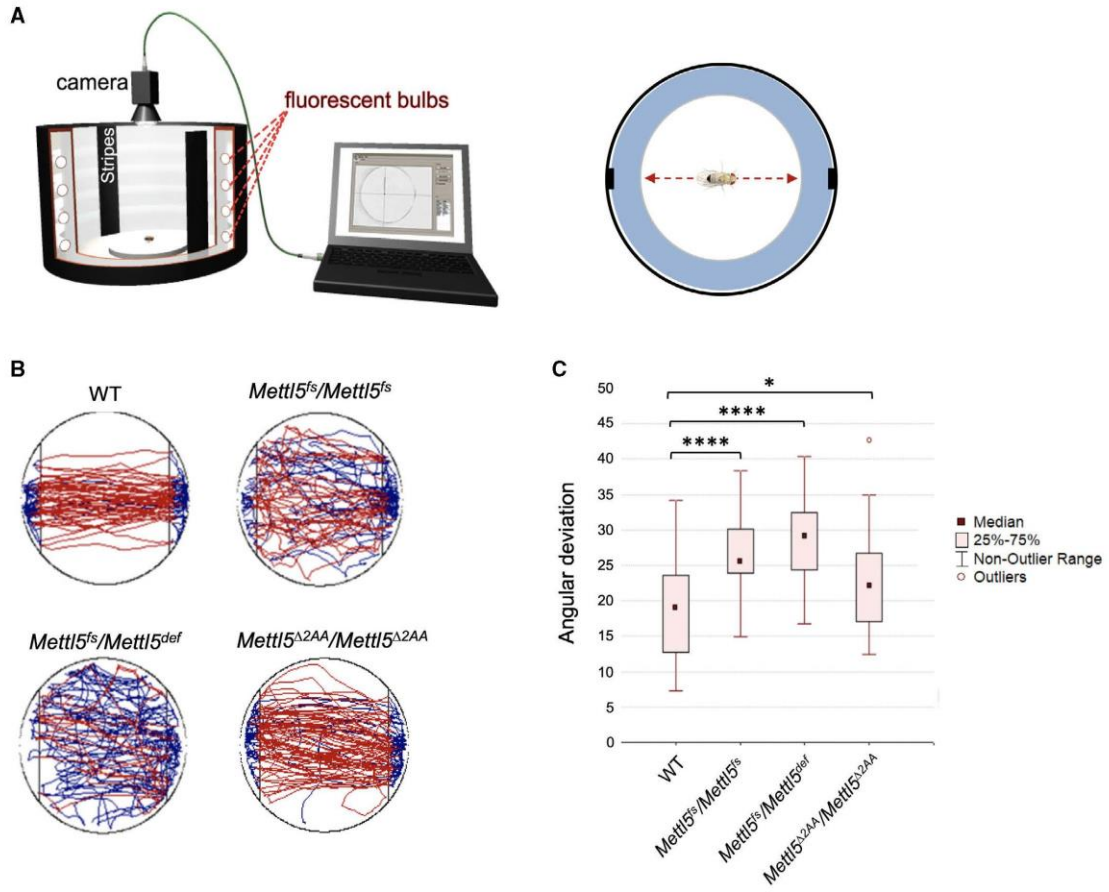

Figure 5. Mettl5 is required for fly orientation.

A Cartoon depicting the experiment with the main components of the setup showing the arena in white, the visual landmarks as black stripes and the camera to record the fly (left, from Ref. [37]), and cartoon showing the normal behavior of a WT fly in the arena. The black rectangles represent the visual landmarks and the red arrow the main trajectory undertaken by WT flies relative to the position of the landmarks (right).

B Representative trajectories of WT and *Mettl5* mutant flies analyzed by Buridan's paradigm. The blue lines indicate when the fly stops and changes direction.

C Orientation evaluated with the help of Buridan's paradigm for *Mettl5* mutant flies. Orientation was measured as the angular deviation from the straight path needed to move from one landmark to another in the arena. Number of flies tested per genotype: 30. Mean ± standard deviation. Shapiro–Wilk test was used to test for normal distribution in each group. Normally distributed groups were tested by *t*-test. Due to multiple comparison, Bonferroni correction was applied (*$P < 0.05$; ****$P < 0.0001$).

Trmt112 KD in S2R+ cells also reduced m^6A level on total RNA (Fig 4C).

We next addressed the expression pattern of *Trmt112*. Like *Mettl5*, *Trmt112* transcript displays strong expression in early embryos (Appendix Fig S6). In subsequent developmental stages, its expression follows a "wavy" pattern with a specific enrichment in adult ovaries. In contrast to Mettl5, Trmt122 localizes predominantly in the nucleus but is also found in the cytoplasm (Fig 2C). This difference in subcellular distribution is not surprising considering that Trmt112 is well-known to interact with additional methyltransferases.

Recently, the structure of human METTL5-TRMT112 was solved at atomic resolution by X-ray crystallography [36]. This revealed that the heterodimeric complex assembles through formation of a parallel ß-zipper involving main chain atoms between ß-strand 3 of METTL5 and ß-strand 4 of TRMT112, resulting in a remarkable continuous eleven-stranded ß-sheet in the complex. To evaluate whether formation of a Mettl5-Trmt112 complex is conserved in *Drosophila*, we modeled the fly Mettl5 and Trmt112 sequences using the 3-D structure of the human complex as template (Fig 4D). This illustrates a near-perfect structural conservation, with most of the major residues involved at the interface between the two subunits

of the complex being conserved between human and fly (Fig 4D and Appendix Fig S7). Upon binding, Trmt112 masks a large hydrophobic area on Mettl5, a region which would otherwise be unfavorable in the water-based environment. Our modeling that predicts the structural conservation of the Mettl5-Trmt112 heterodimer indicates that like in human Trmt112 might be required to stabilize Mettl5 in *Drosophila*.

Mettl5 is required for locomotion and orientation

METTL5 deficiency has recently been associated with neurological symptoms in autosomal recessive intellectual disability (ARID), including microcephaly and intellectual disability with altered behavioral and social skills [38]. Patients with this syndrome carry frameshift mutations in *METTL5*, resulting in truncated products, which, incidentally, is highly reminiscent of our fly mutation *Mettl5*^{fs}. These truncated products are predicted to lack important secondary structure elements of Mettl5, which is expected to alter protein function and is consistent with the destabilization of the corresponding proteins in cell culture experiments [30].

To address whether *Mettl5* mutant flies also display neurological defects, we performed the Buridan's paradigm assay [37]. In this method, individual flies are set onto a lit-up platform surrounded by water, in which two inaccessible black stripes serve as visible landmarks for the flies. Flies move from one stripe to another in a robust manner, enabling the measurement of their activity, orientation, and walking speed in 15-min intervals (Fig 5A). Wild-type flies were used as control and were compared to homozygous mutant animals. We also used trans-heterozygous flies to exclude off-target effects (see Material and Methods).

Although *Mettl5*^{fs} flies displayed normal activity, we found they were severely disoriented as they changed their walking directions more often compared to wild-type flies (Fig 5B and C; Appendix Fig S8A). Both homozygous and trans-heterozygous animals show similar behavior, confirming the specificity of the phenotypes toward *Mettl5* loss of function. In contrast, *Mettl5*$^{\Delta 2AA}$ flies behaved more similar to WT, although a mild angular deviation from the walking tracks could be observed. We conclude that Mettl5 is required for normal walking behavior in *Drosophila* and that its methyltransferase activity plays an important role in this process.

To exclude the possibility that *Mettl5*^{fs} flies are disorientated due to blindness, we re-analyzed in depth our data from the Buridan's assay. If the flies were blind, they would be expected to have the same probability to stay in the area around the black stripes as to stay in the area 90° to the black stripes. Therefore, we split this circled platform into 48 imaginary areas and calculated the frequency with which the flies were in the eight areas around the black stripes compared to the frequency they were in the eight areas 90° to the black stripe. We observed that for all genotypes, the probability that the flies are around the black stripes was highly significantly increased (Appendix Fig S8B). Therefore, this higher propensity to be close to the black stripes demonstrates that the *Mettl5* mutant flies indeed are not blind.

In human cells, METTL5 is mostly found in the nucleolus [33]. In fly, Mettl5 is detected mostly in the cytoplasm, suggesting the existence of ribosome biogenesis specificities. It is possible that in flies, pre-ribosome-bound-Mettl5 follows pre-40S ribosomes to the cytoplasm, while in human cells METTL5 dissociates from pre-40S early on in the nucleus. Small ribosomal RNA base modifications are typically generated late in rRNA processing, but cross-species differences have been reported. For example, the dimethylation installed at the 3′-end of 18S rRNA by DIM1 occurs in the cytoplasm in budding yeast, while it is deposited in the nucleus in human cells [39].

A brief comparison of the absence of phenotype of the *METTL5* knock out in human cells and the behavioral phenotype reported here in fly illustrates the benefits of using complex models (animal) and sophisticated assays (behavioral) to approach the role of conserved rRNA modifications present at essential functional sites on the ribosome. Considering that the m^6A modification deposited by Mettl5 on the 18S rRNA is right at the decoding site, in direct vicinity to the P-site, makes it a likely possibility that the phenotypes observed in mutant flies are explained by differential translation; however, this will require additional work to be tested directly. In conclusion, we propose that the underlying mechanism for the METTL5-associated human neurological disorder is loss of 18S rRNA m^6A modification.

Materials and Methods

Drosophila stocks and genetics

Drosophila melanogaster Canton-S with mutant alleles for *CG9666* was generated using the CRISPR/Cas9 system, as described previously [36]. Guide RNA sequences used were CTTCGCCGCACATAG CCGCGTGCA and AAACTGCACGCGGCTATGTGCGGC as well as CT TCTTCGGCACGAAACACAATGC and AAACGCATTGTGTTTCGTGC CGAAT. For the first allele (*Mettl5*$^{\Delta 2AA}$), a deletion of six base pairs (bp) from base pair 104 to 109 in the genome region chr3L (genome assembly BDGP release 6) containing *CG9666* was produced. For the second allele (*Mettl5*^{fs}), a deletion of 13 bp from base pair 104 to 118 in the genome region chr3L and an insertion of 3 bp were generated. Trans-heterozygous *CG9666* fly mutants were produced by crossing *Mettl5*^{fs} flies with a deficiency fly line for *CG9666* (BL8083-CG9666^{Def}, Bloomington *Drosophila* Stock Center) to rule out possible off-target effects by the CRISPR/Cas9 system.

Drosophila cell line

Drosophila S2R+ are embryonically derived cells obtained from the *Drosophila* Genomics Resource Center (DGRC; Flybase accession FBtc0000150). Mycoplasma contamination was not detected (verified by analyzing RNA sequencing data).

Cloning

The plasmids used for immunohistochemistry and immunoprecipitation assays in S2R+ cells were constructed by cloning the corresponding cDNA or gene region of *Mettl5* and *Trmt112* in the Gateway-based vectors with N-terminal 3XFLAG–6XMyc tag (pPFMW) for Mettl5 and N-terminal 3XHA tag (pAHW) or C-terminal eGFP tag (pAc5.1b) for Trmt112. Furthermore, for the immunofluorescence assay, the UAS promoter in pPFMW and the *Actin* promoter in pAc5.1b were replaced with the endogenous promoters of *Mettl5* and *Trmt112*, respectively.

RNA isolation and mRNA purification

Total RNA from flies as well as S2R+ cells was isolated using TRIzol reagent (Invitrogen), and DNA was removed with DNase-I treatment (NEB). Subsequently, poly(A)$^+$ RNA was isolated by three rounds of purification with Dynabeads Oligo (dT)25 (Invitrogen). Following this, all samples were tested for their quality by capillary electrophoresis using the Bioanalyzer (Agilent).

RT–PCR

qRT–PCR was performed to gain insight into expression levels of CG9666 and CG12975 during development and to assess KD efficiency of fly putative methyltransferase genes (primer list in Table EV2). Staging experiment was performed as previously reported [40], and the RNA was isolated as described above. The RNA was subjected to reverse transcription using the M-MLV Reverse Transcriptase Kit (Promega). Following cDNA synthesis, transcript levels were quantified in technical triplicates for each gene in each developmental stage via qPCR using SYBR Green PCR Master Mix (Thermo Fisher Scientific) and the ViiA 7 Real-Time PCR System (Thermo Fisher Scientific). The qPCR primers TCGAAGGAT ATTGAGGTGGA and TGTCCAAAACTAAATGCAACTGA were used to measure *CG9666* expression levels and CTCAGCACATACAACTT CTTGACC and CGCTCTCCACCACTTCCTTT to measure *CG12975* expression levels.

Immunostaining

Transfection of the tagged constructs in S2R+ cells was performed using Effectene reagent (Qiagen), as described in Ref. [36], co-transfecting both Mettl5 and Trmt112 constructs under the control of their endogenous promoters. Immunostaining of the cells was performed 72 h after transfection, as previously described [36]. To this end, the cells were incubated with primary antibody (mouse anti-Myc, Enzo 9E10, 1:1,000) in 0.2% Triton X-100 PBS supplemented with 10% donkey serum) at 4°C overnight and secondary antibody (anti-mouse AlexaFluor 568, 1:1,000 in 10% donkey serum in PBST) as well as DAPI (1:1,000) for 2 h at RT. Images were taken with Leica SP5 confocal microscope using 63× oil immersion objective.

Cell culture, RNAi and transfection

Drosophila S2R+ cells were grown in Schneider's medium (Gibco) supplemented with 10% FBS (Sigma) and 1% penicillin–streptomycin (Sigma). For RNA interference (RNAi) as well as transfection experiments, S2R+ cells were seeded at a density of 10^6 cells/ml in serum-free and serum-supplemented medium, respectively. For RNAi experiments, PCR templates for the dsRNA were prepared using the T7 megascript Kit (NEB; primer list in Table EV2). dsRNA against bacterial β-galactosidase gene (*lacZ*) was used as a control for all RNA interference (RNAi) experiments. A 7.5 μg of dsRNA was added to 10^6 cells. After 6 h of cell starvation, serum-supplemented medium was added to the cells. dsRNA treatment was repeated after 48 and 96 h, and cells were collected 24 h after the last treatment. The Effectene Transfection Reagent Kit (Qiagen) was used to transfect vector constructs together with the *Actin*-Gal4 driver construct in all overexpression experiments following the manufacturer's protocol.

Co-immunoprecipitation and Western blot analysis

For the co-immunoprecipitation assay, HA-tagged or eGFP-tagged *Trmt112* and FLAG-Myc-tagged *Mettl5* constructs were co-transfected in S2R+ cells, as described above. As controls for GFP co-IP, empty vectors were used. Seventy-two hours after transfection, cells were harvested, washed in DPBS, and pelleted by centrifugation at 500 *g* for 5 min. The pellets were lysed in 1 ml of lysis buffer (50 mM Tris–HCl at pH 7.4, 150 mM NaCl, 0.05% NP-40) supplemented with protease inhibitors and rotated head over tail for 30 min at 4°C. Following five cycles of sonication of 30 s on and 30 s off at the low power setting, the lysates were centrifuged at 20,000 *g* for 10 min at 4°C to remove the remaining cell debris. Protein concentrations were determined using Bradford reagent (Bio-Rad). For the immunoprecipitation, 2 mg of proteins was incubated with 15 μl of pre-washed Protein G beads (Thermo Fischer Scientific) for 1 h at 4°C as a pre-clearing step, to deplete for proteins enrichment based on nonspecific binding to the beads. The lysate with the unbound protein fraction was then added to 15 μl of Protein G beads, which were previously incubated at room temperature for 30 min with 8 μg of either of the following antibodies: mouse anti-HA (clone 12CA5, produced in-house), normal mouse IgG (Santa Cruz Biotechnology, sc-2025), and mouse anti-FLAG (Sigma-Aldrich, M2-F1804) as a pre-coating step to saturate the beads with the antibody. Lysates and pre-coated beads were incubated with head over tail rotation for 2 h at 4°C. The beads were then washed three times with washing buffer (50 mM Tris–HCl at pH 7.4, 150 mM NaCl) and incubated at 70°C for 10 min in 1× NuPAGE LDS buffer (Thermo Fisher) supplemented with 100 mM DTT for denaturation and elution of the immunoprecipitated proteins. Inputs were subjected to the same treatment to denature the proteins prior to Western blot analysis. For Western blot analysis, proteins were separated on a 12% SDS–PAGE gel and transferred to a PVDF membrane (Bio-Rad). After blocking with 5% milk in PBS with 0.05% Tween (PBST) for 1 h at room temperature, the membrane was incubated with primary antibody in blocking solution overnight at 4°C. The primary antibodies used were mouse anti-Myc (1:2,000; Enzo, 9E10), mouse anti-FLAG (1:2,000, Sigma, M2), mouse anti-HA (1:2,000, in-house, 12CA5), and mouse anti-GFP (1:200, Santacruz, B-2). The membrane was washed three times in PBST for 15 min prior incubation for 1 h at room temperature with anti-mouse secondary antibody (Jackson ImmunoResearch) in 5% milk. Protein bands were detected using SuperSignalWest Pico chemiluminescent substrate (Thermo Scientific).

IP, Dimethyl labeling of the samples and proteomic analysis

For proteomic analysis of Mettl5 interactors, the immunoprecipitation was performed using two biological replicates transfected with FLAG-Myc empty plasmid as control and two biological replicates transfected with Mettl5 FLAG-Myc construct, for forward and reverse experiment. Seventy-two hours after transfection, cells were harvested, washed in DPBS, and pelleted by centrifugation at 500 *g* for 5 min. The pellets were lysed in 1 ml of lysis buffer (50 mM Tris–HCl at pH 7.4, 150 mM NaCl, 0.05% NP-40) supplemented with protease inhibitors and rotated head

over tail for 30 min at 4°C. Following five cycles of sonication of 30 s on and 30 s off at the low power setting, the lysates were centrifuged at 20,000 *g* for 10 min at 4°C to remove the remaining cell debris. Protein concentrations were determined using Bradford reagent (Bio-Rad). The antibody used for IP was anti-Myc coupled with magnetic beads (Pierce, 9E10). A 2 mg of proteins was incubated with 15 μl of pre-washed beads for 2 h at 4°C. The beads were washed three times for 10 min with lysis buffer, and immunoprecipitated proteins were eluted at 70°C for 10 min in 1× NuPAGE LDS buffer (Thermo Fisher) supplemented with 100 mM DTT.

Protein lysates were firstly subjected to tryptic digestion, as previously described [41]. Subsequently, the peptides from the four samples were mixed with either formaldehyde-H2 (4% in water, 1 μl) or formaldehyde-D2 (4% in water, 1 μl) and vortexed. Freshly prepared sodium cyanoborohydride (260 mM, 1 μl) was added. The mixture was vortexed again and then let stand for 5 min, for the dimethyl labeling reaction to occur, as described earlier (Hsu JL *et al*, 2003). For the forward experiment, the control sample was labeled with formaldehyde-H2 and the lysate from Mettl5 immunoprecipitation with formaldehyde-D2. The reverse experiment was performed vice versa. The samples were then subjected to mass spectrometry measurements as described previously [42]. Raw files were processed with MaxQuant (version 1.5.2.8, Cox and Mann, 2008) and searched against the UniProt database of annotated *Drosophila* proteins (*D. melanogaster*: 41,850 entries, downloaded January 8, 2015).

LC-MS/MS analysis of m^{6}A levels

Ribonucleoside (rA, N6 mA) standards, ammonium acetate, and LC/MS grade acetonitrile were purchased from Sigma-Aldrich. $^{13}C_9$-A was purchased from Silantes, GmbH (Munich, Germany). $^{2}H_3$-N6 mA was obtained from TRC, Inc (Toronto, Canada). All solutions were prepared using Millipore quality water (Barnstead GenPure xCAD Plus, Thermo Scientific). A 0.1–1 μg of RNA was degraded to nucleosides with 0.003 U nuclease P1 (Roche), 0.01 U snake venom phosphodiesterase (Worthington), and 0.1 U alkaline phosphatase (Fermentas). Separation of the nucleosides from the digested RNA samples was performed with an Agilent 1290 UHPLC system equipped with RRHD Eclipse Plus C18 (95Å, 2.1 × 50 mm, 1.8 μm, Zorbax, USA) with a gradient of 5 mM ammonium acetate (pH 7, solvent A) and acetonitrile (solvent B). Separations started at a flow rate of 0.4 ml/min and linearly increased to 0.5 ml/ml during first 7 min. Then, washing and reconditioning was done at 0.5 ml/min for an additional 3 min and linearly decrease to 0.4 ml/min during the last minute. The gradients were as follows: solvent B linear increase from 0 to 7% for first 3 min, followed by isocratic elution at 7% solvent B for another 4 min; then switching to 0% solvent B for last 4 min, to recondition the column. Quantitative MS/MS analysis was performed with an Agilent 6490 triple quadrupole mass spectrometer in positive ion mode. The details of the method and instrument settings are described elsewhere [43]. MRM transitions used in this study were 269.2→137.2 (rA), 278.2→171.2 ($^{13}C_9$-rA), 282.1→150.1 (N6mrA), and 285.1→153.1 ($^{2}H_3$-N6mrA). The quantification of all samples utilized biological triplicates and the average values with one s.d. are shown.

Phylogenetic analysis

Orthologs of *CG9666* were searched for representative species at increasing taxonomic distances from *Homo sapiens* to eukarya with the assistance of the Protein Path Tracker online tool (PPT; [44]). Identifiers and species names are the following: Q8K1A0, *Mus musculus*; Q9NRN9, *H. sapiens*; F1NZ60, *Gallus gallus*; F1QVR8, *Danio rerio*; F6R9A4, *Ornithorhynchus anatinus*; F6WB92, *Ciona intestinalis*; F7AIW5, *Xenopus tropicalis*; H2P7S0, *Pongo abelii*; H3B2F1, Latimeria chalumnae; Q84TF1, *A. thaliana*; Q8MSW4, *D. melanogaster*; and W4YQG0, *Strongylocentrotus purpuratus*. Multiple sequence alignment of the sequences collected was obtained with MUSCLE as implemented at EBI [45]. ClustalW [46] was used to represent the alignment and to produce a phylogenetic tree.

Modeling the *Drosophila melanogaster* Mettl5 and Trmt112 sequences into the human 3-D structure of the METTL5-TRMT112 complex

The METTL5 and TRMT112 proteins from human and *D. melanogaster* share 59 and 50% sequence identity, respectively. To generate a model of the *D. melanogaster* Mettl5-Trmt112 complex, we processed the co-ordinates of the crystal structure of the human METTL5-TRMT112 complex [36] together with sequence alignments between human and fruit fly proteins using the ROBETTA server [47]. The resulting model exhibits a RMSD value of 0.4 Å over 250 Cα atoms compared to the structure of the human complex. This is typically what is seen when comparing the crystal structures of two proteins sharing between 50 to 60% sequence identity.

Buridan's behavioral paradigm analysis in *Drosophila*

Behavioral tests were performed on 5-day-old flies using the Canton-S strain as wild-type control. Wings were cut under cold anesthesia to one-third of their length on the evening before the experiment. Activity and orientation behavior were analyzed using Buridan's paradigm as described before [48]. All statistical groups were tested for normal distribution with the Shapiro–Wilk test. *t*-Test analysis of variance with Bonferroni correction was used to compare different conditions. $N = 30$ for all genotypes. The sample size was chosen based on a previous study [49], and its power was validated with result analysis. Blinding was applied during the experiment.

Pre-rRNA processing analysis

A 5 μg total RNA extracted from 10 flies was separated on 1.2% denaturing agarose gels and processed for Northern blotting analysis with specific probes, as described in Ref. [50]. The probes used are as follows: LD4533 (ITS1) and LD4534 (ITS2). Mature rRNAs were visualized by ethidium bromide staining of the gels. The ratio of mature rRNAs was established by densitometry on a ChemiDoc MP (Bio-Rad).

Ribosomal RNA modification analysis

18S rRNA was purified on 10–30% sucrose gradient (NaCl 300 mM, Tris–HCl pH8.0 50 mM, $MgCl_2$ 2 mM, EGTA 1 mM, Triton X-100 1%, sodium deoxycholate 0.1%), digested to nucleosides with 2 U

P1 nuclease (Sigma N8630) and 10 μl alkaline phosphatase (Sigma P4252-100U), and analyzed by HPLC as described in [51].

Statistics

In Buridan's paradigm, Shapiro–Wilk's test was used to test for normal distribution in each group. Homogeneity of variances was tested using Levene's test. Normally distributed groups with homogeneous variances were tested by Student's *t*-test. Due to multiple comparison, Bonferroni correction was applied.

m^6A measurements were taken from three biological replicates, and the variance between the groups that are being statistically compared is similar; therefore, the two-tailed unpaired Student's *t*-test was applied.

Expanded View for this article is available online.

Acknowledgements
We thank the Bloomington *Drosophila* Stock Center and the Zurich ORFeome Project (FlyORF) for fly reagents; the *Drosophila* Genomics Resource Center at Indiana University for plasmids and cell line; Roland Strauss and his group for the help with Buridan's paradigm; members of the Roignant and Lafontaine laboratories for helpful discussion; the Genomics and Bioinformatics IMB core facilities for great support. Support by IMB Proteomics core facility is gratefully acknowledged (instrument is funded by DFG INST 247/766-1 FUGG). In particular, we wish to thank Anja Freiwald from IMB Proteomics core facility for sample preparation and Dr. Mario Dejung from Proteomics core facility for data processing. Research in the laboratory of J.-Y.R. is supported by the Deutsch-Israelische Projektkooperation (DIP) RO 4681/6-1 and the Epitran COST action (CA16120). Research in the laboratory of D.L.J.L. is supported by the Belgian Fonds de la Recherche Scientifique (F.R.S./FNRS), the Université Libre de Bruxelles (ULB), the Région Wallonne (DGO6) [grant RIBO*cancer* no. 1810070], the Fonds Jean Brachet, and the International Brachet Stiftung. Research in the laboratory of M.G. is supported by the Agence Nationale pour la Recherche [grant number ANR-16-CE11-0003], the CNRS, Ecole Polytechnique, and the CNRS PICS program [grand number PICS07484].

Author contributions
JL, MS, DLJL, and J-YR conceived the study. JL, MS, LW, MP, MAV, MM, MG, CN, DLJL, and J-YR performed the methodology. PM and MAA-N performed the phylogenetic analysis. JL and MS wrote the draft of the manuscript. All authors reviewed and edited the manuscript. DLJL and J-YR supervised the study.

Conflict of interest
The authors declare that they have conflict of interest.

References

1. Desrosiers R, Friderici K, Rottman F (1974) Identification of methylated nucleosides in messenger RNA from Novikoff hepatoma cells. *Proc Natl Acad Sci USA* 71: 3971 3975
2. Perry R, Kelley D (1974) Existence of methylated messenger RNA in mouse L cells. *Cell* 1: 37 42
3. Dominissini D, Moshitch-Moshkovitz S, Schwartz S, Salmon-Divon M, Ungar L, Osenberg S, Cesarkas K, Jacob-Hirsch J, Amariglio N, Kupiec M *et al* (2012) Topology of the human and mouse m6A RNA methylomes revealed by m6A-seq. *Nature* 485: 201 206
4. Meyer KD, Saletore Y, Zumbo P, Elemento O, Mason CE, Jaffrey SR (2012) Comprehensive analysis of mRNA methylation reveals enrichment in 3' UTRs and near stop codons. *Cell* 149: 1635 1646
5. Shi H, Wei J, He C (2019) Where, when, and how: context-dependent functions of RNA methylation writers, readers, and erasers. *Mol Cell* 74: 640 650
6. Bujnicki JM, Feder M, Radlinska M, Blumenthal RM (2002) Structure prediction and phylogenetic analysis of a functionally diverse family of proteins homologous to the MT-A70 subunit of the human mRNA:m(6)A methyltransferase. *J Mol Evol* 55: 431 444
7. Sledz P, Jinek M (2016) Structural insights into the molecular mechanism of the m(6)A writer complex. *eLife* 5: e18434
8. Wang P, Doxtader KA, Nam Y (2016) Structural basis for cooperative function of Mettl3 and Mettl14 methyltransferases. *Mol Cell* 63: 306 317
9. Wang X, Feng J, Xue Y, Guan Z, Zhang D, Liu Z, Gong Z, Wang Q, Huang J, Tang C *et al* (2016) Structural basis of N(6)-adenosine methylation by the METTL3-METTL14 complex. *Nature* 534: 575 578
10. Yue Y, Liu J, Cui X, Cao J, Luo G, Zhang Z, Cheng T, Gao M, Shu X, Ma H *et al* (2018) VIRMA mediates preferential m(6)A mRNA methylation in 3'UTR and near stop codon and associates with alternative polyadenylation. *Cell Discov* 4: 10
11. Patil DP, Chen CK, Pickering BF, Chow A, Jackson C, Guttman M, Jaffrey SR (2016) m6A RNA methylation promotes XIST-mediated transcriptional repression. *Nature* 537: 369 373
12. Guo J, Tang HW, Li J, Perrimon N, Yan D (2018) Xio is a component of the *Drosophila* sex determination pathway and RNA N(6)-methyladenosine methyltransferase complex. *Proc Natl Acad Sci USA* 115: 3674 3679
13. Knuckles P, Lence T, Haussmann IU, Jacob D, Kreim N, Carl SH, Masiello I, Hares T, Villasenor R, Hess D *et al* (2018) Zc3 h13/Flacc is required for adenosine methylation by bridging the mRNA-binding factor Rbm15/Spenito to the m(6)A machinery component Wtap/Fl(2)d. *Genes Dev* 32: 415 429
14. Wen J, Lv R, Ma H, Shen H, He C, Wang J, Jiao F, Liu H, Yang P, Tan L *et al* (2018) Zc3 h13 regulates nuclear RNA m(6)A methylation and mouse embryonic stem cell self-renewal. *Mol Cell* 69: 1028 1038.e1026
15. Ruzicka K, Zhang M, Campilho A, Bodi Z, Kashif M, Saleh M, Eeckhout D, El-Showk S, Li H, Zhong S *et al* (2017) Identification of factors required for m(6) A mRNA methylation in Arabidopsis reveals a role for the conserved E3 ubiquitin ligase HAKAI. *N Phytol* 215: 157 172
16. Balacco DL, Soller M (2019) The m(6)A writer: rise of a machine for growing tasks. *Biochemistry* 58: 363 378
17. Lence T, Soller M, Roignant JY (2017) A fly view on the roles and mechanisms of the m6A mRNA modification and its players. *RNA Biol* 14: 1232 1240
18. Lence T, Paolantoni C, Worpenberg L, Roignant JY (2019) Mechanistic insights into m(6)A RNA enzymes. *Biochim Biophys Acta Gene Regul Mech* 1862: 222 229
19. Pendleton KE, Chen B, Liu K, Hunter OV, Xie Y, Tu BP, Conrad NK (2017) The U6 snRNA m(6)A methyltransferase METTL16 regulates SAM synthetase intron retention. *Cell* 169: 824 835.e814
20. Shima H, Matsumoto M, Ishigami Y, Ebina M, Muto A, Sato Y, Kumagai S, Ochiai K, Suzuki T, Igarashi K (2017) S-adenosylmethionine synthesis is regulated by selective N(6)-adenosine methylation and mRNA degradation involving METTL16 and YTHDC1. *Cell Rep* 21: 3354 3363
21. Warda AS, Kretschmer J, Hackert P, Lenz C, Urlaub H, Hobartner C, Sloan KE, Bohnsack MT (2017) Human METTL16 is a N(6)-methyladenosine (m

(6)A) methyltransferase that targets pre-mRNAs and various non-coding RNAs. *EMBO Rep* 18: 2004 2014

22. Mendel M, Chen KM, Homolka D, Gos P, Pandey RR, McCarthy AA, Pillai RS (2018) Methylation of structured RNA by the m(6)A writer METTL16 is essential for mouse embryonic development. *Mol Cell* 71: 986 1000.e1011
23. Sloan KE, Warda AS, Sharma S, Entian KD, Lafontaine DLJ, Bohnsack MT (2017) Tuning the ribosome: the influence of rRNA modification on eukaryotic ribosome biogenesis and function. *RNA Biol* 14: 1138 1152
24. Sharma S, Lafontaine DLJ (2015) 'View from a bridge': a new perspective on eukaryotic rRNA base modification. *Trends Biochem Sci* 40: 560 575
25. Piekna-Przybylska D, Decatur WA, Fournier MJ (2008) The 3D rRNA modification maps database: with interactive tools for ribosome analysis. *Nucleic Acids Res* 36: D178 D183
26. Ma H, Wang X, Cai J, Dai Q, Natchiar SK, Lv R, Chen K, Lu Z, Chen H, Shi YG *et al* (2019) N(6-)Methyladenosine methyltransferase ZCCHC4 mediates ribosomal RNA methylation. *Nat Chem Biol* 15: 88 94
27. Lafontaine DL, Preiss T, Tollervey D (1998) Yeast 18S rRNA dimethylase Dim1p: a quality control mechanism in ribosome synthesis? *Mol Cell Biol* 18: 2360 2370
28. Liu PC, Thiele DJ (2001) Novel stress-responsive genes EMC1 and NOP14 encode conserved, interacting proteins required for 40S ribosome biogenesis. *Mol Biol Cell* 12: 3644 3657
29. Eschrich D, Buchhaupt M, Kotter P, Entian KD (2002) Nep1p (Emg1p), a novel protein conserved in eukaryotes and archaea, is involved in ribosome biogenesis. *Curr Genet* 40: 326 338
30. Schosserer M, Minois N, Angerer TB, Amring M, Dellago H, Harreither E, Calle-Perez A, Pircher A, Gerstl MP, Pfeifenberger S *et al* (2015) Methylation of ribosomal RNA by NSUN5 is a conserved mechanism modulating organismal lifespan. *Nat Commun* 6: 6158
31. Bourgeois G, Letoquart J, van Tran N, Graille M (2017) Trm112, a protein activator of methyltransferases modifying actors of the eukaryotic translational apparatus. *Biomolecules* 7: 7
32. Sharma S, Marchand V, Motorin Y, Lafontaine DLJ (2017) Identification of sites of 2′-O-methylation vulnerability in human ribosomal RNAs by systematic mapping. *Sci Rep* 7: 11490
33. Erales J, Marchand V, Panthu B, Gillot S, Belin S, Ghayad SE, Garcia M, Laforets F, Marcel V, Baudin-Baillieu A *et al* (2017) Evidence for rRNA 2′-O-methylation plasticity: Control of intrinsic translational capabilities of human ribosomes. *Proc Natl Acad Sci USA* 114: 12934 12939
34. Krogh N, Jansson MD, Hafner SJ, Tehler D, Birkedal U, Christensen-Dalsgaard M, Lund AH, Nielsen H (2016) Profiling of 2′-O-Me in human rRNA reveals a subset of fractionally modified positions and provides evidence for ribosome heterogeneity. *Nucleic Acids Res* 44: 7884 7895
35. Gehrke CW, Kuo KC (1990) Ribonucleoside analysis by reversed-phase high performance liquid chromatography. *J Chromatogr* 471: 3 36
36. van Tran N, Ernst FGM, Hawley BR, Zorbas C, Ulryck N, Hackert P, Bohnsack KE, Bohnsack MT, Jaffrey SR, Graille M *et al* (2019) The human 18S rRNA m6A methyltransferase METTL5 is stabilized by TRMT112. *Nucleic Acids Res* 47: 7719 7733
37. Colomb J, Reiter L, Blaszkiewicz J, Wessnitzer J, Brembs B (2012) Open source tracking and analysis of adult *Drosophila* locomotion in Buridan's paradigm with and without visual targets. *PLoS ONE* 7: e42247
38. Richard EM, Polla DL, Assir MZ, Contreras M, Shahzad M, Khan AA, Razzaq A, Akram J, Tarar MN, Blanpied TA *et al* (2019) Bi-allelic variants in METTL5 cause autosomal-recessive intellectual disability and microcephaly. *Am J Hum Genet* 105: 869 887
39. Zorbas C, Nicolas E, Wacheul L, Huvelle E, Heurgue-Hamard V, Lafontaine DL (2015) The human 18S rRNA base methyltransferases DIMT1L and WBSCR22-TRMT112 but not rRNA modification are required for ribosome biogenesis. *Mol Biol Cell* 26: 2080 2095
40. Lence T, Akhtar J, Bayer M, Schmid K, Spindler L, Ho CH, Kreim N, Andrade-Navarro MA, Poeck B, Helm M *et al* (2016) m6A modulates neuronal functions and sex determination in *Drosophila*. *Nature* 540: 242 247
41. Hsu JL, Huang SY, Chow NH, Chen SH (2003) Stable-isotope dimethyl labeling for quantitative proteomics. *Anal Chem* 75: 6843 6852
42. Bluhm A, Casas-Vila N, Scheibe M, Butter F (2016) Reader interactome of epigenetic histone marks in birds. *Proteomics* 16: 427 436
43. Schomacher L, Han D, Musheev MU, Arab K, Kienhofer S, von Seggern A, Niehrs C (2016) Neil DNA glycosylases promote substrate turnover by Tdg during DNA demethylation. *Nat Struct Mol Biol* 23: 116 124
44. Mier P, Perez-Pulido AJ, Andrade-Navarro MA (2018) Automated selection of homologs to track the evolutionary history of proteins. *BMC Bioinformatics* 19: 431
45. Edgar RC (2004) MUSCLE: multiple sequence alignment with high accuracy and high throughput. *Nucleic Acids Res* 32: 1792 1797
46. Larkin MA, Blackshields G, Brown NP, Chenna R, McGettigan PA, McWilliam H, Valentin F, Wallace IM, Wilm A, Lopez R *et al* (2007) Clustal W and Clustal X version 2.0. *Bioinformatics* 23: 2947 2948
47. Song Y, DiMaio F, Wang RY, Kim D, Miles C, Brunette T, Thompson J, Baker D (2013) High-resolution comparative modeling with RosettaCM. *Structure* 21: 1735 1742
48. Strauss R, Hanesch U, Kinkelin M, Wolf R, Heisenberg M (1992) No-bridge of *Drosophila melanogaster*: portrait of a structural brain mutant of the central complex. *J Neurogenet* 8: 125 155
49. Poeck B, Triphan T, Neuser K, Strauss R (2008) Locomotor control by the central complex in *Drosophila*-an analysis of the tay bridge mutant. *Dev Neurobiol* 68: 1046 1058
50. Tafforeau L, Zorbas C, Langhendries JL, Mullineux ST, Stamatopoulou V, Mullier R, Wacheul L, Lafontaine DL (2013) The complexity of human ribosome biogenesis revealed by systematic nucleolar screening of Pre-rRNA processing factors. *Mol Cell* 51: 539 551
51. Sharma S, Langhendries JL, Watzinger P, Kotter P, Entian KD, Lafontaine DL (2015) Yeast Kre33 and human NAT10 are conserved 18S rRNA cytosine acetyltransferases that modify tRNAs assisted by the adaptor Tan1/THUMPD1. *Nucleic Acids Res* 43: 2242 2258

Table of Content

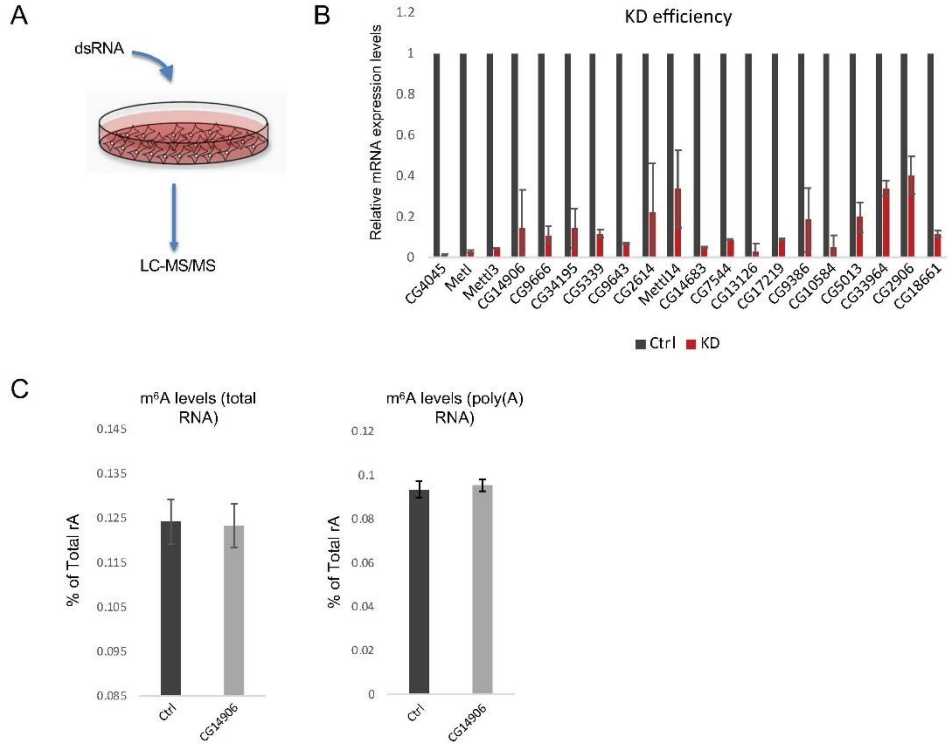

Appendix Figure S1: Design and validation of the candidate-based RNAi screen

(A) Experimental scheme of the RNAi screen performed in *Drosophila* S2R+ cells. After KD prolonged for 6 days, RNA was extracted and submitted to mass spectrometry analysis. (B) Efficiency of the knock down quantified by RT-qPCR. Bar chart represents the mean ± standard deviation of three technical measurements from three biological replicates. (C) LC-MS/MS measurements of m^6A levels in total RNA (left) or in poly(A)+ RNA (right) in S2R+ cells upon depletion of CG14906. Bar charts represent the mean± standard deviation of three technical measurements from three biological replicates.

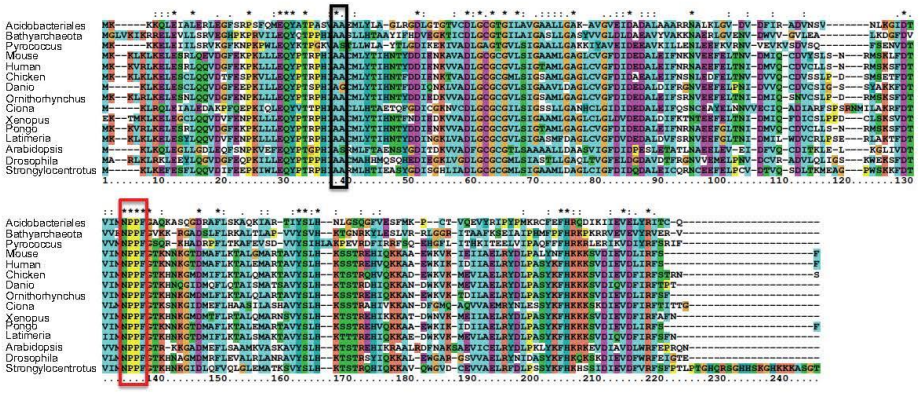

Appendix Figure S2: Phylogenetic analysis

Multiple sequence alignment of Mettl5 (UniProt: Q8MSW4_DROME) and representative orthologs from selected species (see Methods for details and sequence identifiers). Prokaryotic exemplary sequences from archaea (Pyrococcus, Bathyarchaeota) and bacteria (Acidobacteriales) are included as outliers. The red rectangle indicates the conserved NPPF motif and the black rectangle the position of the two amino acids deleted in the *Mettl5*$^{\Delta 2AA}$ allele.

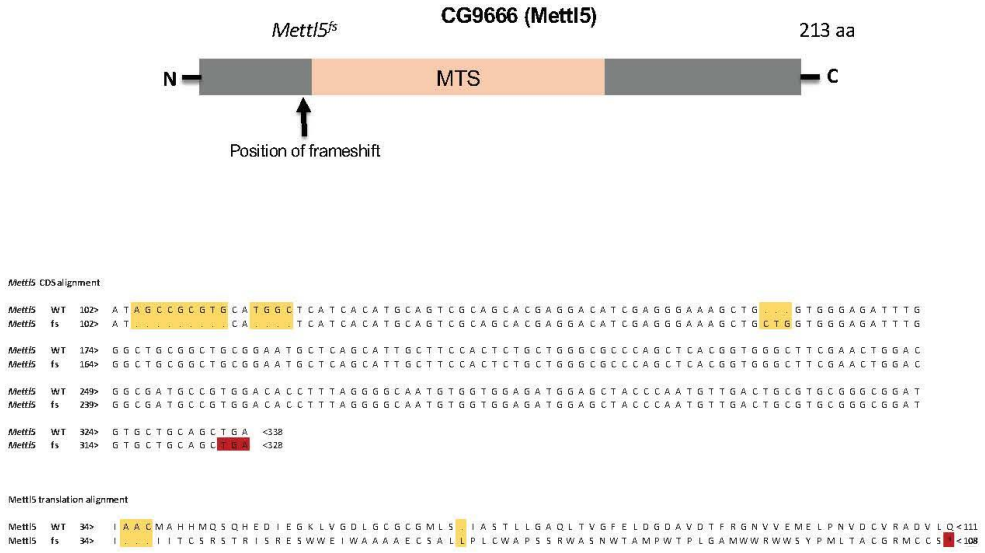

Appendix Figure S3: Description of the *Mettl5*^{fs} mutation

(Top) Representation of the *Mettl5*^{fs} mutant allele generated in this work, consisting of a frameshift mutation leading to a premature stop codon. (Bottom) Nucleotide and protein sequence alignments of WT *Mettl5* and *Metll5*^{fs}. Yellow indicates the changes in the mutant allele. Red indicates the premature stop codon.

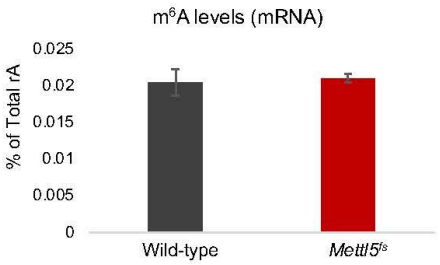

Appendix Figure S4: Methylation levels analysis

LC-MS/MS measurements of m^6A levels in mRNA of WT and *Mettl5*^{fs} mutant flies. Bars represent mean ± standard deviation of measurements of three technical measurements from three biological replicates.

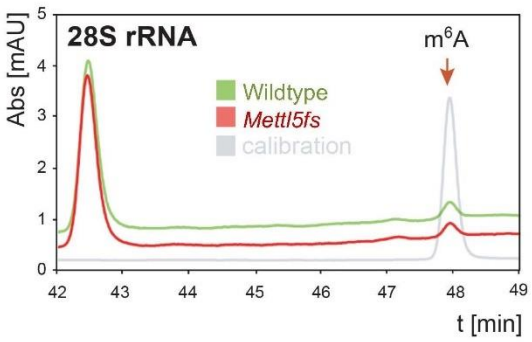

Appendix Figure S5: Analysis of m^6A levels on 28S rRNA by quantitative HPLC

Purified 28S rRNA analyzed for its m^6A content by quantitative HPLC. The 28S RNA was extracted from 60S subunits isolated on sucrose gradients. The calibration control is a commercial source of m^6A (in grey). m^6A elutes at 48 min.

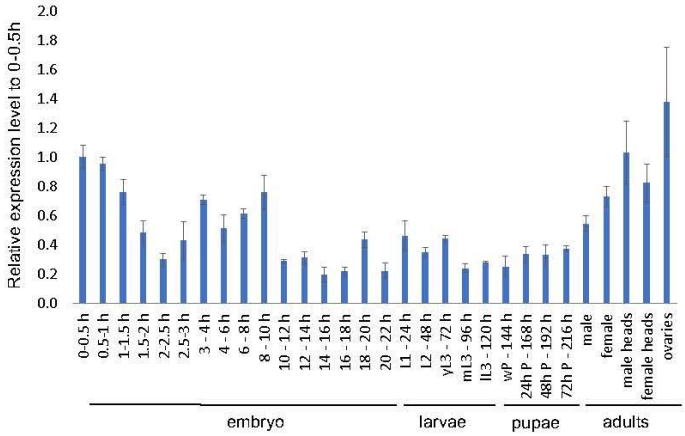

Appendix Figure S6: Expression of *Trmt112* transcript during development

Developmental expression of *Trmt112* transcript assayed by RT-qPCR analysis. The bar chart represents mean± standard deviation of three technical measurements.

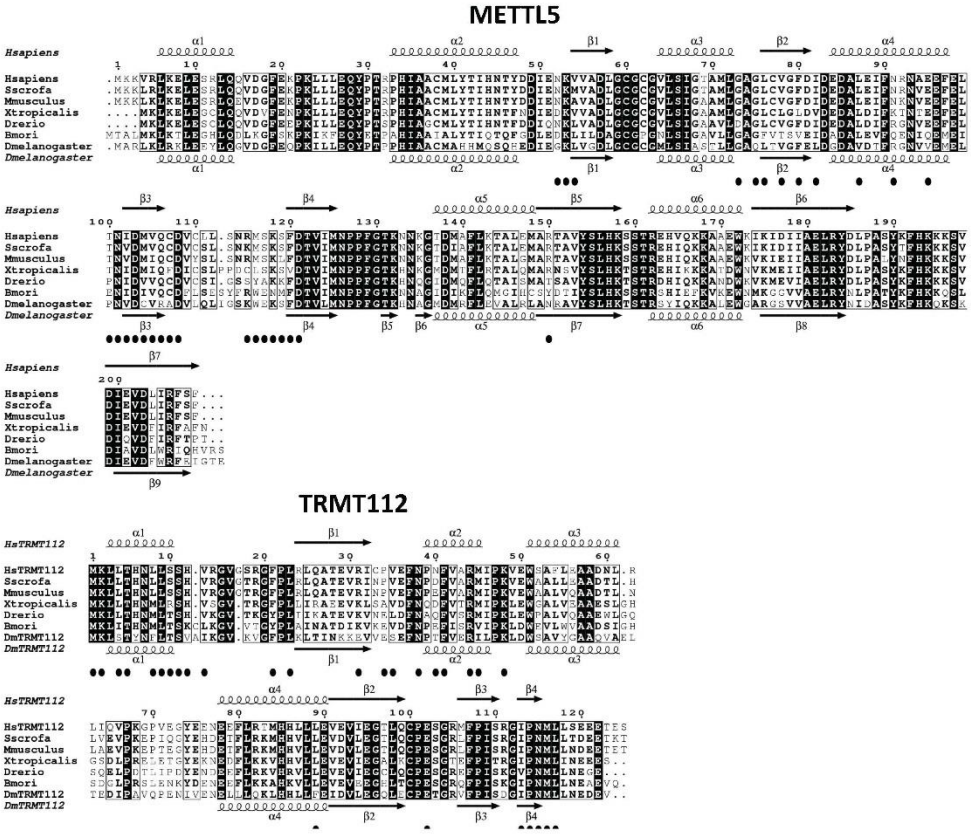

Appendix Figure S7: Secondary structure element analysis of fly Mettl5 and Trmt112

Strictly conserved residues appear in white font on a black background. Partially conserved amino acids are indicated with a grey font. Secondary structure elements assigned on the basis of the *H. sapiens* crystal structure and our fly model (Fig. 4D) are indicated above and below the alignments, respectively. Black circles underneath the multiple sequence alignment indicate residues involved in complex formation. Display generated using the ESpript server (Robert & Gouet, 2014).

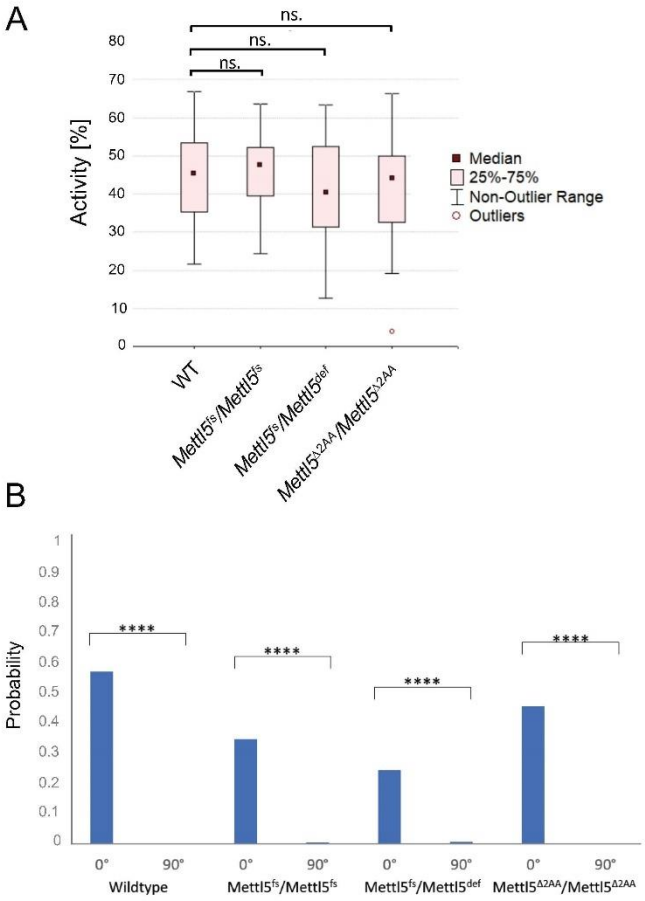

Appendix Figure S8: Statistical analysis of fly activity

(A) Fly activity evaluated with the help of the Buridan's paradigm. Shapiro-Wilk test was used to test for normal distribution in each group. Normally distributed groups were tested by t-test. Due to multiple comparison Bonferroni correction was applied. Number of flies tested: 30 per genotype. (n.s. = not significant). (B) Fixation index analyzed by Buridan's paradigm. 0° indicates area around black stripes, 90° indicates area 90° to the black stripes. Number of flies tested: 30 per genotype. ****P<0.0001 (t-test)

Acknowledgement

Curriculum vitae